UNIVERSITAT POLITÈCNICA DE VALÈNCIA

Geometric Integrators for Schrödinger Equations

PhD Thesis

Author:

Philipp Bader

Advisor:

Prof. Dr. Sergio Blanes Zamora

Valencia, June 2014

Summary

The celebrated Schrödinger equation is the key to understanding the dynamics of quantum mechanical particles and comes in a variety of forms. Its numerical solution poses numerous challenges, some of which are addressed in this work.

Arguably the most important problem in quantum mechanics is the so-called harmonic oscillator due to its good approximation properties for trapping potentials. In Chapter 2, an algebraic correspondence-technique is introduced and applied to construct efficient splitting algorithms, based solely on fast Fourier transforms, which solve quadratic potentials in any number of dimensions exactly - including the important case of rotating particles and non-autonomous trappings after averaging by Magnus expansions. The results are shown to transfer smoothly to the Gross-Pitaevskii equation in Chapter 3. Additionally, the notion of modified nonlinear potentials is introduced and it is shown how to efficiently compute them using Fourier transforms. It is shown how to apply complex coefficient splittings to this nonlinear equation and numerical results corroborate the findings.

In the semiclassical limit, the evolution operator becomes highly oscillatory and standard splitting methods suffer from exponentially increasing complexity when raising the order of the method. Algorithms with only quadratic order-dependence of the computational cost are found using the Zassenhaus algorithm. In contrast to classical splittings, special commutators are allowed to appear in the exponents. By construction, they are rapidly decreasing in size with the semiclassical parameter and can be exponentiated using only a few Lanczos iterations. For completeness, an alternative technique based on Hagedorn wavepackets is revisited and interpreted in the light of Magnus expansions and minor improvements are suggested. In the presence of explicit time-dependencies in the semiclassical Hamiltonian, the Zassenhaus algorithm requires a special initiation step. Distinguishing the case of smooth and fast frequencies, it is shown how to adapt the mechanism to obtain an efficiently computable decomposition of an effective Hamiltonian that has been obtained after Magnus expansion, without having to resolve the oscillations by taking a prohibitively small time-step.

Chapter 5 considers the Schrödinger eigenvalue problem which can be formulated as an initial value problem after a Wick-rotating the Schrödinger equation to imaginary time. The elliptic nature of the evolution operator restricts standard splittings to low order, $p < 3$, because of the unavoidable appearance of negative fractional time-steps that correspond to the ill-posed integration backwards in time. The inclusion of modified potentials lifts the order barrier up to $p < 5$. Both restrictions can be circumvented using complex fractional time-steps with positive real part and sixth-order methods optimized for near-integrable Hamiltonians are presented.

Conclusions and pointers to further research are detailed in Chapter 6, with a special focus on optimal quantum control.

Resumen

La célebre ecuación de Schrödinger es la clave para entender la dinámica de partículas cuánticas y viene en una variedad de formas. Su solución numérica conlleva numerosos desafíos, algunos de los cuales son tratados en esta tesis.

Posiblemente, el problema más importante en mecánica cuántica es el oscilador armónico debido a su uso en aproximar potenciales atractivos. En capítulo 2, se introduce una técnica de correspondencia algebraica entre mecánica clásica y cuántica y es aplicada para construir eficientes algoritmos de escisión (llamados *splittings*), solamente basados en transformadas rápidas de Fourier, que resuelven potenciales cuadráticos exactamente para dimensiones arbitrarias - incluyendo el caso importante de partículas rotantes y potenciales armónicos no autónomos tras la promediación con un desarrollo de Magnus. Los resultados se muestran fácilmente transferibles a la ecuación de Gross-Pitaevskii en capítulo 3. Adicionalmente, la noción de potenciales modificados no lineales es introducida y se su cálculo eficiente mediante transformadas de Fourier es demostrado.

En el límite semiclásico, el operador de evolución se vuelve altamente oscilatorio y métodos estándar de escisión sufren de un crecimiento exponencial en complejidad al incrementar el orden del método. Se han encontrado algoritmos con dependencia del coste respecto al orden solamente cuadrática mediante el algoritmo de Zassenhaus. A diferencia de métodos de escisión clásicos, se permite la apariencia de conmutadores especiales en los exponentes. Su construcción implica un rápido decrecimiento en magnitud con el parametro semiclásico de los conmutadores con la finalidad de poder exponenciarse con unas pocas iteraciones de Lanczos. Por completitud, una técnica alternativa basada en paquetes de onda Hagedorn es revisada e interpretada en términos del desarrollo de Magnus y se proponen algunas mejoras. Con la presencia de dependencias temporales explícitas en el hamiltoniano semiclásico, el algoritmo de Zassenhaus requiere una modificación del paso inicial. Distinguiendo los casos de frecuencias suaves y rápidas, se muestra cómo adaptar el mecanismo para obtener descomposiciones eficientemente calculables de un hamiltoniano efectivo que se ha obtenido tras un desarrollo de Magnus sin tener que resolver las oscilaciones con un paso temporal prohibitivamente pequeño.

En capítulo 5, se considera el problema de autovalores de Schrödinger que se puede formular como problema de valor inicial tras (Wick-)rotar la ecuación de Schrödinger al tiempo imaginario. El carácter elíptico del operador de evolución restringe los métodos de escisión a órdenes bajos, $p < 3$, debido a la apariencia de pasos fraccionales temporales negativos que corresponden a un problema mal condicionado: La integración atrás en el tiempo. La inclusión de potenciales modificados permite aumentar el orden hasta $p < 5$. Ambas restricciones se pueden sobrepasar mediante el uso de pasos fraccionales complejos cuya parte real es positiva y se presentan métodos de orden seis para hamiltonianos casi integrables.

Conclusiones e indicadores para futuros estudios se detallan en capítulo 6, especialmente enfocando el área de control óptimo cuántico.

Resum

La cèlebre equació d'Schrödinguer és la clau per comprendre la dinàmica de partícules quàntiques i es presenta en una gran varietat de forms. La seua resolució numèrica planteja nombrosos reptes, alguns dels quals són referits en aquest treball.

Possiblement, el problema més important en la mecànica quàntica és l'anomenat oscil·lador harmònic degut a la seua capacitat d'aproximar potencials d'atracció.
En el capítol 2, s'introdueix una tècnica de correspondència algebràica i s'aplica per a construer algoritmes eficients d'escissió (anomenats *splittings*), basats únicament en transformacions de Fourier ràpides, que resolen potencials quadràtics en qualsevol nombre exacte de dimensions – inclòs l'important cas de les partícules rotatòries així com la situació, considerablement més comuna, de potencials no autònoms després de promitjar a través de desenvolupaments de Magnus. Els resultats es mostren transferibles acuradament a l'equació de Gross-Pitaveskii en el capítol 3. A més, la noció de potencials no linials modificats s'introdueix i es mostra com computar-los eficientment utilitzant les transformades de Fourier. També es mostra com aplicar *splittings* de coeficients complexos a aquesta equació no linial i resultats numèrics corroboren les troballes.

En el límit semiclàssic, l'operador evolució es converteix en altament oscil·latori i els mètodes estàndards de splitting pateixen un increment exponencial de complexitat quan s'augmenta l'ordre del mètode. Es troben algoritmes amb cost computacional de dependència solament quadràtica respecte l'ordre utilitzant l'algoritme de Zassenhaus. Al contrari que els *splittings* clàssics, es permet l'aparició de commutadors especials en els exponents. La seua construcció implica un ràpid decreixement en magnitud amb el paràmetre semiclàssic dels commutadors i pot ser exponenciat utilitzant unes poques iteracions de Lanczos. Per completar, s'ha revisat i interpretat una tècnica alternativa basada en paquets d'ona de Hagedorn a la llum dels desenvolupaments de Magnus i s'han suggerit millores. En presència de dependències explícites del temps en el Hamiltonià semiclàssic, l'algoritme Zassenhaus requereix un pas d'iniciació especial. Diferenciant els casos de freqüències suaus i ràpides, es mostra com adaptar el mecanisme per a obtindre una descomposició eficientment computable d'un Hamiltonià efectiu que s'ha obtés després del desenvolupament de Magnus, sense haver de resoldre les oscil·lacions prenent un prohibitivament menut pas de temps.

El capítol 5 considera la possibilitat de formular el problema d'autovalors de Schrödinger com un problema de valor inicial després d'aplicar una rotació de Wick al temps imaginari a l'equació de Schrödinger. La naturalesa elíptica de l'operador evolució restringeix els *splittings* estàndars a ordres baixos, $p < 3$, donada la inevitable aparició de pasos fraccionals de temps negatius que corresponen a un mal condicionament del problema: la integració cap a darrere en el temps. La inclusió de potencials modificats eleva la barrera de l'ordre a $p < 5$. Ambdues restriccions poden ser sobrepassades mitjançant l'ús de pasos fraccionals de temps complexos amb part real positiva i es presenten mètodes optimitzats de 6é ordre per a Hamiltonians quasi-integrables.

Les conclusions i les línies a seguir en futures investigacions són detallades en el capítol 6, amb especial atenció al control quàntic òptim.

CONTENTS

Chapter 1

INTRODUCTION

The Schrödinger equation plays a central role in a wide range of applications and is the fundamental model of quantum mechanics [62]. It draws constant attention to theorists and practitioners, ever striving for higher accuracies and faster computation times[1].

This chapter will lay the fundamentals for a variety of Schrödinger equations, in particular, the Gross-Pitaevskii equation, the semiclassical limit and the imaginary time formulation. We briefly discuss many aspects that are crucial for the numerical solution. Furthermore, widely used numerical integrators, including both spatial and temporal discretizations, are introduced with special emphasis on splitting methods and Magnus expansions which will form the core of the numerical techniques that are developed in this work.

1.1 The Schrödinger equation and its varieties

1.1.1 The linear Schrödinger equation

We begin by stating the well-known *time-dependent Schrödinger equation* (TDSE) in one dimension

$$i\hbar\partial_t\psi(x,t) = H\psi(x,t), \quad \psi(x,0) = \psi_0(x), \quad x \in \mathbb{R} \tag{1.1}$$

where the *Hamiltonian* H is a Hermitian operator, usually of the form

$$H = T + V,$$

where T corresponds to the kinetic energy $T = -\frac{\hbar^2}{2m}\Delta$ with the Laplacian Δ and $V : \mathbb{R} \to \mathbb{R}$ is the (scalar) potential energy. Sometimes, we will write the kinetic energy as $T = p^2/2m$ with the *momentum operator* $p = -i\hbar\nabla$. The *wave function* ψ is, unless specified otherwise,

[1] A search in the *ScienceDirect* database with keywords "Schrödinger equation" and "numerical" shows more than 1000 published articles only in 2013.

always assumed to be square-integrable over the reals, i.e., $\psi \in L^2(\mathbb{R})$, and no additional boundary conditions are imposed. Higher dimensions will be explicitly introduced when it is not immediate how to replace $x \in \mathbb{R}$ by $x \in \mathbb{R}^d$. For simplicity in the presentation, it is standard to express the Schrödinger equation in atomic units $\hbar = m = 1$, which will be used throughout the text

$$i\partial_t \psi(x,t) = \left(-\frac{1}{2}\Delta + V(x)\right)\psi(x,t).$$

After the Schrödinger equation was first posed in 1926 [116], it did not take long until Born [33, 32] could identify the squared absolute value of the wave function as a probability density: the probability of finding the described particle in a certain domain Ω at time t is given by $\int_\Omega |\psi(x,t)|^2 dx$. An important feature of the Schrödinger equation is the conservation of the norm,

$$\frac{d}{dt}\int_{\mathbb{R}} |\psi(x,t)|^2 \, dx = 0,$$

which, in the light of viewing ψ as a probability density, has the physical meaning that the number of particles is preserved. With the probabilistic interpretation, we can define expectation values of a (not necessarily linear) Hermitian operator O, in this context called *observable*,

$$\langle O \rangle_\psi \equiv \int_{\mathbb{R}} \psi^*(x)\, O(\psi(x))\, dx.$$

This simplified standard notation in quantum mechanics can be expanded as

$$\langle O \rangle_\psi = \langle \psi | O(\psi) \rangle,$$

where $\langle \cdot \,|\, \cdot \rangle$ denotes the usual scalar product in L^2. As in classical mechanics, the observable associated with the energy is the Hamiltonian H itself, and a simple calculation yields the energy conservation law

$$\frac{d}{dt}\langle H \rangle_{\psi(t)} = 0,$$

for Hamiltonians that do not explicitly depend on time, $\partial_t H = 0$.

More generally speaking, classical quantum theory deals with self-adjoint operators, which we will briefly review. Given a densely defined operator H on some Hilbert space with domain D_H, its adjoint $H^\dagger$ is defined by[2]

$$\langle H^\dagger u | v \rangle = \langle u | H v \rangle, \quad \forall v \in D_H.$$

Such an operator is called *Hermitian* if $\langle Hu|v\rangle = \langle u|Hv\rangle, \quad \forall u, v \in D_H$. A *self-adjoint* operator H is Hermitian and additionally, its domain coincides with the one of its adjoint, $D_H = D_{H^\dagger}$. Obviously, self-adjointness implies Hermiticity, but the converse is not always true, and usually the discrepancy is due to boundary conditions that are imposed. In this work, we will not further address such subtleties and instead refer to [48] for details. Furthermore, we will use the name Hermiticity over self-adjointness, as is standard in the physics literature. This is justified since the Schrödinger operators at hand are self-adjoint under very general conditions, e.g., it suffices to bound the potential from below. By Stone's theorem, self-adjointness guarantees uniqueness and existence of the solution of (1.1) as

$$\psi(x,t) = e^{-itH}\psi_0(x), \tag{1.2}$$

[2] The adjoint of a matrix A is its Hermitian conjugate $A^\dagger$.

and we will use the notation with the exponential to denote the *flow* $\Phi_{H/i}$ associated with a vector field H/i.

Another core result for self-adjoint operators is the so-called spectral theorem: Given a self-adjoint compact operator H on some Hilbert space D, its (point-)spectrum consists of real eigenvalues λ_i and the corresponding eigenfunctions ϕ_i form an orthogonal basis of D. This allows us to write

$$H\psi = \sum_{k=1}^{\infty} \lambda_k \langle \psi, \phi_k \rangle \phi_k, \tag{1.3}$$

and therefore, the evolution (1.2) of some initial condition $\psi_0(x)$ can be written as

$$\psi(x,t) = e^{-itH}\psi_0 = \sum_{k=1}^{\infty} e^{-it\lambda_k} \langle \psi_0, \phi_k \rangle \phi_k. \tag{1.4}$$

For unbounded operators L, a subset of the (generalized) eigenfunctions might not be normalizable and are said to correspond to *unbounded states*, with corresponding eigenvalues in the *continuous spectrum* of L. However, another spectral theorem ensures that a self-adjoint operator can be expanded over generalized eigenfunctions to make sense of (1.3) in the usual case.

In essence, we summarize that if the spectrum is known, the solution of the Schrödinger equation is straightforward by means of (1.4).

For our purposes, two further properties of Hermitian operators H have to be singled out, namely that their eigenvalues are real valued,

$$\lambda_k = \langle \phi_k | H \phi_k \rangle = \langle \phi_k H | \phi_k \rangle = \lambda_k^*$$

and the eigenfunctions corresponding to distinct eigenvalues are orthogonal since,

$$0 = \langle \phi_k | H \phi_l \rangle - \langle \phi_k | H \phi_l \rangle = (\lambda_k - \lambda_l) \langle \phi_k | \phi_l \rangle.$$

1.1.2 The semi-classical limit

The major challenge in quantum chemistry is given by the rapid increase of dimensionality as the number of particles grows: for each particle, one has to add three dimensions to the configuration space and this becomes computationally unfeasible even for small molecules. For illustrative purposes, we write the Hamiltonian for N nuclei with coordinates x_i, electric charge Z_i and mass M_i and n electrons at y_i that interact via Coulomb forces ($\hbar = e = 1$),

$$H = \underbrace{\sum_{k=1}^{N} -\frac{1}{2M_k}\Delta_{x_k}}_{T_{\text{nuclear}}} + \sum_{k=1}^{n} -\frac{1}{2m_e}\Delta_{y_k} + \sum_{j<k} \frac{1}{|y_j - y_k|} + \sum_{j<k} \frac{Z_j Z_k}{|x_j - x_k|} - \underbrace{\sum_{j=1}^{N}\sum_{k=1}^{n} \frac{Z_k}{|x_j - y_k|}}_{\text{electron-nucleus}}. \tag{1.5}$$

Note that the full problem has $3(N+n)$ independent coordinates.

We stress that the timescales of the system are expressed in atomic units and are truly minute, time integration until $T = 1$ corresponds to metric time $T_{\text{real}} = \frac{\hbar}{a_0^2 m} = \frac{\hbar^3 (4\pi\varepsilon_0)^2}{m_e e^4} = 2.419 \times 10^{-17}$s ($\approx 24$ as) for electron mass $m_e = 1$. The Bohr radius is the natural scaling parameter for the space coordinate and is defined to be $a_0 = \frac{4\pi\epsilon_0\hbar^2}{e^2 m_e} = 5.28 \times 10^{-11} m$. From this brief dimensional analysis, we conclude that the time-scales are related to the inverse of the mass.

A standard way to reduce the dimension exploits this intuition and was invented by Born and Oppenheimer [34]. Their approximation is based on a separation of scales: Since the mass of the nuclei is several orders of magnitude larger than the electron mass, the nuclei are assumed to move at a much slower rate - indeed they are assumed to be independent of the electrons and expected to follow classical equations of motion.

Hence, we freeze the coordinates nuclei, thereby neglecting its kinetic energy and, motivated by (1.4), solve the eigenvalue problem of the electronic part of the Hamiltonian $H_e = H - T_{\text{nuclear}}$,

$$H_e \psi_k(x,y) = E_k(x)\psi_k(x,y), \qquad k \in \mathbb{N},$$

where E_k is the $k-$th eigenvalue of H_e. Assuming that the eigenfunctions ψ_k form a (orthonormal) basis of L^2, we can expand the solution of the full problem in these new terms as

$$\psi(t,x,y) = \sum_k \phi_k(x,t)\psi_k(x,y). \tag{1.6}$$

Plugging (1.6) into the SE with the full Hamiltonian (1.5) yields an equation for the nuclei,

$$i\partial_t \sum_k \phi_k(x,t)\psi_k(x,y) = \sum_k \left(\sum_{j=1}^N -\frac{1}{2M_j}\Delta_{x_j} + E_k(x) \right) \phi_k(x,t)\psi_k(x,y).$$

After multiplying from the left with $\psi_k^*(x,y)$ and integrating over the electronic coordinates y, we obtain a Schrödinger equation for the nuclei

$$i\partial_t \phi_k(x,t) = \left(-\frac{\varepsilon^2}{2} \sum_{j=1}^N \Delta_{x_j}\phi_k(x,t) + E_k(x)\phi_k(x,t) \right) + \sum_l C_{k,l}\phi_l(x,t), \tag{1.7}$$

where we have set the nuclear masses identical $M_j = M$ and introduced a new parameter $\varepsilon^2 = m_e/M$, that denotes the relative mass of an electron versus a nucleus. The coupling operator is given by

$$C_{k,l} = -\frac{\varepsilon^2}{2} \int_{\mathbb{R}^n} \psi_k^*(x,y) \sum_{j=1}^N \left((2\partial_{x_j}\psi_l(x,y))\partial_{x_j} + \partial_{x_j}^2 \psi_l(x,y) \right) dy.$$

Until here, all manipulations have been formally exact within the original model (1.5) and in the final step we reduce the equations: The so-called *adiabatic* or Born-Oppenheimer approximation consists of neglecting the coupling terms and assuming that the energy surfaces for the electrons $E_k(x)$ are well-separated which thus results in a system of uncoupled Schrödinger equations

$$i\varepsilon\partial_t \phi_k(x,t) = \left(-\frac{\varepsilon^2}{2}\Delta + E_k(x) \right) \phi_k(x,t), \qquad k \in \mathbb{N}. \tag{1.8}$$

Note that we have scaled the time-coordinate $t \to \varepsilon t$ to guarantee a meaningful limit of the equation as $\varepsilon \to 0$. It is convenient to identify (1.8) with (1.1) via $\varepsilon = \hbar$ and $E_k = V$. For future reference, we write (1.8) for one particle in the standard form, known as *semi-classical Schrödinger equation* (SCSE),

$$i\varepsilon \partial_t \psi(x,t) = \left(-\frac{\varepsilon^2}{2}\Delta + V(x)\right)\psi(x,t), \qquad \psi(x,0) = \psi_0(x) \in L^2(\mathbb{R}) \tag{1.9}$$

The name "semi-classical" is derived from an analogy to classical mechanics, based on the observation that Lie-brackets reduce to Poisson brackets in the limit $\hbar \to 0$ and thus one expects to recover classical mechanical behavior in this limit. Indeed, using Wentzel's, Kramer's and Brillouin's (WKB) approximation, that is formulating the wave function as the exponential of a phase function S^ε,

$$\psi(x,t) = Ae^{\frac{i}{\varepsilon}S^\varepsilon(x,t)},$$

and plugging it into (1.9), we obtain an equation for S^ε,

$$-\partial_t S^\varepsilon = \frac{1}{2}(\partial_x S^\varepsilon)^2 + V - \frac{i\varepsilon}{2}\Delta S^\varepsilon. \tag{1.10}$$

For $\hbar = \varepsilon \to 0$, the classical Hamilton-Jacobi equations are recovered by identifying the momentum $p = \partial_x S$ and as such, the system is interpreted to follow classical trajectories with a small perturbation of size $\mathcal{O}(\varepsilon)$ due to quantum effects.

More information about the solution can be deduced by letting $A = a^\varepsilon(x,t)$ and expanding in powers of the small parameter ε,

$$a^\varepsilon(x,t) = a_0(x,t) + \varepsilon a_1(x,t) + \varepsilon^2 a_2(x,t) + \cdots,$$

with the idea to include the ε-dependence in the "amplitude" a^ε (and hence dropping it in the phase S). As usual, the SE is computed for this ansatz and terms of equal power in ε are collected. A truncation after the first term $a_0 = \mathcal{O}(1)$ then leads to an expression $a_0 \exp({}^{i}/_{\varepsilon} S(x,t))$, where the phase S is now assumed to be slowly varying and certainly independent of ε, as one can expect for a classical approximation by (1.10). Therefore, oscillations should appear on a spatial scale λ proportional to ε, $\lambda \propto \varepsilon$, and a sensible numerical algorithm is expected to resolve the spatial coordinate at least as $\Delta x \propto \varepsilon$.

After these considerations, it is clear that the semi-classical Schrödinger equation poses severe challenges to numerical integration since small values of ε cause the system to oscillate rapidly, which then in turn implies severe step-size restrictions for the numerical integrator. We will address this problem in Chapter 4. For discussions of general and numeric issues, we refer to literature reviews [37, 91, 83].

1.1.3 Many particles and the Gross-Pitaevskii equation

The rich theory of Bose-Einstein condensation, a macroscopic quantum phenomenon, where a large number of indistinguishable particles behave as one (see [107] for details), does not cease to draw attention especially after its first experimental realization [2, 35, 49] and the following nobel prize in 2001. This subsection is devoted to the theoretical description thereof and the

derivation of the nonlinear Schödinger equation whose numerical solution will be addressed in Chapter 3. We commence with the many-particle Schrödinger equation

$$i\frac{d}{dt}\psi(x_1,\dots,x_N) = \left(\frac{1}{2m}\sum_{j=1}^{N}\Delta_j + \sum_{j=1}^{N}V(x_j) + \sum_{j<k}W(x_j,x_k)\right)\psi(x_1,\dots,x_N), \tag{1.11}$$

where x_j represents the position of the j-th particle. All particles are subject to the same external potential V and their kinetic energies are given by the Laplacian Δ_j, acting on the j-th coordinate. We assume identical bosonic particles that are subject to hard-body interaction, modeled by Dirac's $\delta(x)$-function,

$$W(x_j,x_k) = g\delta(x_j - x_k),$$

for some parameter $g \in \mathbb{R}$. Since we are ultimately interested in the lowest energy state, we assume all particles to be identically distributed and thus arrive at the Hartree approximation for the wave function

$$\psi(x_1,\dots,x_N) \approx \Phi(x_1,\dots,x_N) \equiv \prod_{j=1}^{N}\phi(x_j),$$

which is symmetric w.r.t. the interchange of particles and the single-particle wave function is normalized to one, $\int \phi(x)\,dx = 1$. After a simple calculation, the energy functional is obtained to

$$\langle\Phi|H\Phi\rangle = -N\frac{1}{2m}\int \phi^*(x)\Delta\phi(x)\,dx + N\int \phi^*(x)V(x)\phi(x)\,dx + g\frac{N(N-1)}{2}\int|\phi(x)|^4\,dx,$$

where the interaction energy was derived by

$$\begin{aligned}\int\sum_{j<k}^{N}\prod_{l=1}^{N}|\phi(x_l)|^2\delta(x_j-x_k)\,dx^N &= \int\int\sum_{j<k}^{N}|\phi(x_j)|^2|\phi(x_k)|^2\delta(x_j-x_k)\,dx_j\,dx_k\\ &= \sum_{j<k}^{N}\int|\phi(x)|^4\,dx = \frac{N(N-1)}{2}\int|\phi(x)|^4\,dx.\end{aligned}$$

The energy is minimized by treating ϕ and ϕ^* as independent variables and zeroing the functional derivative of ϕ^*,

$$\frac{\delta}{\delta\phi^*}\langle\Phi|H\Phi\rangle = N\int\left[-\frac{1}{2m}\Delta\phi(x) + V(x)\phi(x) + g(N-1)|\phi(x)|^2\phi(x)\right]\delta\phi^*(x)\,dx.$$

To ensure the correct normalization of the variation, we include a Lagrange multiplier μ, the *chemical potential*, $1 = \langle\Phi|\Phi\rangle = \left(\int|\phi(x)|^2\,dx\right)^N$ whose functional derivative

$$\frac{\delta}{\delta\phi^*}\langle\Phi|\Phi\rangle = N\left(\int|\phi(x)|^2\,dx\right)^{N-1}\int\phi(x)\delta\phi^*(x)\,dx = N\int\phi(x)\delta\phi^*(x)\,dx$$

has to be added to yield the extremal equation

$$\frac{\delta}{\delta\phi^*}\left(\langle\Phi|H\Phi\rangle - \mu\langle\Phi|\Phi\rangle\right) = 0.$$

A stationary solution of this variational principle is the time-independent *Gross-Pitaevskii* equation (GPE),

$$-\frac{1}{2m}\Delta\phi(x) + V(x)\phi(x) + gN|\phi(x)|^2\phi(x) = \mu\phi(x),$$

after the approximation $N-1 \simeq N$. In a similar fashion, the stationary point of the action

$$A[\Phi] = \int \left[\frac{1}{2}\left(\langle\Phi|i\partial_t\Phi\rangle + c.c.\right) - \langle\Phi|H\Phi\rangle \right] dt,$$

where $c.c.$ stands for the complex conjugate, gives the time-dependent GPE

$$i\frac{d}{dt}\phi(t,x) = \left(-\frac{1}{2m}\Delta + V(x) + gN|\phi(t,x)|^2\right)\phi(t,x). \tag{1.12}$$

The solution ϕ is still interpreted as a probability density which is preserved by the nonlinear equation (1.12).

Beyond mean-field theory In some contexts, however, the Hartree approximation looses its validity and it is necessary to go beyond mean-field theory. In particular, we mention fragmentation of Bose-Einstein condensates [100], where the single-particle density matrix has more than one macroscopic eigenvalue [88] which in turn implies a macroscopic occupation of more than one state. Instead of assuming a single state as for the Hartree-approach, the quantum mechanical field operator has to be truncated at higher modes. The usual notation is slightly more involved for an N-particle system: The idea is to use the eigenfunctions ψ_j of the single particle Hamiltonian $N = 1$ to write the many-particle states as products of these functions by defining

$$\Phi_{n_0,n_1,n_2,\dots}(x_1,\dots,x_N) \mathrel{\hat{=}} \frac{1}{N!}\prod_{k=0}^{\infty}\sqrt{n_k!}\sum_{j_1\dots j_N}\psi_{j_1}(x_1)\dots\psi_{j_N}(x_N)$$

where the numbers $\sum_{i=0}^{\infty} n_i = N$, $n_i \in \mathbb{N}_0$ indicate the amount of particles in the ith single particle eigenstate and the indices $j_k \in \mathbb{N}_0$ run over all indices k for which $n_k \neq 0$. The states $\Phi_{n_0,n_1,\dots}$ form a complete orthonormal basis, inherited from the ψ_k, and the full Hamiltonian (1.11) reads, written in terms of *field operators* [55],

$$H = \int \hat{\Psi}^\dagger(x)\left(-\frac{\Delta}{2} + V(x)\right)\hat{\Psi}(x)\,dx + \iint \hat{\Psi}^\dagger(x)\hat{\Psi}^\dagger(x')W(x-x')\hat{\Psi}(x')\hat{\Psi}(x)\,dx\,dx'. \tag{1.13}$$

The field operator can be expanded as $\hat{\Psi}(x) = \sum_{k=0}^{\infty}\psi_k(x)\hat{a}_k$, where the *ladder operators* $\hat{a}_j^\dagger$, $\hat{a}_j$ are the creation and annihilation operators (for bosons), respectively. They are defined by their commutation relations $[\hat{a}_k, \hat{a}_{k'}^\dagger] = \delta_{k,k'}$ using Kronecker's delta. Putting this in perspective, a truncation at the lowest mode, i.e., assuming $n_0 = N$ and thus $n_j = 0$ for $j > 0$, or, equivalently $\psi_k = 0$ for $k > 0$, we recover the Gross-Pitaeskii equation for ψ_0 when $W(x) = g\delta(x)$.

More complex phenomena such as fragmentation specifically require the inclusion of higher modes of the expansion (1.13). We have studied the occurrence of fragmentation of bosons

in a time-independent setting for a single trap subject to the relative strength of the couplings of the included modes [8], assuming a general quadratic plus quartic Hamiltonian[3]

$$H = \epsilon_0 \hat{a}_0^\dagger \hat{a}_0 + \epsilon_1 \hat{a}_1^\dagger \hat{a}_1 + \frac{W_{0000}}{2} \hat{a}_0^\dagger \hat{a}_0^\dagger \hat{a}_0 \hat{a}_0 + \frac{W_{1111}}{2} \hat{a}_1^\dagger \hat{a}_1^\dagger \hat{a}_1 \hat{a}_1 + \left(\frac{W_{0011}}{2} \hat{a}_0^\dagger \hat{a}_0^\dagger \hat{a}_1 \hat{a}_1 + \frac{W_{1100}}{2} \hat{a}_1^\dagger \hat{a}_1^\dagger \hat{a}_0 \hat{a}_0 \right) + \frac{A_4}{2} \hat{a}_1^\dagger \hat{a}_1 \hat{a}_0^\dagger \hat{a}_0,$$

with the ϵ_j corresponding to the single particle energies $\epsilon_j = \int \psi_j^*(T+V)\psi_j$, and with interaction coefficients $A_4 = W_{0101} + W_{1010} + W_{1001} + W_{0110}$ and

$$W_{ijkl} = \int d^3x \int d^3x' \psi_i^*(x) \psi_j^*(x') W(x-x') \psi_k(x') \psi_l(x).$$

Further results based on these findings estimate thresholds for the (contact-)interaction strength g to argue that fragmentation exists for harmonically trapped bosons for dimensions $d \leq 2$ [56] and is inhibited for $d = 3$ [9]. Our approach approximates the modes by introducing a variational parameter in the width of the well-known single-particle solutions for the harmonic oscillator which is then minimized to account for interaction between the first relevant many-particle modes.

In this thesis, we will not detail this line of work, however, we pause to explain significant contact points with the main content herein: So far, the (single-particle) ground states have been determined through a semi-quantitative variational analysis which has large room for improvement, and techniques from Chapter 5 can be applied to determine the single-particle states more accurately, aiming for a full solution of the two-mode eigenvalue problem, cf. the following introduction. On the other hand, the dynamics of fragmentation is still barely understood and current simulations rely on the multi-configurational time-dependent Hartree (MCTDH) framework [96], where the full configuration space is projected to the span of a subset of the Hartree products $\psi_{j_1}(x_1) \dots \psi_{j_N}(x_N)$ for which the number of degrees of freedom is truncated by setting $j_k < D$ for some constant D. In other words, the field operator is approximated by $\hat{\Psi} \approx \sum_{k=0}^{D-1} \psi_k \hat{a}_k$. In future work, we intend to apply splitting techniques of Chapter 2 to solve the MCTDH equations, in particular for harmonically trapped particles .

1.1.4 Eigenstates and imaginary time

The last type of Schrödinger equations that we will discuss in this thesis originates from the interest in the spectra of Hamiltonian operators, which is relevant for the understanding of the atomic and molecular structure of matter: In addition to the applications outlined above (Born-Oppenheimer approximation, fragmentation of Bose-Einstein condensates), it determines, e.g., the stability of molecules, band-gaps in semi-conductors etc.

A separation of variable ansatz $\psi(t,x) = e^{-itE_k}\phi(x)$ in (1.1) results in the so-called stationary Schrödinger equation ($\hbar = m = 1$),

$$H\phi_k(x) = E_k \phi_k(x), \qquad k = 0, 1, 2, \dots \tag{1.14}$$

[3]The quartic part is due to pairwise particle interactions, in contrast to the quadratic terms that correspond to non-interacting (uncoupled) many particle systems.

where, again,

$$H = T + V(x) = -\frac{1}{2}\Delta + V(x). \tag{1.15}$$

We recall that the eigenvalues E_k are real and positive (after a shift of the origin) and we assume that their corresponding (real) eigenfunctions $\phi_i(x)$ form a (orthonormal) basis of the underlying Hilbert space.

There are many ways to solve the eigenvalue problem, some of which will be discussed to some extent in Section 5. In this introduction, however, we are interested in the so-called *imaginary time propagation* (ITP): Parting from the TDSE,

$$i\partial_t \psi(t,x) = H\psi(t,x), \tag{1.1}$$

we introduce a Wick rotation of the time coordinate, $t = -i\tau$, which transforms (1.1) into a diffusion type equation

$$-\frac{\partial}{\partial \tau}\psi(x,\tau) = H\psi(x,\tau), \qquad \psi(x,0) = \psi_0(x), \tag{1.16}$$

with formal solution $\psi(x,\tau) = e^{-\tau H}\psi(x,0)$. Analogous to (1.4), we expand the initial condition in the basis functions $\phi_k(x)$ and write

$$\psi_0(x) = \sum_i c_i\, \phi_i(x), \qquad c_i = \left\langle \phi_i(x) \,|\, \psi(x,0) \right\rangle,$$

and the time evolution of (1.16) is given by

$$\psi(x,\tau) = e^{-\tau H}\psi(x,0) = \sum_i e^{-\tau E_i}\, c_i\, \phi_i(x). \tag{1.17}$$

Assuming non-degenerate[4] eigenvalues $E_0 < E_1$, the asymptotic behavior is clearly

$$\psi(x,\tau) \underset{\tau\to\infty}{\longrightarrow} e^{-\tau E_0}\, c_0 \phi_0,$$

since the exponentials with larger exponents decay more rapidly. The convergence rate depends of course on the separation of the eigenvalues. From a formal point of view, the initial condition is required to contain a component of the smallest eigenvalue, $c_0 \neq 0$, however, due to round-off errors - or, equivalently, limits in numerical accuracy - this is not of practical relevance since $c_0 = 0$ will not be exactly maintained along the propagation of the initial condition.

1.2 Spatial discretizations

In the context of PDEs, a major challenge is to deal with the infinite dimensional function space in which the solution evolves with time - a problem that usually goes with the name semi-discretization. Undoubtedly, the most familiar truncation to finite (and thus numerically treatable) dimensions is done by substituting the underlying domain of the function space, say

[4] Practical aspects of degeneracies will be briefly addressed in Section 5.

for simplicity $X \subset \mathbb{R}$, by a finite set of points $x_1, \dots, x_n \in \mathbb{R}$ and thus replacing functions by their values at these grid points. There are several ways of representing spatial derivatives in this basis and a few of them will be discussed subsequently.

Other means of discretizing the space, e.g., finite elements or wavelets are also widely used and an alternative approach using Hagedorn-wave packets will be briefly presented thereafter.

1.2.1 Finite differences

Finite differences (FD) operate on a chosen discretization of the underlying domain by some grid $x_1, \dots, x_n \in \mathbb{R}$. The main idea then consists in approximating the spatial derivatives by linear combinations of the objective function, which has now become a vector, at different grid points. There are many ways to approximate derivatives and the finite difference approach constitutes of a formal Taylor expansion of the ansatz at each point to obtain coefficients up to a certain order and is therefore a *local* approximation.

Suppose that the grid points are equidistantly distributed, i.e., $x_{j+1} = x_j + \Delta x$, then

$$f(x + \Delta x) = f(x) + f'(x)\Delta x + f''(x)\frac{\Delta x^2}{2} + \mathcal{O}\left(\Delta x^3\right),$$

and a first order finite difference approximation of the first derivative is thus readily given by

$$f'(x_j) = \frac{f(x_{j+1}) - f(x_j)}{\Delta x} + \mathcal{O}(\Delta x).$$

Using more grid points, i.e., examining the Taylor expansions of $f(x + k\Delta x)$, we can derive higher order approximations, for example ($k = 2$)

$$f'(x_j) = \frac{f(x_{j+1}) - f(x_{j-1})}{2\Delta x} + \mathcal{O}\left(\Delta x^2\right).$$

The previous formulas are known as forward differences and central differences, respectively. Without going into details, we can observe that higher orders can be easily achieved for the finite difference formulas and it is easy to generalize finite differences to higher derivatives. In this work, due to the virtually periodic structure of the quantum mechanical problems, we will mainly use spectral approximations that converge geometrically in Δx, can be cheaply computed and outperform finite difference methods. In Chapter 4, a comparison between FD and spectral methods is undertaken.

1.2.2 Spectral methods

The previous approach is based on a local approximation of derivatives by mimicking the Taylor expansion of the sought function. Spectral methods follow an opposite direction, they rely on the global interpolation of the objective function and perform the differentiation on the interpolating functions. The following introduction is based on [124]. Suppose $f : \mathbb{R} \to \mathbb{C}$ is a complex-valued function, its *Fourier transform* is then defined as

$$\mathscr{F}[f](k) = \hat{f}(k) = \int_{-\infty}^{\infty} f(x) e^{ikx} dx, \quad k \in \mathbb{R}.$$

We interpret the Fourier transform $\mathscr{F}$ as an expansion of the function f in the basis of plane waves e^{ikx}, where the value of the transform $\hat{f}(k) \in \mathbb{C}$ gives the amplitude of the wave number k. The particular beauty of plane waves is that they are eigenfunctions of the derivative operator, or in other words,

$$\mathscr{F}[\partial_x f(x)](k) = ik\mathscr{F}[f(x)](k) = ik\hat{f}(k). \tag{1.18}$$

Hence, after applying a Fourier transform, derivatives become simple multiplications, yet the transforms still have to be computed.

In order to reduce dimensionality, we discretize in space, thereby passing to so-called spectral collocation: Instead of looking at an expansion in (a finite number of) plane waves at certain different frequencies, the trigonometric interpolation polynomials are considered, an approach that is equivalent on equidistant grids. From here on, we will assume periodic boundary conditions and restrict the spatial domain to the interval $[0, 2\pi]$ on which an odd[5] number $N+1$ of equidistant grid points $x_l = 2\pi(l+1)/(N+1)$, $l = 0, \dots, N$ is chosen.

Trigonometric interpolation [68] consists of expanding the function f as

$$f_N(x) = \sum_{l=0}^{N} f(x_l) h_l(x), \tag{1.19}$$

with Lagrange's trigonometric polynomials

$$h_l(x) = \frac{1}{N+1} \frac{\sin\left(\frac{N+1}{2}(x-x_l)\right)}{\sin\left(\frac{1}{2}(x-x_l)\right)} = \frac{1}{N+1} \sum_{k=-N/2}^{N/2} e^{ik(x-x_l)},$$

or, equivalently, as a (discrete) convolution

$$f_N(x) = \sum_{l=0}^{N} h_N(x-x_l) f(x_l).$$

The interpolant f_N coincides with f at $N+1$ nodes x_l and reproduces exactly all trigonometric polynomials of degree $\leq N/2$.

Differentiation is now easily performed by computing

$$\begin{aligned} f_N'(x) &= \sum_{l=0}^{N} f(x_l) h_l'(x) = \sum_{l=0}^{N} f(x_l) \frac{1}{N+1} \sum_{k=-N/2}^{N/2} ike^{ik(x-x_l)} \\ &= \frac{1}{N+1} \sum_{k=-N/2}^{N/2} ik \sum_{l=0}^{N} f(x_l) e^{ik(x-x_l)} \\ &= \frac{1}{2\pi} \sum_{k=-N/2}^{N/2} \left(\frac{2\pi}{N+1} \sum_{l=0}^{N} f(x_l) e^{-ikx_l} \right) ike^{ikx}. \end{aligned} \tag{1.20}$$

[5] For even $N+1$, analogous expressions exist.

The parenthesis in the last row is called *Discrete Fourier Transform* (DFT) of the function f,

$$\hat{f}_k = \Delta x \sum_{l=0}^{N} f(x_l) e^{-ikx_l}, \qquad k = -\frac{N}{2}, \dots, \frac{N}{2},$$

with the grid size $\Delta x = 2\pi/(N+1)$ and its inverse (IDFT) is given by

$$f_N(x_l) = \frac{1}{2\pi} \sum_{k=-N/2}^{N/2} \hat{f}_k e^{ikx_l}. \tag{1.21}$$

We recognize in (1.20) an application of a DFT followed by multiplication of ik and a consecutive inverse DFT, perfectly analogous to the continuous case. Fortunately, the expansion coefficients $\hat{f}_k$ can be cheaply computed at a cost $N\log(N)$ using the Fast Fourier Transform (FFT) algorithm, which in turn implies that the action of the Laplacian on a discretized function $f(x_l)$ can also be computed with one FFT and one inverse, as in (1.21),

$$\partial_x^r f_N(x) = \mathscr{F}\left[(ik)^r \, \mathscr{F}^{-1}\left[f_N\right](k)\right](x),$$

which is the discrete analogue of (1.18) for the interpolant f_N of (1.19).

It is worth pointing out that, in the limit of infinite order for periodic grids, finite difference schemes coincide with Fourier spectral methods. Furthermore, its matrix representation is given by $\mathbf{DFT}_{k,l} = \Delta x e^{-ikx_l}$ which is a *circulant matrix*, and the discrete Fourier transform can be written in vectorized form as a matrix-vector multiplication,

$$\hat{f} = \mathbf{DFT} f,$$

To conclude, we list a few properties of the Fourier transformation that will be used in the course of this work:

a. Linearity: For two functions $a, b \in L^2(\mathbb{R})$, $\mathscr{F}[a+b](k) = \mathscr{F}[a](k) + \mathscr{F}[b](b)$

b. Differentiation: For $f_x \in L^2(\mathbb{R})$, then $\mathscr{F}[f_x](k) = ik\hat{f}(k)$

c. Real-valued functions: If $f(x)$ is real, then $\hat{f}(k)$ is Hermitian, i.e., $\hat{f}(-k) = \hat{f}(k)^*$, and thus half the coefficients are redundant ($\hat{f}_{-k} = \hat{f}_k^*$). This will lead to a speedup of a factor two in computations.

d. Parseval's identity: $\frac{1}{2\pi}\int_0^{2\pi} |f_N(x)|^2 dx = \sum_k |\hat{f}_k|^2$, which means that the norm is preserved by Fourier transforms. It holds both for the continuous and the discrete case.

e. Spectral convergence: Let $f \in L^2([0, 2\pi])$ be p-times differentiable, then the error committed by trigonometric interpolation is

$$\|f - f_N\|_{L^2([0,2\pi])} \leq aN^{-p} \|f^{(p)}\|_{L^2([0,2\pi])},$$

where f_N is given in (1.19) and a is a constant independent of N and p. For analytic f, we even have exponential convergence

$$\|f - f_N\|_{L^2([0,2\pi])} \leq be^{-cN} \|f\|_{L^2([0,2\pi])},$$

with constants b, c independent of N.

1.2.3 Hagedorn-wavepackets

We have just seen how the differentiation has been simplified by expanding the solution in plane wave states for the spectral method. Obviously, this is not the only useful choice of a basis, as seen, for example for the Born-Oppenheimer approximation in Section 1.1.2. From practical considerations, the important aspect is to ask whether an expansion *and* the dynamics can be efficiently computed in a certain basis. Motivated by the semi-classical Schrödinger equation, it seems promising to use wave-packets that behave similar to classical particles as basis functions. Such wave functions are often associated with the name *coherent states* which means that one can associate them with a classical position and momentum which behave according to classical mechanics and which can be traced back to Schrödinger himself [115]. Heller [67] proposed a variable Gaussian as variational ansatz for the wave function

$$\tilde{\psi}(x,t) = \exp\left(\frac{i}{\varepsilon}\left(\frac{1}{2}\left(x-q(t)\right)^T C(t)\left(x-q(t)\right) + p(t)\cdot\left(x-q(t)\right) + \xi(t)\right)\right).$$

The variational parameters $q(t), p(t)$ correspond to the average position and momentum, respectively, and $\xi(t)$ denotes the global phase. The complex matrix $C(t)$ defines the width of the wave function. After a change of basis which was proposed in [63] and which relies on a factorization $C = PQ^{-1}$, where P, Q satisfy certain relations[6], an orthonormal basis of $L^2(\mathbb{R})$ can be constructed from

$$\phi_0^\varepsilon[p,q,Q,P](x) = \pi^{-1/4}(\varepsilon Q)^{-1/2}\exp\left(\frac{i}{2\varepsilon}PQ^{-1}(x-q)^2 + \frac{i}{2\varepsilon}p(x-q)\right).$$

The construction uses ladder operators, which lead to a recurrence relation

$$Q\sqrt{k+1}\,\phi_{k+1}^\varepsilon(x) = \frac{\sqrt{2}}{\varepsilon}(x-q)\phi_k^\varepsilon(x) - Q^*\sqrt{k}\,\phi_{k-1}^\varepsilon(x).$$

For our purposes, it is sufficient to know that such an orthonormal basis exists and that it can be efficiently evaluated by this recursive formula. Abbreviating the notation by defining $\Pi(t) = (q(t), p(t), Q(t), P(t))$, a given initial condition $\psi(x,0)$ can be expanded as

$$\psi(x,0) = e^{\frac{i}{\varepsilon}S(t)}\sum_{k=0}^{\infty} c_k(t)\phi_k[\Pi(t)], \tag{1.22}$$

where $S(t)$ is a global[7] phase parameter that has been inherited from $\xi(t)$.

The dynamics for the parameters Π, S, i.e., how the basis evolves, are surprisingly simple and can be written as [60]

$$\begin{aligned} \dot{q}(t) &= p(t), & \dot{Q}(t) &= P(t), \\ \dot{p}(t) &= -\nabla V(q(t)), & \dot{P}(t) &= -V^{(2)}(q(t))Q(t), \\ \dot{S}(t) &= \frac{1}{2}p(t)^2 - V(q(t)), \end{aligned} \tag{1.23}$$

[6] Cf. Ref. [91] for details.

[7] A global phase is physically irrelevant, however, since the semi-classical equation is somehow embedded in a larger system, it can become meaningful and we cannot neglect it.

where $V^{(2)}$ is the Hessian of V. The challenge is hidden in the evolution of the weights $c_k(t)$: They obey a linear system of ordinary differential equations (ODEs) which can be derived by plugging (1.22) into the semi-classical SE (1.9). However, the resulting equations, see [63] are difficult to solve and a simpler numerical approach will be discussed in Section 4.2 of Chapter 4.

1.3 Temporal discretizations

In this work, however, the main focus lies on the evolution of the solution in time. For a more complete exposition, we will briefly mention some standard methods that have been widely used in the context of PDEs in general, and in particular for the problems addressed in this work. Supplementary references are given where more details can be found and the methods are placed in context of the geometric integrators to be presented later. After discretization of the spatial domain, we are left with a system of coupled (for now autonomous) ODEs of the form

$$\dot{y}(t) = f(y(t)), \quad y(0) = y_0 \in \mathbb{R}^N,$$

and its solution is given by the *flow* map φ_t as

$$y(t) = \varphi_t^{[f]}(y_0),$$

In the later exposition, we will use an exponential notation for the exact flows which is standard for linear vector fields and can be generalized by means of *Lie-derivatives*: The flow of a (nonlinear) vector field $f(y)$ can be written as

$$e^{t\mathscr{L}_f}(\mathbf{I}(y_0)) \equiv \varphi_t(y_0), \quad \mathscr{L}_f = \sum_{k=1}^{d} f_k \frac{\partial}{\partial y_k},$$

where the sum is to be understood over the components of the vector valued function f. The Lie-derivative acts on the initial conditions by $\mathscr{L}_f g(y) = g'(y)f(y)$, thus

$$e^{t\mathscr{L}_f} g(y_0) = g(\varphi_t^{[f]}(y_0)),$$

and consequently, we obtain the *Vertauschungssatz* for the flows of two vector fields f_1, f_2,

$$e^{t\mathscr{L}_{f_1}} e^{t\mathscr{L}_{f_2}} g(y_0) = g(\varphi_t^{[f_2]} \circ \varphi_t^{[f_1]}(y_0)). \tag{1.24}$$

A *numerical integrator* $\Phi_h^{[f]} : \mathbb{R}^N \to \mathbb{R}^N$ is a map that takes an initial condition y_0 and a step-size $h \in \mathbb{C}$ to an approximation to the exact solution $y(h)$. The quality of the approximation is expressed by its distance from the exact solution in some norm and an integrator is said to be of (local) *order p* if the map satisfies

$$\|\Phi_h^{[f]}(y(0)) - y(h)\| = ch^{p+1} + \mathcal{O}\left(h^{p+2}\right)$$

for some constant c independent of h.

1.3.1 Chebyshev method

The following two subsections are devoted to polynomial interpolations of the exponential. Tal-Ezer and Kosloff[121] have pioneered in the application of Chebyshev interpolation for the time-integration of the Schödinger equation. *Chebyshev polynomials* are defined for $k \in \mathbb{N}$ as

$$T_k(x) = \cos(k \arccos(x)) \qquad x \in [-1, 1]. \tag{1.25}$$

They satisfy the usual three-term recursion relation

$$T_{k+1}(x) = 2xT_k(x) - T_{k-1}(x), \qquad k \geq 1, \tag{1.26}$$

beginning with $T_0(x) = 1$ and $T_1(x) = x$ and we can see that T_k is a polynomial of degree k with roots $x_j = \cos((2j-1)\pi/(2k)), 1 \leq j \leq k$. The polynomials T_k are orthogonal on their domain w.r.t. the weight $w = 1/\sqrt{1-x^2}$. As a family of orthogonal polynomials, they form a basis on $L^2_w([-1,1])$ and we can expand $f \in L^2_w([-1,1])$ as

$$f(x) = \sum_{k=0}^{\infty} c_k T_k(x), \qquad c_k = \frac{1}{\chi_k} \int_{-1}^{1} f(y) T_k(y) \frac{dy}{\sqrt{1-y^2}},$$

with a normalization factor $\chi_k = \int_{-1}^{1} T_k(y)^2/\sqrt{1-y^2}dy$, which gives $\chi_0 = \pi$ and $\chi_k = \pi/2$ for $k > 0$. To evaluate the exponential $f(A) \equiv \exp(A)$ of a matrix A, the matrix has to be scaled by a linear transformation t such that its numerical range lies within the interval $[-1, 1]$, analogously to the scalar case, where the interpolation of a function $f : [a, b] \to \mathbb{R}$ is equivalent to interpolating $f(t(x))$, where $t : [-1, 1] \to [a, b]$, $t(x) = \frac{a+b}{2} + \frac{b-a}{2}x$. Then, one simply computes the (scalar) integrals of the scaled function $f(t(x))$ to obtain the expansion coefficients c_k and finally evaluates the truncated Chebyshev expansion at $t = \frac{a+b-2x}{a-b}$ which is efficiently done by the Clenshaw-algorithm and requires only n matrix-vector products for a n-term expansion, i.e., when setting $c_k = 0$ for $k > n$.

Notice that the coefficients c_k have to be computed only once and the action of (a polynomial in) the Hamiltonian H on a vector v can be computed as $Hv = Tv + Vv$ which, depending on the spatial discretization, is usually cheap: In combination with spectral methods for the Laplacian in T, a matrix-vector multiplication Hv corresponds to the cost of one FFT.

In [91], an error bound for a Hermitian matrix H with eigenvalues within $[-\rho, \rho]$, where $\rho = \rho(H)$ is the spectral radius, is given by

$$\|P_{m-1}(hH)v - e^{-ihH}v\| \leq 4 \left(e^{1-(h\rho/(2m))^2} \left(\frac{h\rho}{2m} \right) \right)^m, \tag{1.27}$$

for the Chebyshev interpolation polynomial of degree $m-1$

$$P_{m-1}(hH) = d_0(h\rho) + 2 \sum_{k=1}^{m-1} d_k(h\rho) T_k\left(H/\rho\right),$$

where the expansion coefficients are proportional to Bessel-functions of the first kind J_k,

$$d_k(h) = (-i)^k J_k(h).$$

The truncation index m has to be chosen such that $m > h\rho$ to reach accuracy. Taking into account that the eigenvalues of $H = T + V$ can be bounded by

$$\rho \in \left[\min_{x \in X} V(x),\ \max_{x \in X} V(x) + \frac{\pi^2}{2\Delta x^2} \right], \tag{1.28}$$

and assuming a finite (discrete) domain X, the dominant term originates from the largest eigenvalue of the Laplacian and eventually leads to the step-size restriction

$$\left(\frac{h\rho}{2m} \right) < 1 \Longrightarrow h < cm\Delta x^2,$$

as $\Delta x \to 0$ for some constant $c > 0$.

1.3.2 Lanczos method

The computation of the exponential of a matrix A is trivial when the matrix is diagonal, and thus the first technique that is taught to students is the diagonalization. In practical applications, a full diagonalization is very costly and thus avoided when possible. Fortunately, in the context of solving linear ODEs, we are only interested in the action of the exponential on a given vector (initial condition) and the underlying idea gives way to a highly efficient scheme which only uses matrix-vector multiplications, a consideration that has already been exploited in the exposition of the Chebyshev interpolation above. A more detailed general treatment of the Lanczos method with original references can be found in [59], and our presentation is borrowed from [91]. The crucial idea for the computation of $e^A v$ is to reduce the dimension of the matrix by introducing *Krylov subspaces*,

$$\mathscr{K}_r(A, v) = \operatorname{span}\{v, Av, A^2 v, \dots, A^{r-1} v\}$$

the linear span of powers of A multiplied by a vector. The aim is now to recursively construct an orthonormal basis of this space and use it to obtain a "partial diagonalization" of A, namely the components that belong to the subspace $\mathscr{K}_r(A, v)$. In the following, we restrict ourselves to Hermitian matrices and present the method that is known as *Lanczos*-iteration. We construct basis vectors of $\mathscr{K}_r(A, v)$ via Gram-Schmidt-orthogonalization, starting from a given initial vector $v_1 = v/\|v\|$, yielding

$$\tau_{k+1,k}\, v_{k+1} = A v_k - \sum_{j=1}^{k} \tau_{j,k} v_j, \tag{1.29}$$

with the expansion coefficients $\tau_{j,k} = v_j^\dagger A v_k$, $j \leq k$, and $\tau_{k+1,k} > 0$ is chosen to normalize v_{k+1}. First, the Krylov dimension is increased by computing Av_k, then orthogonality is achieved by subtracting the orthogonal projections and finally, $\tau_{k+1,k}$ is defined to normalize the new *Lanczos vector* v_{k+1}. If the right hand side vanishes, the Krylov space has become an A-invariant subspace and the iteration terminates.

The algorithm provides us after r steps with a $N \times r$ matrix of orthonormal Lanczos vectors $V_r = (v_1, \dots, v_r)$ and a $r \times r$ coefficient matrix $T_r = (\tau_{k,j})$, where we have set $\tau_{k,j} = 0$ for $j - k > 1$ to rewrite (1.29) in matrix form

$$A V_r = V_r T_r + \tau_{r+1,r} v_{r+1} e_r^T, \tag{1.30}$$

with the rth unit vector $e_r^T = (0, \dots, 0, 1)$. Multiplying (1.30) from the left with the Hermitian conjugate $V_r^\dagger$, and using the orthonormality of the v_k, we get

$$V_r^\dagger A V_r = T_r. \tag{1.31}$$

From (1.31), we deduce that T_r is Hermitian and combined with $\tau_{k+|j|+1,k} = 0$, it follows that T_r is tridiagonal of dimension $r \times r$. The exponential of the (Hermitian) Hamiltonian H can now be approximated by interpreting it as the solution of the initial value problem $i\dot{y}(t) = Hy(t)$, $y(0) = v_1$ at $t = h$ and this will be approximated on the rth Krylov subspace: Using the ansatz for the solution $y_r(t) = \sum_{k=1}^r c_k(t) v_k$, we obtain

$$i\dot{y}_r(t) \equiv i \sum_{k=1}^r \dot{c}_k(t) v_k = H \sum_{k=1}^r c_k(t) v_k, \quad y_r(0) \in \mathbb{C}^N.$$

After multiplication from the left with $v_j^\dagger$, we get

$$i\dot{c}_k(t) = \sum_{j=1}^r \tau_{j,k} c_k(t), \qquad c_1(0) = 1,\, c_l(0) = 0 \quad \forall l > 1, \tag{1.32}$$

or, in matrix form $\dot{c}(t) = T_r c(t)$, with $c(t) = (c_1(t), \dots, c_r(t))$, which is easily exponentiated. An approximation to the solution in the rth Krylov subspace is thus given by the exponential of a small tridiagonal matrix, $r \ll N$, as

$$\exp(-ihH) \approx V_r \exp(-ihT_r) e_1,$$

and unitarity of the exponential is preserved since T_r inherits Hermiticity from H. In a refinement of the results by *Hochbruck & Lubich* [71], cf. Ref. [91], the error committed by the restriction to (Lanczos-)polynomials of degree $< r$ can be bounded by[8]

$$\|e^{-ihH} v - V_r \exp(-ihT_r) e_1\| \le 8 e^{-(h\rho)^2/(4r)} \left(\frac{eh\rho}{2r}\right)^r, \quad \text{for } r \ge h\rho, \tag{1.33}$$

where $\rho = \rho(H)$ is the spectral radius of H, a result similar to Chebyshev interpolation, cf. (1.27). As for the Chebyshev method, a step-size restriction $h < c\Delta x^2 r$ for some constant c can be deduced from (1.28). Assuming exact arithmetics, the procedure (1.29) is cast in algorithmic form in Table 1.1. Round-off errors lead to numerical instability but the cure – re-orthogonalization (cf. [59]) – lies beyond the scope of this introduction.

1.3.3 Splitting methods

Let us consider the separable system of ODEs

$$u' = A(u) + B(u), \qquad u(t_0) = u_0 \in \mathbb{C}^N, \tag{1.34}$$

where we assume that both systems

$$u' = A(u), \qquad u' = B(u) \tag{1.35}$$

[8] For simplicity, we have relaxed the specifications of the theorem by requiring that all eigenvalues of H lie in $[-\rho, \rho]$ which is satisfied by definition.

The Lanczos algorithm

$v_1 := v/\|v\|_2,\ \tau_{1,0} := 0;$
for $j = 1, \dots, r-1$ **do**
$u := Av_j,$
$\tau_{j,j} := v_j^\dagger u,$
$u := u - \tau_{j,j} v_j - \tau_{j,j-1} v_{j-1},$
$\tau_{j+1,j} := \|u\|_2\ (= \tau_{j,j+1}),$
$v_{j+1} := u/\tau_{j+1,j}$
end for
$u := Av_r,\ \tau_{r,r} := v_r^\dagger u,$

Table 1.1: Given a vector v and a Hermitian matrix $A \in \mathbb{C}^{N\times N}$ and an integer $1 \le r \le N$, the algorithm computes a basis of the r-dimensional Krylov subspace $\mathscr{K}_r(A, v)$, in particular the Hermitian coefficient matrix $T_r = (\tau_{j,k})$ and the associated orthonormal Lanczos vectors v_j.

can either be solved in closed form or accurately integrated.

If $\varphi_t^{[A]}$, $\varphi_t^{[B]}$ represent the exact flows associated to (1.35), the solution can be advanced by one time step h by composing the individual flow maps

$$\Phi_h^{[1]} = \varphi_h^{[A]} \circ \varphi_h^{[B]}, \tag{1.36}$$

which gives a first order approximation to the exact flow $\varphi_h^{[A+B]}$, i.e.,

$$\|u(t_0 + h) - \Phi_h^{[1]}(u_0)\| = \mathscr{O}\left(h^2\right).$$

This composition is known as the *Lie-Trotter* method. Sequential application of the two first-order methods $\Phi_h^{[1]}$ and its adjoint $\Phi_h^{[1]\dagger} = \varphi_h^{[B]} \circ \varphi_h^{[A]}$ with half time step yields the well-known *Strang-splitting*[9], second order time-symmetric methods of the form

$$\Phi_{h,A}^{[2]} = \varphi_{h/2}^{[A]} \circ \varphi_h^{[B]} \circ \varphi_{h/2}^{[A]} \tag{1.37}$$
$$\Phi_{h,B}^{[2]} = \varphi_{h/2}^{[B]} \circ \varphi_h^{[A]} \circ \varphi_{h/2}^{[B]} \tag{1.38}$$

(referred as *ABA* and *BAB* compositions). The contraction via the (1-parameter-) group property of the flows that eliminated one computation is called *First Same As Last* (FSAL) property and can also be used with pth-order $m-$*stage* compositions

$$\Phi_h^{[p]} = \varphi_{a_m h}^{[A]} \circ \varphi_{b_m h}^{[B]} \circ \dots \circ \varphi_{a_1 h}^{[A]} \circ \varphi_{b_1 h}^{[B]} \tag{1.39}$$

if $a_m = 0$ or $b_1 = 0$ and for the repeated application of the scheme without requiring output, e.g.,

$$\left(\Phi_{h,A}^{[2]}\right)^n = \varphi_{h/2}^{[A]} \circ \left(\varphi_h^{[B]} \circ \varphi_h^{[A]}\right)^{n-1} \circ \varphi_h^{[B]} \circ \varphi_{h/2}^{[A]}.$$

[9] In the literature, this method sometimes goes with the name *leapfrog*.

If both flows preserve certain geometric properties, such as symplecticity, unitarity, energy, just to mention a few, so will their composition (1.39). For this reason, splitting methods belong to the class of *geometric integrators*.

From here on, we switch to the exponential notation for the exact flows which is standard for linear vector fields and the generalization by Lie-derivatives has been given in the introduction. In this notation, the equation $i\dot{u} = A(u) + B(u)$, whose formal solution for the evolution operator is denoted by $\phi_t^{[A+B]} = e^{-it(A+B)}$, is approximated for one time step, h, by the order p composition (1.39) or, equivalently,

$$\Phi_h^{[p]} \equiv e^{-ihb_1 B} e^{-iha_1 A} \cdots e^{-ihb_m B} e^{-iha_m A}, \tag{1.40}$$

where the order in the composition has been reversed, compared to (1.39), due to the Vertauschungssatz (1.24). We keep in mind that, in a nonlinear problem, if B depends on u, it has to be updated at each stage because u changes during the evolution of $e^{-iha_j A}$.

There exist many different splitting methods which are designed for different purposes, depending on the structure of the problem, the desired order, the required stability, etc. [22, 29, 65, 94, 95, 131, 119].

For the Schrödinger equation, the natural split ($A = T$, $B = V$) is due to the simplicity of Fourier spectral methods: After spatial discretization, the exponential of the kinetic energy operator T is reduced to the exponentials of a diagonal matrix if we encase it in Fourier transforms,

$$e^{-ihT}\phi(x) = \mathscr{F}^{-1}\mathscr{F}e^{-ihT}\phi(x) = \mathscr{F}^{-1}e^{-ih\frac{-(-ik)^2}{2m}}\hat{\phi}(k) = \mathscr{F}^{-1}e^{-ih\frac{k^2}{2m}}\mathscr{F}\phi(x).$$

For the ease of notation, we have dropped the subscripts that indicated trigonometric interpolation, $\phi = \phi_N$, etc. Notice that the exponentials in $e^{-ia_j hT}$ need to be computed only once and can be reused at each step.

We now analyze how to compute the evolution of different parts of the Hamiltonian by spectral methods.

Under the assumption that the potential and its first four derivatives, are bounded, *Jahnke & Lubich* [81] proved that the error of the Strang splitting does not lead to a step size restriction as for Chebyshev or Lanczos methods. Instead, the accuracy depends virtually only on the spatial regularity of the wave function,

$$\|e^{-ihV/2}e^{-ihT}e^{-ihV/2}\phi - e^{-ih(T+V)}\phi\| \le ch^3\langle\phi|(T+\mathbf{I})^2\phi\rangle^{1/2},$$

where $\mathbf{I}$ is the identity operator and the constant is independent of the discretization parameter Δx and the notation has been adapted from [91]. Furthermore, both operators T, V are Hermitian and splitting methods thus conserve the norm of the wave function ϕ. Due to the exact time-integration through the exponential, they also inherit the *gauge-invariance* of the exact solution, i.e., a shift of origin in the energy $H \to H + c$ by some constant will only manifest in a constant global phase of the wave function and thus not alter quadratic observables.

Time dependence

Splitting methods allow for an elegant generalization to non-autonomous separable equations. The fundamental principal is straightforward: re-write the time-dependent equations as an augmented autonomous system, i.e.,

$$\dot{y}(t) = A(y,t), \quad y(0) = y_0 \Longleftrightarrow \frac{d}{dt}\begin{pmatrix} y \\ t_1 \end{pmatrix} = \begin{pmatrix} A(y,t_1) \\ 1 \end{pmatrix}, \quad (y(0), t_1(0)) = (y_0, 0). \tag{1.41}$$

The system is split as

$$\frac{d}{dt}\begin{pmatrix} y \\ t_1 \end{pmatrix} = \begin{pmatrix} A(y,t_1) \\ 0 \end{pmatrix}, \quad \frac{d}{dt}\begin{pmatrix} y \\ t_1 \end{pmatrix} = \begin{pmatrix} 0 \\ 1 \end{pmatrix}.$$

The Strang split (1.38) results in an exponential midpoint rule $\Phi^{[2]}_{h,B} = e^{-hA(y,h/2)}$, which corresponds to freezing the time coordinate at the middle of time integration. An order-three method requires the composition of two exponentials

$$\Phi^{[A]}_h = e^{a_1 hA(y,b_1 h)} e^{a_2 hA(y,b_2 h)},$$

where the coefficients have to be complex and are given by $a_1 = 1/2 - i/(2\sqrt{3}), a_2 = \bar{a_1}$ and $b_1 = 1/4 - i/(4\sqrt{3}), b_2 = b_1 + 1/2$, or alternatively, by the complex conjugate of these values. At this stage, we have silently introduced two subjects which deserve further attention: Firstly, we have derived a method of admittedly little practical relevance, and secondly we assume that the flow can be evaluated at complex times $b_i h$. The first issue leads us to the discussion of order conditions for splitting methods and the latter arises naturally once the order conditions are presented.

Order conditions

The principal tool in the analysis of order conditions is provided by the Baker-Campbell-Hausdorff (BCH) formula

$$\begin{aligned} e^{hA}e^{hB} = e^{\mathrm{BCH}(hA,hB)} = \exp\Big(h(A+B) + \frac{h^2}{2}[A,B] + \frac{h^3}{12}([A,[A,B]] - [B,[A,B]]) \\ - \frac{h^4}{24}[B,[A,[A,B]]] + \mathcal{O}\big(h^5\big)\Big). \end{aligned} \tag{1.42}$$

In Section 1.3.4, a recursion formula (1.63) to compute the expansion to arbitrary order is stated in the context of the Magnus expansion.

From a formal perspective, given some Lie-group G and its associated Lie algebra $\mathfrak{g}$, which is the tangent space TG_1 of G at the identity, the exponential is a map $\exp : \mathfrak{g} \to G$, that satisfies the linear homogeneous differential equation $y'(t) = ay(t)$, $y(0) \in G$ for $a \in \mathfrak{g}$ at $t = 1$, i.e., $y(1) = \exp(a)y(0)$. In other words, the BCH formula answers the question which equation is exactly solved when two exponentials are composed by a (formal) series in the time variable t. Convergence for linear operators is achieved for small t but we refer to standard algebra textbooks, e.g. [126] for precise results. These comments give meaning to

the brackets in (1.42), which are identified as the Lie brackets $[A, B] = AB - BA$, that give structure to the Lie-algebra $\mathfrak{g}$. As an example, the bracket - or *commutator* - of the Lie algebra of vector fields is given as $[X, Y](f) = X(Y(f)) - Y(X(f))$, or, in local coordinates,

$$\left[\sum_i f_i(x)\partial_{x_i}, \sum_j g_j(x)\partial_{x_j}\right] = \sum_i \left(\sum_j \left(f_j \partial_{x_j} g_i - g_j \partial_{x_j} f_i\right)\right)\partial_{x_i},$$

which is again a (linear) vector field.

Dynkin [52] derived an explicit formula for the exponent,

$$\log(e^A e^B) = \sum_{k=1}^{\infty} \frac{(-1)^{k-1}}{k} \sum_{\substack{q_i, p_i \in \mathbb{N}^+ \\ p_i + q_i = k}} \frac{(-1)}{\sum_{i=1}^{k}(p_i + q_i)} \frac{[A^{p_1} B^{q_1} \cdots A^{p_k} B^{q_k}]}{p_1!\, q_1! \cdots p_k!\, q_k!}, \tag{1.43}$$

where the shorthand notation $[A^{p_1} B^{q_1} \cdots A^{p_k} B^{q_k}]$ stands for the right nested commutator which is derived by adding a bracket after each letter beginning from the left, e.g., $[A^2BA] = [A, [A, [B, A]]]$. Additional complications arise because of the linear dependence of certain brackets which is due to the *Jacobi identity*,

$$[A, [B, C]] + [C, [A, B]] + [B, [C, A]] = 0$$

and the antisymmetry condition $[A, B] = -[B, A]$ which hold by definition for any Lie-bracket. Calculations in Lie algebras can thus be substantially simplified by working in a suitable basis. A first example is a Dynkin type basis where we remove linearly dependent commutators of same length (keeping, for example, $[A, B]$ and discarding $[B, A]$). Although it is claimed that a systematic construction of such a basis is possible [42], to the best of our knowledge there exists no practicable algorithm to expand a given element in that basis.

On Hall bases The so-called *Hall* basis on the other hand is well equipped with procedures to compute such expansions and the commutation of basis elements, the way to generate new elements, is the basic building block in the definition of the basis. For completeness, we repeat the definition from [111] of a Hall basis $\mathscr{H}$ of a free Lie-algebra $\mathfrak{g}$ generated by an alphabet $\mathscr{A}$ of letters via commutation $[\cdot, \cdot]$.

(I) $\mathscr{H}$ has a total order $\leq$,

(II) $\mathscr{A} \subset \mathscr{H}$,

(IIIa) (Recursive generation of the basis and the ordering) For any commutator $h = [h', h'']$ in $\mathscr{H} \setminus \mathscr{A}$, it holds that $h'' \in \mathscr{H}$ and

$$h < h''.$$

(IIIb) (Recursive gen. contd.) For any commutator $h = [h', h'']$ in $\mathfrak{g} \setminus \mathscr{A}$, it holds that $h \in \mathscr{H}$ if and only if

$$h', h'' \in \mathscr{H} \quad \text{and} \quad h' < h'',$$

and

$$\text{either } h' \in \mathscr{A}, \quad \text{or} \quad h' = [x, y] \text{ and } y \geq h''.$$

These instructions are easy to cast in a constructive form: (I) Impose an (arbitrary) total order on the letters of the alphabet, here, for simplicity, we have chosen the lexicographical one $\mathscr{A} = \{A, B\}$, $A < B$. Extend it to elements of a Hall-base by (uniquely) mapping[10] each element to a *word* which is done by removing all the brackets, e.g., $[[A, [A, B]], A] \to AABA$. Now, the lexicographical ordering on the words, inherited by the ordering of the alphabet, gives an order on words of the same length, where the length $\mathrm{len} : \mathfrak{g} \to \mathbb{N}$ is defined to be the number of letters a given element contains. For two commutators $w, w' \in \mathscr{H}$, we say $w < w'$ if $\mathrm{len}(w) < \mathrm{len}(w')$. (II) Start the iteration from the set $\tilde{\mathscr{H}} = \mathscr{A}$. (III) Grow the set $\tilde{\mathscr{H}}$ by forming commutators of the elements already in $\tilde{\mathscr{H}}$ and include them in $\tilde{\mathscr{H}}$ when they obey (IIIa) or (IIIb), conditions can be easily verified using the order given by (I).

Such a basis was used by *Casas & Murua* [39] to derive an efficient algorithm to explicitly compute the terms of the BCH formula.

Given a basis and the means of computing the BCH formula, order conditions can be derived for a given splitting/composition method of type (1.39), and several papers [101, 21] have studied the combinatorial structure of the BCH terms to derive formulas for order conditions. Keeping in mind (1.42), we introduce a *grading* on the algebra for which we re-use the length map len from before. The only order condition which we single out is the *consistency*, which assures that, as $h \to 0$, the numerical integrator becomes the exact solution, and which corresponds to satisfying the equations up to $\mathcal{O}\left(h^2\right)$, or

$$\begin{aligned}\log(\Phi_h^{[p]}) &= h\sum_{j=1}^{m} a_j A + h\sum_{j=1}^{m} b_j B + \mathcal{O}\left(h^2\right)\\ &\stackrel{!}{=} h(A+B).\end{aligned}$$

Therefore, the consistency condition is simply $\sum a_j = \sum b_j = 1$.

With the tools presented so far, we can derive higher order composition methods which we will illustrate at the example of the famous *triple-jump* by Yoshida [131]. Given a *symmetric* method $\Phi_h^{[2]}$ of order two, say (1.38), along the lines of (1.42), we can express it formally as a series

$$\Phi_h^{[2]} = \exp\left(hX + h^3 X_3 + \mathcal{O}\left(h^5\right)\right),$$

for the equation $\dot{y}(t) = Xy(t) \equiv (A+B)y(t)$, and X_3 subsumes the commutators of length three. Even powers of h do not appear in the expansion because of the symmetry, $\Phi_{-h}^{[2]} = \left(\Phi_h^{[2]}\right)^{-1}$, a property, which is beautifully explained in [65]. This implies a significant reduction of order conditions and because of good long-term integration properties, usually symmetric splittings are sought for. Symmetrically composing

$$\Phi_h^{[4]} \equiv \Phi_{\gamma h}^{[2]} \circ \Phi_{(1-2\gamma)h}^{[2]} \circ \Phi_{\gamma h}^{[2]}, \tag{1.44}$$

we obtain[11]

$$\Phi_h^{[4]} = \exp\left(hX + h^3(2\gamma^3 + (1-2\gamma)^3)X_3 + \mathcal{O}\left(h^5\right)\right),$$

[10] The uniqueness is guaranteed by the definition of the Hall-base, cf. [111].

[11] Note that consistency is already satisfied by the choice of the coefficients.

and hence a polynomial condition $0 = (2\gamma^3 + (1-2\gamma)^3)$ to reach order four. Among the three solutions $\gamma_k = 1/(2 - 2^{1/3}e^{2\pi ik/3})$, only one is real-valued, $\gamma_0 \approx 1.351$. For complex valued solutions, the numerical values are $\gamma_1 \approx 0.324 + i0.135$ and $\gamma_2 = \bar{\gamma}_1$. From the size of the (real) coefficients, it becomes clear why this scheme has been referred to as triple-jump: The initial vector is first propagated by a large time-step $\gamma_1 > 1$, only to be again pulled back by $(1-2\gamma_1)$, continued by a push to $t = h$. The large effective step sizes γh and $(1-2\gamma)$ lead to large error constants and reduce the stability of the method, nevertheless, the order has been increased from two to four. This procedure has been repeated at arbitrary order in a landmark paper by Yoshida [131] for which it bares his name.

In the preceding subsection, we have already encountered complex time steps, which have already been found and discarded by Yoshida. Assuming everything is well defined for complex time-steps, for a real problem one usually has to face the quadruple cost due to complex arithmetic which has an immense impact on the efficiency of such compositions. However, looking at the real part of $\gamma_{1,2}$, we notice that the time advances only in small steps in the positive direction, taking a detour through the complex plane.

For parabolic problems, for example the imaginary-time Schrödinger equation, the negative time-steps of γ_0 lead to unstable and therefore useless algorithms. The reason for this behavior is that the flow only forms a semi-group and backward integration corresponds to an ill-posed problem. Unfortunately, negative real coefficients - at least one a_i and one b_j - are found for all splitting methods of order higher than two, a result due to [118, 120, 58] and a simple proof can be found in [17]. This restriction is referred to as *order-barrier* for splitting methods. This casts complex coefficients in a different light, especially since the results of *Hansen & Ostermann* [66] and *Castella et al.* [40], who proved that, under certain conditions, the complex flows stay well-defined. Explorations of splitting methods for parabolic equations were performed in [40, 20], where it is assumed that the coefficient multiplying the parabolic operator has positive real part.

For a specific vector field, the commutator algebra has additional structure and most problems that are treated in the following chapters share a particularly useful property which we describe in the following. Recall, that $A = T, B = V$ for the Schrödinger equation and it is possible to compute the commutators explicitly to

$$\begin{aligned} 2[T,V] &= [-\partial_x^2, V(x)] = -\partial_x^2 V(x) + V(x)\partial_x^2 = -V''(x) - 2V'(x)\partial_x, \\ [V,[T,V]] &= (V'(x))^2 . \end{aligned} \tag{1.45}$$

Observe that the second commutator $[V,[T,V]]$ is local, i.e., it only depends on the spatial coordinate x. Hence further commutation with local operators, e.g., V, will make it disappear, $[V,[V,[T,V]]] \equiv 0$. This property is generally exploited in the following since it leads to enormous simplifications in the algebra and further details are provided in Chapter 4. The commutator identity $[V,[V,[T,V]]] \equiv 0$ has also been associated with the names of *Runge-Kutta-Nyström* (RKN) who designed methods for second order ordinary differential equations $\ddot{y} = f(y)$. Augmenting the system by a change of variables $q = y, p = \dot{y}$ yields

$$\frac{d}{dt}\begin{pmatrix} q \\ p \end{pmatrix} = \begin{pmatrix} p \\ f(q) \end{pmatrix}$$

which is equivalent to a classical Hamiltonian system when $H = T + V(q)$, where the kinetic energy is $T = \frac{1}{2}p^2$ and the potential V satisfies $f(q) = -\nabla V(q)$. This Hamiltonian is *quadratic* in the momentum p and the commutators satisfy the relation $\{V, \{V, \{T, V\}\}\} = 0$ for the usual Poisson-bracket $\{\cdot\,, \cdot\}$.

We conclude the introduction on splitting methods by a general treatment of non-autonomous separable systems, which will be combined with an asymmetry in the Lie algebra that in turn motivates the concept of a modified error. First, the system (1.41) is generalized to the separable equation

$$\dot{u} = A(t)u + \epsilon B(t)u, \tag{1.46}$$

which is chosen linear to simplify the notation. Note that we have introduced a small parameter $\epsilon \ll 1$, which makes the two parts, A and $\tilde{B} \equiv \epsilon B$ qualitatively different and is responsible for the asymmetry in the algebra. By asymmetry, we mean an additional structure that implies that the terms[12] $[\tilde{B}, [A, \tilde{B}]] \propto \epsilon^2$ and $[A, [A, \tilde{B}]] \propto \epsilon$ should be treated differently by a numerical method because of their relative sizes. In the context of splitting methods, where one usually assumes that the parts are exactly integrable, a perturbed system like (1.46) is called to as *near-integrable*.

This property has been exploited to design highly efficient splitting methods in Ref. [94], where the terminology below has been introduced.

Excursus: a modified error concept Let Φ_h be a one-step method to approximate the flow φ_h of (1.46) at time h. It is then clear that the error expansion for a consistent method Φ_h can be asymptotically expressed as

$$\Phi_h - \varphi_h = \sum_{j\geq 1} \sum_{k \geq s_j} e_{j,k}\, \epsilon^j h^{k+1} \qquad \text{as } (h, \epsilon) \to (0, 0),$$

where the s_j start from the first non-vanishing error coefficient $e_{s_j,k}$. We say that Φ_h is of *generalized order* $(s_1, s_2, \ldots, s_m)$ (where $s_1 \geq s_2 \geq \cdots \geq s_m$) if the local error satisfies that

$$\Phi_h - \varphi_h = \mathcal{O}(\epsilon h^{s_1+1} + \epsilon^2 h^{s_2+1} + \cdots + \epsilon^m h^{s_m+1}). \tag{1.47}$$

Thus, for a method of generalized order $(8, 2)$, denoted by $\Phi_h^{(8,2)}$, the error reads

$$\Phi_h^{(8,2)} - \varphi_h = e_{1,8}\epsilon h^9 + e_{2,2}\epsilon^2 h^3 + \mathcal{O}\left(\epsilon^2 h^4 + \epsilon^3 h^3\right).$$

For splitting methods, this means that a good choice of coefficients a_j, b_k will zero the polynomials multiplying the dominant commutators $\epsilon\,[A, B]$, $\epsilon\,[A, [A, B]]$, etc. and possibly ignore terms that are already small due to high powers in the small parameter. Thereby, the number of order conditions is reduced and good accuracy can be reached at a smaller number of stages. Throughout the later chapters, we will encounter a multitude of coefficient sets that lead to splitting methods of higher generalized order.

Parting from a non-autonomous system with near-integrable structure (1.46) it is paramount to treat the time-coordinate appropriately in order to preserve the generalized order for splitting

[12] For commutators of different length, similar considerations have to be taken into account.

methods and to yield smaller error coefficients. In continuation, we answer the question of how to properly apply splittings for this kind of equations.

The system (1.46) can be solved by considering the time as two new independent coordinates

$$\frac{d}{dt}\begin{pmatrix} u \\ t_1 \\ t_2 \end{pmatrix} = \underbrace{\begin{pmatrix} A(t_2)u \\ 1 \\ 0 \end{pmatrix}}_{=:f^{[A]}(u,t_1,t_2)^T}, \qquad \frac{d}{dt}\begin{pmatrix} u \\ t_1 \\ t_2 \end{pmatrix} = \underbrace{\begin{pmatrix} \epsilon B(t_1)u \\ 0 \\ 1 \end{pmatrix}}_{=:f^{[B]}(u,t_1,t_2)^T} \tag{1.48}$$

For this choice of the splitting, the time is frozen in each instance of system and the symmetric second order splitting (1.38) yields

$$\varphi^{[A+B]}_{t_n,t_n+h} = e^{\frac{h}{2}\epsilon B(t_n+h)} e^{hA(t_n+\frac{h}{2})} e^{\frac{h}{2}\epsilon B(t_n)} + \mathcal{O}(h^3), \tag{1.49}$$

where $\varphi^{[A+B]}_{t_n,t_n+h}$ denotes the exact flow from t_n to $t_n + h$. It has been pointed out in [28], that for the split (1.48), the proportionality of the errors to powers of the small parameter ϵ is lost and we prove this observation by a straightforward calculation:

The previously linear time-dependent ODE (1.46) has become an autonomous non-linear system (1.48) with associated Lie-operators

$$\mathscr{L}_{f^{[A]}} = A(t_2)u\frac{\partial}{\partial u} + \frac{\partial}{\partial t_1}, \qquad \mathscr{L}_{f^{[B]}} = B(t_1)u\frac{\partial}{\partial u} + \frac{\partial}{\partial t_2}.$$

Their commutator is readily computed by

$$[\mathscr{L}_{f^{[A]}}, \mathscr{L}_{f^{[B]}}] = \sum_{i=1}^{3}\left(\sum_{j=1}^{3}\left(\frac{\partial f_i^{[B]}}{\partial y_j} f_j^{[A]} - \frac{\partial f_i^{[A]}}{\partial y_j} f_j^{[B]}\right)\right)\frac{\partial}{\partial y_i} \tag{1.50}$$

$$= \left(\epsilon[B(t_1), A(t_2)]u + \epsilon\frac{\partial B(t_1)u}{\partial t_1} - \frac{\partial A(t_2)u}{\partial t_2}\right)\frac{\partial}{\partial u}, \tag{1.51}$$

where $(y_1, y_2, y_3) = (u, t_1, t_2)$. In contrast to the original equation, the proportionality of the error term at first order to the small parameter ϵ is lost. This generalizes to commutators at higher order and it is evident that the algebraic structure of the original problem, generated by $A(t)$ and $B(t)$ is completely lost.

On the upside, near-integrability is recovered if we take the time as new variable as follows[13]

$$\frac{d}{dt}\begin{pmatrix} u \\ t_1 \\ t_2 \end{pmatrix} = \begin{pmatrix} A(t_2)u \\ 1 \\ 1 \end{pmatrix}, \qquad \frac{d}{dt}\begin{pmatrix} u \\ t_1 \\ t_2 \end{pmatrix} = \begin{pmatrix} \epsilon B(t_2)u \\ 0 \\ 0 \end{pmatrix}, \tag{1.52}$$

and Strang's splitting then reads

$$\varphi^{[A+B]}_{t_n,t_n+h} = e^{\frac{h}{2}\epsilon B(t_n+h)} \circ \varphi^{[A]}_{t_n,t_n+h} \circ e^{\frac{h}{2}\epsilon B(t_n)} + \mathcal{O}(\epsilon h^3). \tag{1.53}$$

In Table 1.2, the application of this split has been detailed for a general composition. The

[13] Notice that the two equations for t_1, t_2 could be collapsed into a single one.

Splitting algorithm for non-autonomous systems

$t^{[0]} := t_n$
for $i = 1, \dots, m$ **do**
  solve : $\dot{u} = B(u, t^{[i-1]}), \quad t \in [t^{[i-1]}, t^{[i-1]} + b_i h]$
  solve : $\dot{u} = A(u, t), \quad t \in [t^{[i-1]}, t^{[i-1]} + a_i h]$
  $t^{[i]} := t^{[i-1]} + a_i h$
end for
$t_{n+1} := t^{[m]}$

Table 1.2: Algorithm for the numerical integration from t_n to $t_n + h$ of the system (1.52) by the m-stage composition (1.39).

commutator of the associated Lie-operators is now

$$[\mathscr{L}_{f^{[A]}}, \mathscr{L}_{f^{[B]}}] = \epsilon \left([B(t_2), A(t_1)]u + \frac{\partial B(t_2)u}{\partial t_2} \right) \frac{\partial}{\partial u}, \tag{1.54}$$

which coincides with (1.51) except for the last term. In consequence the error is a factor ϵ more accurate and considerably larger time-steps can be used. Furthermore, additional structure can be recovered: Suppose that A, B satisfy the RKN property $[B, [B, [A, B]]] = 0$ and $[B(t), B(t')] = 0$ for all times t, t', then it is clear from (1.54) that the split (1.52) is able to preserve this property, i.e.,

$$[\mathscr{L}_{f^{[B]}}, [\mathscr{L}_{f^{[B]}}, [\mathscr{L}_{f^{[A]}}, \mathscr{L}_{f^{[B]}}]]] = 0.$$

The first split with commutator (1.51) on the contrary also looses this beneficial structure.

This result was proved in [28] for separable Hamiltonian systems. However, as can be concluded from the computations, it is also valid for non-autonomous separable operators in PDEs.

Recently, these considerations have been applied to higher order splitting methods for parabolic non-autonomous equations [117], where the time coordinate is advanced in real space and complex coefficients with positive real part are used in the frozen part to overcome the second-order barrier.

Similar considerations apply to other perturbed problems: Suppose the vector field can be separated in three parts, $f = f_1 + f_2 + \epsilon f_3$. Then, the near-integrable structure that has led to error coefficients proportional to ϵ is only conserved if the split is applied as $(f_1 + f_2) + \epsilon f_3$, whereas the alternatives $f_1 + (f_2 + \epsilon f_3)$ or $f_2 + (f_1 + \epsilon f_3)$ loose this desirable property.

1.3.4 Magnus expansion

Motivated by the findings for non-autonomous systems, where we have elaborated that the proper use of splittings only freezes the time-coordinate in one part of the flow, the solution of the remaining time-dependent part is addressed in this section. The detailed and comprehensive survey on the Magnus expansion [93] by *Blanes et al.* [23] forms the basis of this review. We begin with a linear differential equation formulated in a Lie group,

$$\dot{y} = a(t)y \quad a : \mathbb{R}^+ \to \mathfrak{g}, \quad y(0) = y_0 \in \mathcal{G} \tag{1.55}$$

and remark that a naïve approach to solve this equation $y(t) = \exp(\int_0^t a(\xi)\mathrm{d}\xi)y_0$ will, in general, not produce the solution if the operators $a(t)$ at different times do not commute, i.e., $[a(t_1), a(t_2)] \neq 0$. However, by introducing correction terms in the Lie algebra, e.g.,

$$y(t) = \exp\left(\int_0^t a(\xi)\mathrm{d}\xi + \Delta(t)\right) y_0, \quad \Delta(t) \in \mathfrak{g},$$

the solution can be written in exponential form. With the aim of expressing the flow as $\exp(\Theta(t))$, from simple differentiation,

$$\frac{d}{dt}\exp(\Theta(t)) = \mathrm{dexp}_{\Theta(t)}(\dot{\Theta}(t))\exp(\Theta(t)),$$

where $\mathrm{dexp} : \mathfrak{g} \times \mathfrak{g} \to \mathfrak{g}$ is the differential of the exponential map, it can be seen that the exponent has to satisfy the *dexpinv equation*,

$$\dot{\Theta}(t) = \mathrm{dexp}^{-1}_{\Theta(t)}(a(t)), \qquad \Theta(0) = 0. \tag{1.56}$$

With the help of the *adjoint representation* $\mathrm{ad} : \mathfrak{g} \times \mathfrak{g} \to \mathfrak{g}$, defined by $\mathrm{ad}_x(y) = [x, y]$, and consequently $\mathrm{ad}^k_x(y) = [x, \mathrm{ad}^{k-1}_x(y)]$ for $k \in \mathbb{N}$, it is standard textbook knowledge [126] that the differential of the exponential admits a series expansion

$$\mathrm{dexp}_\Theta = \sum_{k=0}^{\infty} \frac{1}{(k+1)!}\mathrm{ad}^k_\Theta \equiv \frac{\exp(\mathrm{ad}_\Theta) - 1}{\mathrm{ad}_\Theta}, \tag{1.57}$$

and its inverse can be expressed with the help of the Bernoulli numbers B_k as

$$\mathrm{dexp}^{-1}_\Theta = \sum_{k=0}^{\infty} \frac{B_k}{k!}\mathrm{ad}^k_\Theta, \tag{1.58}$$

which is assured to converge for $\|\Theta\| < \pi$. The dexpinv equation (1.56) is solved via Picard's fixed point iteration and, after ordering of the terms, we arrive at the *Magnus expansion*: Using a *grading*, a decomposition in the direct sums $\mathfrak{g} = \bigoplus_{j\in\mathbb{N}} \mathfrak{g}_j$ that propagates under commutation, $[\mathfrak{g}_i, \mathfrak{g}_j] \subset \mathfrak{g}_{i+j}$, the Magnus expansion is the (formal) series

$$\Theta(t) = \sum_{l=1}^{\infty} \Theta_l(t), \tag{1.59}$$

in the grade, $\Theta_l \in \mathfrak{g}_l$, whose components are identified with the terms of same grade in the Picard iteration of (1.56), defined by

$$\begin{aligned}
\Theta^{[0]}(t) &\equiv 0, \\
\Theta^{[n+1]}(t) &= \int_0^t \dot{\Theta}^{[n]}(\xi)\mathrm{d}\xi = \int_0^t \mathrm{dexp}^{-1}_{\Theta^{[n]}(\xi)} a(\xi)\mathrm{d}\xi \\
&= \sum_{k=0}^{\infty} \frac{B_k}{k!}\int_0^t \mathrm{ad}^k_{\Theta^{[n]}(\xi)} a(\xi)\mathrm{d}\xi.
\end{aligned} \tag{1.60}$$

The first three terms are

$$\Theta_1(t) = \int_0^t a(\xi_1)\mathrm{d}\xi_1,$$
$$\Theta_2(t) = \frac{1}{2}\int_0^t \int_0^{\xi_1} [a(\xi_1), a(\xi_2)]\, d\xi_2\, d\xi_1,$$
$$\Theta_3(t) = \frac{1}{6}\int_0^t \int_0^{\xi_1} \int_0^{\xi_2} \Big([a(\xi_1), [a(\xi_2), a(\xi_3)]] + [[a(\xi_1), a(\xi_2)], a(\xi_3)] \Big) d\xi_3\, d\xi_2\, d\xi_1.$$

The same result is achieved by substituting Θ in (1.56) by the ansatz (1.59) and collecting terms of same grade,

$$\begin{aligned} \dot{\Theta}_1 &= a, \\ \dot{\Theta}_n &= \sum_{k=1}^{n-1} \frac{B_k}{k!} S_n^{(k)}, \quad n \geq 2, \end{aligned} \tag{1.61}$$

where the adjoint operation has been expanded in the definition of

$$S_n^{(k)} = \sum_{i_1+\cdots+i_k=n-1} [\Theta_{i_1}, [\ldots [\Theta_{i_k}, a] \ldots]].$$

The resulting equations (1.61) are trivially integrated and the commutators of same grade n, aggregated in $S_n^{(k)}$, can be generated recursively through

$$S_n^{(k)} = \sum_{m=1}^{n-k} [\Theta_m, S_{n-m}^{(k-1)}], \quad 2 \leq k \leq n-1,$$
$$S_n^{(1)} = [\Theta_{n-1}, a], \quad S_n^{(n-1)} = \mathrm{ad}_{\Theta_1}^{(n-1)}(a).$$

Altogether, we state the Magnus expansion in its final form

$$\begin{aligned} \Theta_1(t) &= \int_0^t a(\xi)\, d\xi, \\ \Theta_n(t) &= \sum_{k=1}^{n-1} \frac{B_k}{k!} \int_0^t S_n^{(k)}(\xi)\, d\xi, \quad n \geq 2. \end{aligned} \tag{1.62}$$

The logarithm Θ is known to exist [97] on complete normed (Banach) algebras provided $\int_0^t \|a(\xi)\|_2\, d\xi < \pi$ and the same condition also guarantees the convergence of the Magnus expansion to the solution for bounded linear operators $a(t)$ on some Hilbert space [38, 98].

We highlight the relationship between the Magnus expansion and the BCH formula (1.42) when choosing

$$a(t) = \begin{cases} A & \text{if } 0 \leq t < 1 \\ B & \text{if } 1 \leq t \leq 2 \end{cases}, \tag{1.63}$$

then $e^{\mathrm{BCH}(A,B)} = e^{\Theta^a(2)}$ and the convergence results for the Magnus expansion are carried over to the BCH formula. A word of caution is in place since not all of the obtained terms are linearly independent and it is recommendable to rewrite them in a basis, e.g., the Hall basis, in order to simplify the expression.

Suppose that $a = \mathcal{O}(1)$, then, for small times $t = h$, it is safe to assume that $\Theta_1(h) \propto h$. In the construction of the expansion, we identify two mechanisms: integration and commutation, the

former increases its power in the small parameter h by one, whereas the latter at least retains the size of the two elements. In fact, an additional power in h is gained for the innermost commutator, where

$$\begin{aligned}[a(t_1), a(t_2)] &= [a_0 + t_1 a_1 + \mathcal{O}\left(t_1^2\right), a_0 + t_2 a_1 + \mathcal{O}\left(t_2^2\right)] \\ &= (t_2 - t_1)[a_0, a_1] + \mathcal{O}\left(t_1 t_2 + t_1^2 + t_2^2\right). \end{aligned} \tag{1.64}$$

Furthermore, just as the original equation (1.55), the Magnus expansion and its truncations [80]

$$\Omega_n = \sum_{k=1}^{n} \Theta_k,$$

are *time-symmetric*, i.e., both the exact flow φ and the numerical flow $\Phi = \exp(\Omega_n)$ satisfy

$$\varphi(t, t_0) \circ \varphi(t_0, t) = \mathbf{I}, \qquad \Phi_{t,t_0} \circ \Phi_{t_0,t} = \mathbf{I},$$

with the former being equivalent to $\Theta(t_0, t) = -\Theta(t, t_0)$.

After Taylor expanding $a(t)$ around the midpoint of the interval $[t_n, t_n + h]$, the terms Θ_k and thus also the full expansion Θ contain only odd powers in the time-step h, an observation first made in [80]. Inductively, a size estimate for the terms can be established by first considering

$$\Theta_1 = \mathcal{O}(h), \quad \Theta_2 = \mathcal{O}\left(h^{2+1}\right), \quad \Theta_{2k+1} = \mathcal{O}\left(h^{(2k+1)+1}\right),$$

where the $+1$ is due to (1.64) and finally $\Theta_{2j+1} = \mathcal{O}\left(h^{2j+3}\right)$, $j > 0$ with an additional gain because of the absence of even powers in h. Through simply truncation the Magnus series after the *pth* term, or in other words, by neglecting all terms Θ_n, $n > p$, we obtain a numerical integrator of order $p + 1$ (or $p + 2$ if p is even).

Given the truncated Magnus expansion, several difficulties have to be overcome when actual computation of the terms is desired. If the multidimensional integrals cannot be computed exactly, it has been noted [78] that linear combinations of univariate integrals suffice and hence the number of necessary function evaluations $a(t_i)$ grows only linearly with the order. The standard approach to be portrayed in the following is based on Taylor expanding the vector field a and then integrating the resulting polynomials up to a given order p.

Motivated by the symmetry of the exact Magnus expansion the vector field and its derivatives are evaluated at the midpoint, $t_{1/2} = t + h/2$,

$$a(t) = \sum_{j=0}^{\infty} a_j (t - t_{1/2})^j, \qquad a_j = \frac{1}{j!} \left. \frac{d^j a(t)}{dt^j} \right|_{t=t_{1/2}}. \tag{1.65}$$

The first integrals in (1.62) are readily evaluated up to $\mathcal{O}\left(h^4\right)$ to

$$\begin{aligned} \Theta_1 &= h a_0 + h^3 \frac{1}{12} a_2 + \mathcal{O}\left(h^5\right) \\ \Theta_2 &= h^3 \frac{-1}{12} [a_0, a_1] + \mathcal{O}\left(h^5\right) \end{aligned} \tag{1.66}$$

Notice that, as expected, only odd powers of h appear. However, since the computation of high order derivatives can be costly, we take one step back and interpret the a_j as generators of the

graded free Lie-algebra $FLA(ha_0, h^2a_1, h^3a_2, \ldots)$ which is an approximation to the original algebra $\mathfrak{g}$. In these terms, the (truncated) Magnus expansion is a linear combination of the generators $h^{j+1}a_j$ and commutators thereof. On the other hand, the symmetric momentum integrals

$$A^{(j)} = \frac{1}{h^j}\int_{-h/2}^{h/2} t^j a(t + t_{1/2})\,dt, \qquad j = 0, 1, \ldots$$

provide a way to generate series in the generators a_i. Using again the Taylor expansion (1.65), it becomes clear that by changing the momentum j, and after truncation, linearly independent polynomials can be obtained. In other words, the momentum integrals are generators and one can write

$$\Theta_1 = A^{(0)} + \mathcal{O}\left(h^3\right), \qquad \Theta_2 = [A^{(1)}, A^{(0)}] + \mathcal{O}\left(h^5\right).$$

Keeping in mind that the composition is based on an expansion in powers of h, a single quadrature formula of the desired overall order is sufficient to evaluate the momentum integrals and the choice of quadrature nodes depends on the application. In the later chapters, especially in Sections 2.2 and 4.3, concrete applications of Magnus integrators will be given and in our works [109, 7], Magnus integrators have been studied to obtain efficient solutions for engineering problems. With the framework of how to compute integrals being laid down before us, we now briefly comment on how to avoid commutators in the expansion. It has been noticed [26] that by choosing a proper basis, or - in other words - by properly grouping terms, the number of commutators can be greatly reduced in comparison to the plain application of (1.62). The analysis, however, has been performed in a case by case study for relevant orders up to eight and a general treatment was developed in [18].

In connection with splitting methods, it is even possible to eliminate commutation altogether by considering the BCH formula and the principle goes as follows: a truncated Magnus expansion is nothing else but an element of the free Lie algebra generated by the letters a_j and the aim is to reproduce it by the composition of s exponentials of linear combinations of these letters, i.e.,

$$\prod_{l=1}^{s} \exp\left(\sum_{k=0}^{p} c_{l,k} a_k\right) \stackrel{!}{=} \sum_{j=1}^{p} \Theta_j + \mathcal{O}\left(h^{p+1}\right),$$

with some coefficients $c_{l,k} \in \mathbb{R}$. This is expected to work since most commutators are generated after the combination of the exponentials through the BCH formula, and a fourth-order *commutator-free* Magnus integrator [30, 122] is given by

$$\Omega_{t,t+h}^{[4]} = e^{h\left(\frac{1}{2}a_0 + \frac{1}{6}a_1\right)} e^{h\left(\frac{1}{2}a_0 - \frac{1}{6}a_1\right)}.$$

In the basis of momentum integrals, we equate up to $\mathcal{O}\left(h^5\right)$

$$\begin{aligned}
\Theta_1 + \Theta_2 =& A^{(0)} - [A^{(0)}, A^{(1)}] \\
\stackrel{!}{=}& \log\left(e^{c_{1,0}A^{(0)}+c_{1,1}A^{(1)}} e^{c_{2,0}A^{(0)}+c_{2,1}A^{(1)}}\right) \\
=& (c_{1,0} + c_{2,0})A^{(0)} + (c_{1,1} + c_{2,1})A^{(1)} \\
&+ \frac{1}{2}\left(c_{1,0}c_{2,1} - c_{1,1}c_{2,0}\right)\left[A^{(0)}, A^{(1)}\right] \\
&+ \frac{1}{12}\left(c_{1,0}c_{2,1} - c_{1,1}c_{2,0}\right)\Big((c_{1,0} - c_{2,0})\left[A^{(0)}, \left[A^{(0)}, A^{(1)}\right]\right] \\
&\qquad + (c_{1,1} - c_{2,1})\underbrace{\left[A^{(1)}, \left[A^{(0)}, A^{(1)}\right]\right]}_{=\mathcal{O}\left(h^5\right)}\Big) + \mathcal{O}\left(h^5\right).
\end{aligned}$$

The polynomial equations in the coefficients $c_{l,k}$ to be satisfied are then

$$\begin{aligned}
\mathcal{O}(h): &\quad A^{(0)}, && 1 &&= c_{1,0} + c_{2,0} \\
\mathcal{O}\left(h^2\right): &\quad A^{(1)}, && 0 &&= c_{1,1} + c_{2,1} \\
\mathcal{O}\left(h^3\right): &\quad \left[A^{(0)}, A^{(1)}\right], && -2 &&= c_{1,0}c_{2,1} - c_{1,1}c_{2,0} \\
\mathcal{O}\left(h^4\right): &\quad \left[A^{(0)}, \left[A^{(0)}, A^{(1)}\right]\right], && 0 &&= (c_{1,0} - c_{2,0}).
\end{aligned}$$

and the solution yields the time-symmetric decomposition

$$\tilde{\Omega}^{[4]}_{t,t+h} = e^{\frac{1}{2}A^{(0)}+2A^{(1)}} e^{\frac{1}{2}A^{(0)}-2A^{(1)}}. \tag{1.67}$$

From a geometric point of view, the key to understanding the Magnus expansion comes from the dexpinv equation: The original problem was posed on some Lie-group $\mathcal{G}$ and has been pulled back to an ODE (1.56) on a linear space: The Lie algebra $\mathfrak{g}$. Therefore, the approximation that arises after truncation of the Magnus expansion will still be in the algebra and respect the geometric structure. Taking the exponential thus guarantees that the numerical solution stays in the correct space: In the context of Schrödinger equations, unitarity will be preserved.

For nonlinear equations, the same formalism can be employed by means of Lie-derivatives and there exist several links between the Magnus series and other ways of writing the solution of time-dependent ODEs, e.g., the Dyson series based on time-ordered products or the Chen-Fliess series for nonlinear vector fields. For details and extensive collection of examples, we refer to the review in [23] and only remark that the sufficient convergence criterion in the nonlinear case becomes to $\int_0^t \|\mathcal{L}_a(\xi, x_0)\| d\xi < 1.08686$, where, as usual, $\mathcal{L}_a$ denotes the Lie-derivative associated with the vector field a. For completeness, we mention that Iserles & Nørsett developed a graph-theoretic approach to construct the terms Θ_k [78] which drew much attention to the study of Magnus expansions as numerical integrators and has motivated many of the exhibited results.

Chapter 2

LINEAR SCHRÖDINGER EQUATIONS

After spatial discretization, the Schrödinger equation reduces to a system of ordinary differential equations,

$$i\frac{d}{dt}\psi(t) = \hat{H}\psi(t), \quad \psi(0) = \psi_0 \in \mathbb{C}^N.$$

Since we are mainly interested in temporal accuracy, we use the same symbol for the function and the corresponding discretized vector, $\psi(x_j, t) \approx (\psi(t))_j$ for the chosen grid points x_j and will also drop the hat that indicated the discretized version of the Hamiltonian.

The resulting ODE can be numerically solved by standard all purpose methods, however, because of the particular structure of this problem, different numerical methods can differ considerably in accuracy as well as computational cost and stability. In addition, the structural properties of the system lead to the existence of several preserved quantities like the norm and energy (for the autonomous case). The accurate preservation of these quantities[1] as well as the error propagation and performance of splitting methods explain why they are frequently recommended for the time integration [15, 106, 123] and make them subject of investigation in this work.

With the aim of an efficient use of split-step methods, a family of potentials is studied. In particular, we derive algorithms to exactly solve the $d-$dimensional harmonic oscillator [4] using only Fourier transforms through a correspondence principle with its isomorphic classical mechanical algebra.

The developed technique is powerful enough to be applied to time-dependent potentials that are (multivariate) polynomials of degree at most two, thus including linear perturbations and the important angular momentum due to rotating traps. Numerical examples corroborate the efficiency of embedding the obtained decomposition algorithms with standard splitting methods.

[1] The energy is only nearly conserved, for details see Ref. [50].

2.1 The Harmonic Oscillator

The exposition is based on the article [4].

Motivated by the importance of parabolic potentials in the study of the Schrödinger equation and its nonlinear counterpart, we consider the numerical integration of the harmonic oscillator, i.e., a potential of the form $V_{\mathrm{HO}}(x) = \frac{1}{2}\omega^2 x^2$, which can be solved exactly.

In many applications, the wave function is expected to evolve in the vicinity of a minimum at, w.l.o.g., $x = 0$ of the potential V and locally, we interpret V as a perturbed harmonic oscillator

$$V = V_{\mathrm{HO}} + \epsilon \underbrace{(ax^3 + bx^4 + \cdots)}_{=:V_\epsilon},$$

The model Hamiltonian in this section is thus taken to be

$$H = \frac{1}{2m}p^2 + \frac{1}{2}m\omega^2 x^2 + \epsilon V_\epsilon. \tag{2.1}$$

Another example, to be detailed in Chapter 3, is the Gross-Pitaevskii equation for a trapped BEC,

$$i\frac{\partial}{\partial t}\psi = H_{\mathrm{HO}}\psi + \left(\epsilon V_\epsilon(x) + \sigma|\psi|^2\right)\psi,$$

where the Hamiltonian of the *harmonic oscillator* is defined as

$$H_{\mathrm{HO}} = \frac{1}{2m}p^2 + \frac{1}{2}m\omega^2 x^2. \tag{2.2}$$

In the standard approach, i.e., the split in $T = p^2/(2m)$ and some (nonlinear) potential V, while the RKN property is satisfied $[V,[V,[T,V]]] = 0$, important information about the problem is lost and as established in the introduction, it is of great importance to preserve the near-integrable structure through appropriate splittings when possible.

Remarkably, the split in $A = H_{\mathrm{HO}}$ and $B = \epsilon V_\epsilon + \sigma|\psi|^2$ recovers the RKN structure of the original algebra T, V since $[B,[B,[B,A]]] = 0$. Additionally, if σ and ϵ are small, so will be the commutators $[A,B]$ and highly accurate results are obtained [15, 51, 106, 123].

We will refer to the alternative splits in two parts A, B, which are claimed [106] to be the most efficient in comparison with a variety of standard integrators, as

(i) Fourier (F)-split.

$$A = \frac{1}{2m}p^2, \qquad B = \frac{1}{2}m\omega^2 x^2 + V_\epsilon(x). \tag{2.3}$$

Here, A and B are diagonal in the momentum and coordinate spaces, respectively, and we can change between them using Fourier transforms.

(ii) Harmonic oscillator (HO)-split.

$$A = \frac{1}{2m}p^2 + \frac{1}{2}m\omega^2 x^2, \qquad B = \epsilon V_\epsilon(x). \tag{2.4}$$

The usual approach to propagate part A uses Hermite functions and will be explained below. Since B is diagonal in the coordinate space, it will act in both cases as a simple multiplication on a wave function that is discretized on a grid.

The harmonic oscillator is a standard problem in both classical and quantum mechanics and its spectrum is well-understood. For simplicity, we have rescaled the units such that $m = \omega = 1$ and the normalized eigenfunctions of H_{HO} become

$$\phi_n(x) = \frac{1}{\pi^{1/4}\sqrt{2^n n!}} \mathscr{H}_n(x) e^{-x^2/2}, \qquad n = 0, 1, \dots, \tag{2.5}$$

where $\mathscr{H}_n(x)$ are the Hermite polynomials, which obey the recurrence relation

$$\mathscr{H}_{k+1}(x) = 2x\mathscr{H}_k(x) - 2k\mathscr{H}_{k-1}, \qquad k = 1, 2, \dots,$$

starting from $\mathscr{H}_0(x) = 1,\ \mathscr{H}_1(x) = 2x$. The corresponding eigenvalues are

$$E_n = n + \frac{1}{2}, \qquad n = 0, 1, \dots \ , \quad (H_{\mathrm{HO}}\phi_n = E_n\phi_n),$$

and the eigenvectors form a complete orthonormal system on $L^2(\mathbb{R})$. An initial condition, ψ_0, can then be propagated easily by

$$\psi(t, x) = \sum_{n=0}^{\infty} c_n e^{-iE_n t}\phi_n(x), \tag{2.6}$$

where the weights c_n are the orthogonal projections on the eigenfunctions, $c_n = \langle\phi_n|\psi_0\rangle \equiv \int_{\mathbb{R}} \phi_n(x)^*\psi_0(x)\,dx$. For a numerical method, the sum in (2.6) has to be truncated and the expansion coefficients c_n need to be computed in each step, in other words it requires a change of basis between the HO eigenfunctions and coordinate space for the remaining potential ϵV_ϵ and the integrals for c_n are evaluated on a chosen mesh x_j, e.g., using the Gauss-Hermite quadrature [91] or some rule on equidistant grid points [106],

$$\psi(x_j, t) \approx \psi_M(x_j, t) = \sum_{n=0}^{M} c_n e^{-iE_n t}\phi_n(x_j), \tag{2.7}$$

with $c_n = \sum w_j\phi_n(x_j)^*\psi_0(x_j)$. A (Galerkin) truncation error bound for truncation after M terms for a perturbation $V(x) = (1 + x^2)B(x)$ with bounded B is given by [91]

$$\|\psi_M(t) - \psi(t)\| \le CM^{-s/2}(1 + t) \max_{0\le\tau\le t} \left\|\hat{a}^{s+2}\psi(\tau)\right\|, \tag{2.8}$$

for some $s \le M/2$ such that $\hat{a}^{s+2}\psi(\tau)$ exists, where $\hat{a} \equiv \frac{1}{\sqrt{2}}(x + ip)$ is a so-called ladder operator[2] that acts on HO eigenfunctions by $\hat{a}\phi_k = \sqrt{k}\phi_{k-1}$ for $k \in \mathbb{N}$ and $\hat{a}\phi_0 = 0$ and a constant C independent of M and t. Notice that the bound depends on both smoothness and decay of the solution which makes practical estimates difficult.

The change between Hermite basis functions and the coordinate space is not efficient when the number of basis terms in the expansions has to be altered along the integration or taken

[2] See also the discussion following Section 1.1.3.

very large, being the case for time dependent trap frequencies $\omega(t)$ or strong nonlinearities σ to be studied in Section 2.2 and Chapter 3, respectively.

The Fourier type methods can be implemented with FFT algorithms since the trapping potential V causes the wave function to vanish asymptotically which in turn allows us to consider the problem as periodic on a sufficiently large spatial interval. Their advantages are high accuracy with a moderate number of mesh points and low computational cost.

In general, the split **(i)** can be considered faster and simpler since $A \equiv T$ can be computed in the momentum space, and one can easily and efficiently change from momentum to coordinate space via FFTs. The choice **(ii)**, on the other hand, allows us to take advantage of the structure of a near-integrable system if, roughly speaking, $\|B\| < \|A\|$, but it requires to solve the equation for the (time-dependent) harmonic potential exactly (or with high accuracy). The evolution of the constant oscillator is easily computed using Hermite polynomials (see [106, 123, 91]), but the evolution for the explicitly time-dependent problem is more involved.

Motivated by these results, we show how both methods are combined to retain both the accuracy of the Hermite method and the speed of the Fourier transforms, i.e., to rewrite the Hermite method as a single simple pseudospectral Fourier scheme. We have found, that this approximation performs, for the studied problem classes, always equal to or better than the original Fourier method and therefore has to compete with Hermite expansions only.

We show that the exact solution of the autonomous problem, in our setting the dominant part H_{HO} of (2.1),

$$i\frac{\partial}{\partial t}\psi = \left(\frac{1}{2m}p^2 + \frac{1}{2}m\omega^2 x^2\right)\psi \tag{2.9}$$

is easily computed for a time step using Fourier transforms. Before giving the details on the time integration, some remarks on the formal solution are necessary.

It is clear that H_{HO} is an element of the Lie algebra spanned by the operators $\{E = x^2/2, F = p^2/2, G = \frac{1}{2}(px + xp)\}$, where $m = \omega = 1$ for simplicity, and their commutators are

$$[E, F] = iG, \quad [E, G] = 2iE, \quad [F, G] = -2iF. \tag{2.10}$$

This Lie algebra is three-dimensional and the solution, $\psi(x, t) = U(t, 0)\psi(x, 0)$, of (2.9) can be expressed as a product of exponentials [127]. Our objective is to obtain a factorization of the solution which only involves terms proportional to E or F since they are easy to compute by FFTs as shown in Section 1.2.

2.1.1 Solving the harmonic oscillator by Fourier methods

We propose a new method which combines the advantages of both splittings. It retains the advantages of the HO-split **(ii)** while being as fast to compute as the F-split in **(i)**. For this purpose, we briefly review some basic concepts of Lie algebras.

Given X, Y two elements of a given Lie algebra, it is well known that

$$e^X Y e^{-X} = e^{\mathrm{ad}_X} Y = Y + [X, Y] + \frac{1}{2}[X, [X, Y]] + \ldots \tag{2.11}$$

For analytic functions in their arguments, $X(x), P(p)$ and $F(x,p)$, we are interested in the following adjoint actions[3]

$$\begin{aligned} e^{-itX}F(x,p)e^{itX} &= F(x,p+tX') \\ e^{-itP}F(x,p)e^{itP} &= F(x-tP',p) \end{aligned} \tag{2.12}$$

where $X' = dX/dx$, $P' = dP/dp$. In classical mechanics, this corresponds to a kick and a drift. As we have seen, the exponentials $\exp(\alpha x^2/2)$ and $\exp(\beta p^2/2)$ can be easily computed by Fourier spectral methods. It is then natural to ask the question if it is possible to write the solution of (2.9) as a product of exponentials which are solvable by spectral methods. The answer is positive and it is formulated in the following lemma. We present a new proof for a result already obtained in Ref. [47] that allows an elegant generalization to the time-dependent case.

Lemma 2.1.1. *Let* $A_1 = \frac{1}{2}p^2$, $B_1 = \frac{1}{2}x^2$ *and*

$$f(t) = (1-\cos(t))\,/\,\sin(t), \qquad g(t) = \sin(t). \tag{2.13}$$

Then, the following property is satisfied for $|t| < \pi$*:*

$$e^{-it(A_1+B_1)} = e^{-if(t)A_1}\, e^{-ig(t)B_1}\, e^{-if(t)A_1} \tag{2.14}$$

$$= e^{-if(t)B_1}\, e^{-ig(t)A_1}\, e^{-if(t)B_1} \tag{2.15}$$

Proof. A new constructive way to derive the functions f, g makes use of the parallelism with the one-dimensional classical harmonic oscillator with Hamiltonian function $H = \frac{1}{2}p^2 + \frac{1}{2}q^2$ and Hamilton's equations

$$\frac{d}{dt}\begin{pmatrix} q \\ p \end{pmatrix} = \begin{pmatrix} 0 & 1 \\ -1 & 0 \end{pmatrix}\begin{pmatrix} q \\ p \end{pmatrix} = (A+B)\begin{pmatrix} q \\ p \end{pmatrix}, \tag{2.16}$$

where

$$A \equiv \begin{pmatrix} 0 & 1 \\ 0 & 0 \end{pmatrix}, \qquad B \equiv \begin{pmatrix} 0 & 0 \\ -1 & 0 \end{pmatrix}. \tag{2.17}$$

The Lie algebra generated by the matrices A, B is the same as the Lie algebra associated to the operators A_1, B_1 for the Schrödinger equation with the harmonic potential (2.2).

The exact evolution operator of (2.16) is

$$O(t) = \begin{pmatrix} \cos(t) & \sin(t) \\ -\sin(t) & \cos(t) \end{pmatrix}, \tag{2.18}$$

which is an orthogonal and symplectic 2×2 matrix. For the split parts, the flows are easily computed to

$$e^{f(t)A} = \begin{pmatrix} 1 & f(t) \\ 0 & 1 \end{pmatrix}, \qquad e^{g(t)B} = \begin{pmatrix} 1 & 0 \\ -g(t) & 1 \end{pmatrix},$$

[3] The expressions can be easily derived using the series expansion of F and the fact that all nested commutators vanish.

and then, equating the symmetric composition

$$e^{fA}e^{gB}e^{fA} = \begin{pmatrix} 1-f\cdot g & 2f-f^2\cdot g \\ -g & 1-f\cdot g \end{pmatrix}$$

to (2.18), we obtain (2.13) which is valid for $|h| \leq \pi$. The decomposition (2.15) is derived analogously. Using the Baker-Campbell-Hausdorff-formula, it is clear, that both results remain valid, up to the first singularity at $t = \pm\pi$, when replacing the matrices A, B by the corresponding linear operators A_1, B_1, since all computations are done in identical Lie algebras.

Given the functions f, g, we can prove the lemma directly by recalling that two operators are identical on a sufficiently small time interval if they satisfy the same first order differential equation with the same initial conditions[130]. We thus verify that the right-hand side of (2.14) also solves the propagator equation

$$i\dot{U} = (A_1 + B_1)U, \qquad U(0) = I, \tag{2.19}$$

and is therefore identical to the propagator on the left-hand side. Now set

$$\tilde{U}(t) = e^{-if(t)A_1}e^{-ig(t)B_1}e^{-if(t)A_1}$$

and plugging it into (2.19) yields

$$(A_1 + B_1)\tilde{U} \stackrel{!}{=} \left(\dot{f}A_1 + e^{-ifA_1}\,\dot{g}B_1\,e^{ifA_1} + e^{-ifA_1}\,e^{-igB_1}\,\dot{f}A_1\,e^{igB_1}\,e^{ifA_1}\right)\tilde{U}.$$

Using (2.12), we obtain two independent non-linear differential equations for $f(t)$ and $g(t)$ with initial condition $f(0) = g(0) = 0$ in order to satisfy $\tilde{U}(0) = I$. It is then easy to check that f, g given in (2.13) solve these equations. As a result, we have that $\tilde{U}(t) = U(t)$ locally in a neighborhood of the origin and (2.14) is proved identically. □

For practical purposes, the singularities occur at sufficiently large times and hence do not impose limits for the time-steps of numerical methods.

Remark 2.1.2. *By simply replacing* (2.18) *with*

$$O(t) = \begin{pmatrix} \cos(\omega t) & \frac{1}{m\omega}\sin(\omega t) \\ -m\omega\sin(\omega t) & \cos(\omega t) \end{pmatrix},$$

the lemma immediately generalizes to the equation

$$i\frac{\partial}{\partial t}\psi(x,t) = \left(\frac{1}{2m}p^2 + m\frac{\omega^2}{2}x^2\right)\psi(x,t),$$

for $m, \omega > 0$ *when we substitute* (2.13) *with*

$$f = m\omega\frac{1-\cos(\omega t)}{\sin(\omega t)}, \qquad g = \frac{1}{m\omega}\sin(\omega t). \tag{2.20}$$

This result is valid for $|t| < t^* \equiv \pi/\omega$.

2.1.2 Higher dimensions

Although the results in the previous section have been developed for one-dimensional problems, it is straightforward to extend them to arbitrary dimension. Keeping in mind the proof-technique based on the isomorphy of the Lie algebras, we state the $d-$dimensional classical Hamiltonian

$$H = \frac{1}{2}p^T \Lambda p + \frac{1}{2}q^T \Omega q, \quad p, q \in \mathbb{R}^d,$$

with symmetric positive definite (spd) matrices $\Lambda, \Omega \in \mathbb{R}^{d\times d}$. The corresponding classical (linear) system is given by

$$\frac{d}{dt}\begin{pmatrix} q \\ p \end{pmatrix} = \begin{pmatrix} 0 & \Lambda \\ -\Omega & 0 \end{pmatrix}\begin{pmatrix} q \\ p \end{pmatrix}.$$

The matrix exponential is computed to[4]

$$\begin{aligned}
\exp\left(t\begin{pmatrix} 0 & \Lambda \\ -\Omega & 0 \end{pmatrix}\right) &= \sum_{k=0}^{\infty} \frac{t^{2k}}{(2k)!}\begin{pmatrix} 0 & \Lambda \\ -\Omega & 0 \end{pmatrix}^{2k} + \sum_{k=0}^{\infty} \frac{t^{2k+1}}{(2k+1)!}\begin{pmatrix} 0 & \Lambda \\ -\Omega & 0 \end{pmatrix}^{2k+1} \\
&= \sum_{k=0}^{\infty} \frac{t^{2k}}{(2k)!}(-1)^k \begin{pmatrix} (\Lambda\Omega)^k & 0 \\ 0 & (\Omega\Lambda)^k \end{pmatrix} \\
&\quad + \sum_{k=0}^{\infty} \frac{t^{2k+1}}{(2k+1)!}(-1)^k \begin{pmatrix} \Lambda & 0 \\ 0 & -\Omega \end{pmatrix}\begin{pmatrix} 0 & (\Omega\Lambda)^k \\ (\Lambda\Omega)^k & 0 \end{pmatrix} \\
&= \begin{pmatrix} \cos(t\sqrt{\Lambda\Omega}) & \Lambda(\sqrt{\Omega\Lambda})^{-1}\sin(t\sqrt{\Omega\Lambda}) \\ -\Omega(\sqrt{\Lambda\Omega})^{-1}\sin(t\sqrt{\Lambda\Omega}) & \cos(t\sqrt{\Omega\Lambda}) \end{pmatrix}. \qquad (2.21)
\end{aligned}$$

It is known that products of real spd matrices $\Lambda\Omega, \Omega\Lambda$ can be diagonalized and have positive eigenvalues [74, Corr. 7.6.2], which means that the positive square root in (2.21) exists and is unique. We further note that the product $\Lambda\Omega$ is symmetric iff $[\Lambda, \Omega] = 0$. For the decomposition, we multiply the exponentials

$$\begin{pmatrix} \mathbf{I} & 0 \\ -B & \mathbf{I} \end{pmatrix}\begin{pmatrix} \mathbf{I} & A \\ 0 & \mathbf{I} \end{pmatrix}\begin{pmatrix} \mathbf{I} & 0 \\ -B & \mathbf{I} \end{pmatrix} = \begin{pmatrix} \mathbf{I} - AB & A \\ -2B + BAB & \mathbf{I} - BA \end{pmatrix}, \qquad (2.22)$$

where $\mathbf{I} \in \mathbb{R}^{d\times d}$ denotes the identity matrix. Equating (2.22) and (2.21) yields

$$A = \Lambda(\sqrt{\Omega\Lambda})^{-1}\sin(t\sqrt{\Omega\Lambda}) = \sum_{k=0}^{\infty} \frac{t^{2k+1}}{(2k+1)!}(-1)^k \Lambda(\Omega\Lambda)^k$$

and

$$\cos(t\sqrt{\Omega\Lambda}) \overset{!}{=} \mathbf{I} - BA = \mathbf{I} - B\Lambda(\sqrt{\Omega\Lambda})^{-1}\sin(t\sqrt{\Omega\Lambda}),$$

from which we deduce

$$\begin{aligned}
B &= \left(\mathbf{I} - \cos(t\sqrt{\Omega\Lambda})\right)\sin(t\sqrt{\Omega\Lambda})^{-1}(\sqrt{\Omega\Lambda})\Lambda^{-1} = \sqrt{\Omega\Lambda}\,\frac{\mathbf{I} - \cos(t\sqrt{\Omega\Lambda})}{\sin(t\sqrt{\Omega\Lambda})}\Lambda^{-1} \\
&= \sqrt{\Omega\Lambda}\,\tan\left(\frac{t}{2}\sqrt{\Omega\Lambda}\right)\Lambda^{-1}.
\end{aligned}$$

[4] The calculation is performed explicitly to keep track of the order of multiplication.

Taking into account that $\Lambda\cos(t\sqrt{\Omega\Lambda})\Lambda^{-1} = \cos(t\sqrt{\Lambda\Omega})$, which can be seen by writing out the series expansion of the cosine,

$$\begin{aligned}\Lambda\cos(t\sqrt{\Omega\Lambda})\Lambda^{-1} &= \sum_{k=0}^{\infty}\frac{(-1)^k t^{2k}}{(2k)!}\Lambda(\Omega\Lambda)^k\Lambda^{-1}\\ &= \sum_{k=0}^{\infty}\frac{(-1)^k t^{2k}}{(2k)!}(\Lambda\Omega\Lambda\Lambda^{-1})^k = \cos(t\sqrt{\Lambda\Omega}),\end{aligned}$$

it is trivial to verify $\mathbf{I} - AB = \cos(t\sqrt{\Lambda\Omega})$. The remaining condition is

$$\begin{aligned}-\Omega(\sqrt{\Lambda\Omega})^{-1}\sin(t\sqrt{\Lambda\Omega}) &\stackrel{!}{=} -2B + BAB\\ &= -B(\mathbf{I} + (\mathbf{I} - AB)) = -B(\mathbf{I} + \cos(t\Lambda\Omega))\\ &= -\sqrt{\Omega\Lambda}\tan\left(\frac{t}{2}\sqrt{\Omega\Lambda}\right)\Lambda^{-1}(\mathbf{I} + \Lambda\cos(t\sqrt{\Omega\Lambda})\Lambda^{-1})\\ &= -\sqrt{\Omega\Lambda}\,\frac{\mathbf{I} - \cos(t\sqrt{\Omega\Lambda})}{\sin(t\sqrt{\Omega\Lambda})}\left(\mathbf{I} + \cos(t\sqrt{\Omega\Lambda})\right)\Lambda^{-1}\\ &= -\sqrt{\Omega\Lambda}\sin(t\sqrt{\Omega\Lambda})\Lambda^{-1}\\ &= -(\sqrt{\Omega\Lambda})\Lambda^{-1}\sin(t\sqrt{\Lambda\Omega}),\end{aligned}$$

and equality holds since

$$\begin{aligned}&(\sqrt{\Omega\Lambda})\Lambda^{-1} &&= \Omega(\sqrt{\Lambda\Omega})^{-1} = \Lambda^{-1}\Lambda\Omega(\sqrt{\Lambda\Omega})^{-1} = \Lambda^{-1}\sqrt{\Lambda\Omega}\\ \Leftrightarrow\quad &\Lambda(\sqrt{\Omega\Lambda})\Lambda^{-1} &&= \sqrt{\Lambda\Omega},\end{aligned}$$

which is true because both $\Omega\Lambda$ and $\Lambda\Omega$ have nonnegative eigenvalues [69, Cor. 1.3.4]. The transition to the quantum mechanical Hamiltonian is made as in 1D and the calculations are summarized in the following

Theorem 2.1.3. *For symmetric positive definite matrices $\Lambda, \Omega \in \mathbb{R}^{d\times d}$ and functions*

$$f(h,\Lambda,\Omega) = \sqrt{\Omega\Lambda}\tan\left(\frac{h}{2}\sqrt{\Omega\Lambda}\right)\Lambda^{-1}, \qquad g(h,\Lambda,\Omega) = \Omega^{-1}\sqrt{\Omega\Lambda}\sin\left(h\sqrt{\Omega\Lambda}\right),$$

the following identity is satisfied for $|h\lambda_{\max}(\sqrt{\Omega\Lambda})| < \pi$:

$$e^{-ih\frac{1}{2}(p^T\Lambda p + q^T\Omega q)} = e^{-i\frac{1}{2}q^T f(h,\Lambda,\Omega)q}e^{-i\frac{1}{2}p^T g(h,\Lambda,\Omega)p}e^{-i\frac{1}{2}q^T f(h,\Lambda,\Omega)q}, \tag{2.23}$$

where $q^T = (x_1, x_2, \dots, x_d)$ and $p^T = -i(\partial_{x_1}, \partial_{x_2}, \dots, \partial_{x_d})$ and the stepsize $|h|$ is restricted by the largest eigenvalue $\lambda_{\max}$ of $\sqrt{\Omega\Lambda}$.

Remark 2.1.4. *From a formal point of view, the symmetry of Λ and Ω as well as the positivity are not necessary and could be replaced by invertibility. These conditions only play a role when we express the formal series in terms of trigonometric functions with the help of the (positive) matrix square root. For quantum mechanics, however, we require Hermitian operators, e.g., for $p^T\Lambda p$, $\Lambda^\dagger = \Lambda$ is implied. Furthermore, since the corresponding operators commute, there is a degree of freedom in the representation of the matrices in the Hamiltonian. By choosing the matrices real and requiring Hermiticity, Λ, Ω are uniquely determined.*

2.1.3 The Hermite-Fourier methods

With the presented exact decompositions at hand, we now solve the discretized perturbed harmonic oscillator, $H = H_{\mathrm{HO}} + \epsilon V_\epsilon$, by splitting methods using the symmetric compositions (1.37) and (1.38). Let us first consider the case $\omega = 1$ and take the HO split $A = H_{\mathrm{HO}} = A_1 + B_1$, $B = \epsilon V_\epsilon$,

$$\Phi_{h,A}^{[2]} = e^{-ih(A_1+B_1)/2}\, e^{-ihB}\, e^{-ih(A_1+B_1)/2}, \tag{2.24}$$

$$\Phi_{h,B}^{[2]} = e^{-ihB/2}\, e^{-ih(A_1+B_1)}\, e^{-ihB/2}. \tag{2.25}$$

Replacing the exponentials $e^{-ih(A_1+B_1)}$ by (2.14) or (2.15), we obtain four different methods whose computational costs differ considerably. At first sight, using the FSAL property, both (2.24) and (2.25) are equivalent from the computational point of view and require one exponential of B and another one of $A_1 + B_1$ per step. However, a significant difference arises when we plug in the decompositions (2.14) or (2.15). Only the combination (2.25) with (2.15) yields a method that involves only one FFT and one inverse FFT call per step

$$\begin{aligned}\Phi_h^{[2]} &= e^{-ihB/2}\, e^{-ih(A_1+B_1)}\, e^{-ihB/2} \\ &= e^{-ihB/2}\, e^{-if(h)B_1}\, e^{-ig(h)A_1}\, e^{-if(h)B_1}\, e^{-ihB/2} \\ &= e^{-i(hB/2+f(h)B_1)}\, e^{-ig(h)A_1}\, e^{-i(hB/2+f(h)B_1)},\end{aligned} \tag{2.26}$$

and solves exactly the harmonic oscillator for $|h| < h^*$. For any other combination, more kinetic terms have to be computed per step since the FSAL property cannot be exploited to full extent and hence result in more costly[5] methods for the same accuracy.

The general splitting method (1.40) can be rewritten in the same way by replacing each flow e^{-ia_iA} by the composition (2.15)

$$\begin{aligned}\Phi_h \equiv\ & e^{-i(hb_mB+\alpha_mB_1)}\, e^{-ig(a_mh)A_1}\, e^{-i(hb_mB+\alpha_{m-1}B_1)} \\ & \cdots e^{-i(hb_1B+\alpha_1B_1)}\, e^{-ig(a_1h)A_1}\, e^{-i\alpha_0B_1},\end{aligned} \tag{2.27}$$

where $\alpha_k = f(a_{k+1}h) + f(a_kh)$, $k = 0, 1, \ldots, m+1$ with $a_0 = a_{m+1} = 0$. This method is valid for $|a_ih| < h^*$, $i = 1, \ldots, m$ and requires only m calls of the FFT and its inverse, just like the standard Fourier pseudospectral methods, but reaches the same accuracy as if the Hermite functions were used.

For stability reasons, it seems convenient to look for splitting methods whose value of $\max_i\{|a_i|\}$ is as small as possible.

[5] More precisely, the computational costs are due to a change of coordinates realized by the Fourier transform which is for this type of problem equivalent to the number of kinetic terms.

2.1.4 Numerical results

We analyze the performance of the methods considered in this section for the one-dimensional problem (2.1) with $m = \omega^2 = 1$, and to illustrate the validity of the decomposition presented in Lemma 2.1.1, we first study the pure harmonic trap, i.e., $V_\epsilon = 0$.

The ground state ϕ_0 at $t = 0$ is taken as the initial condition, with exact solution

$$\psi(x,t) = e^{-it/2}\phi_0(x) = \frac{1}{\pi^{1/4}} e^{-it/2} e^{-x^2/2}.$$

Restricting the spatial interval on $[-10, 10]$ ensures that the wave function and its first derivatives vanish up to round off at the boundaries, and for high accuracy it is sampled at $N = 1024$ equidistant grid points x_j. We integrate with only one time step from $t = 0$ to T for $T \in [-\pi, \pi]$, i.e., forward and backward in time. The error in the wave function is defined by $\mathrm{err}(T) = |\Psi(T) - \psi(T)|$, where $\Psi(T)$ denotes the approximate numerical solution obtained using the specified method and $\psi(T)$ is the exact solution on the discretized mesh. It is standard to measure the error in the wave function by the discrete L^2 norm,

$$\|\mathrm{err}(T)\|_2 \equiv \sqrt{\Delta x \sum_{j=1}^{N} |\mathrm{err}_j(T)|^2}. \tag{2.28}$$

The result of this comparison is illustrated in Fig. 2.1 (left). The split (2.15) reproduces, for $|T| < \pi$, the exact solution up to round off, as expected. The right panel in Fig. 2.1 displays a zoom near a singularity where the error grows rapidly due to double precision arithmetic. Next,

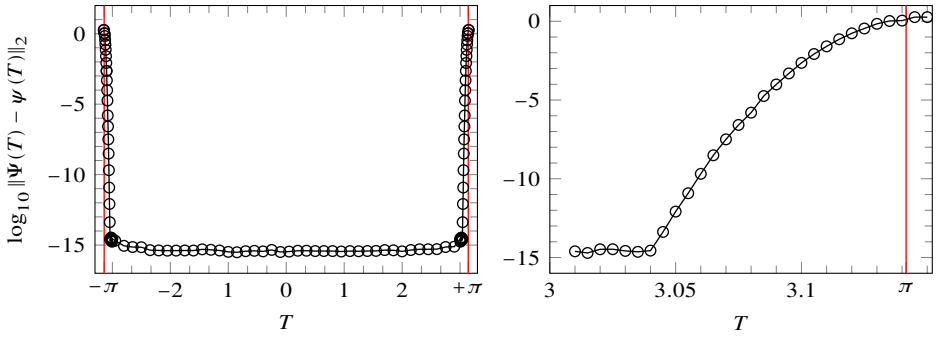

Figure 2.1: Error in logarithmic scale for the integration of the ground state of the Harmonic potential using the split (2.15) for $T \in [-\pi, \pi]$ (integration forward and backward in time). The right panel shows a zoom about $T = \pi$.

we examine how the approximation properties of the Hermite decomposition (2.7) strongly depend on the function in question and on the chosen number of basis functions, M. We compute the M required to reach round-off precision for the evolution of a displaced ground state as initial condition, $\psi_\delta(x,0) = e^{-(x-\delta)^2/2}/\pi^{1/4}$ from $t = 0$ to $T = 10$ in one time step. From initial conditions discretized on an equidistant mesh, this can be accomplished as follows [106]:

$$\Psi(T) = e^{-iT(A_1+B_1)}u_0 \approx K^\dagger e^{-iTD_1} K\, u_0 \tag{2.29}$$

where $D_1 = \mathrm{diag}\{\frac{1}{2}, \frac{3}{2}, \dots, M - \frac{1}{2}\}$, M is the number of basis elements considered, and $K_{j,k} = \sqrt{\Delta x}\, \phi^*_{j-1}(x_k)$, $j = 1, \dots, M$, $k = 1, \dots, N = 512$ with $\phi_n(x)$ given in (2.5), $x \in [-10, 10]$. For $\delta = \frac{1}{10}$, round off accuracy is achieved with $M = 8$ while for $\delta = 2$ it is necessary to take $M = 29$. Using an estimate of type (2.8), cf. [91, Th. 1.2], similar minimum values of M are attained if the integrals were calculated exactly without using a mesh, which justifies the use of equidistant grid points (and thus the trapezoidal rule) instead of the possibly more natural Gauss-Hermite quadrature points in the computation of K. As expected, the Hermite decomposition is very sensitive to the initial conditions. The Hermite basis works efficiently as far as the initial conditions as well as the exact solution can be accurately approximated using a few number of basis elements and one has to keep in mind that, especially for nonlinear problems, the number of basis functions necessary to reach a given accuracy can vary along the time integration.

HO-split versus F-split

We analyze now the advantages of the HO-split versus the F-split as given in (2.4) and (2.3).

In this experiment, the symmetric second order *BAB* composition (1.38) is used to integrate each of the splits. For the HO-split, we compute the harmonic part either with the decomposition (2.15) or in the Hermite basis (2.29) with different numbers of basis terms. The following configurations are used for numerical experiments:

a. The Morse potential [99]

$$V(x) = D_e \left(1 - e^{-a(x-x_e)}\right)^2,$$

with $D_e = 10$, $a = 0.3$ and $x_e = 0$ in atomic units [61], which approximates the energy curve of a molecular bound using the dissociation energy, D_e, and a parameter for the width of the potential, a. The energy spectrum, that corresponds to different vibrational excitations of the molecule, is finite and the eigenvalues are given by

$$E_n = \omega_0 \left(n + \frac{1}{2}\right) \left(1 - \frac{\omega_0 \left(n + \frac{1}{2}\right)}{4D_e}\right), \qquad n = 0, 1, \dots, n_{max},$$

where n_{max} is the largest integer smaller than $2D_e/\omega_0 - 1$ and $\omega_0 = a\sqrt{2D_e}$ is the (classical) vibrational frequency. The corresponding fundamental states are given by

$$\phi_n(x) \propto e^{-z/2} z^{-1/2+\lambda-n} L_n^{-1+2\lambda-2n}(z), \qquad n = 0, 1, \dots, n_{max},$$

with the generalized Laguerre polynomials $L_n^{\alpha}(z)$ and after the coordinate change $z = 2\lambda e^{-a(x-x_e)}$, where we have introduced the constant $\lambda = \sqrt{2D_e}/a$. As initial condition, we have chosen a superposition of the two lowest energy eigenstates,

$$\psi_0 = \frac{1}{\sqrt{2}}\phi_0 + \frac{1}{\sqrt{2}}\phi_1,$$

for which we can trivially compute the reference solution at the final time $T = 10\pi$ to

$$\psi(T) = \frac{1}{\sqrt{2}} \left(e^{-iTE_0}\phi_0 + e^{-iTE_1}\phi_1\right).$$

b. The Pöschl-Teller potential [110] has been introduced as an example of an anharmonic oscillator which is solvable in closed form. We will treat the particular case

$$V(x) = \frac{\lambda(\lambda+1)}{2}\left(1 - \operatorname{sech}(x)^2\right), \tag{2.30}$$

with $\lambda = 4$. The energy spectrum is finite and can be computed to (for $\lambda \in \mathbb{N}_0$)

$$E_n = -\frac{(\lambda - n)^2}{2}, \qquad n = 0, \dots, \lambda - 1,$$

The fundamental states are

$$\phi_n(x) \propto L_n^{\lambda}(\tanh(x)), \qquad n = 0, \dots, \lambda - 1,$$

with the associated Legendre functions L_n^{α}. Again, the superposition of the lowest eigenvectors will be the initial condition, $\psi_0 = \frac{1}{\sqrt{2}}(\phi_0 + \phi_1)$, and the reference solution is computed at the final time $T = 10$ using the eigenvalues.

c. The harmonic oscillator perturbed by a Pöschl-Teller potential

$$V(x) = \frac{1}{2}\omega^2 x^2 + \frac{\lambda(\lambda+1)}{2}\left(1 - \operatorname{sech}(x)^2\right),$$

with $\omega = 2$ and $\lambda = 1$. No closed form solution to this problem is known, but parts of the spectrum can be calculated by the imaginary time propagation, cf. Chapter 5. As initial condition, we have used the superposition of the lowest eigenvectors, that have been obtained numerically to sufficiently high precision, $\psi_0 = \frac{1}{\sqrt{2}}(\phi_0 + \phi_1)$, and the reference solution at final time $T = 10$ is computed directly using the corresponding eigenvalues.

The experiments are based on the leapfrog (LF) method (1.38), and we denote by LF_F, LF_H and $\mathrm{LF}_H M$ its implementations with the F-split, the HO-split using the new Hermite-Fourier method (with the composition (2.15)) and the HO-split using M Hermite basis functions in (2.29), respectively. For all integrations, we use equidistant grid points and the chosen spatial and temporal intervals are specified in the labels of Fig. 2.2a,b,c. We measure the error versus the number of basis changes, i.e., FFTs or Hermite transforms, which can be considered proportional to the computational cost and plot the results in Fig. 2.2. The main observations are that, as expected, the standard Hermite method has to be calibrated to get a sufficiently large number of basis vectors to reach high accuracy. The Fourier-Hermite split does not show this behavior. In the worst case, it behaves like the standard Fourier-split, however, if the harmonic part is dominant, it will perfectly recover the Hermite method. We point out that, even though the harmonic oscillator does not dominate in the first two examples, the HO split $(T + \frac{1}{2}\omega^2 x^2) + (V(x) - \frac{1}{2}\omega^2 x^2)$ does not deteriorate in comparison to the Fourier split since T and V are of comparable size for the chosen initial conditions and it comes at the same computational cost.

To validate the results in higher dimensions graphically, we have studied the evolution of a two-dimensional perturbed harmonic oscillator with a constant isotropic mass-matrix $\Lambda = \mathrm{diag}\{1, 1\}$,

$$H = \frac{1}{2}p^T \Lambda p + \frac{1}{2}q^T \Omega q + \frac{1}{100}x^4, \qquad p^T = (p_x, p_y), \quad q^T = (x, y), \tag{2.31}$$

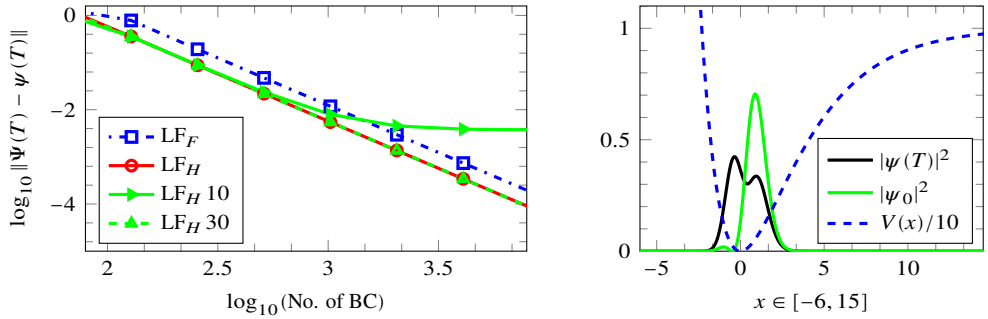

(a) Morse potential, $T = 10\pi$, $N = 512$

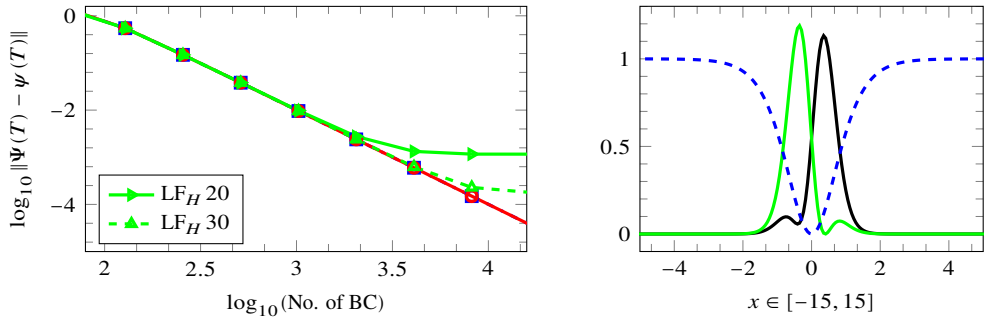

(b) Pöschl-Teller potential, $T = 10$, $N = 512$

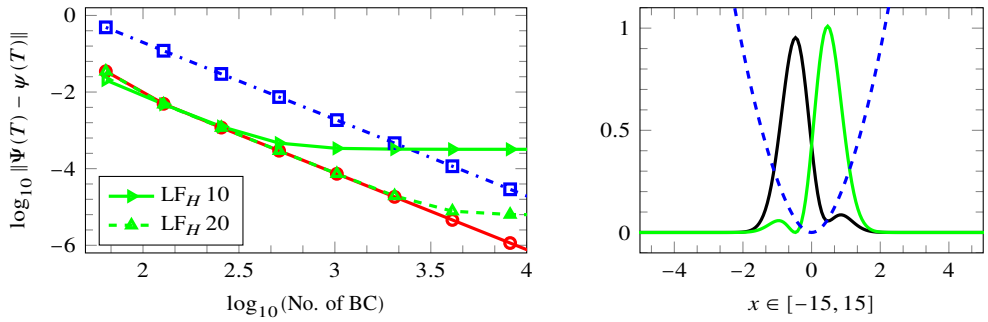

(c) Perturbed Pöschl-Teller potential, $T = 10$, $N = 512$

Figure 2.2: The left column shows the error vs. the number of basis changes (BC), i.e., Fourier or Hermite transforms, in logarithmic scale for the integration of three test potentials using the HO split (subscript H) and the standard split (subscript F) using the leapfrog method (1.38). In the right column, the initial condition (green), the exact solution (black) and the potentials (dashed blue), scaled by $1/10$ to fit the axes, are shown. Unless specified otherwise, the legends of the first row are also valid for remaining parts.

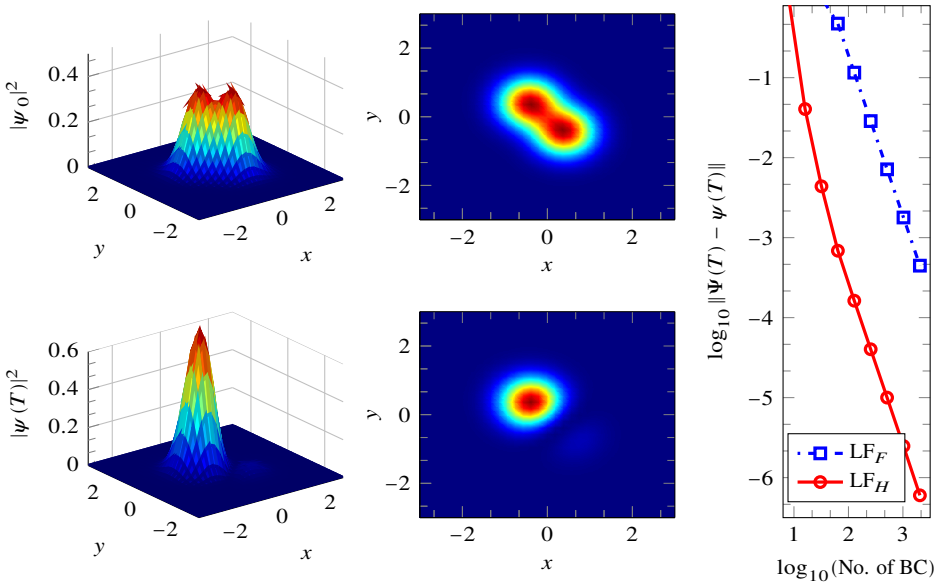

Figure 2.3: The rightmost column shows the efficiency curves for the 2D perturbed harmonic oscillator (2.31) integrated using $N_x = N_y = 128$ equidistant grid points on $[-10, 10]^2$. In the first row, the squared absolute value of the initial condition, in 3D (left) and from above (center), is displayed, whereas the evolution at time $T = 10$ is depicted in the second row, both in 3D (left) and from above (center).

and frequency matrix $\Omega = \left(\begin{smallmatrix} 4 & 1 \\ 1 & 4 \end{smallmatrix}\right)$. The spatial coordinates are discretized with 128×128 equidistant grid points on the square $[-10, 10] \times [-10, 10]$ and we integrate until the final time $T = 10$. We compare the leapfrog method using the F-split (LF$_F$) and the HO-split (LF$_H$), based on (2.23). Note that the Fourier transforms have to be replaced by their two-dimensional counterpart. The results are reproduced in Fig. 2.3. As expected, near integrability and thus small error coefficients are recovered by the HO-split.

2.2 The Harmonic Oscillator: non-autonomous

The previous results lend their methodology to the important generalization for time-dependent potentials. In this section, we show how to build splitting methods for time-dependent potentials, with a special focus on the important cases of harmonic trapping (see Ref. [90] and citations thereof) or linear potentials that usually arise from Laser-interactions.

2.2.1 Varying trap frequency

For general time-dependencies, the quantum harmonic oscillator problem can be stated as

$$i\partial_t \psi(x,t) = \left(\frac{1}{2m(t)}p^2 + \frac{1}{2}m(t)\omega(t)^2x^2\right)\psi(x,t), \quad \psi(x,0) \in L^2(\mathbb{R}). \tag{2.32}$$

The associated Lie algebra again has three basis elements, $E = x^2/2$, $F = p^2/2$, and $G = \frac{1}{2}(xp + px)$ and the solution, $\psi(x,t) = U(t,0)\psi(x,0)$, of (2.32) can be expressed as a single exponential using the Magnus series expansion, cf. Section 1.3.4 [93, 23], or as a product of exponentials [127]. It is possible to formulate the evolution operator $U(t,0)$ in many different ways, the most appropriate depending on the particular purpose, e.g., using the Magnus expansion

$$U(t,0) = \exp\left(f_1(t)E + f_2(t)F + f_3(t)G\right) \tag{2.33}$$

for certain functions $f_i(t)$. The reason is that since F, G, E form a basis of the Lie algebra of the problem, there exist functions $f_i(t)$ that correspond to the summation of the Magnus series. The functions can be obtained by solving a set of differential equations, cf. Ref. [130].

On the other hand, approximations of (2.33) for one time step, h, are easily obtained, e.g., a fourth-order commutator-free method is given by [31]

$$\begin{aligned} U(t+h,t) = \exp\left(-i\,\frac{h}{2}\left(\frac{1}{2m_L}p^2 + \frac{1}{2}m_L\omega_L^2x^2\right)\right) \\ \times \exp\left(-i\,\frac{h}{2}\left(\frac{1}{2m_R}p^2 + \frac{1}{2}m_R\omega_R^2x^2\right)\right) + \mathcal{O}(h^5), \end{aligned} \tag{2.34}$$

where

$$\begin{aligned} m_L &= \alpha m_1 + \beta m_2, & m_R &= \beta m_1 + \alpha m_2, \\ m_L\omega_L^2 &= \alpha m_1\omega_1^2 + \beta m_2\omega_2^2, & m_R\omega_R^2 &= \beta m_1\omega_1^2 + \alpha m_2\omega_2^2, \end{aligned}$$

with $\omega_j = \omega(t_n + c_j h), m_j = m(t_n + c_j h)$, $c_1 = \frac{1}{2} - \frac{\sqrt{3}}{6}$, $c_2 = \frac{1}{2} + \frac{\sqrt{3}}{6}$, and $\alpha = \frac{1}{2} - \frac{1}{\sqrt{3}}$, $\beta = 1 - \alpha$. It can be considered as the composition of the evolution for half a time step of two oscillators with averaged frequencies, using the fourth-order Gauss-Legendre quadrature rule to evaluate $\omega(t)$. Different quadrature rules can also be be used and correspond to different averages along the time step, see Refs. [31, 23]. In the limit when ω is constant, the exact solution is recovered. Higher order approximations are available, if more accurate results are desired, by approximating the functions f_j in (2.33) via truncated Magnus expansions.

The following theorems extend this idea to decompositions of operators that appear after the approximation of the time dependent parts via (2.33) or by the composition (2.34).

Theorem 2.2.1. *Let α, β, γ be constants, $\eta = \sqrt{\alpha\gamma - \beta^2}$ and*

$$\begin{aligned} g(t) &= \gamma/\eta \cdot \sin(\eta t), \\ f(t) &= \frac{1}{g(t)}\left(1 - \cos(\eta t) + \frac{\beta}{\eta}\sin(\eta t)\right), \\ e(t) &= \frac{1}{g(t)}\left(1 - \cos(\eta t) - \frac{\beta}{\eta}\sin(\eta t)\right). \end{aligned} \tag{2.35}$$

Then, the following decomposition holds for $0 \leq t < \pi/\eta$*:*

$$e^{-i\frac{t}{2}\left(\alpha x^2+\beta(xp+px)+\gamma p^2\right)} = e^{-if(t)\frac{1}{2}x^2}\ e^{-ig(t)\frac{1}{2}p^2}\ e^{-ie(t)\frac{1}{2}x^2}. \tag{2.36}$$

Proof. The proof follows the lines of the proof of Lemma 2.1.1. The evolution operator associated to the classical Hamiltonian $H = \frac{1}{2}\left(\alpha x^2 + 2\beta xp + \gamma p^2\right)$ is given by

$$\begin{pmatrix} \cos(\eta t) + \frac{\beta}{\eta}\sin(\eta t) & \frac{\gamma}{\eta}\sin(\eta t) \\ -\frac{\alpha}{\eta}\sin(\eta t) & \cos(\eta t) - \frac{\beta}{\eta}\sin(\eta t) \end{pmatrix},$$

and equality to the right hand side of (2.36) is verified by straightforward computation of the matrix exponentials. The solution is valid until the first singularity at $t = \pi/\eta$. Using (2.12), it can be checked that both sides of (2.36) satisfy the same differential equation and initial conditions. Now, the initial conditions become $f(0) = -e(0)$, $g(0) = 0$ because the loss of symmetry in the decomposition has to be taken into account. □

Theorem 2.2.2. *Let* $m_k, \omega_k \in \mathbb{R}$, $c_k = \cos(\omega_k h/2)$, $s_k = \sin(\omega_k h/2)$ *for* $k = L, R$ *and*

$$\begin{aligned} g(h) &= s_L c_R/(m_L\omega_L) + c_L s_R/(m_R\omega_R), \\ f(h) &= \frac{1}{g(h)}\left(1 - c_L c_R + \frac{m_L\omega_L}{m_R\omega_R}s_L s_R\right), \\ e(h) &= \frac{1}{g(h)}\left(1 - c_L c_R + \frac{m_R\omega_R}{m_L\omega_L}s_L s_R\right). \end{aligned} \tag{2.37}$$

Then, the following decomposition

$$e^{-i\frac{h}{2}\left(\frac{1}{2m_L}p^2+\frac{1}{2}m_L\omega_L^2x^2\right)}\ e^{-i\frac{h}{2}\left(\frac{1}{2m_R}p^2+\frac{1}{2}m_R\omega_R^2x^2\right)} = e^{-if(h)\frac{1}{2}x^2}\ e^{-ig(h)\frac{1}{2}p^2}\ e^{-ie(h)\frac{1}{2}x^2}$$

is satisfied for $0 \leq h < h^*$*, where* h^* *is the smallest positive root of* $g(h)$*.*

The proof is similar to the previous one. □

2.2.2 The driven oscillator

Only a minor ingredient is needed to extend the previous results to the more general case of a quantum mechanical particle subject to some laser interaction. The Laser acts on the dipole momentum of the particle which is proportional to the position operator and the Hamiltonian in its general form can be written as

$$H_0(t) = \sum_{j=1}^{6} f_j(t)E_j \tag{2.38}$$

with $E_1 = 1, E_2 = x, E_3 = p, E_4 = \frac{1}{2}x^2, E_5 = \frac{1}{2}p^2, E_6 = \frac{1}{2}(xp + px)$. The operators E_i are basis elements of an algebra $\mathfrak{g}_{\mathrm{HO}}$that is closed under commutation and the nonzero commutators are

$$\begin{aligned} &[E_4, E_5] = iE_6, \quad [E_4, E_6] = 2iE_4, \quad [E_5, E_6] = -2iE_5, \\ &[E_4, E_3] = iE_3, \quad [E_5, E_2] = -iE_2, \quad [E_2, E_3] = iE_1. \end{aligned} \tag{2.39}$$

After applying a time-averaging mechanism that works within the algebra, e.g., the Magnus expansion, it remains to compute the exponential of some element

$$\mathbf{g} = \frac{1}{2}\left(\alpha x^2 + \beta(px + xp) + \gamma p^2\right) + \delta x + \lambda p + \xi \quad \in \mathfrak{g}_{\mathrm{HO}}. \tag{2.40}$$

The main result is stated in the following

Theorem 2.2.3. *For an element* $\mathbf{g} \in \mathfrak{g}_{HO}$ *written as* (2.40)*, the following decomposition holds for* $0 \leq h < \pi/\eta$*:*

$$\exp\left(-ih \cdot \mathbf{g}\right) = e^{-i(\phi + h\xi)} e^{-i(fq^2/2 + d_1 q)} e^{-i(gp^2/2 + d_2 p)} e^{-i(eq^2/2 + d_3 q)} \tag{2.41}$$

where

$$\begin{aligned}
\eta &= \sqrt{\alpha\gamma - \beta^2}, \qquad D_1 = \frac{\delta\gamma - \lambda\beta}{\eta^2}, \qquad D_2 = \frac{\lambda\alpha - \delta\beta}{\eta^2}, \\
f(h) &= \frac{\eta}{\gamma}\tan\left(\frac{\eta h}{2}\right) + \frac{\beta}{\gamma}, & d_1(h) &= D_1 \cdot f(h), \\
g(h) &= \frac{\gamma}{\eta}\sin\left(\eta h\right), & d_2(h) &= D_2 \cdot g(h), \\
e(h) &= \frac{\eta}{\gamma}\tan\left(\frac{\eta h}{2}\right) - \frac{\beta}{\gamma}, & d_3(h) &= D_1 \cdot e(h), \\
\phi(h) &= \frac{h}{2\beta}\left(D_1 D_2 \eta^2 - \lambda\delta\right) + \frac{D_2^2}{2} g(h) + \frac{D_1^2}{2}\left(f(h) - \frac{\beta}{\gamma}\right).
\end{aligned}$$

Proof. The proof differs from the previous in a small but important detail: The classical mechanical algebra does not know about global phases: A constant shift of the potential will not enter the equations of motion. For quantum mechanical problems, on the other hand, such a shift implies a global (constant) phase of the wave function. This phase will not have any physical effects, but for correctness and completeness of the decomposition, we have to pay attention to this peculiarity.

We will proceed as follows: First, we establish a system of differential equations to which the decomposition (2.40) is equivalent, and then construct the solution which can then be verified by the first part. Since the l.h.s. of (2.40) is the solution of the Schrödinger equation (for the evolution operator)

$$i\frac{d}{dt}U(t) = \mathbf{g}\,U, \quad U(0) = 1, \tag{2.42}$$

the right hand side of (2.40) is required to solve the same differential equation for small times to confirm the identity. Defining $U_1 = e^{fx^2 + d_1 x} e^{gp^2 + d_2 p} e^{ex^2 + d_3 x} e^{\phi}$ and plugging it into (2.42) yields

$$\begin{aligned}
\frac{d}{dt}U_1 =& (\dot{f}x^2 + \dot{d}_1 x)U_1 \\
&+ e^{fx^2 + d_1 x}(\dot{g}p^2 + \dot{d}_2 p)e^{-(fx^2 + d_1 x)}U_1 \\
&+ e^{fx^2 + d_1 x} e^{gp^2 + d_2 p}(\dot{e}x^2 + \dot{d}_3 x)e^{-(gp^2 + d_2 p)} e^{-(fx^2 + d_3 x)}U_1 \\
&+ \dot{\phi}U_1.
\end{aligned}$$

Now, using (2.12) to evaluate the kicks and drifts, one obtains the equations

$$\begin{aligned}
x^2: \quad \alpha/2 =& \dot{e}(t)\left(\dot{f}(t) + (1-4f(t)g(t))^2\right) + 4f(t)^2\dot{g}(t),\\
x: \quad \lambda/2 =& \dot{d}_1(t) + (4f(t)g(t)-1)\left(-\dot{d}_3(t) + 2\dot{e}(t)\left(d_2(t)+2d_1(t)g(t)\right)\right)\\
&+ 2f(t)\left(\dot{d}_2(t) + 2d_1(t)\dot{g}(t)\right),\\
p^2: \quad \gamma/2 =& 4g(t)^2\dot{e}(t) + \dot{g}(t),\\
p: \quad \delta/2 =& \dot{d}_2(t) + 2d_1(t)\dot{g}(t) - 2\dot{e}(t)g(t)\left(\dot{d}_3(t) - 2\left(d_2(t)+2d_1(t)g(t)\right)\right),\\
px+xp: \quad \beta =& 4f(t)\dot{g}(t) - 4g(t)\dot{e}(t)\left(1-4f(t)g(t)\right),\\
1: \quad \phi'(t) =& \dot{e}(t)\left(d_2(t)+2d_1(t)g(t)\right)\left(\dot{d}_3(t) - \left(d_2(t)+2d_1(t)g(t)\right)\right)\\
&- d_1(t)\left(\dot{d}_2(t) + d_1(t)\dot{g}(t)\right).
\end{aligned} \tag{2.43}$$

With the initial condition $U_1(0) = 1$, it is easily checked that the functions of Theorem 2.2.3 satisfy the above equations.

For the construction of the functions, we examine the corresponding classical Hamiltonian (cf. (2.40))

$$H = \frac{1}{2}\left(\alpha x^2 + \beta(px+xp) + \gamma p^2\right) + \delta x + \lambda p + \xi \tag{2.44}$$

and we want to decompose it in blocks

$$H_1 = f\frac{1}{2}x^2 + d_1 x, \quad H_2 = g\frac{1}{2}p^2 + d_2 p, \quad H_3 = e\frac{1}{2}x^2 + d_3 x.$$

The corresponding flows are trivial to compute and their composition becomes

$$\begin{aligned}
&\varphi_h^{H_1} \circ \varphi_h^{H_2} \circ \varphi_h^{H_2}\\
&= \begin{pmatrix} 1-h^2gf & hg \\ -h\left(f+e-h^2egf\right) & 1-h^2eg \end{pmatrix}\begin{pmatrix} q_0 \\ p_0 \end{pmatrix} - h\begin{pmatrix} -d_2 + hgd_1 \\ d_1 + d_3 + ed_2 - h^2egd_1 \end{pmatrix}
\end{aligned} \tag{2.45}$$

The full Hamiltonian leads to equations of motion

$$\frac{d}{dt}\begin{pmatrix} q(t) \\ p(t) \end{pmatrix} = \underbrace{\begin{pmatrix} \beta & \gamma \\ -\alpha & -\beta \end{pmatrix}}_{=:A}\begin{pmatrix} q_0 \\ p_0 \end{pmatrix} + \begin{pmatrix} -\lambda \\ \delta \end{pmatrix},$$

which are solved by variation of constants

$$\begin{pmatrix} q(t) \\ p(t) \end{pmatrix} = \exp(tA)\begin{pmatrix} q_0 \\ p_0 \end{pmatrix} + A^{-1}\left(\exp(tA) - 1\right)\begin{pmatrix} -\lambda \\ \delta \end{pmatrix}. \tag{2.46}$$

The exponential of this 2×2 matrix is easily computed to

$$\exp(tA) = \begin{pmatrix} \cos(t\eta) + \beta\frac{\sin(t\eta)}{\eta} & \gamma\frac{\sin(t\eta)}{\eta} \\ -\alpha\frac{\sin(t\eta)}{\eta} & \cos(t\eta) - \beta\frac{\sin(t\eta)}{\eta} \end{pmatrix}$$

with $\eta = \sqrt{\alpha\gamma - \beta^2}$ and the inverse is

$$A^{-1} = \frac{1}{\eta^2}\begin{pmatrix} -\beta & -\gamma \\ \alpha & \beta \end{pmatrix}.$$

Equating (2.45) and (2.46), we obtain a simple system of equations for the functions e, f, g, d_j whose solutions are stated in the theorem. Now, it is trivial to solve the equation for ϕ in (2.43). □

2.2.3 Numerical results

The test bench will be a harmonic oscillator with time-dependent frequency perturbed by a weak static quartic anharmonicity

$$i\frac{\partial}{\partial t}\psi = \left(\frac{1}{2}p^2 + \frac{1}{2}\omega^2(t)x^2\right)\psi + \varepsilon_Q\frac{1}{4}x^4\psi. \tag{2.47}$$

We first consider the case

$$\omega^2(t) = A(1 + \epsilon\cos(wt)) \tag{2.48}$$

with $w = 1/2,\ A = 4,\ \epsilon = 0.1,\ \varepsilon_Q = 0.01$ and the initial condition is taken to be

$$\psi_0 = \frac{1}{(\pi/\omega(0))^{1/4}}e^{-x^2/(2/\omega(0))}.$$

As reference, we take a highly accurate numerical approximation, $\psi(T)$, as exact solution and restrict the spatial domain to $[-20, 20]$ for all experiments in this subsection. We compare the Hermite-Fourier method with the plain Fourier split, since Hermite polynomials are not appropriate in a time-dependent setting.

To be able to appreciate the precision of the Magnus integrator, the methods have to be used with higher order splittings. In particular, we choose the fourth-order, six-stage split $\mathrm{RKN}_6 4$ and the method V84 of generalized order (8,4). Both methods can be found in Table3.2.

For fast oscillating systems and if high accuracy is needed, the two-exponential fourth-order approximation of the harmonic oscillator (2.34) can be improved by taking, for example, a higher order Magnus expansion (2.33). As we have seen, the solution of

$$iU' = \left(\frac{1}{2}p^2 + \frac{1}{2}\omega^2(t)x^2\right)U$$

can be written as

$$U(t,0) = e^{-i\frac{t}{2}\left(\alpha x^2 + \beta(xp+px) + \gamma p^2\right)}, \tag{2.49}$$

and we have considered, for example, a sixth-order Magnus integrator [23] to approximate the evolution operator for one fractional time step, $a_j h$, i.e., $U(t, t + a_j h)$. This is equivalent to taking $t = a_j h$ in (2.49) and the parameters α, β, γ are given by:

$$\alpha = \tfrac{1}{18}(5\omega_1 + 8\omega_2 + 5\omega_3) + \tfrac{(a_j h)^2}{486}(\tfrac{17}{4}(\omega_1^2 + \omega_3^2) + 8\omega_2^2 + \omega_1\omega_2 + \omega_2\omega_3 - \tfrac{37}{2}\omega_1\omega_3),$$
$$\beta = a_j h\sqrt{\tfrac{5}{3}}(\omega_3 - \omega_1)(\tfrac{1}{12} + \tfrac{(a_j h)^2}{3240}(5\omega_1 + 8\omega_2 + 5\omega_3)),$$
$$\gamma = 1 + \tfrac{(a_j h)^2}{54}(\omega_1 - 2\omega_2 + \omega_3),$$

with $\omega_k = \omega(t_n + c_k a_j h),\ k = 1, 2, 3$ and $c_1 = 1/2 - \sqrt{15}/10,\ c_2 = 1/2,\ c_3 = 1/2 + \sqrt{15}/10$, corresponding to a sixth-order Gaussian quadrature rule. The obtained operator is then decomposed according to Theorem 2.2.1.

The results are given in Fig. 2.4a and corroborate the superiority of the HO split.

Another interesting example is given by an intense short pulse modeled via

$$\omega(t) = w_0 \left(1 + \frac{At}{\cosh^2(B(t-2))} \right). \tag{2.50}$$

Varying the parameters A and B, the pulse can be sharpened while keeping its time-average and hence its strength relative to the anharmonicity constant. Figure 2.4b shows the results obtained for a relatively slow variation of the harmonic potential, for the parameters: $w_0 = 4$, $A = 0.25$, $B = 2$. Again, the advantageousness of the presented decomposition can be appreciated. It is already noticeable, that the error introduced by the time-dependence becomes dominant, and this effect increases for more rapidly varying potentials, e.g., for $B \gg 1$. In that case, higher order approximations of the Magnus expansion are necessary to maintain the benefits of the Hermite decomposition.

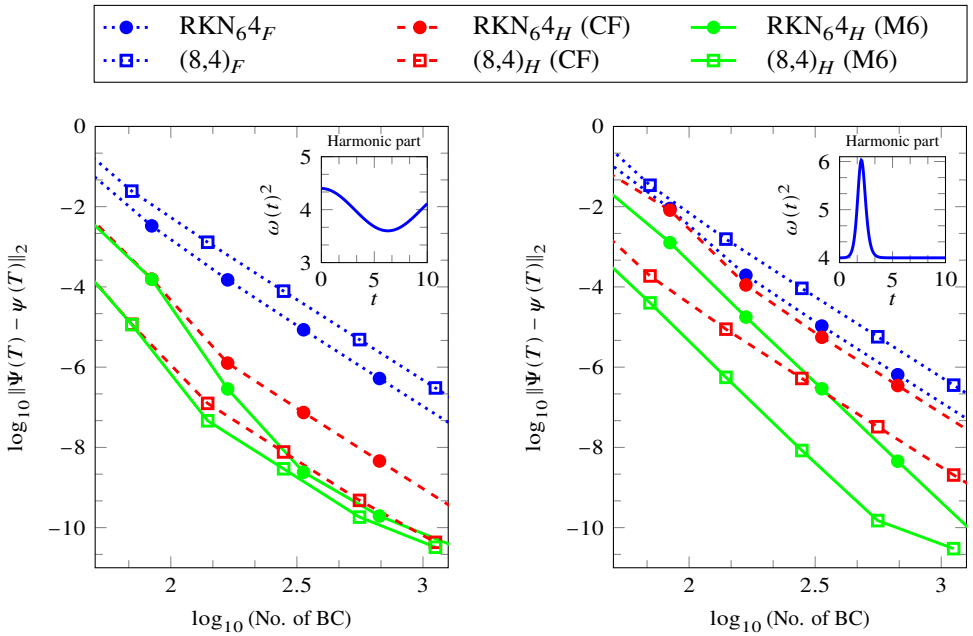

(a) Time-dependence (2.48) with parameters $w = 1/2$, $A = 4$, $\epsilon = 0.1$, and with a small anharmonicity $\varepsilon_Q = 0.01$.

(b) Time-dependence (2.50) with parameters $w_0 = 4$, $A = 0.25$, $B = 2$, $\varepsilon_Q = 0.01$.

Figure 2.4: Comparison of Fourier and Fourier-Hermite splittings for two fourth-order methods for the model potential (2.47), integrated until final time $T = 10$ with $N = 512$ equidistant points on $[-20, 20]$. The (red) dashed line indicates the two-exponential approximation (2.34), the (green) solid line corresponds to the sixth-order Magnus approximation presented in the text (2.49). The insets show the evolution of the harmonic trap frequency $\omega(t)^2$ and the parameters used for the Hamiltonian are given in the sub-captions.

2.3 Rotating traps

A particularly challenging problem is given when a rotation term is included in the potential, i.e., a term that mixes momentum and position coordinates which complicates the splitting procedures that rely on the separability thereof. Recent approaches have been exploiting the closed form availability of the solution of harmonically trapped particles subject to a rotation term via Laguerre polynomials [16, 73]. However, the main drawbacks are a mix of different spatial discretizations, when three-dimensional problems are considered and the computational cost due to the Laguerre transform.

The objective is to use the tools developed in the previous sections to achieve a decomposition that can be computed using only Fourier transforms.

We consider the two-dimensional Hamiltonian

$$H = p_x^2 + p_y^2 + \Omega L_z + V(x,y), \quad \Omega \in \mathbb{R}, \tag{2.51}$$

where the angular momentum operator is given by $L_z = (xp_y - yp_x)$. For $\Omega = 0$, the standard split separates momentum and spatial coordinates, which both lead to diagonal matrices in their respective basis and exponentiation is trivial. Our goal is to compute the exponential e^{-ihH} to high order in h by a split of type

$$e^{f(x,y)} e^{g_1(x,p_y)} e^{e(p_x,p_y)} e^{g_2(y,p_x)} e^{f(x,y)}, \tag{2.52}$$

where each exponent is diagonal in an efficiently computable basis. We point out that mixed terms, as for example yp_x, can be cheaply diagonalized by using a one-dimensional FFT and the only terms to avoid involve both momentum and position in the same coordinate, e.g., $xp_x, yp_y, x + p_x$, etc.

2.3.1 Angular momentum algebra

Before addressing the full problem, we present exact decompositions for certain subproblems, beginning with only the rotation term ΩL_z.

Its components xp_y and yp_x generate a finite dimensional algebra $\mathfrak{g}_1$, since

$$\begin{aligned}
[xp_y, yp_x] &= xp_x p_y y - yp_y p_x x = xp_x(-i + yp_y) - yp_y(-i + xp_x) \\
&= -i(xp_x - yp_y), \\
[xp_y, [xp_y, yp_x]] &= -i([xp_y, xp_x] - [xp_y, yp_y]) \\
&= -i\left((x^2 p_x - xp_x x)p_y - x(p_y yp_y - yp_y^2)\right) \\
&= -i\left((ix)p_y - x(-ip_y)\right) = 2xp_y, \\
[yp_x, [xp_y, yp_x]] &= -2yp_x,
\end{aligned}$$

and by setting $E = xp_y$, $F = -yp_x$ and $G = (xp_x - yp_y)$, we obtain a three-dimensional algebra with commutators

$$[E,F] = iG, \quad [E,G] = 2iE, \quad [F,G] = -2iF. \tag{2.53}$$

This algebra is isomorphic to the algebra of the simple harmonic oscillator (2.10) which allows us to apply the decomposition given in Lemma 2.1.1 and state the following

Lemma 2.3.1. *Let* $A = xp_y$, $B = -yp_x$ *and*

$$f(t) = (1 - \cos(t\Omega))\,/\sin(\Omega), \quad g(t) = \sin(t\Omega).$$

Then, the following property is satisfied for $|t\Omega| < \pi$*:*

$$e^{-it\Omega L_z} = e^{-if(t)A}\, e^{-ig(t)B}\, e^{-if(t)A} \tag{2.54}$$

$$= e^{-if(t)B}\, e^{-ig(t)A}\, e^{-if(t)B}. \tag{2.55}$$

Proof. Since $L_z = A + B$ and A, B correspond via the algebra isomorphism (2.53)→(2.10) to the kinetic and potential energy operators of the standard harmonic oscillator, the proof of Lemma 2.1.1 can be reused. The rotational strength Ω is accounted for by (2.20) with the identifications $\frac{1}{m} = \Omega$ and $m\omega^2 = \Omega$ which are trivially solved by $\omega = \Omega$. □

This allows us to compute the rotation exactly with two 2D-FFTs, the computational complexity being $\mathcal{O}\big(N^2 \log N\big)$. However, one has to keep in mind that this term is usually embedded in a more complex Hamiltonian where the remaining terms are diagonal in either spatial or momentum coordinates and therefore, two additional 1D-FFTs become necessary at the beginning and at the end of the decomposition. The total is two 2D- and $2N$ 1D-FFTs, or equivalently[6] three 2D-FFTs.

2.3.2 The rotation kernel

Including the kinetic energy, the generators are

$$p_x^2,\ p_y^2,\ p_x y,\ p_y x,$$

and apart from the previously obtained identities, the additional non-vanishing commutators are

$$\begin{aligned} [p_x^2, p_y x] &= -2ip_x p_y, & [p_y^2, p_x y] &= -2ip_x p_y, \\ [p_x^2, x p_x] &= -2ip_x^2, & [p_y^2, y p_y] &= -2ip_y^2, \\ [p_x p_y, p_y x] &= -ip_y^2, & [p_x p_y, p_x y] &= -ip_x^2. \end{aligned}$$

We deduce that $[p_x^2 + p_y^2, L_z] = 0$ and thus for $|t| < \pi/\Omega$,

$$e^{-itH} = e^{-i\frac{t}{2}(p_x^2+p_y^2)} e^{-it\Omega L_z} = e^{-it(p_x^2+p_y^2)} e^{-if(t)(-yp_x)}\, e^{-ig(t)xp_y}\, e^{-if(t)(-yp_x)},$$

with the result of Lemma 2.3.1. Taking into account the considerations after the previous lemma, one step imposes an additional 2D-FFT to change from momentum to coordinate space $(p_x, p_y) \to (x, y)$.

[6] For a rectangular grid of $N \times N$ equispaced points, the cost of a 2D-FFT is $2N^2 \log(N)$, whereas a transformation in one coordinate requires N 1D-FFTs and thus only half as many operations.

This result can be improved by eliminating repetitions of diagonalized operators. In other words, whenever the basis has been changed by means of Fourier transforms, we allow all operators that are diagonal to appear in the corresponding exponent. The decomposition stated in the following lemma requires only two 2D-FFT plus the embracing 1D transformations, hence the inclusion of the kinetic terms comes without extra cost.

Lemma 2.3.2. *Given the Hamiltonian* $H = \frac{1}{2m}(p_x^2 + p_y^2) + \Omega L_z$ *and for functions*

$$\begin{aligned} f_1(t) &= \tan(t\Omega/2), \quad & g_1(t) &= t/(m + m\cos(t\Omega)), \\ f_2(t) &= \sin(t\Omega), & g_2(t) &= t\cos(t\Omega)/m, \end{aligned} \tag{2.56}$$

the following identities are satisfied for $|t\Omega| < \pi$*:*

$$\begin{aligned} e^{-itH} &= e^{-i(g_1(t)\frac{1}{2}p_x^2 - f_1(t)yp_x)} e^{-i(g_2(t)\frac{1}{2}p_y^2 + f_2(t)xp_y)} e^{-i(g_1(t)\frac{1}{2}p_x^2 - f_1(t)yp_x)} \\ &= e^{-i(g_1(t)\frac{1}{2}p_y^2 + f_1(t)xp_y)} e^{-i(g_2(t)\frac{1}{2}p_x^2 - f_2(t)yp_x)} e^{-i(g_1(t)\frac{1}{2}p_y^2 + f_1(t)xp_y)}. \end{aligned}$$

Proof. Using the machinery of the previous lemmata, we identify the quantum mechanical problem with its classical counterpart and first solve the system which corresponds to $H = \frac{1}{2}(p_x^2 + p_y^2) + \Omega(xp_y - yp_x)$, namely,

$$\frac{d}{dt}\begin{pmatrix} x \\ y \\ p_x \\ p_y \end{pmatrix} = \begin{pmatrix} 0 & -\Omega & 1/m & 0 \\ \Omega & 0 & 0 & 1/m \\ 0 & 0 & 0 & -\Omega \\ 0 & 0 & \Omega & 0 \end{pmatrix}\begin{pmatrix} x \\ y \\ p_x \\ p_y \end{pmatrix} = (A + B)\begin{pmatrix} x \\ y \\ p_x \\ p_y \end{pmatrix}, \tag{2.57}$$

where

$$A = \begin{pmatrix} 0 & -\Omega & 1/m & 0 \\ 0 & 0 & 0 & 0 \\ 0 & 0 & 0 & 0 \\ 0 & 0 & \Omega & 0 \end{pmatrix}, \qquad B = \begin{pmatrix} 0 & 0 & 0 & 0 \\ \Omega & 0 & 0 & 1/m \\ 0 & 0 & 0 & -\Omega \\ 0 & 0 & 0 & 0 \end{pmatrix}.$$

The matrices A, B generate the same algebra as $\frac{1}{2}p_x^2 - \Omega yp_x$ and $\frac{1}{2}p_y^2 + \Omega xp_y$, respectively. Furthermore, they are both nilpotent, $A^2 = B^2 = 0$. We will identify A_T, B_T with the parts originating from the kinetic energy ($\propto 1/m$) and A_{L_z}, B_{L_z} with the remainder such that

$$A = \frac{1}{m}A_T + \Omega A_{L_z}, \quad B = \frac{1}{m}B_T + \Omega B_{L_z}.$$

Introducing the functions f_j, g_k, we proceed to calculate the exponentials of $\tilde{A} = g_1 A_T + f_1 A_{L_z}$ and $\tilde{B} = g_2 B_T + f_2 B_{L_z}$ to

$$e^{\tilde{A}} = \begin{pmatrix} 1 & -f_1 & g_1 & 0 \\ 0 & 1 & 0 & 0 \\ 0 & 0 & 1 & 0 \\ 0 & 0 & f_1 & 1 \end{pmatrix} \quad \text{and} \quad e^{\tilde{B}} = \begin{pmatrix} 1 & 0 & 0 & 0 \\ f_2 & 1 & 0 & g_2 \\ 0 & 0 & 1 & -f_2 \\ 0 & 0 & 0 & 1 \end{pmatrix}.$$

The flow of (2.57) is readily computed to

$$O(t) = \begin{pmatrix} \cos(h\Omega) & -\sin(h\Omega) & h\cos(h\Omega)/m & -h\sin(h\Omega)/m \\ \sin(h\Omega) & \cos(h\Omega) & h\sin(h\Omega)/m & h\cos(h\Omega)/m \\ 0 & 0 & \cos(h\Omega) & -\sin(h\Omega) \\ 0 & 0 & \sin(h\Omega) & \cos(h\Omega) \end{pmatrix},$$

and equating $O(t) = e^{\tilde{A}} e^{\tilde{B}} e^{\tilde{A}}$ results in a simple system whose solution are precisely the functions f_j, g_k stated in the lemma. As before, we conclude that the results can be carried over to the quantum mechanical problem. □

Remark 2.3.3. *For non-isotropic masses, i.e.,* $H = \frac{1}{2m_x} p_x^2 + \frac{1}{2m_y} p_y^2 + \Omega L_z$*, the functions* g_1, g_2 *have to be replaced by*

$$g_1(t) = \frac{m_x(t\Omega - \sin(t\Omega)) + m_y(t\Omega + \sin(t\Omega))}{2m_x m_y \Omega(\cos(t\Omega) + 1)},$$
$$g_2(t) = \frac{(m_x - m_y)\sin(t\Omega) + t\Omega(m_x + m_y)\cos(t\Omega)}{2m_x m_y \Omega}.$$

2.3.3 Isotropic trap

Along the lines of Lemma 2.3.2, the system can be generalized to the following

Lemma 2.3.4. *Given the Hamiltonian* $H = \frac{1}{2m}\left(p_x^2 + p_y^2\right) + \Omega L_z + \frac{1}{2} m\omega \left(x^2 + y^2\right)$ *and for functions* $\chi(t) = \cos(t\Omega) + \cos(t\omega)$ *and*

$$\begin{aligned} f_1(t) &= m\omega \sin(t\omega)/\chi(t), & f_2(t) &= m\omega \cos(t\Omega)\sin(t\omega), \\ g_1(t) &= \sin(t\omega)/(m\omega\chi(t)), & g_2(t) &= \cos(t\Omega)\sin(t\omega)/(m\omega), \\ e_1(t) &= \sin(t\Omega)/\chi(t), & e_2(t) &= \cos(t\omega)\sin(t\Omega), \end{aligned} \tag{2.58}$$

the following identities are satisfied for $|t|$ *less than the smallest root of* $\chi(t)$

$$\begin{aligned} e^{-itH} &= e^{-i(f_1 \frac{1}{2}x^2 + g_1 \frac{1}{2}p_y^2 + e_1 x p_y)} e^{-i(f_2 \frac{1}{2}y^2 + g_2 \frac{1}{2}p_x^2 - e_2 y p_x)} e^{-i(f_1 \frac{1}{2}x^2 + g_1 \frac{1}{2}p_y^2 + e_1 x p_y)} \\ &= e^{-i(f_1 \frac{1}{2}y^2 + g_1 \frac{1}{2}p_x^2 - e_1 y p_x)} e^{-i(f_2 \frac{1}{2}x^2 + g_2 \frac{1}{2}p_y^2 + e_2 x p_y)} e^{-i(f_1 \frac{1}{2}y^2 + g_1 \frac{1}{2}p_x^2 - e_1 y p_x)}. \end{aligned}$$

The t-dependence of the functions f_j, g_k, e_l *has been omitted for brevity.*

Proof. The proof is virtually identical to the one above. The resulting equations in the corresponding classical mechanical system are easy to solve. □

2.3.4 Anisotropic trap

The same principles can be applied for a rotating gas subject to anisotropic harmonic trapping, which corresponds to the Hamiltonian

$$H = \frac{1}{2m}\left(p_x^2 + p_y^2\right) + \frac{1}{2} m\omega_x^2 x^2 + \frac{1}{2} m\omega_y^2 y^2 + \Omega L_z.$$

The Hamiltonian can be written in a simpler form as [103]

$$H = \frac{1}{2}\left(p_x^2 + p_y^2 + (1+\eta)x^2 + (1-\eta)y^2\right) + \tilde{\Omega} L_z,$$

where the length has been rescaled in units of the harmonic oscillator $l = 1/\sqrt{m\omega_0}$ with the mean frequency $\omega_0^2 = (\omega_x^2 + \omega_y^2)/2$. The rotation frequency then becomes $\tilde{\Omega} = \Omega/\omega_0$,

and the anisotropy parameter is given by $\eta = (\omega_x^2 - \omega_y^2)/\omega_0^2$. Naturally, the corresponding classical mechanical system can still be easily exponentiated after diagonalizing the matrix ∇H, however, the obtained expressions are lengthy and will not be repeated here. A similar treatment using ladder operators can be found in [92]. Instead, we follow Ref. [103], where an elegant linear canonical transformation[7] to diagonalize the Hamiltonian has been used,

$$u = \gamma_x \left(\cos(\phi)x - \sin(\phi)p_y\right), \qquad p_u = \frac{1}{\gamma_x}\left(\sin(\phi)y + \cos(\phi)p_x\right),$$
$$v = \gamma_y \left(\cos(\phi)y - \sin(\phi)p_x\right), \qquad p_v = \frac{1}{\gamma_y}\left(\sin(\phi)x + \cos(\phi)p_y\right),$$

where $\tan(2\phi) = \frac{2\tilde{\Omega}}{\eta}$ and

$$\gamma_x = \left[\frac{1 + \frac{\eta}{2} + \sqrt{\tilde{\Omega}^2 + \left(\frac{\eta}{2}\right)^2}}{1 - \frac{\eta}{2} + \sqrt{\tilde{\Omega}^2 + \left(\frac{\eta}{2}\right)^2}}\right]^{1/4}, \qquad \gamma_y = \left[\frac{1 - \frac{\eta}{2} - \sqrt{\tilde{\Omega}^2 + \left(\frac{\eta}{2}\right)^2}}{1 + \frac{\eta}{2} - \sqrt{\tilde{\Omega}^2 + \left(\frac{\eta}{2}\right)^2}}\right]^{1/4}.$$

Denoting the eigenvalues by

$$\lambda_u = \sqrt{1 + \tilde{\Omega}^2 + 2\sqrt{\tilde{\Omega}^2 + \left(\frac{\eta}{2}\right)^2}}, \qquad \lambda_v = \sqrt{1 + \tilde{\Omega}^2 - 2\sqrt{\tilde{\Omega}^2 + \left(\frac{\eta}{2}\right)^2}},$$

the Hamiltonian becomes

$$H = \frac{1}{2}\lambda_u \left(p_u^2 + u^2\right) + \frac{1}{2}\lambda_v \left(p_v^2 + v^2\right). \tag{2.59}$$

The condition for bounded states, i.e., a spectrum that is bounded from below, is given by $\eta \leq 1 - \tilde{\Omega}^2$. Using this diagonalization, it has been observed [103] that the new coordinate pairs u, p_u and v, p_v satisfy the canonical commutator relations, i.e., they generate the same algebra as for example p_x and x. Furthermore, the new Hamiltonian is the sum of two uncoupled harmonic oscillators in the new coordinates. The diagonal form of the Hamiltonian has been exploited to apply the decomposition results for the standard harmonic oscillator, however, our correspondence technique yields the same results but is, of course, less elegant than a simple change of coordinates. Finally, for a numerical scheme, one composes

$$e^{-i(C_{p_u}(h)p_u^2 + C_v(h)v^2)} e^{-i(C_{p_u}(h)u^2 + C_v(h)p_v^2)} e^{-i(C_{p_u}(h)p_u^2 + C_v(h)v^2)},$$

with functions $C_j(h)$, for which we refer to the original reference [47]. Note that three 2D-FFTs are necessary for one step of the algorithm.

2.3.5 Time dependence for rotating traps

The most general situation is given if we allow for time-dependencies in the frequencies. Having a splitting in mind where the trapping plays the role of the dominant part H_0, as in Section 2.2.1, a non-autonomous problem has to be solved and we, again, turn towards the Magnus

[7] This transformation corresponds to a change from an inertial to a rotating coordinate system.

expansion. Clearly, the algebra becomes more involved, now bearing commutators of all the elements of the Hamiltonian H_0. Of course, it is perfectly valid to restrict ourselves to commutator free Magnus methods, in this case, however, all the necessary tools have been exhibited in the preceding subsections. Here, we will elaborate a decomposition of an arbitrary order Magnus expansion for arbitrary time-dependencies

$$H_0(t) = \sum_{j=1}^{15} \alpha_j(t) E_j, \tag{2.60}$$

in the algebra $\mathfrak{g}$ with basis

$$\begin{aligned} &E_1 = x, && E_2 = p_x, && E_3 = \tfrac{1}{2}x^2, && E_4 = \tfrac{1}{2}p_x^2, && E_5 = \tfrac{1}{2}\left(xp_x + p_x x\right), \\ &E_6 = y, && E_7 = p_y, && E_8 = \tfrac{1}{2}y^2, && E_9 = \tfrac{1}{2}p_y^2, && E_{10} = \tfrac{1}{2}\left(yp_y + p_y y\right), \\ &E_{11} = xy, && E_{12} = p_x p_y, && E_{13} = xp_y, && E_{14} = yp_x, && E_{15} = 1. \end{aligned} \tag{2.61}$$

Computationally difficult terms that ought to be avoided, are the ones mixing momenta and position of the same coordinate: xp_x and yp_y.

A careful examination of the structure coefficients of the algebra[8] shows that a symmetric ansatz as before,

$$e^{-i(f_1 \frac{1}{2}y^2 + g_1 \frac{1}{2}p_x^2 - e_1 y p_x)} e^{-i(f_2 \frac{1}{2}x^2 + g_2 \frac{1}{2}p_y^2 + e_2 x p_y)} e^{-i(f_1 \frac{1}{2}y^2 + g_1 \frac{1}{2}p_x^2 - e_1 y p_x)},$$

is not able to generate the terms $xp_x, yp_y, p_x p_y, xy$ as well as the linear terms x, y, p_x, p_y. The latter group could be recovered by change of coordinates, or by directly including them in the exponents, the former, on the other hand, requires us to create a new path since, of course, direct inclusion of mixed terms is not viable because of a lack of diagonalization techniques.

As for the time-dependent harmonic oscillator in Theorem 2.2.1, the symmetry condition has to be dropped and we employ the ansatz

$$e^{-i(x^2+x+y+xy)} e^{-i(y^2+p_x^2+p_x-yp_x)} e^{-i(x^2+p_y^2+p_y+xp_y)} e^{-i(y^2+p_x^2+p_x-yp_x)} e^{-i(x^2+x+y+xy)},$$

where the coefficients multiplying the operators have been omitted to improve readability. Unfortunately, the until here successful correspondence methods reaches its limits since the resulting equations become too complicated to find a closed form solution. From a numerical point of view, this is only a minor restriction since the Hamiltonian H_0 is only an approximation obtained after, say, a Magnus expansion and is thus of limited accuracy. Instead of aiming for a closed form solution, it is sufficient to approximate the (averaged) Hamiltonian up to its order.

Before going into tedious and lengthy algebra, let us examine the important case of a varying trapping potential, i.e., only the quadratic terms x, y are subject to time-dependency. Magnus expanding the Hamiltonian, $H(t) = T + \omega_x(t)^2 x^2 + \omega_y(t)^2 y^2 + \Omega L_z$ implies the computation of commutators of $H(t)$ at different instances of time, which turn out to form a proper subalgebra $\mathfrak{g}_1 \subset \mathfrak{g}$, containing the elements

$$\mathfrak{g}_1 = \mathfrak{g} \setminus \operatorname{span}\{x, y, p_x, p_y, 1\}.$$

[8] Cf. Appendix Table A.1

Thus, after rescaling as in the previous subsection, the averaged Hamiltonian can be written as

$$H_{\text{avg.}} = \frac{1}{2}(p_x^2 + p_y^2) + \frac{1}{2}\left(\omega_x x^2 + \omega_y y^2\right) + \Omega_x x p_y - \Omega_y y p_x + \frac{1}{2}\alpha(x p_x p_x x) + \frac{1}{2}\beta(y p_y + p_y y) + \gamma xy + \delta p_x p_y. \quad (2.62)$$

Notice the asymmetry that has been introduced in the angular momentum term due to the time-averaging. The corresponding classical mechanical system is linear, with equations

$$\frac{d}{dt}\begin{pmatrix} x \\ y \\ p_x \\ p_y \end{pmatrix} = \begin{pmatrix} \alpha & -\Omega_y & 1 & \delta \\ \Omega_x & \beta & \delta & 1 \\ -\omega_x & -\gamma & -\alpha & -\Omega_x \\ -\gamma & -\omega_y & \Omega_y & -\beta \end{pmatrix}\begin{pmatrix} x \\ y \\ p_x \\ p_y \end{pmatrix}.$$

We stress that the algebra that is generated by the underlying classical mechanical system is equivalent to the quantum mechanical one, and so is the matrix representation. Along the lines of our previous exposition, and for each time step, we exponentiate the 4×4 matrix and set it equal to the composition

$$\Psi_h = e^{n_1 x^2} e^{f_1 y^2 + g_1 p_x^2 - e_1 y p_x} e^{f_2 x^2 + g_2 p_y^2 + e_2 x p_y} e^{f_3 y^2 + g_3 p_x^2 - e_3 y p_x}, \quad (2.63)$$

which can be easily computed in the matrix formalism. The outcome is a matrix whose entries are multivariate polynomials of degree four[9]. There are ten degrees of freedom in the original Hamiltonian, one for each basis element. For the composition, we omit the difficult mixed terms xp_x, yp_y as well as xy and $p_x p_y$ and complete the system by introducing additional variables, as seen in (2.63). In total, one step of the algorithm requires the application of two 1D-FFTs and two 2D-FFTs, at the cost of three 2D-FFTs, and prior to evolving the wave function, the coefficients are determined through exponentiating a 4×4 matrix and solving a small nonlinear system. The effort for the solution of the formally over-determined system, which can be done by a least-square algorithm, is marginal since - for small time steps - the solution is not far from $0 \in \mathbb{R}^{10}$. If further speed-up is necessary, the number of variables and equations can be reduced by simple algebra or using a Gröbner basis.

Special cases In passing, we mention some further special cases, for which the algebra simplifies.

- Isotropic trap,

  $$H = \frac{1}{2m(t)}\left(p_x^2 + p_y^2\right) + \frac{1}{2}m(t)\omega(t)^2(x^2 + y^2) + \Omega(t)L_z$$

  Due to cancellations, the commutators of H at different instances lie in the span of $\{p_x^2 + p_y^2, x^2 + y^2, L_z, (xp_x + p_x x) + (yp_y + p_y y)\}$ and any Magnus integrator can be written as effective Hamiltonian

  $$\tilde{H}_{t,t+h} = a_{t,t+h}(p_x^2 + p_y^2) + b_{t,t+h}(x^2 + y^2) + c_{t,t+h}L_z + d_{t,t+h}\left((xp_x + p_x x) + (yp_y + p_y y)\right).$$

[9] For the full matrix, see Appendix Section A.3

- Linear interaction,

$$H = \frac{1}{2}\left(p_x^2 + p_y^2\right) + \frac{\omega_0^2}{2}\left(x^2 + y^2\right) + \xi_x(t)x + \xi_y(t)y + \Omega L_z$$

  The following terms in algebra do not appear: $xy, p_x p_y, xp_x, yp_y$, therefore, a symmetric composition is sufficient.

For more complicated Hamiltonians, in particular, when linear terms are involved, the described procedure fails to a certain degree: As for the one dimensional problem, the phase relation cannot be recovered. Nevertheless, it is an easy exercise to compute the corresponding classical equations, just as in 1D, cf. (2.45) and (2.46). In principle, one could approximate the phase numerically, by evaluating the scalar functions on a fixed grid which partitions the time-step interval $[t_n, t_n + h]$ and then solve the differential equations which are analogous to (2.43) numerically, or alternatively make use of the BCH formula.

This effort can be spared since only the global phase information is lost which is not observable. The polynomial system to be solved then needs additional degrees of freedom to cater for the linear contributions and to close the discussion, we conjecture that there exist (under mild assumptions[10]) imaginary coefficients, such that

$$\Psi_h = e^{n_1 x^2 + m_1 x} e^{f_1 y^2 + g_1 p_x^2 - e_1 y p_x + k_1 p_x} e^{f_2 x^2 + g_2 p_y^2 + e_2 x p_y + k_2 p_y} e^{f_3 y^2 + g_3 p_x^2 - e_3 y p_x + k_3 p_x} e^{n_2 x^2 + m_2 x},$$

is the solution of the SE with Hamiltonian (2.60) for small values of the α_j.

2.3.6 Numerical results

To numerically verify the proposed algorithm, we choose the Hamiltonian

$$H_L(t) = \frac{1}{2}\left(p_x^2 + p_y^2\right) + \frac{1}{2}\left(\omega_x(t)^2 x^2 + \omega_y(t)^2 y^2\right) + \Omega L_z, \tag{2.64}$$

where $\omega_x(t)^2 = 4(1 + \sin(t/2))$, $\omega_y(t)^2 = (4 - \sin(t/2))$ and $\Omega = 1/10$. The spatial domain is discretized with 128×128 grid points on $[-10, 10]^2$ and we integrate the normalized initial condition $\psi_0 \propto (x + iy)e^{-(x^2+y^2)/2}$ until the final time $T = 3$. For the time-averaging we choose a fourth-order Magnus integrator that is in turn based on the fourth-order Gauss-Legendre quadrature,

$$\Theta_{t,t+h}^{[4]} = -i\frac{h}{2}\left(H(t_1) + H(t_2)\right) + \frac{h^2}{4\sqrt{3}}[-iH(t_1), -iH(t_2)],$$

[10] In order to recover the mixed terms xp_x, yp_y, a pair of possible generators must be present in the Hamiltonian, e.g., x, p_x^2 can generate xp_x through commutation.

where $t_j = t + hc_j$ with the standard Gauss-nodes $c_{1,2} = (1 \mp 1/\sqrt{3})/2$. Evaluating the commutator leads to

$$\begin{aligned} i\Theta^{[4]}_{t,t+h} = \frac{1}{2}\left(p_x^2 + p_y^2\right) + \frac{1}{2}\frac{\omega_x(t_1)^2 + \omega_x(t_2)}{2}x^2 + \frac{1}{2}\frac{\omega_y(t_1)^2 + \omega_y(t_2)}{2}y^2 + h\Omega L_z \\ + \frac{1}{4\sqrt{3}}\left(\frac{xp_x + p_x x}{2}\left(\omega_x(t_2)^2 - \omega_x(t_1)^2\right) + \frac{yp_y + p_y y}{2}\left(\omega_y(t_2)^2 - \omega_y(t_1)^2\right)\right) \\ + \frac{\Omega}{4\sqrt{3}}xy\left(\left(\omega_y(t_2)^2 - \omega_y(t_1)^2\right) - \left(\omega_x(t_2)^2 - \omega_x(t_1)^2\right)\right). \end{aligned}$$

In a first experiment, we compare the split (2.63) against a standard symmetric approach which uses the same number of FFTs per step,

$$\begin{aligned} \Psi^{[2]}_{t,t+h} = e^{-i\frac{h}{2}(\omega_x(t)^2x^2 + \omega_y(t)^2y^2)/2} e^{-i\frac{h}{2}\left(p_x^2/2 - \Omega y p_x\right)} e^{-ih\left(p_y^2/2 + \Omega x p_y\right)} \\ e^{-i\frac{h}{2}\left(p_x^2/2 - \Omega y p_x\right)} e^{-i\frac{h}{2}(\omega_x(t+h)^2x^2 + \omega_y(t+h)^2y^2)/2}. \end{aligned} \tag{2.65}$$

Notice that the time has been advanced in the center step which assures overall symmetry of the method. The results are shown in Fig. 2.5 and clearly show the correct order and high accuracy of the new method.

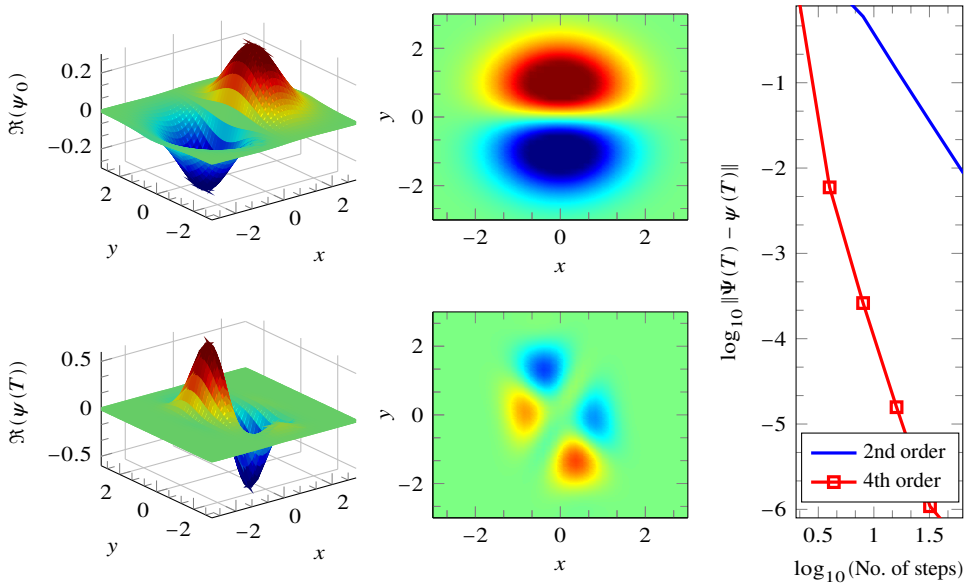

Figure 2.5: The rightmost column shows the efficiency curves for the 2D rotating harmonic oscillator (2.64) integrated using $N_x = N_y = 128$ equidistant grid points on $[-10, 10]^2$. In the first row, the initial condition with real (left) and imaginary part (center) are displayed, whereas the evolution at time $T = 3$ is depicted in the second row, both for real (left) and imaginary part (center). The imaginary part is shown from above and the colormaps are kept constant in each row, i.e., the same color corresponds to the same value.

In a second experiment, the Hamiltonian H_L is perturbed by a quartic potential,

$$H(t) = H_L(t) + \frac{1}{10}x^4 \tag{2.66}$$

and the experimental setup is taken as above. Instead of embedding our method within a higher-order splitting, we chose a simple Strang-type approach where the perturbation $H - H_L$ is appended on both sides of the method. Of course, despite the fourth-order Magnus expansion, we only expect a second-order integrator, however, with much smaller error terms when compared to (2.65) due to the smallness of the perturbation. The results in Fig. 2.6 confirm the predicted behavior.

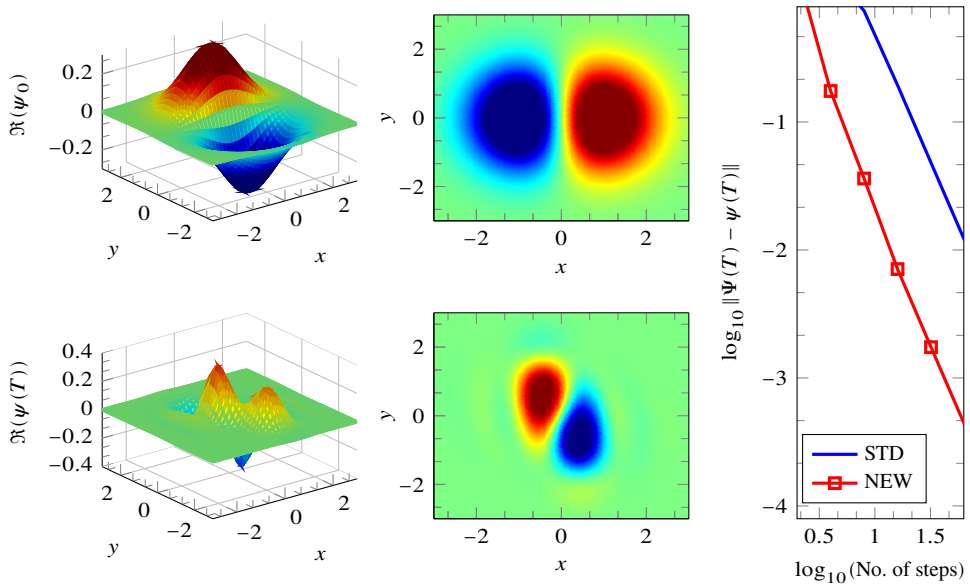

Figure 2.6: For detailed captions, cf. Fig. 2.5. Results for the perturbed Hamiltonian (2.66). The top row shows the real (left) and imaginary part (center) of the initial condition, whereas the corresponding pictures for the exact solution at $T = 3$ are displayed in the bottom row. The right panel demonstrates the smaller error constant for the proposed decomposition (2.63) (red squares) in comparison with the standard scheme (2.65) (blue).

Chapter 3

NON-LINEAR EQUATIONS: GROSS-PITAEVSKI

The numerical integration of the Gross-Pitaevskii equation (GPE)

$$i\frac{\partial}{\partial t}\psi(x,t) = \left(-\frac{1}{2m}\Delta + V(x,t) + \sigma(t)|\psi(x,t)|^2\right)\psi(x,t), \qquad \psi(x,0) \in L^2(\mathbb{R}^d)$$

$x \in \mathbb{R}^d$, describing the ground state of interacting bosons at zero temperature, the Bose-Einstein condensates, has attracted great interest [13, 106, 123] after the first experimental realizations [2, 35, 49].

We present a new efficient way to solve a special class of GPE, namely that of weakly interacting bosons in a single time-dependent trap. To be more specific, the potential trap V is taken to be a perturbation of the (time-dependent) d-dimensional harmonic oscillator, i.e. $V(x,t) = x^T M(t)x + \varepsilon V_I(x,t)$ where $M(t) \in \mathbb{R}^{d\times d}$ is a positive definite matrix and $\varepsilon V_I(x,t)$ is a small perturbation. The real scalar function σ originates from the mean-field interaction between the particles and corresponds to repulsive or attractive forces for positive or negative values of $\sigma(t)$, respectively [107]. It has been demonstrated recently, that $\sigma(t)$ can vary as much as seven orders of magnitude using Feshbach resonances [108]. Notice that the non-interacting case, $\sigma \equiv 0$, corresponds to the linear Schrödinger equation.

Several methods have been analyzed to compute both the time evolution and the ground state of the GPE in the course of the last decade [13, 15, 51, 106, 123], among them finite differences, Galerkin spectral methods and pseudospectral methods for Fourier or Hermite basis expansions. It has been concluded [106] that these pseudospectral methods perform best for a wide parameter range for the GPE.

3.1 Near-integrable systems

When the Hamiltonian can be considered as a perturbed system, i.e., $H = H_0 + \varepsilon V_\varepsilon(x)$ with an exactly solvable part $H_0 = T + V_0(x)$ and a small (possibly nonlinear) perturbation $\varepsilon V_\varepsilon(x)$, it is advantageous to split the Hamiltonian into the dominant part H_0 and its perturbation $\varepsilon V_\varepsilon$. In the introduction, Section 1.3.3, we have defined the concept of generalized order $(s_1, s_2, \dots, s_m)$ in (1.47), which means that the local error of a method Ψ_h satisfies

$$\Psi_h - e^{-ihH} = \mathcal{O}(\varepsilon h^{s_1+1} + \varepsilon^2 h^{s_2+1} + \cdots + \varepsilon^m h^{s_m+1}),$$

where $s_1 \geq s_2 \geq \cdots \geq s_m$. Two very successful splitting methods among this category of Ref. [94] that are used for reference throughout this work are reprinted in Table 3.2.

Even if $\varepsilon = \mathcal{O}(1)$, such methods can be profitable. For instance, suppose one takes a sufficiently fine mesh, then $\|T\| \gg \|V\|$ and the previous considerations apply (with $H_0 = T$). Also, if $V(x) = |x|^n$, then the virial theorem[1] for bounded states ψ,

$$2\langle \psi \, | T \, \psi \rangle = \langle \psi \, | \nabla V(x) x \, \psi \rangle,$$

leads to $\langle T \rangle_\psi = \frac{n}{2} \langle V \rangle_\psi$ and the potential takes the role of the large part for higher degree polynomial potentials.

3.1.1 Spectral methods for the nonlinear Hamiltonian

In this first part, we consider the numerical integration of the Gross-Pitaevskii equation with a potential trap given by a time-dependent harmonic potential or a small perturbation thereof. The purpose is to illustrate how the results obtained in Chapter 2 translate to the nonlinear equation and to demonstrate the superiority of the Fourier-Hermite splitting over standard Hermite methods in the presence of large nonlinearities.

Recalling the results for harmonic oscillators from Chapter 2, the Hermite expansion suggests the split

$$A = \frac{1}{2}(p^2 + x^2), \qquad B(t) = \varepsilon V_I(x,t) + \sigma(t)|\psi|^2, \tag{3.1}$$

where the solution for the equation $i\dot{u} = Au$ can be approximated using a finite number of Hermite basis functions or by Fourier methods with the exact decomposition from Lemma 2.1.1. We take the time as a new coordinate, as in (1.52), and evolve it with A, which is now autonomous and exactly solvable, and freeze the time in B, which is then solved using the result from Lemma 3.1.1.

In the more general situation with a time-dependent frequency, $\omega(t)$,

$$A(t) = \frac{1}{2}(p^2 + \omega^2(t)x^2), \qquad B(t) = \varepsilon V_I(x,t) + \sigma(t)|\psi|^2, \tag{3.2}$$

starting from the HO splitting, the harmonic part is first approximated by Magnus expansions (2.33) or (2.34) and the time is frozen in the remainder, $B(t)$. Theorems 2.2.1 and 2.2.2 then

[1] This theorem only holds in this form for the linear SE, where $\sigma = 0$.

provide decompositions to write the product of exponentials in a similar way as in (2.27) but now $\alpha_k = f(a_{k+1}h) + e(a_k h)$ and it is valid for $|a_j h| < t^*,\ j = 1, \dots, m$ where t^* is the first zero of $g(t)$. At each stage, one has to compute the scalar numbers $f(a_j h), g(a_j h), e(a_j h)$ from $\omega(t)$.

For the remaining part, the following well-known result is very useful and we include the proof for the convenience of the reader.

Lemma 3.1.1. *For real-valued functions $F : \mathbb{R} \times \mathbb{R}^d \times \mathbb{d} \to \mathbb{R}$, the equation*

$$i\frac{\partial}{\partial t}\psi(x,t) = F(t,x,|\psi(x,t)|)\psi(x,t), \tag{3.3}$$

leaves the modulus invariant, $|\psi(x,t)| = |\psi(x,0)|$, and then

$$\psi(x,t) = e^{-i\int_0^t F(s,x,|\psi(x,0)|)\,ds}\psi(x,0), \tag{3.4}$$

which simplifies for autonomous F to

$$\psi(x,t) = e^{-itF(x,|\psi(x,0)|)}\psi(x,0).$$

Proof. Taking the complex conjugate of (3.3) we get $-i\psi_t^* = F(t,x,|\psi|)\psi^*$ and with the product rule

$$\frac{d}{dt}|\psi|^2 = \big(-iF(t,x,|\psi|)\psi\big)\psi^* + \psi\big(iF(t,x,|\psi|)\psi^*\big) = 0,$$

the result $|\psi(x,t)| = |\psi(x,0)|$ follows. Hence, the evolution of (3.3) is governed

$$i\frac{\partial}{\partial t}\psi(x,t) = F(t,x,|\psi(x,0)|)\psi(x,t),$$

whose solution is given by (3.4). □

Commutators For two Lie operators, $\hat{A} = A\partial_\psi + A^*\partial_{\psi^*}$ and $\hat{B} = B\partial_\psi + B^*\partial_{\psi^*}$, a simple calculation confirms that [65]

$$[\hat{A},\hat{B}] = C\partial_\psi + C^*\partial_{\psi^*},$$

with

$$C = \frac{\partial B}{\partial\psi}A - \frac{\partial A}{\partial\psi}B + \frac{\partial B}{\partial\psi^*}A^* - \frac{\partial A}{\partial\psi^*}B^*.$$

In the context of the GPE, the operators take the form

$$\hat{A} = \hat{T} = i\Delta\psi\,\partial_\psi - i\Delta\psi^*\,\partial_{\psi^*}, \quad \hat{B} = \hat{V} = -i(V+\sigma|\psi|^2)\psi\,\partial_\psi + i(V+|\psi|^2)\psi^*\,\partial_{\psi^*},$$

and their commutator $[\hat{T},\hat{V}] = C\partial_\psi + C^*\partial_{\psi^*}$ is readily computed, see also (1.50), with

$$\begin{aligned}
C &= -i(V+2|\psi|^2)(i\Delta\psi) - (i\Delta)\left(-i(V+\sigma|\psi|^2)\psi\right) + (-i\psi^2)(-i\Delta\psi^*) - 0\\
&= [-iV, i\Delta]\psi + 2\sigma|\psi|^2\Delta\psi - \sigma\Delta(|\psi|^2\psi) - \sigma\psi^2\Delta\psi^*\\
&= [-iV, i\Delta]\psi + 2\sigma|\psi|^2\Delta\psi - \sigma\nabla(\psi_x^*\psi^2 + 2\sigma|\psi|^2\psi_x) - \sigma\psi^2\Delta\psi^*\\
&= [V,\Delta]\psi - \sigma\left((\Delta\psi^*)\psi^2 + 2(\nabla\psi^*)\psi\psi_x + 2\left((\nabla\psi^*)\psi(\nabla\psi) + \psi^*(\nabla\psi)(\nabla\psi)\right)\right)\\
&\qquad - \sigma\psi^2\Delta\psi^*\\
&= [V,\Delta]\psi - \sigma\left(2\psi^2\Delta\psi^* + 4\psi(\nabla\psi)\cdot(\nabla\psi^*) + 2\psi^*(\nabla\psi)\cdot(\nabla\psi)\right).
\end{aligned}$$

Table 3.1: Computation of Lie-commutators with MATHEMATICA, with inputs of the form $\hat{O} = (O_R(P, P^*) + iO_I(P, P^*))\partial_P + (O_R(P^*, P) - iO_I(P^*, P))\partial_{P^*}$.

```
LieCom[A_, B_] := Module[{CA, CB, maxder = 10, Dv},
(* Assuming real parameters, the conjugate is taken by replacing P ↔ CP and i ↔ −i *)
  CA = A /. Complex[a_,b_]:>Complex[a,−b] /. P −> PP /. CP −> P /. PP −> CP;
  CB = B /. Complex[a_,b_]:>Complex[a,−b] /. P −> PP /. CP −> P /. PP −> CP;
  Dv[exp_, var_, v_] :=
    D[exp, var[x]]*v + Sum[D[exp, Derivative[k][var][x]]*D[v, {x, k}], {k, 1, maxder}];
(* Output *)
  Dv[B, P, A] − Dv[A, P, B] + Dv[B, CP, CA] − Dv[A, CP, CB]
]
```

A computation using the algorithm in Table 3.1 confirms that $[\hat{V}, [\hat{V}, [\hat{V}, \hat{T}]]] = 0$, and the RKN property also holds for the nonlinear Schrödinger equation.

In the present near-integrable setting, our new method substantially improves the Hermite performance, and it can indeed be regarded as the optimal choice for the number of Hermite basis functions (for an equidistant grid) at each time step.

For the ease of notation, we restrict ourselves to the one-dimensional problem

$$i\frac{\partial}{\partial t}\psi = H_0(t)\psi + \left(\varepsilon V_I(x,t) + \sigma(t)|\psi|^2\right)\psi \tag{3.5}$$

where

$$H_0(t) = \frac{1}{2\mu}p^2 + \frac{1}{2}\mu\omega^2(t)x^2 \tag{3.6}$$

and $p = -i\frac{\partial}{\partial x}$. As in Chapter 2, the boundary conditions imposed by the trap require the wave function to go to zero at infinity, and up to any desired accuracy, we can assume $\psi(x,t)$ and all its derivatives to vanish outside a finite region, say $[a,b]$, which we divide using a mesh (usually with $N = 2^k$ points to allow a simple use of the FFT algorithms). Then, the partial differential equation (3.5) transforms into a system of ordinary differential equations[2] of the same form.

3.1.2 Numerical results

Next, we study the values $\sigma = 10^{-2}, 1, 10^2$ for the nonlinearity parameter and assume the trapping frequency to be constant $\omega = 1$. The case $\sigma = 10^{-2}$ illustrates the performance of the new methods if applied to problems (linear or nonlinear) which are small perturbations of the Harmonic potential whereas the values $\sigma = 1, 10^2$ are large enough to demonstrate the nonlinearity effects on the approximation properties of the methods. Physically, σ is proportional to the number of particles in a Bose-Einstein condensate and to the interaction strength, cf. (1.12) [107].

For all cases, we choose the initial condition $\psi(x,0) = \pi^{-1/4}e^{-x^2/2}$, which is normalized to $\|\psi(x,0)\|_2 = 1$ in the discrete L^2 norm (2.28). We show in Fig. 3.1 the value of $|\psi(x,t)|^2$ at

[2] As we are only interested in the temporal error, we do not distinguish formally between the spatially discretized and the full solution.

the initial and final time, which has been computed numerically to high accuracy. The spatial interval is adjusted to ensure the wave function vanishes (up to round off) at the boundaries, here $[-30, 30]$ (we only show the interval $x \in [-5, 5]$) and discretized at $N = 1024$ equidistant points. One can appreciate that for strong nonlinearities the wave function can considerably penetrate the potential barrier. Then, we expect that an accurate approximation of these wave functions requires a large number of Hermite functions when using (2.7) what renders this procedure inappropriate.

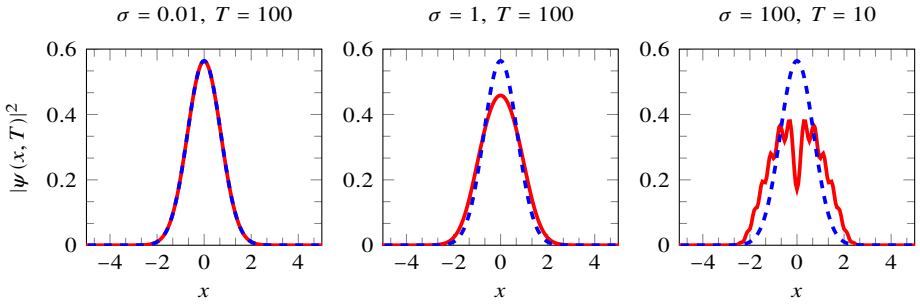

Figure 3.1: Exact evolution at $t = T$ (solid red line) from the initial conditions given by $\psi(x, 0) = \pi^{-1/4} e^{-x^2/2}$ (dashed blue line).

In order to assess the relative performances of different splitting approaches, we use the standard Leapfrog method (1.38)

$$\Psi(nh) = \left(e^{\frac{h}{2}B} e^{hA} e^{\frac{h}{2}B} \right)^n , \tag{3.7}$$

with $A = H_0$, $B = \sigma|\psi|^2$ and $A = T$, $B = \frac{1}{2}x^2 + \sigma|\psi|^2$ for the Hermite and plain Fourier splits, respectively. The results reproduced in Fig. 3.2 show that the Hermite-Fourier method proposed in this work (using the composition (2.15)) is clearly superior for weak perturbations and it keeps similar performance to the F-split for strong nonlinearities. Overall, we conclude that the Fourier-Hermite split is superior since it attains the best performance for all situations where the wave function is localized in a single minimum of the potential by combining the best of both worlds.

Finally, we analyze the performance of different higher order splitting methods which are useful when high accuracies are desired. The following methods (whose coefficients are collected in Table 3.2 for the convenience of the reader) are considered:

- $\text{RKN}_6$4 (the 6-stage fourth-order method from [29]). This is a Runge-Kutta-Nyström method and it is designed for algebras where $[B, [B, [B, A]]] = 0$, being the case for both the F-split and the HO-split.
- V82 (the 4-stage (8,2) *BAB* method from [94]). This method is addressed to perturbed systems. One expects a high performance if the contribution from B is small.
- V84 (the 5-stage (8,4) *BAB* method from [94]).

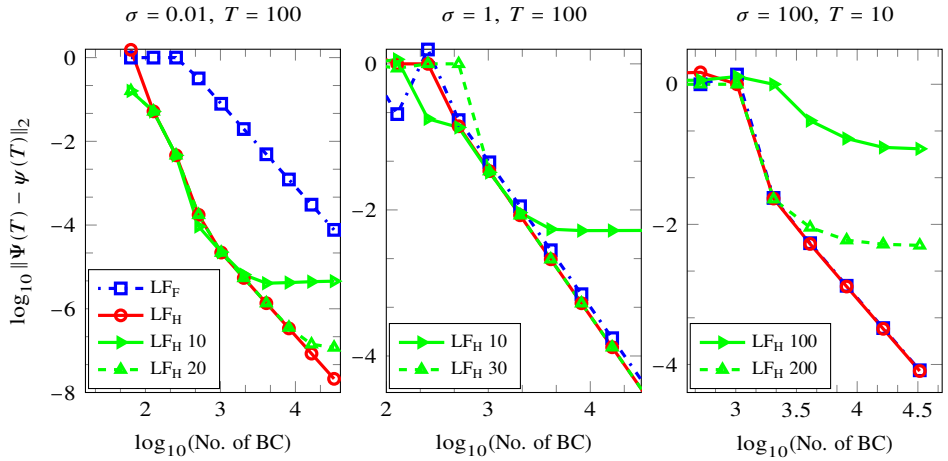

Figure 3.2: Error versus the number of basis changes (BC), i.e., Fourier (dashed blue line) or Hermite transforms, in logarithmic scale for different splittings for the Leap-Frog method (3.7).

Table 3.2: Coefficients for several splitting methods.

The 6-stage $4th$-order method: $\mathrm{RKN}_6 4$ [29]	
$b_1 = 0.0829844064174052$	$a_1 = 0.245298957184271$
$b_2 = 0.396309801498368$	$a_2 = 0.604872665711080$
$b_3 = -0.0390563049223486$	$a_3 = 1/2 - (a_1 + a_2)$
$b_4 = 1 - 2(b_1 + b_2 + b_3)$	$a_4 = a_3,\ a_5 = a_2,\ a_6 = a_1$
$b_5 = b_3,\ b_6 = b_2,\ b_7 = b_1$	
The 4-stage (8,2) method: V82 [94]	
$b_1 = 1/20$	$a_1 = 1/2 - \sqrt{3/28}$
$b_2 = 49/18$	$a_2 = 1/2 - a_1$
$b_3 = 1 - 2(b_1 + b_2)$	$a_3 = a_2,\ a_4 = a_1$
$b_4 = b_2,\ b_5 = b_1$	
The 5-stage (8,4) method: V84 [94]	
$b_1 = 0.811862738544516$	$a_1 = -0.00758691311877447$
$b_2 = -0.677480399532169$	$a_2 = 0.317218277973169$
$b_3 = 1/2 - (b_1 + b_2)$	$a_3 = 1 - 2(a_1 + a_2)$
$b_4 = b_3,\ b_5 = b_2,\ b_6 = b_1$	$a_4 = a_2,\ a_5 = a_1$

We analyze in Figures 3.3-3.5 the three problems specified in Fig. 3.2. In the left panels, the Leap-Frog methods, LF, are compared with the second order V82 methods. In the right panels, we compare the $\mathrm{RKN}_6 4$ methods against the V84 methods jointly with the best among the previous second order methods. Additional experiments with different initial conditions, e.g., for a displaced Gaussian, show that the improvement for the HO-split can be much more pronounced for intermediate values of the nonlinearity parameter, $\sigma = \mathcal{O}(1)$. Note that the number of Hermite basis functions has not been taken into account for the cost in the effi-

ciency plots, and it would further deteriorate their performance. We thus advocate, backed with Fig. 3.2 that they should be discarded in favor of the combined Fourier-Hermite split.

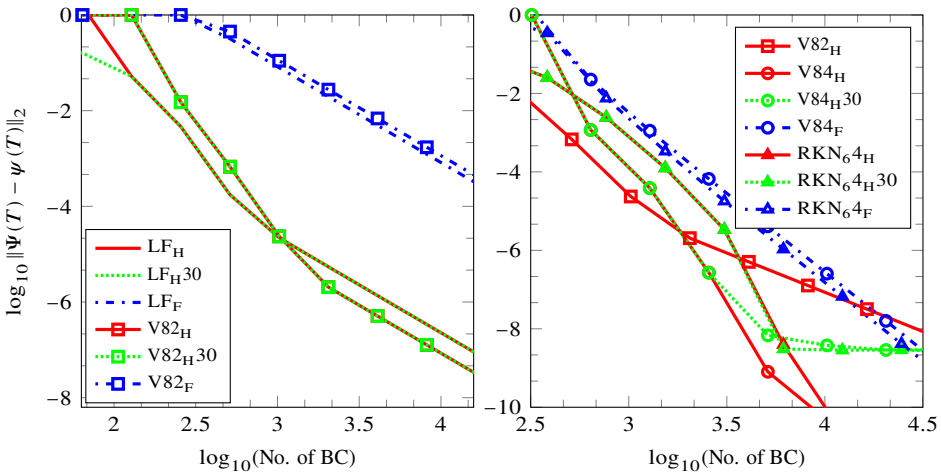

Figure 3.3: Comparison of second order (left panel) and fourth-order (right panel) methods for the different splittings and decompositions discussed in the text and $\sigma = 0.01$. In the both panels and for a wide range of precision, the dashed curves overlap with the solid ones that correspond to the same composition method X_H, i.e., X_H overlaps with X_H30.

For a weak nonlinearity, when the system can be considered as a perturbed harmonic oscillator, we clearly observe that the HO-split is superior to the F-split. In this case, with a relatively small number of Hermite functions, it is possible to approach accurately the solution, but this procedure has a limited accuracy which can deteriorate along the time integration and depends on the initial conditions. Overall, the methods addressed to perturbed problems show the best performance: The $V82_H$ method performs best among the compared when a relatively low accuracy is desired and the $V84_H$ method takes its place for higher accuracies.

Figure 3.4 shows the results for $\sigma = 1$. It is qualitatively similar to the previous case yet the HO-split does not outperform the plain F-split (2.3) as significantly as before. For higher order methods and high accuracies, the improvement is only marginal. Nevertheless, it is important to observe that, again, the best result is obtained for the HO-split. Notice that a higher number of Hermite basis functions is necessary to achieve the same accuracy as the Hermite-Fourier decomposition.

Figure 3.5 shows the results for $\sigma = 100$. The HO-split cannot be expected to be particularly useful because the system is far from being a harmonic oscillator. From Fig. 3.2, we expect a great number of Hermite basis functions to be required for a sufficiently accurate expansion. The results in Fig. 3.5 demonstrate this rather intuitive expectation, i.e., almost negligible precision despite the large number of basis terms $M = 200$. Remarkably, the proposed HO decomposition does not show these limitations and reaches the precision of the F-split (2.3) because we are solving the harmonic potential exactly up to spectral accuracy. For this problem, we observe that the V82 method has the best performance when a relatively low accuracy

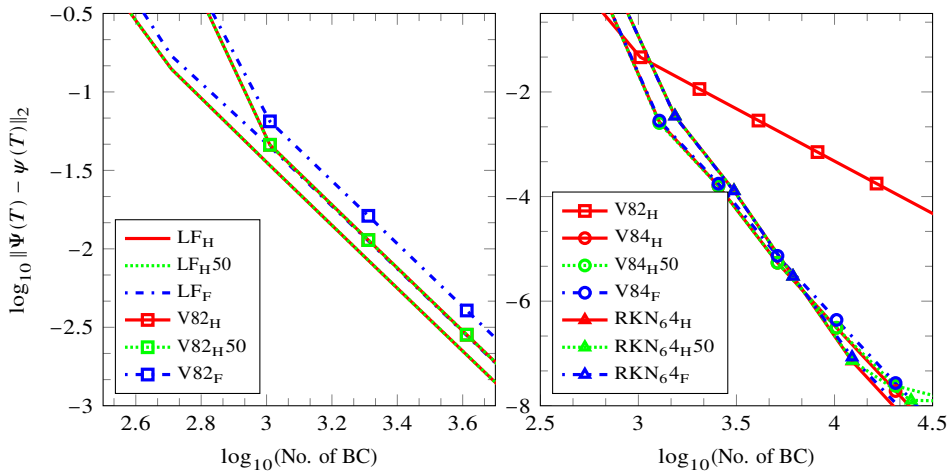

Figure 3.4: Same as Fig. 3.3 for $\sigma = 1$. In the left panel, $\mathrm{LF_H}$ and $\mathrm{V82_H}$ coincide with $\mathrm{LF_H50}$ and $\mathrm{V82_H}$, respectively.

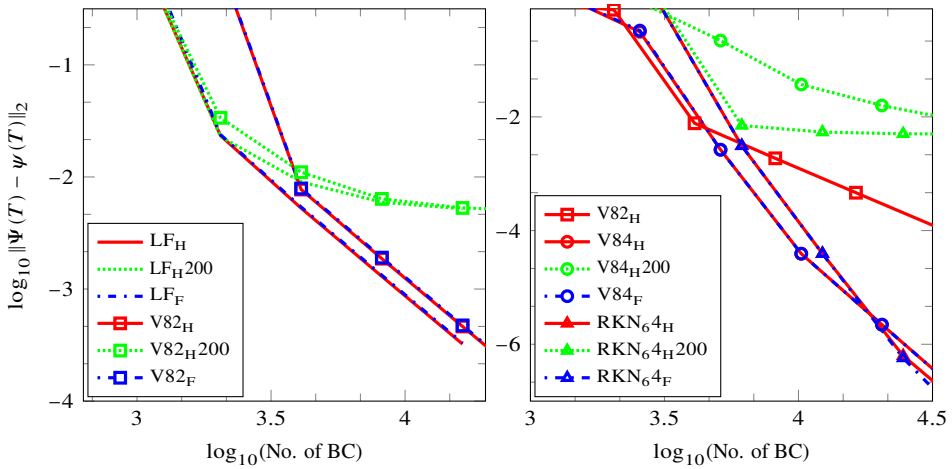

Figure 3.5: Same as Fig. 3.3 for $\sigma = 100$. F-splittings (blue dashed) overlap with the corresponding (solid red) Fourier-Hermite curves.

is desired, the V84 method shows the best performance for medium accuracies and the $\mathrm{RKN_6}4$ is the method of choice for higher accuracies.

3.2 Unconventional splitting methods

3.2.1 Modifying nonlinear potentials

The starting point is the well-known concept of modifying potentials [86], which comes from the observation that the commutator $[V(x),[V(x),\partial_x^2]] = 2(\partial_x V)^2$ is a function of the spatial coordinate only, and it can be cheaply exponentiated together with the potential, see also the discussion following (1.45) of Section1.3.3.

For the nonlinear SE, the expression becomes slightly more involved, namely,

$$\begin{aligned}[\hat{B},[\hat{A},\hat{B}]](\mathbf{I})(\psi) = {} & +i\epsilon^2 V_x^2\psi - 2i\sigma\epsilon|\psi|^2 V_{xx}\psi \\ & + i\sigma^2\Big(|\psi|^2\left(-6|\psi_x|^2 - 2\psi^*\psi_{xx}\right) + \psi^2\left(-2\psi^*\psi_{xx}^* - \psi_x^{*2}\right) - \psi^{*2}\psi_x^2\Big)\psi,\end{aligned}$$

with Lie operators $\hat{A},\hat{B}$ associated with the vector fields $B = -i(\epsilon V + \sigma|\psi|^2)\psi$ and $A = -i(\frac{1}{2}\Delta + W(x))\psi$, respectively. The right-hand side can be rewritten as

$$[\hat{B},[\hat{A},\hat{B}]](\mathbf{I})(\psi) = +i\epsilon^2 V_x^2\psi - 2i\sigma\epsilon|\psi|^2 V_{xx}\psi - i\sigma^2\Big(2(\Delta(|\psi|^2))|\psi|^2 + (\nabla(|\psi|^2))^2\Big)\psi. \tag{3.8}$$

After this simplification, it is clear that Lemma 3.1.1 can be applied to exponentiate (3.8) since the absolute value of the wave function remains constant.

At the expense of having to compute derivatives, we introduce the *modified nonlinear potential*

$$\begin{aligned}\tilde{V}_{a,b}(h) = {} & ah\left(\epsilon V + \sigma|\psi|^2\right) - bh^3\left(\epsilon^2(\nabla V)^2 - 2\epsilon\sigma|\psi|^2(\Delta V)\right) \\ & + bh^3\sigma^2\Big(2(\Delta(|\psi|^2))|\psi|^2 + (\nabla(|\psi|^2))^2\Big).\end{aligned}$$

In contrast to the linear case for which we will revisit the modifying potentials in Chapter 5, here, each computation of $\tilde{V}$ requires an FFT and two inverse transformations to compute the derivatives, and is thus roughly as costly as adding one and a half extra stage to the splitting. Optimal implementation can save the first FFT since we are already in Fourier space after having evaluated the T exponent and thus, we will only account for two extra FFTs when the modified potential is preceded by some calculation in Fourier space, e.g., $\cdots e^{-ia_j hT} e^{-i\tilde{V}_{b_j,c_j}(h)} e^{-ia_{j+1}hT}\cdots$. For this reason, it is recommendable to only use the modified potential in the center step, e.g., as in the well-known fourth-order method [86, 44],

$$\Psi^{[4]} = e^{-i\frac{h}{6}V} e^{-i\frac{h}{2}T} e^{-i\tilde{V}_{\frac{2}{3},\frac{1}{72}}(h)} e^{-i\frac{h}{2}T} e^{-i\frac{h}{6}V}, \tag{3.9}$$

which requires six FFTs. Adding an extra stage while imposing symmetry and consistency, we arrive at

$$e^{-ihb_1V} e^{-iha_1T} e^{-i\tilde{V}_{1/2-b_1,c}(h)} e^{-ih(1-2a_1)T} e^{-i\tilde{V}_{1/2-b_1,c}(h)} e^{-iha_1T} e^{-ihb_1V}$$

at the cost of ten FFTs and with two free parameters which is enough to reach order (6,4),

$$a_1 = \frac{1}{2}\left(1 - \frac{1}{\sqrt{5}}\right),\ b_1 = \frac{1}{12},\ c = \frac{1}{576}\left(13 - 5\sqrt{5}\right).$$

At the same computational cost, the following composition offers an additional degree of freedom for optimizations

$$e^{-ihb_1V}e^{-iha_1T}e^{-ihb_2V}e^{-iha_2T}e^{-i\tilde{V}_{b_3,c}}e^{-iha_2T}e^{-ihb_2V}e^{-iha_1T}e^{-ihb_1V}$$

and we have computed an (8,4) method with only positive coefficients

$$a_1 = \frac{7-\sqrt{21}}{14},\ b_1 = 1/20,\ b_2 = 1/20,\ c = \frac{3861-791\sqrt{21}}{64800}, \tag{3.10}$$

and for consistency $a_2 = 1/2 - a_1,\ b_3 = 1 - 2(b_1 + b_2)$.

For completeness, we mention that adding an extra stage to a splitting method while keeping it symmetric will also cost two additional FFTs and introduces one free parameter. Overall, it is thus comparable to the modified potential approach.

3.2.2 Complex coefficients

In the introduction, we already came across Yoshida's device to construct arbitrary order methods from a low order approximation. Apart from the real-valued solution for the order conditions, there are two complex-valued ones with positive real part at each composition step, e.g., from order two to order four. For real-valued problems as common in classical mechanics, a numerical integrator based on complex fractional time-steps needs an additional projection step which implies a loss of the geometric properties[3] and furthermore implies quadruple computational cost which is due to multiplication of complex numbers instead of reals.

In the quantum mechanical setting, the situation is slightly more beneficial since the wave functions are already complex-valued and complex time-steps not even double the overall cost since only the real-valued exponentials are replaced by complex ones, thus the products are between complexes and complexes instead of reals and complexes. In addition, the obtained methods will not be unitarity and some normalization has to be applied to the wave function.

With the aim of integrating the Hamiltonian

$$H = (T + W)\psi + (\varepsilon V + \sigma|\psi|^2)\psi$$

under the assumption that we have an efficient solver for $T + W$, e.g., by FFTs (for $W = 0$) or when the eigenfunctions of $T + W$ are known, cf. Chapter 2, we have constructed splitting methods of two types that are optimized for near-integrable systems, where $a_j \in \mathbb{R}$, $b_j \in \mathbb{C}$ and $a_j, b_j \in \mathbb{C}$. The latter family turned out to be unstable in numerical experiments, which is due to exponents of the form $-ia_jhT$ and of course either all $a_j \in \mathbb{R}$ or at least one a_k has negative imaginary part[4]. In fact, the same holds to some degree for complex b_j for unbounded potentials V. The stability of the methods will then crucially depend on the truncation of the spatial domain in order to artificially bound the potential.

Before going into details, we address how to solve the nonlinear part in complex time.

[3] Although it has been shown, that certain geometric properties are preserved up to higher order

[4] This follows immediately from the consistency condition $\sum_j a_j = 0$.

A variant of the complex Ginzburg-Landau equation Let us consider the PDE which corresponds to the potential nonlinear part of the GPE,

$$i\psi_t = (V + \sigma|\psi|^2)\psi, \quad \psi(x,0) = \psi_0(x).$$

Now, the vector-field is not holomorphic but we can borrow a trick from [19], which has been successfully applied to the complex Ginzburg-Landau equation. However, their derivation is incomplete and therefore generalized in the following to be applicable for any kind of GPE, in real and imaginary time:

$$\psi_t = \alpha\Delta\psi + \beta\psi + \gamma|\psi|^2\psi, \qquad t \in \mathbb{C},$$

where α, β, γ are complex-valued linear operators to also account for the complex Ginzburg-Landau equation. The starting point is to write the system as sum of real and imaginary parts, i.e., $\psi = v + iw$

$$\partial_t v + i\partial_t w = (\alpha\Delta + \beta)(v + iw) + (\gamma_R + i\gamma_I)(v^2 + w^2)(v + iw). \tag{3.11}$$

Now, we identify the real and imaginary parts on both sides and introduce new (complex) coordinates $\tilde{v} = -\frac{i}{2}(v + iw)$, $\tilde{w} = \frac{1}{2}(v - iw)$, which, after simple algebra, yields the now holomorphic system

$$\begin{aligned} \partial_t\tilde{v} &= (\alpha\Delta + \beta)\tilde{v} + \gamma\tilde{M}\tilde{v}, \\ \partial_t\tilde{w} &= (\alpha^*\Delta + \beta^*)\tilde{w} + \gamma^*\tilde{M}\tilde{w}, \end{aligned} \tag{3.12}$$

with $\tilde{M} = 4i\tilde{v}\tilde{w}$. The kinetic part can be solved with spectral methods and for the remainder, i.e., for $\alpha = 0$, the equation becomes *local* and can be solved easily as an ODE: As is standard for the Ginzburg-Landau equation, we solve the equation by first considering the "norm", $\tilde{M}$, which is governed by

$$\partial_t\tilde{M} = 4i\left(\tilde{v}_t\tilde{w} + \tilde{v}\tilde{w}_t\right) = (\beta + \beta^*)\tilde{M} + (\gamma + \gamma^*)\tilde{M}^2, \quad \tilde{M}(0) = M_0 := 4i\tilde{v}(0)\tilde{w}(0),$$

and which can be solved by separation of variables, using the shorthand $\beta_R = \Re(\beta)$, $\gamma_R = \Re(\gamma)$, to

$$\tilde{M}(t) = \frac{\beta_R e^{2\beta_R t} M_0}{\beta_R - \gamma_R(e^{2\beta_R t} - 1)M_0}.$$

Now, the original equations (3.12) can be easily solved by evaluating

$$\begin{aligned} \tilde{v}(t) &= \exp\left(\beta t + \gamma\int_0^t \tilde{M}(z)\,dz\right)\tilde{v}_0, \\ \tilde{w}(t) &= \exp\left(\beta^* t + \gamma^*\int_0^t \tilde{M}(z)\,dz\right)\tilde{w}_0, \end{aligned} \tag{3.13}$$

where

$$\int_0^t \tilde{M}(z)dz = -\frac{1}{2\gamma_R}\log\left(\frac{\gamma_R}{\beta_R}M_0\left(1 - e^{2\beta_R t}\right) + 1\right).$$

For the nonlinear Schrödinger equation, both β and γ are purely imaginary and in the limit $\beta_R, \gamma_R \to 0$, the evolution (3.13) simplifies to

$$\tilde{v}(t) = e^{t(\beta + \gamma\tilde{M}_0)}\tilde{v}_0, \qquad \tilde{w}(t) = e^{t(\beta^* + \gamma^*\tilde{M}_0)}\tilde{w}_0, \quad \tilde{M}_0 = 4i\tilde{v}_0\tilde{w}_0.$$

The α-part is trivially solved by

$$\tilde{v}(t) = e^{t\alpha\Delta}\tilde{v}_0, \qquad \tilde{w}(t) = e^{t\alpha^*\Delta}\tilde{w}_0, \tag{3.14}$$

and we have all ingredients to apply a composition with complex coefficients. As is evident from (3.14), twice as many Fourier transforms are necessary due to the increase of dimensionality.

3.2.3 Numerical experiments

A preliminary search to find new splitting methods with real a_i and complex b_j gave promising results in terms of accuracy, however, the double cost, when counting only FFTs, in comparison to real-coefficient classical splittings overcompensates and the efficiency of a range of complex coefficient methods that we have tested[5] is not competitive. As mentioned above, stability becomes an issue since complex fractional times lead to a loss of unitarity which is particularly pronounced for unbounded potentials on large domains. Therefore, we restrict ourselves to a proof of concept type exposition to show that the correct orders of accuracy are attained when integrating the Gross-Pitaevskii equation with the new procedures based on nonlinear modifying potentials and complex coefficients.

For reference, the successful standard splitting methods Leapfrog, V84, $\text{RKN}_6$4, see Table 3.2, have been used and compared against the following group of methods:

- GPE-4M (the fourth-order splitting with nonlinear modifying potential (3.9)).
- GPE-84M (the (8,4) method (3.10)).
- Castella-4 (the fourth-order *BAB* method from [40]). The coefficients are $a_j = 1/4$ and $b_1 = \frac{1-i/3}{10}$, $b_2 = \frac{4+2i}{15}$, $b_3 = \frac{4-3i}{15}$, $b_4 = b_2$, $b_5 = b_1$.

Bounded potentials First, we treat the simpler bounded case, as exemplified by the familiar Pöschl-Teller potential (2.30),

$$V = \frac{\lambda(\lambda+1)}{2}\left(1 - \operatorname{sech}(x)\right)^2, \tag{3.15}$$

with $\lambda = 4$. In this setting, complex values of b_j are not likely to cause stability problems since the exponent $-ib_jhV$ remains relatively small. The nonlinearity is chosen as $\sigma = 0.01$ and $\sigma = 10$ and the respective spatial domain has been truncated to the interval $[-15, 15)$, discretized at $N = 1024$ equidistant grid points, $x_j = j\frac{30}{N} - 15$, $j = 0, \ldots, N-1$. As initial condition, we choose the corresponding ground states ψ_0 which have been computed to ten digit accuracy with the imaginary time method, cf. Chapter 5. The exact solution is obtained by propagating the ground state until the final time $T = 10$ through $\psi(T) = e^{-i\mu T}\psi_0$ using the eigenvalue $\mu = \langle T + V + \sigma|\psi_0|\rangle_{\psi_0}$.

The results for both values of σ are illustrated in Fig. 3.6. We appreciate the fourth-order behavior of the new methods which confirms our theory. However, the classical methods V84

[5] The results are not reproduced in the text.

and $\mathrm{RKN}_6 4$ are extremely competitive and it remains to be seen whether a parameter optimization for complex coefficient methods will be able to close the gap and create more efficient methods. On the other hand, the new modifying potential is competitive and the optimized (8,4) method is improving on the standard when the nonlinearity plays the role of the small part, see Fig. 3.6a.

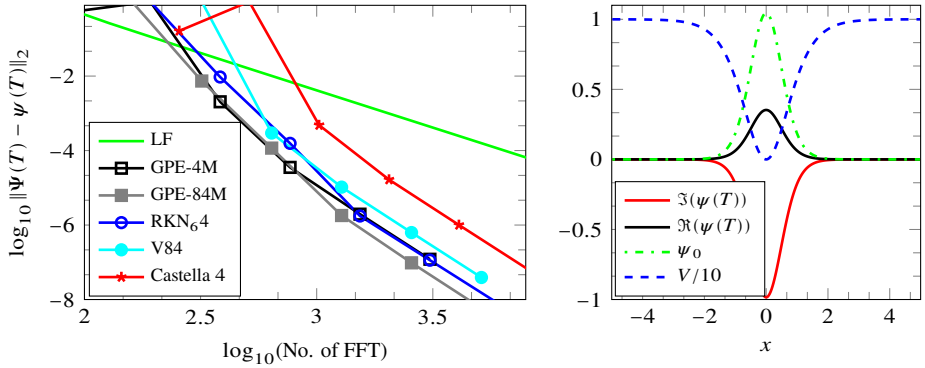

(a) Weak interaction strength, $\sigma = 0.01$

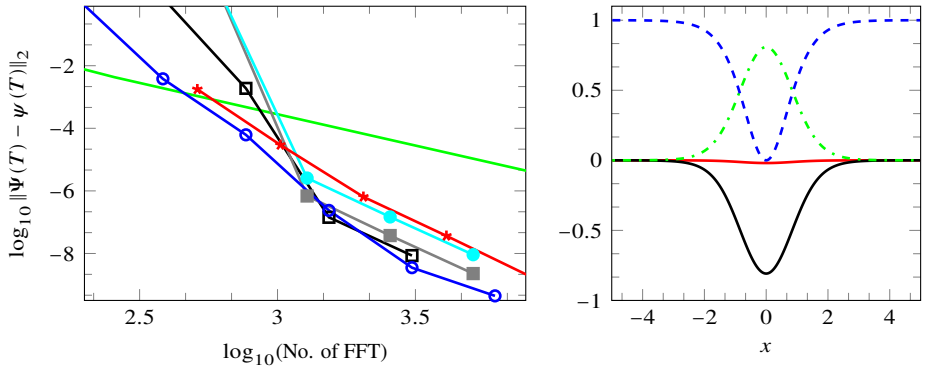

(b) Intermediate interaction strength, $\sigma = 10$. Legend as above in Fig. 3.6a.

Figure 3.6: Efficiency plot of various splitting methods for the Pöschl-Teller potential (3.15) for $N = 1024$ grid points on the domain $x \in [-15, 15]$. On the abscissa, the number of N-point FFTs is shown for each method.

Unbounded potentials In this experiment, we take the harmonic oscillator potential $V = \frac{1}{2}x^2$ and leave the remaining parameters as before, i.e., we integrate the respective ground states for $\sigma = 0.01$ and $\sigma = 10$ until $T = 10$ using $N = 1024$ equidistant grid points on $[-15, 15)$.

For each method and configuration, the two splits, $(T+V)+\sigma|\psi|^2$ (HO) and $T+(V+\sigma|\psi|^2)$ (F) have been compared. The HO-split solves the harmonic part exactly with the Fourier methods discussed in Chapter 2

The results in Fig. 3.7 show the instabilities for large values of the time-step in the complex do-

main. Furthermore, as predicted, for the HO-split when only the nonlinearity is propagated in complex time, the stability domain is greatly enlarged. The calculations confirm the expected order of the methods and whether an improvement over the real standard splittings is possible is subject of further research.

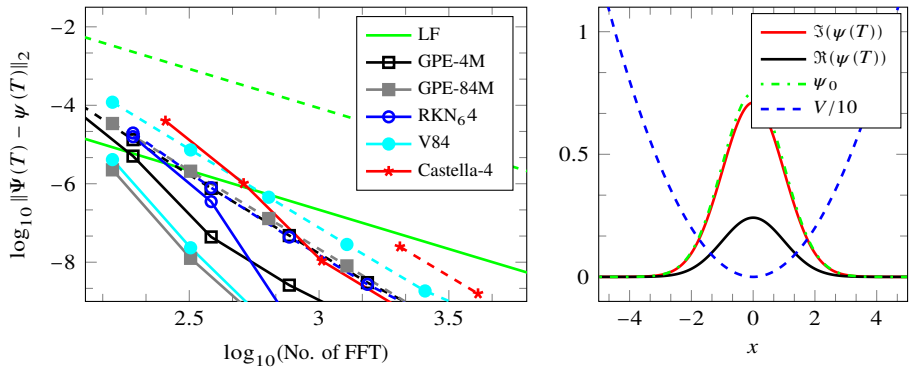

(a) $\sigma = 0.01$

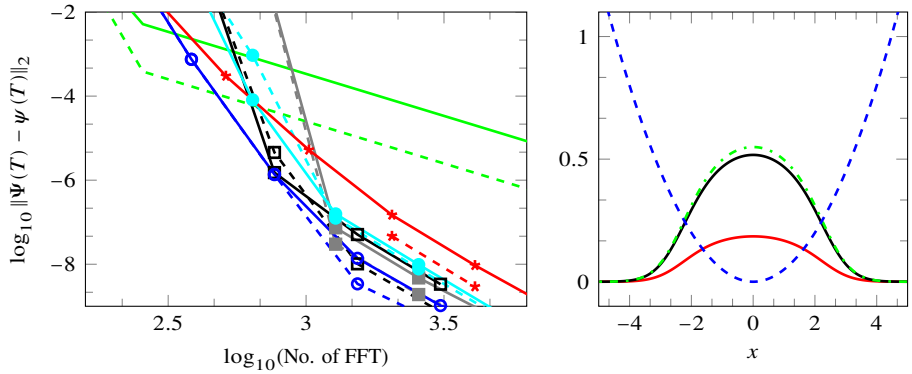

(b) $\sigma = 10$

Figure 3.7: Efficiency plot of various splitting methods for the harmonic potential $V = \frac{1}{2}x^2$ and two different strengths of the interaction parameter σ. Same symbols correspond to same splitting coefficients, and the type of splitting is indicated by the line style: Dashed lines originate from the F-split, where the kinetic part is propagated separately from the potential, whereas the solid lines have been computed with the HO-split for which the nonlinearity is separately evolved. The right column shows a zoom of the initial conditions, the exact solution and the external potential $V(x)$.

Chapter 4

THE SEMI-CLASSICAL LIMIT

The computation of the semi-classical Schrödinger equation (SCSE) presents a variety of challenges [83] and in this section, we present a new method for the numerical evolution of the SCSE defined in (1.9). After suitable rescaling of the spatial variable and using atomic units, cf. Section 1.1.2, we arrive at the problem

$$i\varepsilon\partial_t\psi(x,t) = -\varepsilon^2\frac{\partial^2}{\partial x^2}\psi(x,t) + V(x,t)\psi(x,t), \qquad x \in [-1,1], \tag{4.1}$$

given with an initial value and periodic boundary conditions, where the potential V is a periodic function in space. In accordance with the considerations in previous chapters, this formulation is also valid to simulate bounded states on unbounded domains since they rapidly decay on a sufficiently large spatial interval. Although we address the problem in only one spatial dimension, the methodology extends in a straightforward fashion to problems with moderately large dimension d.

The small size of ε is a source of substantial difficulties in the numerical discretization of (4.1) because rapid oscillations require a resolution of $\mathcal{O}(\varepsilon)$ in both space and time which is often impractical or exceedingly expensive.

From the WKB analysis in Section 1.1.2 following (1.10), it is clear that the spatial resolution $\Delta x = \mathcal{O}(\varepsilon)$ must be maintained. However, there is no such restriction for the time domain and we therefore pursue alternative approaches, based in the main on the concept of exponential splittings [53, 83, 91, 95].

4.1 The autonomous case

The exposition is based on the article [10].

Let us consider the autonomous situation by dropping the time-dependence in the potential. It is convenient to rewrite (4.1) as

$$i\frac{\partial \psi}{\partial t} = -\omega^{-1}\frac{\partial^2 \psi}{\partial x^2} + \omega V(x)\psi, \qquad x \in [-1,1], \tag{4.2}$$

where $\omega = \varepsilon^{-1} \gg 1$. At this stage, we will assume a given spatial discretization and replace the second derivative operator and the multiplication by the interaction potential by matrices $\mathscr{K}$ and $\mathscr{D}$, respectively, in order to reformulate (4.1) as a system of ordinary differential equations of the form

$$iu' = (-\omega^{-1}\mathscr{K} + \omega\mathscr{D})u, \qquad u \in \mathbb{C}^N \tag{4.3}$$

where $u(0)$ is sampled from the initial conditions on the spatial grid. The exact solution of (4.3) is of course

$$u(t) = \exp\left(it(\omega^{-1}\mathscr{K} - \omega\mathscr{D})\right)u(0) \tag{4.4}$$

and a natural temptation is to approximate it (using small time steps) by any of many methods to compute the matrix exponential, $e^{ih(\omega^{-1}\mathscr{K}-\omega\mathscr{D})}$. However, both summands in the exponent, $\omega^{-1}\mathscr{K}$ and $\omega\mathscr{D}$ are scaling with ω as we will see in continuation and therefore require either very small time steps h or extreme numerical efforts to approximate the exponential (e.g., Krylov subspace methods of dimension $\approx N$) to attain reasonable accuracy.

The alternative is to separate scales by means of an exponential splitting and we begin by pointing out a few aspects that have to be considered for this highly oscillatory problem.

Limitations of classical splittings As in the previous sections, the working horse of the splitting family, the Strang splitting

$$e^{ih(\omega^{-1}\mathscr{K}-\omega\mathscr{D})} = e^{-i\frac{h}{2}\omega\mathscr{D}}e^{ih\omega^{-1}\mathscr{K}}e^{-i\frac{h}{2}\omega\mathscr{D}} + \mathscr{O}\left(h^3\right), \tag{4.5}$$

delivers advantageous properties: separation of scales on the one hand and cheap computability of each exponential by spectral methods. The downside is that higher order methods require a large number of exponentials.

Under the assumptions that all derivatives of the potentials are bounded in the L^∞-norm and that the derivatives of the exact solution do not grow larger than

$$\left\| \frac{\partial^{m_1+m_2}}{\partial x^{m_1}\partial t^{m_2}}\psi(x,t) \right\|_{C([0,T];L^2(-1,1))} \leq \frac{C_{m_1+m_2}}{\varepsilon^{m_1+m_2}},$$

for some positive constants C_m, it has been derived in Ref. [14] that a meshing strategy of $\Delta x = \mathscr{O}(\varepsilon)$ and $h = \mathscr{O}(\varepsilon)$ will yield an error bound for the first order Lie-trotter splitting (1.36) after n time-steps of size h,

$$\|\psi^\varepsilon(nh) - u_{\text{int}}^{\varepsilon,n}\|_{L^2((a,b)} \leq G_m\frac{T}{h}\left(\frac{\Delta x}{\varepsilon(b-a)}\right)^m + \frac{CTh}{\varepsilon}, \quad n = 0,1,\dots,T/h, \tag{4.6}$$

for constants $C, G_m > 0$ independent of ε and C independent of m. On time intervals of size $T = \mathcal{O}(1)$, an L^2 error of size $\mathcal{O}(\delta)$ can thus be guaranteed by choosing $h/\varepsilon = \mathcal{O}(\delta)$ and $\Delta x/\varepsilon = \mathcal{O}\big((\delta h)^{1/m}\big)$.

The proof of this result makes use of the Taylor expansion of the splitting and estimates the local error through the commutator $[hT, hV]$, which is then calculated to be of size $\mathcal{O}\big(h^2/\varepsilon\big)$ and which constitutes the right part of the estimate (4.6).

For the Strang split, e.g., after spatial discretization in (4.5), the error terms are

$$h^3[\varepsilon\partial_x^2, [\varepsilon\partial_x^2, \varepsilon^{-1}V]] \text{ and } h^3[\varepsilon^{-1}V, [\varepsilon^{-1}V, \varepsilon\partial_x^2]],$$

which result, with the help of Table 4.1, in terms of size $\mathcal{O}\big(h^3\varepsilon^{-1}\big)$. Indeed, any higher-order commutator of length n will be of size $h^n\varepsilon^{-1}$ and we can expect to relax the meshing restriction for an order p splitting method to

$$h^p/\varepsilon = \mathcal{O}(\delta) \quad \text{and} \quad \Delta x/\varepsilon = \mathcal{O}\big((\delta h)^{1/m}\big). \tag{4.7}$$

If high order is desired, an inordinately large number of exponentials is required, e.g., the simple composition method of Yoshida (1.44), calls for $r = 3^{p-1}$ compositions of Leapfrog schemes, or $2 \cdot 3^{p-1} + 1$ exponentials after concatenation, to attain order $2p$.

Introduction to an asymptotic approach We present new splittings that require far fewer exponentials to attain a given order, to be precise, the number of exponentials is shown to grow linearly, rather than exponentially, with order. Moreover, the exponents will become of increasingly smaller size which will yield an *asymptotic splitting*. Ultimately, even though some non-diagonal matrices will appear in the splittings, the computation of the exponentials can still be cheaply performed because of their small exponents by low-dimensional Lanczos-methods. The final method will be of the form

$$e^{-ih(-\omega^{-1}\mathscr{H}+\omega\mathscr{D})} = e^{\mathscr{R}_0}e^{\mathscr{R}_1}\cdots e^{\mathscr{R}_s}e^{\mathscr{T}_{s+1}}e^{\mathscr{R}_s}\cdots e^{\mathscr{R}_1}e^{\mathscr{R}_0} = \mathcal{O}\left(\varepsilon^{s+1/2}\right), \tag{4.8}$$

where

$$\begin{aligned}
\mathscr{R}_0 &= \mathscr{R}_0(h, \varepsilon, \mathscr{H}, \mathscr{D}) = \mathcal{O}\left(\varepsilon^{-1/2}\right), \\
\mathscr{R}_k &= \mathscr{R}_k(h, \varepsilon, \mathscr{H}, \mathscr{D}) = \mathcal{O}\left(\varepsilon^{k-3/2}\right), \qquad k = 1, \dots, s, \\
\mathscr{T}_{s+1} &= \mathscr{T}_{s+1}(h, \varepsilon, \mathscr{H}, \mathscr{D}) = \mathcal{O}\left(\varepsilon^{s-1/2}\right),
\end{aligned}$$

(recall that $\omega = \varepsilon^{-1}$) and variations on this theme. Note a number of critical differences between (4.8) and standard exponential splittings.

Firstly, the error is quantified in the small parameter ε under which we have subsumed the other small quantities h and $1/N$ (where N is the number of degrees of freedom in the semi-discretization) by introducing a power law relationship between ε and the choices of h and N.

Secondly, we allow the exponents to contain both potentials and derivatives, originating from commutators, which can be understood as a generalization of modifying potentials. Usually, a mix of momentum and spatial coordinates is avoided since the result cannot be diagonalized

by simple FFTs. In our approach, the separation of scales will enable us to overcome this limitation and to achieve an efficient computation of the exponentials by means of Krylov-subspace methods. And finally, we highlighted the linear growth in order with the number of exponentials as the most striking benefit.

The outline of this section is as follows: We present the Lie algebraic concepts which form the core of our method, the symmetric BCH formula and the Zassenhaus splitting. Thereafter, the new splitting algorithm based on a recursive application of the symmetric BCH formula is developed and some technical problems concerning the stability after discretization are resolved. We comment on the computation of the exponentials and conclude with some numerical experiments.

4.1.1 The Lie algebraic setting

An algebra of operators

The vector field in the linear Schrödinger equation (4.3) is a linear combination of the action of two operators, ∂_x^2 and the multiplication by the interaction potential V. Since the calculation of exponential splittings entails nested commutation, the focus of our interest is on the free Lie algebra

$$\mathfrak{F} = \mathrm{FLA}\{\partial_x^2, V\},$$

i.e., the linear-space closure of all nested commutators generated by ∂_x^2 and V. The elements of $\mathfrak{F}$ are operators, acting on the initial value of (4.3): for the sake of simplicity, we assume that the initial value, and hence the solution of (4.3) for moderate values of $t \geq 0$, is a periodic function in $\mathrm{C}^\infty[-1,1]$, but our results extend in a straightforward manner to functions of lower smoothness.

To compute commutators, we need in principle to describe their action on functions, e.g.,

$$[V, \partial_x^2]u = V(\partial_x^2 u) - \partial_x^2(Vu) = -(\partial_x^2 V)u - 2(\partial_x V)\partial_x u$$

implies that $[V, \partial_x^2] = -(\partial_x^2 V) - 2(\partial_x V)\partial_x$. We list the lowest-order further commutators which form a so-called Hall basis[1] [111] of the free Lie algebra $\mathfrak{F}$ in Table 4.1. "Grade" therein refers to the number of "letters" V and ∂_x^2 in the expression, while χ_j is the coefficient of this term in the symmetric BCH formula, cf. (1.42) in Section 1.3.3. Additionally, Table 4.1 collects the explicitly computed terms H_j, $j = 3, 4, \dots, 8$. We note that all the terms belong to the set

$$\mathfrak{G} = \left\{ \sum_{k=0}^{n} y_k(x)\partial_x^k \,:\, n \in \mathbb{Z}_+,\ y_0, \dots, y_n \in \mathrm{C}^\infty[-1,1] \text{ periodic with period } 2 \right\}.$$

It is trivial to observe that $\mathfrak{G}$ is itself a Lie algebra. There are numerous cancellations, similar to $H_8 = 0$, because of the RKN structure induced by the letters ∂_x^2 and $V(x)$. Nevertheless, for our exposition it is more appropriate to operate in the larger Lie algebra $\mathfrak{G}$, where all

[1] cf. Section 1.3.3.

Table 4.1: The terms of the Hall basis of $\mathfrak{F}$ of grade ≤ 4.

j	Basis element in $\mathfrak{F}$	χ_j	corresponding expression in $\mathfrak{G}$
Grade 1			
H_1	∂_x^2	1	∂_x^2
H_2	V	1	V
Grade 2			
H_3	$[V, \partial_x^2]$	0	$-(\partial_x^2 V) - 2(\partial_x V)\partial_x$
Grade 3			
H_4	$[[V, \partial_x^2], \partial_x^2]$	$-\frac{1}{24}$	$(\partial_x^4 V) + 4(\partial_x^3 V)\partial_x + 4(\partial_x^2 V)\partial_x^2$
H_5	$[[V, \partial_x^2], V]$	$-\frac{1}{12}$	$-2(\partial_x V)^2$
Grade 4			
H_6	$[[[V, \partial_x^2], \partial_x^2], \partial_x^2]$	0	$-(\partial_x^6 V) - 6(\partial_x^5 V)\partial_x - 12(\partial_x^4 V)\partial_x^2 - 8(\partial_x^3 V)\partial_x^3$
H_7	$[[[V, \partial_x^2], \partial_x^2], V]$	0	$4[(\partial_x V)(\partial_x^3 V) + (\partial_x^2 V)^2] + 8(\partial_x V)(\partial_x^2 V)\partial_x$
H_8	$[[[V, \partial_x^2], V], V]$	0	0

cancellations will be taken care of by simple computation of the commutators, according to

$$\left[\sum_{i=0}^{n} f_i(x)\,\partial_x^i, \sum_{j=0}^{m} g_j(x)\,\partial_x^j\right] = \sum_{i=0}^{n}\sum_{j=0}^{m}\sum_{l=0}^{i}\binom{i}{l} f_i(x)\left(\partial_x^{i-l} g_j(x)\right)\partial_x^{l+j} - \sum_{j=0}^{m}\sum_{i=0}^{n}\sum_{l=0}^{j}\binom{j}{l} g_j(x)\left(\partial_x^{j-l} f_i(x)\right)\partial_x^{l+i}. \tag{4.9}$$

The symmetric BCH formula

Let X and Y be two terms in a Lie algebra $\mathfrak{g}$. The *symmetric Baker–Campbell–Hausdorff formula* (also symmetric BCH or sBCH formula) is

$$e^{\frac{1}{2}X} e^{Y} e^{\frac{1}{2}X} = e^{\mathrm{sBCH}(X,Y)}, \tag{4.10}$$

where

$$\begin{aligned}\mathrm{sBCH}(hX, hY) =& h(X+Y) - h^3\left(\frac{1}{24}[[Y,X],X] + \frac{1}{12}[[Y,X],Y]\right)\\ &+ h^5\Big(\frac{7}{5760}[[[[Y,X],X],X],X] + \frac{7}{1440}[[[[Y,X],X],X],Y]\\ &+ \frac{1}{180}[[[[Y,X],X],Y],Y] + \frac{1}{720}[[[[Y,X],Y],Y],Y]\\ &+ \frac{1}{480}[[[Y,X],X],[Y,X]] - \frac{1}{360}[[[Y,X],Y],[Y,X]]\Big) + \mathcal{O}\left(h^7\right).\end{aligned} \tag{4.11}$$

Higher-order terms can be obtained by means of the standard BCH formula (1.42) and an efficient algorithm has been provided in Ref. [39]. Terms up to order 7 are reproduced in the appendix, (A.1). Since (4.10) is symmetric, only odd powers of h feature in the expansion and with the substitution $X = \partial_x^2$ and $Y = V$, the coefficients can be identified with the numbers χ_j from Table 4.1.

The Zassenhaus splitting

The *Zassenhaus splitting* [105] gives a somehow inverse approach to the BCH formula. Given a separable exponent, it provides a way to decompose in exponentials of increasing grade in the exponents:

$$e^{h(X+Y)} = e^{hX} e^{hY} e^{h^2 U_2(X,Y)} e^{h^3 U_3(X,Y)} e^{h^4 U_4(X,Y)} \cdots, \tag{4.12}$$

where

$$\begin{aligned}
U_2(X,Y) &= \frac{1}{2}[Y,X], \\
U_3(X,Y) &= \frac{1}{3}[[Y,X],Y] + \frac{1}{6}[[Y,X],X], \\
U_4(X,Y) &= \frac{1}{24}[[[Y,X],X],X] + \frac{1}{8}[[[Y,X],X],Y] + \frac{1}{8}[[[Y,X],Y],Y].
\end{aligned}$$

In other words, the functions U_j quantify the discrepancy from commuting case $e^X e^Y = e^{X+Y}$. As usual, more terms can be generated using the non-symmetric BCH formula.

The splitting (4.12) is not well-known and seldom used in computation because it lacks symmetry and the involved commutators are expected to be costly. We remedy the first issue by symmetrizing and thus considering a splitting of the form

$$e^{h(X+Y)} = \cdots e^{h^5 Q_5(X,Y)} e^{h^3 Q_3(X,Y)} e^{\frac{1}{2}hX} e^{hY} e^{\frac{1}{2}hX} e^{h^3 Q_3(X,Y)} e^{h^5 Q_5(X,Y)} \cdots \tag{4.13}$$

where we can deduce by inspection of (4.11), that

$$Q_3(X,Y) = \frac{1}{48}[[Y,X],X] + \frac{1}{24}[[Y,X],Y].$$

For higher-order terms, such as Q_5, simple addition of terms will not be sufficient since the inner block (Q_3) generates new terms that have to be taken care of. Fortunately, it is easy to cast the procedure in an easy algorithmic form [77]. We commence from the symmetric BCH formula (4.11),

$$e^{-\frac{1}{2}hX} e^{h(X+Y)} e^{-\frac{1}{2}hX} = e^{\mathrm{sBCH}(-hX, h(X+Y))},$$

which we rewrite in the form

$$e^{h(X+Y)} = e^{\frac{1}{2}hX} e^{\mathrm{sBCH}(-hX, h(X+Y))} e^{\frac{1}{2}hX}. \tag{4.14}$$

It follows from (4.11) that

$$\mathrm{sBCH}(-hX, h(X+Y)) = \mathscr{W}^{[1]} = hY + \mathcal{O}\left(h^3\right),$$

and we note that we have extracted the outer term hX from the inner exponent. We iterate (4.14) over the resulting term and continue to symmetrically pull-out the lowest order terms, one by one, until the central exponent reaches the desired high order,

$$\begin{aligned}\exp\left(h(X+Y)\right) &= e^{\frac{1}{2}hX} e^{\mathrm{sBCH}(-hX,h(X+Y))} e^{\frac{1}{2}hX} \\ &= e^{\frac{1}{2}hX} e^{\frac{1}{2}hY} e^{\mathrm{sBCH}(-hY,\mathrm{sBCH}(-hX,h(X+Y)))} e^{\frac{1}{2}hY} e^{\frac{1}{2}hX}.\end{aligned}$$

Notice that by pulling-out, we essentially subtract a term and add higher-order corrections. It is important to observe that the order of the exponent given by the sBCH formula (4.14) is never decreased by this procedure[2] and thus we can easily control the order of the approximation error when truncating the BCH formula. With the notation

$$\mathscr{W}^{[k+1]} = \mathrm{sBCH}(-W^{[k]}, \mathscr{W}^{[k]}), \quad \mathscr{W}^{[0]} = h(X+Y), \tag{4.15}$$

the result after s steps can be written as

$$\exp h(X+Y) = e^{\frac{1}{2}W^{[0]}} e^{\frac{1}{2}W^{[1]}} \cdots e^{\frac{1}{2}W^{[s]}} e^{\mathscr{W}^{[s+1]}} e^{\frac{1}{2}W^{[s]}} \cdots e^{\frac{1}{2}W^{[1]}} e^{\frac{1}{2}W^{[0]}}.$$

We emphasize that, in principle, we can freely choose the elements $W^{[k]}$ that we want to extract. A first idea is to choose the $W^{[k]} = \mathcal{O}\left(h^{2k-1}\right)$ for $k > 0$ and $W^{[0]} = \mathcal{O}(h)$, which yields a separation of powers, analogous to (4.13), and thus for s stages and approximating $\mathscr{W}^{[s+1]} = W^{[s+1]} + \mathcal{O}\left(h^{2s+3}\right)$, we obtain a symmetric Zassenhaus splitting of order $2s+2$.

4.1.2 An asymptotic splitting

In standard splittings, e.g., in the context of a numerical solution of Hamiltonian ordinary differential equations, there is usually a single small parameter, h (the time step), and it is sensible to group terms in powers of h. However, after the discretization of (4.2), we have three small parameters to deal with:

a. The oscillatory parameter of the system $\varepsilon = \omega^{-1}$;

b. The time step h;

c. $1/N$, where N is the number of degrees of freedom in the spatial discretization.

Although we derive our splitting before the infinite-dimensional operator ∂_x^2 has been discretized, we must keep in mind the eventual spatial discretization: For actual computation, we need to replace ∂_x^2 with a differentiation matrix acting on an appropriate N-dimensional space, where N is the number of nodal values or of Fourier modes. It is elementary that the norm of a differentiation matrix corresponding to ∂_x^n scales as $\mathcal{O}(N^n)$, $n \in \mathbb{N}$. We propose to unify the three small parameters by introducing the following scaling laws which will specify the parameters h and N,

$$N = \mathcal{O}(\omega^{\rho}) = \mathcal{O}(\varepsilon^{-\rho}), \qquad h = \mathcal{O}(\omega^{-\sigma}) = \mathcal{O}(\varepsilon^{\sigma}), \tag{4.16}$$

[2] Unless a non-existing term is subtracted and thus newly introduced instead of removed.

where $\rho, \sigma > 0$ are given. For the derivatives, this implies the assumption that each ∂_x^n scales like $\mathcal{O}(\varepsilon^{-n\rho})$.

While we have already established that $\rho = 1$ is necessary to resolve the highly oscillatory behavior in space, we will choose $\sigma = \frac{1}{2}$ for the time-step.

In the following, we will conduct the steps necessary to achieve an asymptotic splitting (4.8) with an error of $\mathcal{O}\left(\varepsilon^{7/2}\right)$. We will expand the commutators in powers of ε and successively remove them from the core of our expansion, aiming for $W^{[j]} = \mathcal{O}\left(\varepsilon^{j-3/2}\right)$ for $j > 1$. Motivated by (4.4), the exponential we ultimately want to decompose, we introduce the abbreviation

$$\tau = -ih = \mathcal{O}\left(\varepsilon^{1/2}\right).$$

Note that $\tau\omega^{-1}\partial_x^2 = \mathcal{O}\left(\varepsilon^{-1/2}\right)$ and $\tau\omega V = \mathcal{O}\left(\varepsilon^{-1/2}\right)$, or more generally

$$\tau^l \omega^m \partial_x^n = \mathcal{O}\left(\varepsilon^{l/2-m-n}\right), \qquad \varepsilon \to 0. \tag{4.17}$$

We can now commence the algorithm (4.15), setting

$$\mathscr{W}^{[0]} = -\tau\omega^{-1}\partial_x^2 + \tau\omega V, \qquad W^{[0]} = \tau\omega V.$$

With the help of (4.11), we compute the commutators in $\mathscr{W}^{[1]} = \mathrm{sBCH}(-W^{[0]}, \mathscr{W}^{[0]})$ according to (4.9). This task confronts us with long and tedious algebra but can, however, be automatized with a computer algebra program. It is worth pointing out that all simplifications, such as $[V, \partial_x^2], V], V] = 0$ are automatically performed once we work in the larger Lie algebra $\mathfrak{S}$ with differential operators and scalar functions. Likewise, there is no need for a representation of expansion elements in, say, the Hall basis because this is done automatically in $\mathfrak{G}$.

Substituting and aggregating terms of the same order of magnitude, we obtain

$$\begin{aligned}
\mathscr{W}^{[1]} = \; & -\overbrace{\tau\omega^{-1}\partial_x^2}^{\mathcal{O}(\varepsilon^{-1/2})} - \overbrace{\tfrac{1}{12}\tau^3\omega(\partial_x V)^2 - \tfrac{1}{3}\tau^3\omega^{-1}(\partial_x^2 V)\partial_x^2}^{\mathcal{O}(\varepsilon^{1/2})} \\
& - \overbrace{\tfrac{1}{3}\tau^3\omega^{-1}(\partial_x^3 V)\partial_x + \tfrac{1}{45}\tau^5\omega^{-3}(\partial_x^4 V)\partial_x^4}^{\mathcal{O}(\varepsilon^{3/2})} \\
& + \overbrace{\tau^5\left\{\omega\tfrac{1}{60}(\partial_x V)^2(\partial_x^2 V) - \omega^{-1}\left(\tfrac{4}{45}(\partial_x^2 V)^2 - \tfrac{1}{90}(\partial_x V)(\partial_x^3 V)\right)\partial_x^2\right\}}^{\mathcal{O}(\varepsilon^{3/2})} \\
& - \overbrace{\tau^3\omega^{-1}\tfrac{1}{12}(\partial_x^4 V) - \tau^5\omega^{-1}\{\tfrac{1}{6}(\partial_x^2 V)(\partial_x^3 V) - \tfrac{1}{90}(\partial_x V)(\partial_x^4 V)\}\partial_x}^{\mathcal{O}(\varepsilon^{5/2})} \\
& + \overbrace{\tfrac{2}{45}\tau^5\omega^{-3}(\partial_x^5 V)\partial_x^3 - \tau^7\omega\{\tfrac{1}{945}(\partial_x^2 V)^2(\partial_x V)^2 + \tfrac{1}{840}(\partial_x^3 V)(\partial_x V)^3\}}^{\mathcal{O}(\varepsilon^{5/2})} \\
& - \overbrace{\tau^7\omega^{-1}\{\tfrac{26}{945}(\partial_x^2 V)^3 + \tfrac{13}{945}(\partial_x V)(\partial_x^2 V)(\partial_x^3 V) + \tfrac{1}{630}(\partial_x V)^2(\partial_x^4 V)\}\partial_x^2}^{\mathcal{O}(\varepsilon^{5/2})} \\
& + \overbrace{\tau^7\omega^{-3}\{\tfrac{1}{315}(\partial_x^3 V)^2 + \tfrac{22}{945}(\partial_x^2 V)(\partial_x^4 V) - \tfrac{1}{945}(\partial_x V)(\partial_x^5 V)\}\partial_x^4}^{\mathcal{O}(\varepsilon^{5/2})} \\
& - \overbrace{\tau^7\omega^{-5}\tfrac{2}{945}(\partial_x^6 V)\partial_x^6}^{\mathcal{O}(\varepsilon^{5/2})} + \mathcal{O}\left(\varepsilon^{7/2}\right).
\end{aligned} \tag{4.18}$$

In principle, we could pursue with the next iteration, i.e., identifying the largest term $W^{[1]} = -\tau\omega^{-1}\partial_x^2$ and extracting it with the same procedure. Unfortunately, a closer look at (4.18) reveals a number of difficulties, namely the appearance of non-Hermitian operators in form of multiplications $V^{(k)}\partial_x^j$ and odd order derivatives ∂_x at higher order. On the other hand, skew-Hermitian operators form a Lie algebra and since the (symmetric) BCH formula only involves commutators and linear combinations thereof, skew-Hermiticity is preserved but this applies only to the expression $\mathscr{W}^{[1]}$ as a whole. For the purpose of stability of our expansion, we need to ensure that in each step, only skew-Hermitian operators are extracted. Both ∂_x^2 and multiplication by V are Hermitian operators, which in turn implies that their product with an odd power of τ is skew-Hermitian (multiplication with the imaginary unit) and its exponential is thus unitary. This survives under eventual discretization, because any reasonable approximation of ∂_x^2 preserves Hermiticity. However, ∂_x and odd powers thereof are a skew-symmetric operators and so are their reasonable approximations. Furthermore, products of Hermitian operators are only Hermitian if they commute. Therefore, a naïve collection of terms in the same power could lead to a loss of unitarity and we need an additional step to avoid stability problems. The idea is to rewrite odd derivatives as a linear combination of even derivatives, thereby enabling us to identify the Hermitian operators of a given size in ε and the following result is due to *Iserles* [10].

Excursus: getting even

Let y be a continuously differentiable function. The starting point for our current construction is the identity

$$y(x)\partial_x = -\frac{1}{2}\int_{x_0}^{x} y(\xi)\,\mathrm{d}\xi\,\partial_x^2 - \frac{1}{2}\partial_x y(x) + \frac{1}{2}\partial_x^2\left[\int_{x_0}^{x} y(\xi)\,\mathrm{d}\xi\,\cdot\right], \tag{4.19}$$

where x_0 is arbitrary: Its direct proof is trivial. Note that, whilst we have ∂_x on the left, the right-hand side features ∂_x^0 and ∂_x^2, which are both even powers of the differentiation operator. Since in principle we might be interested in expanding beyond $\mathcal{O}\left(\varepsilon^{3/2}\right)$ or employing different values of ρ and σ, we wish to cater not just for ∂_x but for all its odd powers. The following theorem generalizes (4.19) to express $y(x)\partial_x^{2s+1}$, $s \in \mathbb{N}$, solely by means of even derivatives. We remark that the procedure introduces different powers in ε by generating higher-order derivatives.

Theorem 4.1.1 (*Iserles*)**.** *Let $s \in \mathbb{N}$, define the real sequence $\{\beta_k\}_{k\geq 0}$ by*

$$\sum_{k=0}^{\infty}\frac{(-1)^k\beta_k}{(2k+1)!}T^k = \frac{1}{T}\left(1 - \frac{T^{1/2}}{\sinh T^{1/2}}\right)$$

and set

$$Q_k(x) = (-1)^{s-k+1}\beta_{s-k}\binom{2s+1}{2k}\partial_x^{2s-2k+1}y(x), \qquad k = 0, 1, \ldots, s, \tag{4.20}$$

$$Q_{s+1}(x) = \frac{1}{2s+2}\int_{x_0}^{x} y(\xi)\,\mathrm{d}\xi, \tag{4.21}$$

$$P_k(x) = -\sum_{l=k}^{s+1}\binom{2l}{2k}\partial_x^{2l-2k}Q_l(x), \qquad k = 1, 2, \ldots, s+1. \tag{4.22}$$

Then

$$y(x)\partial_x^{2s+1} = \sum_{k=0}^{s+1} P_k(x)\partial_x^{2k} + \sum_{k=0}^{s+1} \partial_x^{2k}[Q_k(x)\cdot]. \tag{4.23}$$

Proof. We act on the second sum on the right-hand side of (4.23) with the Leibniz rule, whereby

$$\begin{aligned} y\partial_x^{2s+1} &= \sum_{k=1}^{s+1} P_k\partial_x^{2k} + \sum_{l=0}^{s+1}\sum_{k=0}^{2l}\binom{2l}{k}(\partial_x^{2l-k}Q_l)\partial_x^k \\ &= \sum_{k=1}^{s+1} P_k\partial_x^{2k} + \sum_{k=0}^{s+1}\left[\sum_{l=k}^{s+1}\binom{2l}{2k}(\partial_x^{2(l-k)}Q_l)\right]\partial_x^{2k} \\ &\quad + \sum_{k=0}^{s}\left[\sum_{l=k+1}^{s+1}\binom{2l}{2k+1}(\partial_x^{2(l-k)-1}Q_l)\right]\partial_x^{2k+1}. \end{aligned}$$

Equating powers of ∂_x on both sides, we obtain (4.21), (4.22) and the equations

$$\sum_{l=k+1}^{s+1}\binom{2l}{2k+1}\partial_x^{2(l-k)-1}Q_l = 0, \qquad k = s-1, s-2, \dots, 0. \tag{4.24}$$

Our contention is that there exist coefficients $\{\beta_k\}_{k\geq 0}$ such that (4.20) is true. Indeed, substituting (4.20) into (4.24) yields, after simple algebra, the triangular linear system

$$\sum_{l=k+1}^{s}(-1)^{s-l}\binom{2s-2k}{2s+1-2l}\beta_{s-l} = \frac{1}{2s-2k+1}, \qquad k = 0, 1, \dots, s-1.$$

We deduce that

$$\sum_{l=0}^{k-1}(-1)^l\binom{2k}{2l+1}\beta_l = \frac{1}{2k+1}, \qquad k \in \mathbb{N}.$$

Finally, we multiply the last equation by $T^{k-1}/(2k)!$ and sum up for $k \in \mathbb{N}$. On the left we have

$$\begin{aligned} \sum_{k=1}^{\infty}\frac{1}{(2k)!}\sum_{l=0}^{k-1}(-1)^l\binom{2k}{2l+1}\beta_l T^{k-1} &= \sum_{l=0}^{\infty}\frac{(-1)^l\beta_l}{(2l+1)!}\sum_{l=k+1}^{\infty}\frac{T^{k-1}}{(2k-2l-1)!} \\ &= \sum_{l=0}^{\infty}\frac{(-1)^l\beta_l}{(2l+1)!}T^l\sum_{k=0}^{\infty}\frac{T^k}{(2k+1)!} \\ &= \frac{\sinh T^{1/2}}{T^{1/2}}\sum_{l=0}^{\infty}\frac{(-1)^l\beta_l}{(2l+1)!}T^l, \end{aligned}$$

while on the right we obtain

$$\sum_{k=1}^{\infty}\frac{T^{k-1}}{(2k+1)!} = \frac{1}{T}\left(\frac{\sinh T^{1/2}}{T^{1/2}} - 1\right).$$

This confirms (4.20) and completes the proof. □

The first few values are $\beta_0 = \frac{1}{6}$, $\beta_1 = \frac{7}{60}$, $\beta_2 = \frac{31}{126}$, $\beta_3 = \frac{127}{120}$, $\beta_4 = \frac{511}{66}$, $\beta_5 = \frac{1414477}{16380}$ and $\beta_6 = \frac{8191}{6}$. Practically, just

$$
\begin{aligned}
y\partial_x &= -\frac{1}{2}\int_0^x y(\xi)\,\mathrm{d}\xi\,\partial_x^2 - \frac{1}{2}\partial_x y + \frac{1}{2}\partial_x^2\left[\int_0^x y(\xi)\,\mathrm{d}\xi\,\cdot\right],\\
y\partial_x^3 &= -(\partial_x y)\partial_x^2 - \frac{1}{4}\int_0^x y(\xi)\,\mathrm{d}\xi\,\partial_x^4 + \frac{1}{4}\partial_x^3 y - \frac{1}{2}\partial_x^2[(\partial_x y)\cdot] + \frac{1}{4}\partial_x^4\left[\int_0^x y(\xi)\,\mathrm{d}\xi\,\cdot\right],\\
y\partial_x^5 &= \frac{4}{3}(\partial_x^3 y)\partial_x^2 - \frac{5}{3}(\partial_x y)\partial_x^4 - \frac{1}{6}\int_0^x y(\xi)\,\mathrm{d}\xi\,\partial_x^6 - \frac{1}{2}\partial_x^5 y + \frac{7}{6}\partial_x^2[(\partial_x^3 y)\cdot]\\
&\quad - \frac{5}{6}\partial_x^4[(\partial_x y)\cdot] + \frac{1}{6}\partial_x^6\left[\int_0^x y(\xi)\,\mathrm{d}\xi\,\cdot\right].
\end{aligned}
$$

are ever likely to be needed in practical computation.

An asymptotic splitting of the first kind

Now, all necessary tools are available and we dedicate this subsection to illustrate how to compute the splitting (4.8) with the algorithm in Table 4.2 on page 90. Using (4.19) to replace all the occurrences of ∂_x in (4.18), the new core $\mathscr{W}^{[1]}$ becomes

$$
\begin{aligned}
\mathscr{W}^{[1]} = &-\overbrace{\tau\omega^{-1}\partial_x^2}^{\varepsilon^{-1/2}}\\
&-\overbrace{\tfrac{1}{12}\tau^3\omega(\partial_x V)^2 - \tfrac{1}{6}\tau^3\omega^{-1}\{\partial_x^2,(\partial_x^2 V)\}_+}^{\varepsilon^{1/2}}\\
&+\overbrace{\tfrac{1}{60}\tau^5\omega(\partial_x V)^2(\partial_x^2 V) + \tfrac{1}{90}\tau^5\omega^{-3}\{\partial_x^4,\partial_x^4 V\}_+}^{\varepsilon^{3/2}}\\
&-\overbrace{\tfrac{2}{45}\tau^5\omega^{-1}\left(\{\partial_x^2,(\partial_x^2 V)^2\}_+ - \tfrac{1}{8}\{\partial_x^2,(\partial_x V)(\partial_x^3 V)\}_+\right)}^{\varepsilon^{3/2}}\\
&+\overbrace{\tfrac{1}{12}\tau^3\omega^{-1}(\partial_x^4 V) - \tau^7\omega\left(\tfrac{1}{945}(\partial_x V)^2(\partial_x^2 V)^2 + \tfrac{1}{840}(\partial_x V)^3(\partial_x^3 V)\right)}^{\varepsilon^{5/2}}\\
&-\tfrac{1}{3780}\overbrace{\tau^7\omega^{-1}\{\partial_x^2,52(\partial_x^2 V)^3 + 26(\partial_x V)(\partial_x^2 V)(\partial_x^3 V) + 3(\partial_x V)^2(\partial_x^4 V)\}_+}^{\varepsilon^{5/2}}\\
&+\overbrace{\tau^7\omega^{-3}\tfrac{1}{1890}\{\partial_x^4,3(\partial_x^3 V)^2 + 22(\partial_x^2 V)(\partial_x^4 V) - (\partial_x V)(\partial_x^5 V)\}_+}^{\varepsilon^{5/2}}\\
&-\overbrace{\tau^7\omega^{-5}\tfrac{1}{945}\{\partial_x^6,(\partial_x^6 V)\}_+}^{\varepsilon^{5/2}} + \mathscr{O}\left(\varepsilon^{7/2}\right),
\end{aligned}
$$

where we have introduced the *anti-commutator*,

$$
\{A,B\}_+ = AB + BA. \tag{4.25}
$$

Recall that we have started the algorithm with

$$
\mathscr{R}_0 = \frac{1}{2}W^{[0]} = \frac{1}{2}\tau\omega V
$$

and to progress to the second stage, we choose to eliminate the lowest ε-order term,

$$\mathscr{R}_1 = \frac{1}{2}W^{[1]} = -\frac{1}{2}\tau\omega^{-1}\partial_x^2 = \mathcal{O}\left(\varepsilon^{-1/2}\right),$$

from $\mathscr{W}^{[1]}$, which is of the same size as the $W^{[0]}$ for this choice of parameters $\rho = 1$. Although the new $W^{[1]}$ and $\mathscr{W}^{[1]}$ are more complicated, the computations are now much simpler. The main reason is that the ε-order behaves under commutation like

$$[\tau^{i_1}\omega^{j_1}f(x)\partial_x^{k_1}, \tau^{i_2}\omega^{j_2}g(x)\partial_x^{k_2}] = \mathcal{O}\left(\tau^{i_1+i_2}\omega^{j_1+j_2}\partial_x^{k_1+k_2-1}\right), \tag{4.26}$$

and thus, the order increases under very general assumptions. The first commutators then become

$$[W^{[1]}, \mathscr{W}^{[1]}] = \mathcal{O}\left(\varepsilon^1\right) \text{ and } [[\mathscr{W}^{[1]}, W^{[1]}], W^{[1]}],\ [[\mathscr{W}^{[1]}, W^{[1]}], \mathscr{W}^{[1]}] = \mathcal{O}\left(\varepsilon^{3/2}\right).$$

Each commutation with $W^{[1]}$ or $\mathscr{W}^{[1]}$ introduces a factor $\varepsilon^{1/2}$ and we need to compute commutators up to length 5 to reach an accuracy of $\mathcal{O}\left(\varepsilon^{7/2}\right)$. The next step still involves lengthy algebra and we obtain

$$\begin{aligned}
\mathscr{W}^{[2]} &= \mathrm{sBCH}(-W^{[1]}, \mathscr{W}^{[1]}) \\
&= -\overbrace{\tfrac{1}{12}\tau^3\omega(\partial_x V)^2 - \tfrac{1}{6}\tau^3\omega^{-1}\left\{\partial_x^2, (\partial_x^2 V)\right\}_+}^{\varepsilon^{1/2}} \\
&\quad + \overbrace{\tfrac{1}{60}\tau^5\left(\omega V'^2 V'' - \tfrac{1}{2}\omega^{-1}\left\{\partial_x^2, 7V''^2 + V'V'''\right\}_+ - \omega^{-3}\left\{\partial_x^4, V^{(4)}\right\}_+\right)}^{\varepsilon^{3/2}} \\
&\quad + \overbrace{\tfrac{1}{12}\tau^3\omega^{-1}V^{(4)} - \tfrac{1}{840}\tau^7\omega V'^2\left(V'V''' - 3V''^2\right)}^{\varepsilon^{5/2}} \\
&\quad + \overbrace{\tfrac{1}{1680}\tau^7\omega^{-1}\left\{\partial_x^2, -34V''^3 + 18V'V''V''' + V'^2V^{(4)}\right\}_+}^{\varepsilon^{5/2}} \\
&\quad + \overbrace{\tfrac{1}{3360}\tau^7\omega^{-3}\left\{\partial_x^4, 45V'''^2 - 76V''V^{(4)} - V'V^{(5)}\right\}_+}^{\varepsilon^{5/2}} \\
&\quad - \overbrace{\tfrac{1}{1680}\tau^7\omega^{-5}\left\{\partial_x^6, V^{(6)}\right\}_+}^{\varepsilon^{5/2}} + \mathcal{O}\left(\varepsilon^{7/2}\right),
\end{aligned} \tag{4.27}$$

with the usual shorthand $V' \equiv \partial_x V$, etc. In the next iteration, we pull out the $\mathcal{O}\left(\varepsilon^{1/2}\right)$ term,

$$2\mathscr{R}_2 = W^{[2]} = -\tfrac{1}{12}\tau^3\omega(\partial_x V)^2 - \tfrac{1}{6}\tau^3\omega^{-1}\left\{\partial_x^2, (\partial_x^2 V)\right\}_+,$$

and need to compute $\mathscr{W}^{[3]}$. Due to the symmetry of our procedure, only commutators of odd length appear and since

$$[[\mathscr{W}^{[2]}, W^{[2]}], W^{[2]}],\ [[\mathscr{W}^{[2]}, W^{[2]}], \mathscr{W}^{[2]}] = \mathcal{O}\left(\varepsilon^{9/2}\right),$$

we can disregard all commutators from here on. The next smaller term is thus $\mathscr{W}^{[3]} = \mathscr{W}^{[2]} - W^{[2]} = \mathcal{O}\left(\varepsilon^{3/2}\right)$ and the remainders can be read off (4.27) to arrive at

$$\mathscr{W}^{[4]} = \mathscr{W}^{[2]} - W^{[2]} - W^{[3]} + \mathcal{O}\left(\varepsilon^{5/2}\right), \qquad \mathscr{W}^{[4]} - \mathscr{T}_4 = \mathcal{O}\left(\varepsilon^{7/2}\right),$$

and the asymptotic splitting is therefore

$$\mathcal{S}^{[1]}_{(1,\frac{1}{2}),3} = e^{\mathscr{R}_0} e^{\mathscr{R}_1} e^{\mathscr{R}_2} e^{\mathscr{R}_3} e^{\mathscr{T}_4} e^{\mathscr{R}_3} e^{\mathscr{R}_2} e^{\mathscr{R}_1} e^{\mathscr{R}_0}, \tag{4.28}$$

where

$$\begin{aligned}
\mathscr{R}_0 &= \tfrac{1}{2}\tau\omega V = \mathcal{O}\left(\varepsilon^{-1/2}\right), \\
\mathscr{R}_1 &= -\tfrac{1}{2}\tau\omega^{-1}\partial_x^2 = \mathcal{O}\left(\varepsilon^{-1/2}\right), \\
\mathscr{R}_2 &= -\tfrac{1}{24}\tau^3\omega(\partial_x V)^2 - \tfrac{1}{12}\tau^3\omega^{-1}\left\{\partial_x^2, (\partial_x^2 V)\right\}_+ = \mathcal{O}\left(\varepsilon^{1/2}\right), \\
\mathscr{R}_3 &= \tfrac{1}{120}\tau^5\left(\omega V'^2 V'' - \tfrac{1}{2}\omega^{-1}\left\{\partial_x^2, 7V''^2 + V'V'''\right\}_+ - \omega^{-3}\left\{\partial_x^4, V^{(4)}\right\}_+\right), \\
\mathscr{T}_4 &= \tfrac{1}{12}\tau^3\omega^{-1}V^{(4)} - \tfrac{1}{840}\tau^7\omega V'^2\left(V'V''' - 3V''^2\right) \\
&\quad + \tau^7\Big(\tfrac{1}{1680}\omega^{-1}\left\{\partial_x^2, -34V''^3 + 18V'V''V''' + V'^2V^{(4)}\right\}_+ \\
&\quad + \tfrac{1}{3360}\omega^{-3}\left\{\partial_x^4, 45V'''^2 - 76V''V^{(4)} - V'V^{(5)}\right\}_+ \\
&\quad - \tfrac{1}{1680}\omega^{-5}\left\{\partial_x^6, V^{(6)}\right\}_+\Big) = \mathcal{O}\left(\varepsilon^{5/2}\right).
\end{aligned} \tag{4.29}$$

The notation $\mathcal{S}^{[1]}_{(1,\frac{1}{2}),3}$ is mostly self-explanatory: $(1, \frac{1}{2})$ refers to the values of ρ and σ, while $s = 3$. The superscript $^{[1]}$ stands for an asymptotic splitting of the *first kind* (1st) and in continuation, we consider an alternative splitting (with initial $W^{[0]}$ equaling $-\tau\omega^{-1}\partial_x^2$), which we designate as an asymptotic splitting of the *second kind* (2nd).

Once we replace derivatives by differentiation matrices, the evaluation of a single time step $u_{n+1} = \tilde{\mathcal{S}}^{[1]}_{(1,\frac{1}{2}),3} u_n$ requires in principle 9 exponentials. Here and in the remainder of this section, the tilde indicates that the operator has been semidiscretized. However, we note that, once we use nodal values in semi-discretization, the discretized matrix $\mathscr{R}_0$ is diagonal and the computation of its exponential can be accomplished in $\mathcal{O}(N)$ operations.[3] The second exponent $\mathscr{R}_1$ can be cheaply diagonalized in the Fourier basis at cost $\mathcal{O}(N \log N)$. This is an important point because $\mathscr{R}_0$ and $\mathscr{R}_1$ are the largest matrices present. All other matrices are $\mathcal{O}\left(\varepsilon^{1/2}\right)$ or less, and, as will become clear in Section 4.1.4, their computation with Krylov subspace methods is very affordable.

An asymptotic splitting of the second kind

Our choice of $W^{[0]}$ in the first approach was somewhat arbitrary and we will now pursue the alternative, i.e., we start from

$$2\mathscr{R}_0 = W^{[0]} = -\tau\omega^{-1}\partial_x^2, \qquad \mathscr{W}^{[0]} = -\tau\omega^{-1}\partial_x^2 + \tau\omega V.$$

This results in

$$\mathscr{W}^{[1]} = \mathrm{sBCH}(-W^{[0]}, \mathscr{W}^{[0]}) = \sum_{j=-1}^{\infty} \mathscr{W}_j^{[1]}, \quad \text{where} \quad \mathscr{W}_j^{[l]} = \mathcal{O}\left(\varepsilon^{j+1/2}\right),\ l \in \mathbb{N}_0,$$

[3] Using a Fourier basis the cost is $\mathcal{O}(N \log N)$.

Symmetric Zassenhaus algorithm

$s := 0; \quad \mathscr{W}^{[0]} := \tau(-\omega^{-1}\partial_x^2 + \omega V(x)); \quad W^{[0]} := \tau\omega V(x)$

do

$s := s + 1$

compute $\mathscr{W}^{[s]} := \mathrm{sBCH}(-W^{[s-1]}, \mathscr{W}^{[s-1]})$

rewrite $\mathscr{W}^{[s]}$ in even derivatives, cf. (4.23)

expand result in powers of ε

define $W^{[s]} := \mathscr{O}\left(\varepsilon^{s-3/2}\right)$, s.t. $W^{[s]} - \mathscr{W}^{[s]} = \mathscr{O}\left(\varepsilon^{s-1/2}\right)$

while $s <$ desired order $s_{\max}$

Resulting method:

$$e^{\mathscr{W}^{[0]}} = e^{W^{[0]}/2} e^{W^{[1]}/2} \cdots e^{W^{[s_{\max}]}} \cdots e^{W^{[1]}/2} e^{W^{[0]}/2} + \mathscr{O}\left(\varepsilon^{1+s_{\max}/2}\right)$$

Table 4.2: Symmetric Zassenhaus splitting of the first kind in even-order derivatives

and

$$\begin{aligned}
\mathscr{W}_{-1}^{[1]} &= \tau\omega V, \\
\mathscr{W}_{0}^{[1]} &= \tfrac{1}{6}\tau^3\omega(\partial_x V)^2 + \tfrac{1}{12}\tau^3\omega^{-1}\left\{\partial_x^2, (\partial_x^2 V)\right\}_+, \\
\mathscr{W}_{1}^{[1]} &= \tfrac{2}{45}\tau^5\omega(\partial_x V)^2(\partial_x^2 V) - \tfrac{1}{60}\tau^5\omega^{-1}\left\{\partial_x^2, (\partial_x^2 V)^2 - 2(\partial_x V)(\partial_x^3 V)\right\}_+ \\
&\quad + \tfrac{1}{240}\tau^5\omega^{-3}\left\{\partial_x^4, (\partial_x^4 V)\right\}_+, \\
\mathscr{W}_{2}^{[1]} &= -\tfrac{1}{24}\tau^3\omega^{-1}(\partial_x^4 V) + \tau^7\omega\Big(\tfrac{1}{630}(\partial_x^3 V)(\partial_x V)^3 + \tfrac{13}{945}(\partial_x^2 V)^2(\partial_x V)^2\Big) \\
&\quad + \tfrac{1}{1890}\tau^7\omega^{-1}\left\{\partial_x^2, 2(\partial_x^2 V)^3 + (\partial_x V)(\partial_x^2 V)(\partial_x^3 V) + 9(\partial_x V)^2(\partial_x^4 V)\right\}_+ \\
&\quad + \tfrac{1}{5040}\tau^7\omega^{-3}\left\{\partial_x^4, 15(\partial_x^3 V)^2 - 16(\partial_x^2 V)(\partial_x^4 V) + 9(\partial_x V)(\partial_x^5 V)\right\}_+ \\
&\quad + \tfrac{1}{10080}\tau^7\omega^{-5}\left\{\partial_x^6, (\partial_x^6 V)\right\}_+.
\end{aligned}$$

We next remove $\mathscr{R}_1 = \frac{1}{2}W^{[1]} = \frac{1}{2}\mathscr{W}_{-1}^{[1]} = \mathscr{O}\left(\varepsilon^{1/2}\right)$ and obtain, with the short hand $X = -W^{[1]}$, $Y = \mathscr{W}^{[1]}$,

$$\mathscr{W}^{[2]} = \mathrm{sBCH}(X, Y) = X + Y - \frac{1}{24}[[Y, X], X] - \frac{1}{12}[[Y, X], Y] + \mathscr{O}\left(\varepsilon^{7/2}\right) = \sum_{j=0}^{\infty} \mathscr{W}_j^{[2]},$$

where

$$\begin{aligned}
\mathscr{W}_{0}^{[2]} &= \tfrac{1}{6}\tau^3\omega(\partial_x V)^2 + \tfrac{1}{12}\tau^3\omega^{-1}\left\{\partial_x^2, (\partial_x^2 V)\right\}_+, \\
\mathscr{W}_{1}^{[2]} &= \tfrac{7}{120}\tau^5\omega(\partial_x^2 V)(\partial_x V)^2 - \tfrac{1}{60}\tau^5\omega^{-1}\left\{\partial_x^2, (\partial_x^2 V)^2 - 2(\partial_x V)(\partial_x^3 V)\right\}_+ \\
&\quad + \tfrac{1}{240}\tau^5\omega^{-3}\left\{\partial_x^4, (\partial_x^4 V)\right\}_+, \\
\mathscr{W}_{2}^{[2]} &= -\tfrac{1}{24}\tau^3\omega^{-1}(\partial_x^4 V) + \tau^7\omega\left(\tfrac{1}{140}(\partial_x^3 V)(\partial_x V)^3 + \tfrac{17}{840}(\partial_x^2 V)^2(\partial_x V)^2\right) \\
&\quad - \tfrac{1}{3360}\tau^7\omega^{-1}\left\{\partial_x^2, 12(\partial_x^2 V)^3 + 6(\partial_x V)(\partial_x^2 V)(\partial_x^3 V) - 23(\partial_x V)^2(\partial_x^4 V)\right\}_+ \\
&\quad + \tfrac{1}{5040}\tau^7\omega^{-3}\left\{\partial_x^4, 15(\partial_x^3 V)^2 - 16(\partial_x^2 V)(\partial_x^4 V) + 9(\partial_x V)(\partial_x^5 V)\right\}_+ \\
&\quad + \tfrac{1}{10080}\tau^7\omega^{-5}\left\{\partial_x^6, (\partial_x^6 V)\right\}_+.
\end{aligned}$$

Next,

$$\mathscr{R}_2 = \frac{1}{2}W^{[2]} = \frac{1}{2}\mathscr{W}_0^{[2]} = \tfrac{1}{12}\tau^3\omega(\partial_x V)^2 + \tfrac{1}{24}\tau^3\omega^{-1}\left\{\partial_x^2, (\partial_x^2 V)\right\}_+,$$

and we deduce that the relevant terms of $\mathscr{W}^{[3]} = \sum_{j=1}^{\infty}\mathscr{W}_j^{[3]}$ are

$$\begin{aligned}
\mathscr{W}_1^{[3]} =& \tfrac{7}{120}\tau^5\omega(\partial_x^2 V)(\partial_x V)^2 - \tfrac{1}{60}\tau^5\omega^{-1}\left\{\partial_x^2, (\partial_x^2 V)^2 - 2(\partial_x V)(\partial_x^3 V)\right\}_+ \\
&+ \tfrac{1}{240}\tau^5\omega^{-3}\left\{\partial_x^4, (\partial_x^4 V)\right\}_+, \\
\mathscr{W}_2^{[3]} =& -\tfrac{1}{24}\tau^3\omega^{-1}(\partial_x^4 V) + \tfrac{1}{840}\tau^7\omega\left(17(\partial_x^2 V)^2 + 6(\partial_x V)(\partial_x^3 V)\right) \\
&- \tfrac{1}{3360}\tau^7\omega^{-1}\left\{\partial_x^2, 12(\partial_x^2 V)^3 + 6(\partial_x V)(\partial_x^2 V)(\partial_x^3 V) - 23(\partial_x V)^2(\partial_x^4 V)\right\}_+ \\
&+ \tfrac{1}{5040}\tau^7\omega^{-3}\left\{\partial_x^4, 15(\partial_x^3 V)^2 - 16(\partial_x^2 V)(\partial_x^4 V) + 9(\partial_x V)(\partial_x^5 V)\right\}_+ \\
&+ \tfrac{1}{10080}\tau^7\omega^{-5}\left\{\partial_x^6, (\partial_x^6 V)\right\}_+.
\end{aligned}$$

And, finally, we can read off the results

$$\mathscr{R}_3 = \frac{1}{2}\mathscr{W}_1^{[3]}, \qquad \mathscr{T}_4 = \mathscr{W}_2^{[3]},$$

since the commutators are negligible, $[W^{[3]}, \mathscr{W}^{[3]}] \equiv [\mathscr{W}_1^{[3]}, \mathscr{W}^{[3]}] = \mathcal{O}\left(\varepsilon^4\right)$, and no new terms of relevant size greater than $\mathcal{O}\left(\varepsilon^{7/2}\right)$ are generated. The outcome is the splitting

$$\mathcal{S}^{[2]}_{(1,\frac{1}{2}),3} = e^{\mathscr{R}_0}e^{\mathscr{R}_1}e^{\mathscr{R}_2}e^{\mathscr{R}_3}e^{\mathscr{T}_4}e^{\mathscr{R}_3}e^{\mathscr{R}_2}e^{\mathscr{R}_1}e^{\mathscr{R}_0}, \tag{4.30}$$

where

$$\begin{aligned}
\mathscr{R}_0 =& -\tfrac{1}{2}\tau\omega^{-1}\partial_x^2, \\
\mathscr{R}_1 =& \tfrac{1}{2}\tau\omega V, \\
\mathscr{R}_2 =& \tfrac{1}{12}\tau^3\omega(\partial_x V)^2 + \tfrac{1}{24}\tau^3\omega^{-1}\left\{\partial_x^2, (\partial_x^2 V)\right\}_+, \\
\mathscr{R}_3 =& \tfrac{7}{240}\tau^5\omega(\partial_x^2 V)(\partial_x V)^2 - \tfrac{1}{120}\tau^5\omega^{-1}\left\{\partial_x^2, (\partial_x^2 V)^2 - 2(\partial_x V)(\partial_x^3 V)\right\}_+ \\
&+ \tfrac{1}{480}\tau^5\omega^{-3}\left\{\partial_x^4, (\partial_x^4 V)\right\}_+, \\
\mathscr{T}_4 =& -\tfrac{1}{24}\tau^3\omega^{-1}(\partial_x^4 V) + \tfrac{1}{840}\tau^7\omega\left(17(\partial_x V)^2(\partial_x^2 V)^2 + 6(\partial_x V)^3(\partial_x^3 V)\right) \\
&- \tfrac{1}{3360}\tau^7\omega^{-1}\left\{\partial_x^2, 12(\partial_x^2 V)^3 + 6(\partial_x V)(\partial_x^2 V)(\partial_x^3 V) - 23(\partial_x V)^2(\partial_x^4 V)\right\}_+ \\
&- \tfrac{1}{5040}\tau^7\omega^{-3}\left\{\partial_x^4, 15(\partial_x^3 V)^2 - 16(\partial_x^2 V)(\partial_x^4 V) + 9(\partial_x V)(\partial_x^5 V)\right\}_+ \\
&+ \tfrac{1}{10080}\tau^7\omega^{-5}\left\{\partial_x^6, (\partial_x^6 V)\right\}_+.
\end{aligned}$$

Comparing (4.30) with (4.28), we have again 9 exponentials, and again, the outermost exponentials $\mathscr{R}_0, \mathscr{R}_1$ are cheap to compute since, after discretization, they are either diagonal or diagonal after a FFT. The remaining terms $\tilde{\mathscr{R}}_2 = \mathcal{O}\left(\varepsilon^{1/2}\right)$, $\tilde{\mathscr{R}}_3 = \mathcal{O}\left(\varepsilon^{3/2}\right)$ and $\tilde{\mathscr{T}}_4 = \mathcal{O}\left(\varepsilon^{5/2}\right)$ need to be computed with Krylov subspace methods but the small magnitude of both these matrices means that only a small number of Krylov iterations will be necessary.

Note that the FSAL property can be exploited for splittings of both types, (4.28) and (4.30).

Generalizations to different pairs (ρ, σ)

The presented algorithm is by no means restricted to the chosen values of ρ, σ and other choices can be pursued to obtain different splittings as long as the subsequent exponents are guaranteed to decrease in size. Here, we will briefly discuss the implications on the length of the commutators and occurrence of derivatives.

For initial computation of the asymptotic method, the computationally challenging part is the symmetric BCH formula in high orders and we are interested in truncating as soon as the desired order is achieved. In general, the algorithm parts from either the kinetic term $A = -\tau\varepsilon\partial_x^2$ or the potential $B = \tau V/\varepsilon$ and the first commutators of odd length are

$$[A,[A,B]] = \mathcal{O}\left(\varepsilon^{1+3\sigma-2\rho}\right), \quad [B,[B,A]] = \mathcal{O}\left(\varepsilon^{-1+3\sigma}\right).$$

According to our construction rules, the smaller of the two will be pulled out in the next step, and since we have to require $\rho \geq 1$ to resolve spatial oscillations, the right commutator is identified to be smaller or of equal size (for $\rho = 1$).

For the derivation of the algorithm, one is dealing with an exponentially growing number of terms in the sBCH formula and it is important to know at what grade the commutators can be safely truncated. Suppose that we have arrived at the kth step ($k > 0$), for arbitrary σ, ρ, and let $W^{[k]} = \mathcal{O}(\varepsilon^p)$ for some $p > 0$ and consequently $\mathscr{W}^{[k]} = W^{[k]} + \mathcal{O}\left(\varepsilon^{p+\delta}\right)$, for some $\delta > 0$, then the leading (odd) commutators are (cf. (4.26))

$$[W^{[k]},[W^{[k]},\mathscr{W}^{k}]] = \mathcal{O}\left(\varepsilon^{3p+\delta+2\rho}\right), [\mathscr{W}^{[k]},[W^{[k]},\mathscr{W}^{k}]] = \mathcal{O}\left(\varepsilon^{3p+\delta+2\rho}\right),$$

where the 2ρ contribution is due to the ever lowering degree in the derivatives and the extra gain δ is caused by to the innermost commutator. For the splitting of the first kind, we had, e.g., $W^{[2]} = \mathcal{O}\left(\varepsilon^{1/2}\right)$ and $\mathscr{W}^{[2]} - W^{[2]} = \mathcal{O}\left(\varepsilon^{3/2}\right)$ which we identify with $p = 1/2$ and $\delta = 1$ and reproduce the previous estimates.

For odd derivatives, the odd-even substitution will increase the size by a factor $\varepsilon^{-\rho}$, which, however, will not impact on the overall size since terms of the same magnitude are already present, a fact that follows from the stability considerations that we examine next.

4.1.3 Stability

The convergence of classical methods for initial-value partial differential equations is governed by the Lax equivalence theorem: Convergence equals consistency plus stability [75]. Our method is clearly consistent and stability is equivalent to

$$\lim_{\varepsilon\to 0}\limsup_{n\to\infty} \|(\tilde{\mathcal{S}}^{[1]}_{(1,\frac{1}{2}),3})^n\|_2 < \infty, \tag{4.31}$$

for a semi-discretized method $\tilde{\mathcal{S}}$ obtained above in the usual Euclidean norm. We are going to show that the proposed splittings yield unitary schemes and thus trivially satisfy (4.31). Furthermore they can be regarded as geometric integrators in the sense of Refs. [53, 65, 91] since the exact evolution operator is also unitary. Additionally, the method preserves the gauge invariance since a constant shift of the potential will only appear in the first step (or second for splits of the second kind) and automatically cancels in consecutive steps due to the commutations.

Theorem 4.1.2. *Supposing that the splitting* (4.8) *has been derived by the symmetric Zassenhaus algorithm of 4.2, it is true that* $W^{[j]} \in \mathfrak{su}(\mathbb{C})$ *for all* $j \geq 0$ *and thus also* $\mathscr{R}_0, \mathscr{R}_1, \dots, \mathscr{R}_s$, *and* $\mathscr{T}_{s+1} \in \mathfrak{su}(\mathbb{C})$ *and in consequence, the scheme is unitary.*

Proof. The basic argument goes as follows: The operator at the initial step, $\mathscr{W}^{[0]} = \tau H$, is skew-Hermitian and, in each step, a term $W^{[j]}$ is pulled out via the symmetric BCH formula (4.11). Assume, that $W^{[j]}$ is skew-Hermitian, then so will be $\mathscr{W}^{[j+1]}$ because skew-Hermiticity is preserved under commutation and summation, i.e., let A, B be skew-Hermitian, then

$$[A,B]^\dagger = (AB - BA)^\dagger = (B^\dagger A^\dagger - A^\dagger B^\dagger) = [B,A] = -[A,B].$$

What remains to be shown is that at each step, the lowest order ε terms in $\mathscr{W}^{[j]}$, after the 'odd to even' substitution (4.19), namely $W^{[j]}$, are indeed skew-Hermitian.

Problematic terms are of the form $f(x)\partial_x^k$ and we need to ensure, that they occur in a symmetric way, i.e., they come in pairs $\tau^{2l+1}\left(f(x)\partial_x^{2k} + \partial_x^{2k}(f(x)\cdot)\right)$ that clearly constitute a skew-Hermitian operator since f, ∂_x^{2k} are symmetric.

All commutators iC produced by the symmetric Zassenhaus algorithm are of odd length and can be written - after the 'odd to even' substitution - as, $iC = i\sum f_k \partial_x^{2k} + \partial_x^{2k}(g_k\cdot)$, for some scalar functions f_k, g_k. Since C, f_k, g_k and ∂_x^{2k} are symmetric, it follows that

$$\sum_{k=0}^{n} [f_k - g_k, \partial_x^{2k}] = 0. \tag{4.32}$$

Computing the highest derivative gives $[f_n - g_n, \partial_x^{2n}] = -2n(f_n - g_n)'\partial^{2n-1} + r$. The remaining terms of (4.32), $k < n$, cannot cancel this derivative and hence $f_n - g_n = \text{const.}$ and $r = 0$. It follows by induction that $f_k - g_k = \text{const.}$ and thus, symmetry of each pair is verified. Since our algorithm does not separate terms of same size, the pairs will not be split and consequently, $W^{[j]} \in \mathfrak{su}(\mathbb{C})$.

The same proof is valid after spatial discretization if the derivatives ∂_x^2 are approximated by a symmetric matrix $\mathscr{K}$ and the functions by (trivially symmetric) diagonal matrices $\mathscr{D}$, and then $W^{[j]} \in \mathfrak{su}(\mathbb{C})$. □

4.1.4 Computing the exponential

The asymptotic splittings (4.28) and (4.30) are expressed in operatorial terms and as indicated in the stability proof, to render them into proper computational algorithms, we must replace ∂_x^2 with an appropriate differentiation matrix, acting on an N-dimensional space.

It is common in the numerical solution of the Schrödinger equation to use spectral discretization [53, 83] since they can be cheaply computed with the FFT algorithm and are of infinite order in space.

As discussed earlier, the large exponentials depend only on either the space or the momentum coordinate, respectively, and are thus either already diagonal or can be diagonalized by a FFT. The smaller terms can be computed with the Lanczos method, cf. Section 1.3.2, which greatly benefits from the smallness of the exponents. For convenience of the reader, we repeat the

error estimates of Ref. [91]: The error committed by the restriction to (Lanczos-)polynomials of degree $< r$ can be bounded by ($h = 1$)

$$\|e^{\mathscr{R}}v - V_r \exp(-iT_r)e_1\| \leq 8e^{-\rho^2/(4r)} \left(\frac{e\rho}{2r}\right)^r, \quad \text{for } r \geq \rho, \tag{1.33'}$$

where $\rho = \rho(\mathscr{H})$ is the spectral radius of the Hermitian operator $\mathscr{H} = i\mathscr{R}$. Suppose that $\rho(\mathscr{R}) \leq c\varepsilon^p$, then the r.h.s. of (1.33') becomes

$$\leq 8e^{-c^2\varepsilon^{2p}/(4r)} \left(\frac{ec\varepsilon^p}{2r}\right)^r \leq 8\left(\frac{ec}{2r}\right)^r \varepsilon^{rp}.$$

For the presented algorithms, we are facing exponents of powers $1/2$, $3/2$ and $5/2$ in ε and to reach an overall error of magnitude $\varepsilon^{7/2}$, we require 7, 3 and 2 Lanczos iterations, respectively. In each iteration, a matrix-vector product has to be calculated, but even though the matrices are dense, it is still possible to resort to Fast Fourier Transforms to ease up the computational complexity by expanding the expression, just as for standard Hamiltonians, $\tilde{H}\psi = \mathscr{K}\psi + \mathscr{D}_V\psi$.

An efficient implementation minimizes the number of basis changes (FFTs). Suppose that the initial value is given in the space where $\mathscr{R}_0$ is diagonal, then, one FFT and its inverse are needed to compute the action of $e^{\mathscr{R}_1}$ (which occurs twice per step because of symmetry). For order $\mathcal{O}\left(\varepsilon^{3/2}\right)$, we can truncate after $\mathscr{R}_2$ and need three Lanczos-iterations, each requiring two FFTs and two inverse FFTs. For the next exponentials, by storing the transformed vector $\mathscr{F}(\psi)$, one FFT can be saved for each new anti-commutators: Suppose the exponent comprises of n anti-commutators $\{\partial_x^{2k}, f_{2k}(x)\}_+$, $k = 1, \ldots, n$, then $3n + 1$ FFTs are needed to evaluate one Lanczos-iteration. For arbitrary order, $\mathcal{O}\left(\varepsilon^{s+1/2}\right)$, we can calculate the cost to be

$$n = 2 \cdot \underbrace{2}_{\mathscr{R}_0, \mathscr{R}_1} + 2 \sum_{k=2}^{s} \underbrace{\overbrace{\left\lceil \frac{s+1/2}{k-3/2} \right\rceil}^{\text{iterations}} \cdot \overbrace{(3(k-1)+1)}^{\text{anti-commutators}}}_{\mathscr{R}_k} + \underbrace{\overbrace{2}^{\text{iterations}} \cdot \overbrace{(3(s-1)+1)}^{\text{anti-commutators}}}_{\mathscr{T}_{s+1}}, \quad s \geq 2, \tag{4.33}$$

where $\lceil x \rceil$ is the smallest integer $m \leq x$. The proof is obvious due to the construction of the algorithm: The stages $\mathscr{R}_k$ do not change if higher-order accuracy is required, only the number of Lanczos iterations has to be adjusted to meet the sought precision and the required number is immediate from (1.33'). The number of anti-commutators grows in each step by one since we have to cater for higher derivatives and the first few values together with some standard numerical methods are collected in Table 4.3.

As mentioned in the summary on classical splittings (4.7), the scaling $h = \mathcal{O}(\epsilon^\sigma)$ implies an error of size $\mathcal{O}\left(\epsilon^{p\sigma-1/2}\right)$ for a method of local order p. The presented methods with the choice $\sigma = 1/2$ thus show a scaling similar to an order 8 method!

It is illustrative to establish the cost of Yoshida's composition, based on the Strang splitting, which requires $n = 2 \cdot 3^p$ FFTs for classical order $2(p+1)$ or ε-order $\mathcal{O}\left(\varepsilon^{p+1/2}\right)$ in contrast to the scaling $n \propto \mathcal{O}\left(p^2\right)$ for the Zassenhaus method. And from ε-order $11/2$ onwards (classical order 12), the new algorithm requires less (about half as many) FFTs.

Method	Order $\mathcal{O}(\varepsilon^p)$	No. anti-commutators	No. FFTs
LF	1/2	0	2
Chin-4M	3/2	0	4
Split of 1st/2nd kind	3/2	1	14
$\mathrm{RKN}_{11}6$	5/2	0	22
1st/2nd	5/2	3	49
1st/2nd	7/2	6	120
Yoshida (order 8, $p = 3$)	7/2	0	54

Table 4.3: Collection of numerical costs per time-step for a selection of numerical methods. The methods are referenced in Table 4.4.

4.1.5 Numerical results

As proof of concept, we have conducted numerical experiments that confirm our theoretical considerations. We define a potential on the domain $x \in [-10, 10]$,

$$V(x) = \cos(\pi x) e^{-x^2/2}, \tag{4.34}$$

and follow the proposed scaling laws: The number of grid points is $N = 8\varepsilon^{-1}$ and $h = \varepsilon^{-1/2}$. The integrations are performed for one time-step and for various methods, cf. Table 4.4. As initial condition, we take a normalized shifted Gaussian, $\psi_0(x) \propto e^{-(x-1)^2/2}$. The reference solution ψ at each ε has been computed using the most accurate method ($\mathrm{RKN}_{11}6$) on a finer mesh ($N_{\mathrm{ref}} = 16N$) and by dividing the time-step in 50 sub-steps. The results are shown in Fig. 4.1, where the superior order of the new methods can be clearly appreciated. We conjecture that the new methods become useful for small values of ε, when the curves intersect. One can expect that for a long time integration, the error curves lie closer together since the particular error terms greatly depend on the wave function which does not change for one time-step. It is worth to stress that each new iteration of the Zassenhaus-algorithm increases the epsilon order by one, just as an iteration of Yoshida's device. However, only two new exponentials are generated with an overall polynomial growth in the cost (4.33), in contrast to the geometric growth of Yoshida, where the number of exponentials is triplicated.

Method	Error exponent ε^p	Reference
First kind (1st)	3.500	Eqn. (4.28)
Second kind (2nd)	3.502	Eqn. (4.30)
LF	0.500	Eqn. (4.5)
V82	0.500	Table 3.2
$\mathrm{RKN}_{11}6$	2.525	Method SRKN^b_{11} of [29]
Chin-4M	1.503	Eqn. (5.10)
$\mathrm{T86M}_5$	2.497	Table 5.3

Table 4.4: Observed slopes in Fig. 4.1 between the data points corresponding to the smalles values of ε. The references direct to detailed descriptions of the respective methods in this text. All methods reproduce the predicted local order.

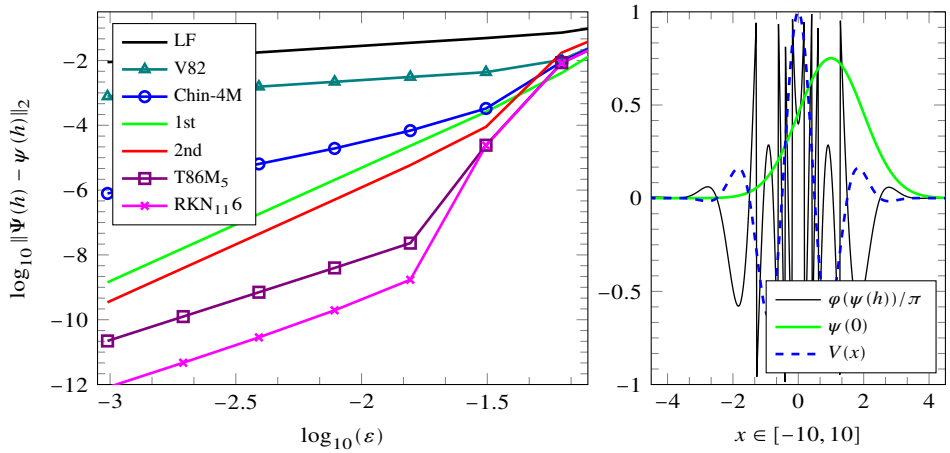

Figure 4.1: The left panel shows the logarithmic error in the discrete L^2-norm of the discretized wave function $\Psi(h)$ with respect to a reference solution $\psi(h)$ after a time step $h = \sqrt{\varepsilon}$ versus the logarithm of the oscillatory parameter ε. On the right, the dashed curve (blue) visualizes the potential (4.34) and the solid lines represent the initial condition (green) and the phase of the complex valued exact solution at $h = \sqrt{\varepsilon}$ with $\varepsilon = 1/128$. The phase has been chosen to instead of the usual absolute value since it cannot be distinguished from the initial condition for one small time-step in this resolution.

Remark on a modified extension The great virtue of standard splitting methods for the Schödinger equation is that the kinetic and potential parts can be exponentiated virtually exactly, rather independently of the size of the exponents. Furthermore, by virtue of modifying potentials, functions that only depend on the spatial coordinate, additional order conditions can be cheaply satisfied. With these two remarks in mind, we revise the previously obtained algorithms: The first two terms are exactly the simply-computable exponentials from standard splittings, and for the interior, smaller exponentials, functions that only depend on x re-appear. Since the exponential of a diagonal matrix is not expected to suffer from a mix of scales, we are tempted to combine the position-dependent terms with the plain potential term $V(x)$. Thereby, at no additional cost, one could expect a slightly better truncation error for expansions where fewer terms are included. The procedure goes as follows, instead of extracting $\tau\omega V(x)$, we set $W^{[1]} = \tau\omega V(x) + \tau^3 V_3 + \tau^5 V_5 + \tau^7 V_7 + \ldots$ and after reaching the final stage s of the expansion, we define the V_k elements to cancel the purely position dependent errors in $\mathscr{W}^{[s]}$. However, since the computational effort is solely determined by the number of FFTs, the outcome can only be a minor improvement over the previous methods and for completeness we state the final result, at order $\mathcal{O}\left(\varepsilon^{7/2}\right)$ for $\sigma = 1/2,\ \rho = 1$, in the usual notation:

$$
\begin{aligned}
\mathscr{R}_0 &= \tfrac{1}{2}\tau\omega V - \tfrac{1}{24}\tau^3\left(-\omega(\partial_x V)^2 + \omega^{-1}(\partial_x^4 V)\right) + \tfrac{1}{120}\tau^5\omega(\partial_x V)^2(\partial_x^2 V) \\
&\quad - \tfrac{1}{10080}\tau^7\omega\left(17(\partial_x V)^2(\partial_x^2 V)^2 + 6(\partial_x V)^3(\partial_x^3 V)\right), \\
\mathscr{R}_1 &= -\tfrac{1}{2}\tau\omega^{-1}\partial_x^2, \\
\mathscr{R}_2 &= -\tfrac{1}{12}\tau^3\omega^{-1}\left\{\partial_x^2, (\partial_x^2 V)\right\}_+, \\
\mathscr{R}_3 &= -\tfrac{1}{120}\tau^5\omega^{-1}\left\{\partial_x^2, V''^2 - 2V'V'''\right\}_+ + \tfrac{7}{360}\tau^5\omega^{-3}\left\{\partial_x^4, V^{(4)}\right\}_+
\end{aligned}
$$

$$\begin{aligned}\mathcal{T}_4 = \tau^7\Big(&\tfrac{1}{15120}\omega^{-1}\left\{\partial_x^2, 18V''^3 + 114V'V''V''' + 87V'^2V^{(4)}\right\}_+\\ &+ \tfrac{1}{378}\omega^{-3}\left\{\partial_x^4, 4V'''^2 - V''V^{(4)} - V'V^{(5)}\right\}_+\\ &- \tfrac{31}{2520}\omega^{-5}\left\{\partial_x^6, V^{(6)}\right\}_+\Big).\end{aligned}$$

4.2 Propagators based on Hagedorn wave-packets

In this section, we briefly dissect a method of Ref. [54] based on Hagedorn-wavepackets that has been analyzed recently [60] in order to propose improvements along the lines of the latter. Recall from the introduction, Section 1.2.3, that in this approach, the wave function is approximated as a linear combination of the scaled and shifted Gaussian,

$$\phi_0^\varepsilon[p,q,Q,P](x) = \pi^{-1/4}(\varepsilon Q)^{-1/2}\exp\Big(\frac{i}{2\varepsilon}PQ^{-1}(x-q)^2 + \frac{i}{2\varepsilon}p(x-q)\Big),$$

and "excited states", constructed via the recurrence relation

$$Q\sqrt{k+1}\phi_{k+1}^\varepsilon(x) = \frac{\sqrt{2}}{\varepsilon}(x-q)\phi_k^\varepsilon(x) - Q^*\sqrt{k}\phi_{k-1}^\varepsilon(x).$$

The ϕ_k form an orthonormal basis of $L^2\mathbb{R}$, and writing $\Pi(t) = (q(t),p(t),Q(t),P(t))$, a given initial condition $\psi(x,0)$ can be expanded as

$$\psi(x,0) = e^{\frac{i}{\varepsilon}S(t)}\sum_{k=0}^{\infty} c_k(t)\phi_k[\Pi(t)],$$

where $S(t)$ is the global phase. Let the Hamiltonian be of the form $H = T+V(x)$ with potential $V(x) = U_q(x) + W_q(x)$ separated into its linear and quadratic part $U_q(x)$ at some point q plus a remainder $W_q(x)$,

$$U_q(x) = V(q) + V'(q)(x-q) + \frac{1}{2}V''(q)(x-q)^2.$$

It has been shown in Ref. [54] that the action of each part on the wave packets can be computed easily and the details are repeated in Th. 4.2.1 and Prop. 4.2.2 below. In fact, the free Schrödinger equation $H = T$ as well as the linear-quadratic part $U_q(x)$ only act on the coordinates subsumed under Π and leave the expansion coefficients c_k unchanged. For this reason, *Faou et al.* [54] proposed to use a splitting method to compute the evolution (1.22) with a splitting

$$e^{-i\frac{h}{2}T}e^{-ihU}e^{-ihW}e^{-i\frac{h}{2}T},$$

yielding a method of second order in Π with global convergence rate $\mathcal{O}\left(h^2/\varepsilon\right)$. Notice that despite the apparent asymmetric composition, it is indeed symmetric since U and W commute. This method has been improved in Ref. [60] to higher order, first by using a fourth-order (Yoshida-)splitting

$$e^{-i\frac{\Theta h}{2}T}e^{-i\Theta hV}e^{-i(1-\Theta)\frac{h}{2}T}e^{-i(1-2\Theta)hV}e^{-i(1-\Theta)\frac{h}{2}T}e^{-i\Theta hV}e^{-i\frac{\Theta h}{2}T},$$

for $\Theta = 1/(2 - 2^{1/3})$. Then, the V parts are decomposed in a step for U and a step for W and convergence of order h^4/ε was observed. Finally, a semiclassical splitting is introduced which can be written as

$$e^{-i\frac{h}{2}(T+U)}e^{-ihW}e^{-i\frac{h}{2}(T+U)}, \tag{4.35}$$

and assuming high accuracy in the computation for the outer exponentials[4], the convergence is shown to be $\mathcal{O}\left(\varepsilon^{1/2}h^2\right)$. The factor $\sqrt{\varepsilon}$ comes from the fact that W is a cubic polynomial and that the dynamics of the coordinates Π are independent of ε.

4.2.1 An interpretation of Hagedorn dynamics

A closer look at the system reveals that there are actually two different sets of dynamics, clearly separated into the coordinates Π and the weights c_k, which will also explain the favorable convergence of the method (4.35).

First, we repeat two central results for the construction of numerical methods.

Theorem 4.2.1 (*Hagedorn* [63], Th. 3.4)**.** *Let p, q, P, Q, S be any solution of*

$$\begin{aligned} \dot{q}(t) &= p(t), & \dot{Q}(t) &= P(t), \\ \dot{p}(t) &= -\nabla V(q(t)), & \dot{P}(t) &= -V''(q(t))Q(t), \\ \dot{S}(t) &= \frac{1}{2}p(t)^2 - V(q(t)), \end{aligned} \tag{4.36}$$

for $V(x) = a + bx + \frac{1}{2}cx^2$ a polynomial of degree 2, then, for every k,

$$\psi(x,t) = e^{\frac{i}{\varepsilon}S(t)}c_k(t)\phi_k[\Pi(t)]$$

satisfies the Schrödinger equation

$$i\varepsilon\partial_t\psi(x,t) = H\psi(x,t)$$

for the Hamiltonian $H = -\frac{\varepsilon^2}{2}\Delta + U$.

Proposition 4.2.2 (*Faou et al.* [54], Prop. 2.3)**.** *For the propagation of a potential W, and fixing Π, the Galerkin approximation in $\mathcal{M}(\Pi) = \operatorname{span}\{\psi_k(\Pi)\}_{k\in\mathcal{K}}$ for some set $\mathcal{K} \subset \mathbb{N}_0$ and $\partial_t u \in \mathcal{M}$,*

$$\forall k \in \mathcal{K}, \qquad \langle \phi_k,\ \varepsilon i\partial_u - Wu\rangle = 0$$

is equivalent [54] to the linear system of ODEs

$$i\varepsilon\frac{dc_k}{dt} = \sum_{l\in\mathcal{K}} f_{k,l}c_l, \qquad k \in \mathcal{K},$$

where $f_{k,l} = \langle\phi_k|W\phi_l\rangle$ are the matrix elements of W in the basis ϕ_k of $\mathcal{M}$. Thus, the evolution of c_k under W can be written as

$$c(t) = \exp(-it/\varepsilon F)c(0),$$

when we aggregate the components as vectors and matrices, $c = (c_j)_{j\in\mathcal{K}}$ and $F = (f_{j,k})$, respectively.

[4] An approximation using a composition of a large number $N(\varepsilon, h)$ of Strang splittings with time step $h/2N$ is proposed.

The simple Lie-Trotter splitting will be sufficient for our analysis: Approximate $e^{-ihH}\psi(0)$ by n steps

$$\left(e^{-i\frac{h}{n}(T+U_q)}e^{-i\frac{h}{n}W_q}\right)^n$$

and look at the limit $n \to \infty$. Since the method is convergent, this limit reproduces the exact solution at h. From the above theorem and proposition, it is clear that the dynamics of the left exponential is completely independent of the right one. Therefore, in this limit, we regard W as function depending on time, and its dynamics must thus be described as

$$i\varepsilon\,\dot{c}(t) = F(\Pi(t))c(0), \tag{4.37}$$

where $\Pi(t)$ is a solution of (4.36). Of course, this system is predestined to be solved by Magnus integrators as seen in previous chapters, since it preserves unitarity. Suppose we use a second order Magnus integrator, where the only integral has been approximated by the midpoint rule, then we rediscover method (4.35) by writing

$$c(h) = e^{-i\frac{h}{\varepsilon}F\left(\Pi\left(\frac{h}{2}\right)\right)}c(0). \tag{4.38}$$

The dynamics of the coordinate function $\Pi(t)$ is described by (4.36), which in fact corresponds to a classical autonomous Hamiltonian system[5]

$$\frac{d}{dt}\begin{pmatrix}q(t)\\p(t)\end{pmatrix} = \begin{pmatrix}p(t)\\-\nabla U_{q(t)}(q(t))\end{pmatrix} = \begin{pmatrix}p(t)\\-\nabla V(q(t))\end{pmatrix}, \tag{4.39}$$

whose solution gives the time-dependent function of the non-autonomous harmonic oscillator

$$\frac{d}{dt}\begin{pmatrix}Q(t)\\P(t)\end{pmatrix} = \begin{pmatrix}P(t)\\-\nabla V''(q(t))Q(t)\end{pmatrix}. \tag{4.40}$$

The phase S is completely independent and can be computed separately. Therefore and because of its physical irrelevance, we omit its discussion.

The procedure for an efficient numerical integration is now clear: Approximate (4.38) up to the desired order by a Magnus expansion. Using momentum integrals and numerical quadrature thereof, this implies the need to evaluate $\Pi(t)$ at the quadrature points b_j and we have to compute $\Pi(b_j h)$ to high precision. This can be done by splitting the combined system (4.39), (4.40) into kinetic and potential parts and using a high-order splitting method with a fractional (ε-dependent) time-step, in particular, we propose the use of method $\mathrm{RKN}_{11}6$, see Table 4.4. Thereby, only $N \propto (\varepsilon\Delta t^2)^{1/6}$ intermediate steps are needed. Alternatively, one could compute the smaller system (4.39) and solve (4.40) trivially by computing the integral $\int V''(q(s))ds$ using the obtained values for $q(s)$ in the previous step.

A careful examination of the proofs in Ref.[60] allows us to identify the sources of the global error. First, notice that the time-steps for the evaluation of Π are chosen such that its error is of comparable size as the algorithm for the weights c_k, which is the bottleneck of the algorithm. By construction, the matrix F can be shown to be of size $\mathcal{O}\left(\varepsilon^{3/2}\right)$, which will lead to an overall scaling[6] of $\varepsilon^{3/2}/\varepsilon^1 = \sqrt{\varepsilon}$ multiplying the error. Furthermore, commutators of $\frac{1}{\varepsilon}F$,

[5] We suspect that this was the motivation for the notation q, p, Q, P in Ref. [54].

[6] The factor ε^{-1} comes from the left-hand side of (4.37).

which originate from a Magnus expansion, are of even smaller size, $[\frac{1}{\varepsilon}F_1, \frac{1}{\varepsilon}F_2] = \mathcal{O}(\varepsilon)$ and could be ignored. In essence, the overall error of the procedure will thus be determined (neglecting ε terms) by the error of the quadrature formula for

$$c(t) = e^{-i\frac{1}{\varepsilon}\int_0^t F(\Pi(s))ds} c(0).$$

For example, for the fourth-order Gauss-Legendre quadrature with weights b_1, b_2 after one time-step h, we have

$$c(h) = e^{-i\frac{1}{2\varepsilon}(F(\Pi(b_1 h))+F(\Pi(b_2 h)))} c(0)$$

and the local error is $\mathcal{O}\left(\sqrt{\varepsilon}h^5 + \varepsilon h^3\right)$. Using a commutator-free fourth-order method instead [30], (1.67), one gets $\mathcal{O}\left(\sqrt{\varepsilon}h^5 + \varepsilon h^5\right)$ at the cost of another exponential. If the matrices are too large to compute the commutator efficiently, then the direct method would require four products per Lanczos iteration, $(F_1 + F_2 + [F_1, F_2])c = F_1(1 + F_2)c + F_2(1 - F_1)c$, whereas a commutator-free method just requires two, one per exponential and iteration.

4.3 Time-dependent potentials

After this short interlude, we return to the symmetric Zassenhaus splitting. It is then natural to ask whether the machinery can be carried over to semi-classical equations with explicitly time-dependent potentials, arising, e.g., from particles subject to external (electric) fields.

As having seen throughout this work, the Magnus expansion presents an excellent tool to obtain a formal solution for the non-autonomous setting, and indeed, it has been successfully applied to this problem class [57, 85], however, with temporal resolution much finer than the spatial one. Convergence issues due to the unbounded nature of the kinetic and potential operators for the standard TDSE are discussed in Ref. [72] and it turns out that the correct order for classical Magnus integrators is recovered if the solution has sufficient spatial regularity.

In the semi-classical context, one has to identify the relevant terms in the Magnus series in order to consequently apply the Zassenhaus algorithm with the goal to decompose the suitably truncated expansion into exponentials of decreasing size. Two qualitatively distinct problems are addressed: On the one hand, slow time-dependencies and on the other, frequencies that scale with the fast parameter, $\propto 1/\varepsilon$, as occurring for realistic laser interactions [64]. The difference will become crucial for the evaluation of the algorithm. For slowly varying potentials, standard techniques such as the momentum integrals in the Magnus expansion can be used. Since the quality of the underlying Taylor expansion depends greatly on the size of the time-derivatives of the potentials, this approach will fail for rapidly changing fields and a different approach will be developed in the second part.

4.3.1 Slowly varying external field

Suppose that, for some given value ε, the SE is of the form

$$i\partial_t \psi(x,t) = H(t)\psi(x,t) \equiv \left(-\varepsilon\Delta + \frac{1}{\varepsilon}V(x,\omega t)\right)\psi(x,t),$$

where ω is assumed to be of size $\mathcal{O}(1)$. The idea is to evaluate the Magnus expansion $\exp(\Omega_h)$ using the Taylor series of the Hamiltonian $H(t)$ around $t_{1/2} = t_0 + \frac{h}{2}$, as in (1.65). Given that the masses are constant, the simplifications due to the RKN structure of the algebra are dramatic. Letting $H_j = -i\,\frac{1}{j!}\frac{d^j H(t)}{dt^j}\Big|_{t=t_{1/2}}$, the Magnus expansion up to order 8 in h can be written as [23]

$$\Omega^{[8]} = \sum_{k=1}^{6} \Omega_k, \tag{4.41}$$

where

$$\begin{aligned}
\Omega_1 &= hH_0 + \tfrac{h^3}{12}H_2 + \tfrac{h^5}{80}H_4 + \tfrac{h^7}{448}H_6,\\
\Omega_2 &= -\tfrac{h^3}{12}[H_0,H_1] - \tfrac{h^5}{80}[H_0,H_3] - \tfrac{h^7}{448}[H_0,H_5],\\
\Omega_3 &= h^5\left(\tfrac{1}{360}[H_0,[H_0,H_2]] - \tfrac{1}{240}[H_1,[H_0,H_1]]\right)\\
&\qquad + h^7\left(\tfrac{1}{1680}[H_0,[H_0,H_4]] + \tfrac{1}{6048}[H_2,[H_0,H_2]] - \tfrac{1}{840}[H_3,[H_0,H_1]]\right),\\
\Omega_4 &= h^5\tfrac{1}{720}[H_0,[H_0,[H_0,H_1]]] + h^7\left(\tfrac{1}{6720}[H_0,[H_0,[H_0,H_3]]]\right.\\
&\qquad \left. + \tfrac{1}{4032}[H_0,[H_2,[H_0,H_1]]] + \tfrac{11}{60480}[H_1,[H_0,[H_0,H_2]]]\right),\\
\Omega_5 &= h^7\left(\tfrac{-1}{15120}[H_0,[H_0,[H_0,[H_0,H_2]]]] - \tfrac{1}{30240}[H_0,[H_0,[H_1,[H_0,H_1]]]]\right.\\
&\qquad \left. + \tfrac{1}{7560}[H_1,[H_0,[H_0,[H_0,H_1]]]]\right),\\
\Omega_6 &= h^7\tfrac{-1}{30240}[H_0,[H_0,[H_0,[H_0,[H_0,H_1]]]]].
\end{aligned}$$

Defining $iH_0 = -\varepsilon\Delta + \frac{1}{\varepsilon}V_0$ and $iH_j = \frac{1}{\varepsilon}V_j$, the size of the expressions in terms of the small parameter ε can be determined while we keep the scaling $\Delta x \propto \varepsilon$ and $h \propto \varepsilon^{1/2}$, ($\rho = 1$, $\sigma = 1/2$). Spatial differentiation is hidden within the commutators which will be computed to be able to group terms by their ε-scaling. We briefly remark their effect on the overall size of the elements to justify the truncation of the Magnus expansion: The innermost commutator is of size $\mathcal{O}(\varepsilon^{-\rho})$ and each further appearance of the kinetic operator εT will increment the degree of the occurring derivatives by one, and given the choice of scaling parameters, the power in ε remains unchanged. Commutation with $\varepsilon^{-1}V_j$ has the opposite effect and reduces the degree of differentiation, but in turn is counteracted by multiplication with the large parameter $1/\varepsilon$. Hence, the composite term H_0 will not increase the size of a commutator and to achieve an approximation of degree ε^p is equivalent to truncating the Magnus series at $h^{(p+\rho)/\sigma}$. In other words, the leading error of a (classical) nth-order Magnus integrator is of size $\mathcal{O}(\varepsilon^{(n+1)\sigma-\rho})$ and we truncate the integrator (4.41) at order six to achieve

the $\mathcal{O}(\varepsilon^{5/2})$ accurate method

$$\begin{aligned}\Omega^{[6]} = \tau\left(-\varepsilon\partial_x^2 + \varepsilon^{-1}V_0\right) + \tau^3\left(-\tfrac{1}{12}\varepsilon^{-1}V_2 + i\tfrac{1}{6}(\partial_x V_1)\partial_x + i\tfrac{1}{12}(\partial_x^2 V_1)\right)\\ + \tau^5\varepsilon^{-1}\left(-\tfrac{1}{180}(\partial_x V_0)(\partial_x V_2) + \tfrac{1}{120}(\partial_x V_1)^2 + \tfrac{1}{80}V_4\right)\\ - i\tau^5\left(\tfrac{1}{40}(\partial_x V_3) + \tfrac{1}{180}(\partial_x V_1)(\partial_x^2 V_0) + \tfrac{1}{60}(\partial_x V_0)(\partial_x^2 V_1)\right)\partial_x\\ - \tfrac{1}{90}\tau^5\varepsilon\left((\partial_x^2 V_2)\partial_x^2 + (\partial_x^3 V_2)\partial_x\right)\\ - i\tau^5\tfrac{1}{720}\varepsilon^2\left(8(\partial_x^3 V_1)\partial_x^3 + 12(\partial_x^4 V_1)\partial_x^2 + 6(\partial_x^5 V_1)\partial_x\right) + \mathcal{O}\left(\varepsilon^{5/2}\right),\end{aligned}$$

with $\tau = h/i$. The careful reader will notice the appearance of the imaginary unit, i, which is due to the commutators of even length in the Magnus expansion. Furthermore, derivatives of odd degree appear and have to be dealt with as for the autonomous case. This is also the reason why some terms, such as $\tau^5\varepsilon(\partial_x^3 V_2)\partial_x = \mathcal{O}\left(\varepsilon^{5/2}\right)$ have not been discarded yet: After rewriting in even derivatives, a factor of $1/\varepsilon$ is gained and if it had been dropped prematurely, the result would not form a skew-Hermitian operator. The underlying reason is that only the entire commutators form (skew-)Hermitian operators and we can only discard them *after* the odd-even-substitution.

From here on, we proceed as before: The odd-degree derivatives are rewritten as linear combinations of even ones, the terms of same size are identified and extracted with the symmetric Zassenhaus formula.

Given the algorithm in Table 4.2, only the starting points $\mathscr{W}^{[0]},\ W^{[0]}$ of the expansion need to be modified to compute the decomposition. With the aim of a $\mathcal{O}(\varepsilon^{5/2})$ integrator, the algorithm is initiated with the sixth-order Magnus expansion

$$\mathscr{W}^{[0]} = \Omega^{[6]},$$

and, as before, there are several alternatives for the initial iterations.

A closer look reveals a difficulty that is unique to the non-autonomous setting: After conversion to even derivatives, we are facing terms

$$\mathscr{W}^{[0]} = ih/\omega\,\partial_x^2 - i\omega h V_0 + \tfrac{1}{12}h^3\left[\partial_x^2, V_1\right]_- + \mathcal{O}\left(\sqrt{\varepsilon}\right),$$

and all scale as $\varepsilon^{-1/2}$. The now appearing commutator is due to $[H_0, H_1]$ and cannot be diagonalized by Fourier transforms. This is a major drawback since our algorithm relied on the already achieved decrease of size for terms that had to be computed with Lanczos' method. Before, only the diagonal (after FFT) terms $\partial_x^2,\ V$ were growing with $\varepsilon^{-1/2}$.

Fortunately, we can borrow ideas from Section 2.2.1, where we computed a commutator of length two using three simpler exponentials. Thus, we attempt to compute

$$e^{-ki\omega h^2 V_1}e^{i/\omega h\partial_x^2}e^{ki\omega h^2 V_1} = e^{i/\omega h\partial_x^2 + \frac{1}{12}h^3[\partial_x^2, V_1] + \mathcal{O}\left(\varepsilon^{1/2}\right)},$$

and a simple application of the BCH formula leads to $k = \frac{1}{12}$. The composition is related to *(post-)processing*, where a method Ψ_h is embraced by a processor P and its inverse, $P\Psi_h P^{-1}$

in order to reduce the error. Finally, we set

$$\begin{aligned} W^{[0]} &= \log\left(e^{-\frac{1}{12}i\omega h^2 V_1} e^{i/\omega h\partial_x^2} e^{\frac{1}{12}i\omega h^2 V_1}\right) \\ &= i\frac{h}{\omega}\partial_x^2 - \frac{1}{12}h^3\left[\partial_x^2, V_1\right]_- - \frac{1}{144}ih^5\omega(\partial_x V_1)^2 \end{aligned}$$

Remarkably, this composition of exponents has very nice features for RKN algebras. Recalling (2.11), the following expression is exact,

$$e^{-khV}e^{hT}e^{khV} = e^{hT - h^2k[V,T] - \frac{1}{2}h^3k^2[[V,T],V]}. \tag{4.42}$$

This property could also be useful for commutator-free Magnus integrators but will not be explored further in this work.

Instead, we return to the Zassenhaus splitting. Having defined $W^{[0]}$ in a way that all derivatives of large size in the small parameters are included and that only requires one FFT plus its inverse to exponentiate, the first iteration effectively removes derivatives to yield

$$\begin{aligned} \mathscr{W}^{[1]} &= \mathrm{sBCH}(-W^{[0]},\ \mathscr{W}^{[0]}) \\ &= -ih\omega V_0 - \tfrac{1}{12}ih^3\left(\omega\left(V_2 - 2(\partial_x V_0)^2\right) + \frac{1}{\omega}\{\partial_x^2,\ (\partial_x^2 V_0)\}_+\right) + \mathcal{O}(\sqrt{\varepsilon}) \end{aligned}$$

We proceed with the next largest term, $W^{[1]} = -ih\omega V_0$ and after computing commutators up to length five, the next term is identified to be

$$\begin{aligned} W^{[2]} = &-\tfrac{1}{12}ih^3\left(\omega\left(V_2 - 2(\partial_x V_0)^2\right) + \frac{1}{\omega}\{\partial_x^2,\ (\partial_x^2 V_0)\}_+\right) \\ &- \tfrac{1}{240}h^5\left[\partial_x^2, 3V_3 + 2\int\left(2V_1'V_0'' + V_0'V_1''\right)\right]_- - \tfrac{1}{360}\frac{1}{\omega^2}h^5[\partial_x^4,\ (\partial_x^2 V_1)]_- = \mathcal{O}(\sqrt{\varepsilon}), \end{aligned} \tag{4.43}$$

where the integral has to be understood in the sense of (4.19). We terminate the computation at the next step by identifying the $\mathcal{O}\left(\varepsilon^{3/2}\right)$ terms in $\mathscr{W}^{[2]} = \mathrm{sBCH}(-W^{[2]}, \mathscr{W}^{[1]})$ to achieve a method of order $\mathcal{O}(\varepsilon^{5/2})$. The rather lengthy result is

$$\begin{aligned} W^{[3]} = &-ih^5\Big(\omega\left(\tfrac{1}{80}V_4 + \tfrac{1}{720}(\partial_x V_1)^2 - \tfrac{1}{30}(\partial_x V_0)(\partial_x V_2) + \tfrac{7}{120}(\partial_x V_0)^2(\partial_x^2 V_0)\right) \\ &- \frac{1}{\omega}\left\{\partial_x^2,\ \tfrac{1}{60}(\partial_x V_0)^2 + \tfrac{1}{80}(\partial_x^2 V_2) - \tfrac{1}{30}(\partial_x V_0)(\partial_x^3 V_0)\right\}_+ + \tfrac{1}{240}\frac{1}{\omega^3}\left\{\partial_x^4,\ (\partial_x^4 V_0)\right\}_+\Big) \\ &- h^7\Bigg(\tfrac{1}{4320}\Big[\partial_x^2,\ \int(9V_3'(\partial_x^2 V_0) + 14V_1'(\partial_x^2 V_0)^2 + 5V_1'(\partial_x^2 V_2) + 18V_0'(\partial_x^2 V_0)(\partial_x^2 V_1) \\ &\qquad + 27V_0'(\partial_x^2 V_3) + 30V_0'(\partial_x V_1)(\partial_x^3 V_0) + 24(\partial_x V_0)^2(\partial_x^3 V_1))\Big]_- \\ &\quad - \tfrac{1}{8640}\frac{1}{\omega^2}\Big[\partial_x^4,\ \int(10(\partial_x^2 V_1)(\partial_x^3 V_0) + 2(\partial_x^2 V_0)(\partial_x^3 V_1) + 9(\partial_x^3 V_3) \\ &\qquad + 8(\partial_x V_1)(\partial_x^4 V_0) + 26(\partial_x V_0)(\partial_x^4 V_1))\Big]_- + \tfrac{1}{3240}\frac{1}{\omega^4}\left[\partial_x^6, (\partial_x^4 V_1)\right]_-\Bigg), \end{aligned} \tag{4.44}$$

and combining the results, we obtain the method

$$e^{\frac{1}{2}W^{[0]}}e^{\frac{1}{2}W^{[1]}}e^{\frac{1}{2}W^{[2]}}e^{W^{[3]}}e^{\frac{1}{2}W^{[2]}}e^{\frac{1}{2}W^{[1]}}e^{\frac{1}{2}W^{[0]}} = e^{\Omega_h} + \mathcal{O}\left(\varepsilon^{5/2}\right).$$

The numerical effort for the computation of one step, ignoring differentiation and integration, can be determined by counting the necessary FFTs: The outermost exponentials $W^{[0]}$ only require four FFTs in total, the next one $W^{[1]}$ is already diagonal in coordinate space, and it remains to estimate $W^{[3]}$ and $W^{[4]}$. Since an overall accuracy of $\mathcal{O}\left(\varepsilon^{5/2}\right)$ is desired and $W^{[3]} = \mathcal{O}\left(\varepsilon^{1/2}\right)$, we conclude with (1.33') that five Lanczos iterations per exponential are necessary. The exponent contains two commutators[7] which sum up to seven FFTs. The smallest term only requires two Lanczos iterations, but contains three commutators that sum up to 10 FFTs. In total, $4 + 5 \times 7 + 2 \times 10 = 59$ FFTs per step have to be evaluated. However, as for autonomous potentials, this number is growing quadratically with increasing precision.

We remark that all arguments translate perfectly to the formulation of the Magnus expansion in terms of momentum integrals.

4.3.2 Highly oscillating time dependence

The standard Magnus techniques heavily rely on the smoothness of the time-dependency of the potential, or in other words, on tight bounds for its temporal derivatives. The important case of laser interactions, however, has a qualitatively different character and must be resolved in the fast timescale, proportional to $1/\varepsilon$.

A fairly general interaction with an external field can be modeled by the Hamiltonian[8]

$$H = -\frac{\varepsilon}{2}\Delta + \frac{1}{\varepsilon}V(x) + \frac{1}{\varepsilon}f\left(\frac{t}{\varepsilon}\right)W(x). \tag{4.45}$$

The Hamiltonian thus consists of two parts, a constant contribution due to kinetic energy and a intrinsic potential plus some external interaction $W(x)$ which is modulated by a scalar function f. Staying with the example of an external laser field, $W(x)$ could be either just a linear function in x or take more sophisticated forms modeling the underlying dipole moment, e.g., $\mu = xe^{ax}$ [132].

It has been pointed out in the context of (modified) Magnus expansions [76, 114, 84] (see [23] for more references) and for more general multivariate integrations [79, 84] that the appearing integrals in the expansion should actually be beneficial for an oscillating function. However, the whole machinery heavily relies on either the fact that the oscillations stem from the equation in form of a larger parameter, a completely different setting, or on the truncation of the series expansion around the small parameter h:

With the aim of keeping a large time-step $h \propto \sqrt{\varepsilon}$, this approach is rendered futile since the correct expansion has to be done around $\varepsilon = 0$ for $f(1/\sqrt{\varepsilon})$ which leads to growing error terms proportional to inverse (fractional) powers of the small parameter ε.

In the spirit of the Zassenhaus splitting for the semiclassical expansion, we employ a different approach: We carefully study the terms of the Magnus expansion to discover that the multivariate integrals are only scalar and thus cheap to compute to sufficiently high accuracy, in contrast to the more common problem when the time-dependencies are inside some matrix

[7] Anti-commutators can be computed together with commutators at no extra computational cost.

[8] The semiclassical parameter has been included in the Hamiltonian which thus corresponds to the Schrödinger equation $i\partial\psi = H\psi$.

structure and thereby increase the complexity. In this work, we assume to be able to compute the integrals exactly, and then only have to deal with the commutators, which can be done in a similar fashion as for the slow setting above.

In the following, we will write $\tilde{f}(t) = f(\omega t)$ and assume that this scalar function is of size $\mathcal{O}(1)$.

Structure of the Magnus expansion 1: the commutators Working in a Dynkin basis, it is clear from the recursive construction of the Magnus expansion (1.62) that all commutators are of the form $[H(s_1), [\dots, H(s_n)] \cdots]$.

Working in the algebra generated by $A = \varepsilon T + V/\varepsilon$ and $B = W/\varepsilon$, such a general commutator can be expanded to yield simple (nested) commutators in A and B multiplied by scalar functions in the time-coordinates s_j. Assuming the usual scaling $\Delta x \propto \varepsilon$, the simple term $H(s)$ is of size $1/\varepsilon$ and the first commutator

$$\begin{aligned}[H(s_1), H(s_2)] &= \left(\tilde{f}(s_n) - \tilde{f}(s_{n-1})\right)[A, B] \\ &= \left(\tilde{f}(s_n) - \tilde{f}(s_{n-1})\right)\left((\partial_x^2 W) + 2(\partial_x W)\partial_x\right) = \mathcal{O}\left(\varepsilon^{-1}\right).\end{aligned}$$

To estimate the size after further commutation, we can study the effects of A and B separately due to the linearity of the bracket. We conclude as for the slow case that commutation with either A, or B leaves the size in ε invariant, since commuting with the kinetic (potential) operator increases (decreases) the degree of the derivatives by one which is compensated by the multiplication with the small (large) parameter ε ($1/\varepsilon$). Overall, we can conclude that all commutators are of size

$$[H(s_1), [\dots, H(s_n)] \cdots] = \mathcal{O}\left(\varepsilon^{-1}\right), \tag{4.46}$$

which must be taken into account for a suitable truncation of the Magnus expansion. Hence, the decrease in size must come from nested integrals, which we will estimate in continuation.

Structure of the Magnus expansion 1: the integrals Suppose that $f(t)$ is sufficiently smooth, or in other words, it contains no fast frequencies which we will formalize as

$$f(t) = \sum_{k \in \mathbb{Z}} \hat{f}_k e^{(2\pi i)kt}, \qquad \sum_{k \in \mathbb{Z}} \frac{|\hat{f}_k|}{k} \leq C,$$

for a constant C independent of the small parameter ε. Hence, $f(t)$ is slow and integrating over a full time-step, we get

$$\begin{aligned}\int_0^h f(s/\varepsilon)\, ds &= \int_0^h \sum_k \hat{f}_k e^{2\pi i k s/\varepsilon}\, ds \\ &= \varepsilon \sum_k \frac{\hat{f}_k}{2\pi i k}\left(e^{2\pi i k h} - 1\right) \leq \varepsilon \sum_k 2\, \frac{|\hat{f}_k|}{2\pi |k|} = \mathcal{O}(\varepsilon).\end{aligned}$$

In a multivariate integration, we will estimate one of the occurring integrals by this procedure and use the standard estimation that another power of h is gained in each integration (using a constant majorant) to derive

$$\int_0^h \int_0^{s_1} \cdots \int_0^{s_n} f(\omega s_j)\, ds_n\, ds_0 = \mathcal{O}\left(h^n \varepsilon\right).$$

Notice that for the general case where $f(\omega s_j)$ has to be replaced by linear combinations of oscillating functions $f(\omega s_k)$, this estimation still holds since we assumed that $f(t) = \mathcal{O}(1)$.

We summarize these estimates to yield a growth law for the Magnus expansion in the small parameter:

Theorem 4.3.1. *Let $H = \varepsilon T + V/\varepsilon + f(t/\varepsilon)W/\varepsilon$, with f independent of ε, and discretizing in space and time as $\Delta x = \mathcal{O}(\varepsilon)$ and $h = \varepsilon^\sigma$, the Magnus expansion* (1.62) *truncated after p terms is of effective order $\varepsilon^{p\sigma}$.*

$$\sum_{k=1}^{\infty} \Theta_k = \sum_{k=1}^{p} \Theta_k + \mathcal{O}\left(\varepsilon^{p\sigma}\right), \qquad p \geq 2.$$

At this point, we are able to apply the symmetric Zassenhaus algorithm and in the remainder, a method of epsilon-order $3/2$ will be constructed. From Th. 4.3.1, it is clear that it suffices to include the first three terms $\Theta_j, j = 1, 2, 3$ for an approximation error $\mathcal{O}\left(\varepsilon^{3/2}\right)$. The expression is easy to compute and we set (recall $\omega = \varepsilon^{-1}$)

$$\begin{aligned}
\mathscr{W}^{[0]} &= \Theta_1 + \Theta_2 + \Theta_3 \\
&= -i\left(h\frac{1}{\omega}T + h\omega V + f_{1,1}W\right) + f_{2,1}[W,T] \\
&\qquad + if_{3,1}\Big[\omega V + \tfrac{1}{\omega}T, [T,W]\Big] + if_{3,2}\omega\Big[W,[T,W]\Big] \\
&= \underbrace{-ih\left(-\frac{1}{\omega}\partial_x^2 + \omega V\right)}_{\mathcal{O}(\varepsilon^{-1/2})} \underbrace{-i\omega f_{1,1}W}_{\mathcal{O}(\varepsilon^0)} \underbrace{-2f_{2,1}W'\partial_x}_{\mathcal{O}(\varepsilon^{1/2})} \underbrace{-f_{2,1}W''}_{\mathcal{O}(\varepsilon^{3/2})} \\
&\qquad \underbrace{+2if_{3,1}\left(\omega V'W' + 2\frac{1}{\omega}W''\partial_x^2\right) + 4if_{3,2}\omega(\partial_x W)^2}_{\mathcal{O}(\varepsilon^1)} \underbrace{+4i\frac{f_{3,1}}{\omega}(\partial_x^3 W)\partial_x}_{\mathcal{O}(\varepsilon^2)} + \mathcal{O}\left(\varepsilon^3\right).
\end{aligned}$$

The functions $f_{j,k}$ are of size $\mathcal{O}\left(\varepsilon h^{j-1}\right) = \mathcal{O}\left(\varepsilon^{(j+1)/2}\right)$, in particular,

$$\begin{aligned}
f_{1,1} &= \textstyle\int_0^h ds \tilde{f}(s), \\
f_{2,1} &= \tfrac{1}{2}\textstyle\int_0^h ds_1 \int_0^{s_1} ds_2 \Big(\tilde{f}(s_2/\omega) - \tilde{f}(s_1/\omega)\Big), \\
f_{3,1} &= \tfrac{1}{6}\textstyle\int_0^h ds_1 \int_0^{s_1} ds_2 \int_0^{s_2} ds_3 \Big(\tilde{f}(s_3) - 2\tilde{f}(s_2) + \tilde{f}(s_1)\Big), \\
f_{3,2} &= \tfrac{1}{6}\textstyle\int_0^h ds_1 \int_0^{s_1} ds_2 \int_0^{s_2} ds_3 \Big(2\tilde{f}(s_1)\tilde{f}(s_3) - \tilde{f}(s_2)(\tilde{f}(s_1) + \tilde{f}(s_3))\Big),
\end{aligned}$$

with the shorthand $\tilde{f}(s) = f(s/\omega)$. The application of the Zassenhaus algorithm is almost straightforward: Convert $\mathscr{W}^{[0]}$ to even derivatives and identify the largest terms. As before, the conversion to even derivatives will increase the size of the first commutator which originates from Θ_2 and we apply the construction (4.42) to avoid its direct computation. The starting point is set to

$$\begin{aligned}
W^{[0]} &= \log\left(e^{kW}e^{ih\partial_x^2/\omega}e^{-kW}\right) \\
&= i\frac{h}{\omega}\partial_x^2 + f_{2,1}[\partial_x^2, W]_- - i\frac{f_{2,1}^2\omega}{h}(\partial_x W)^2,
\end{aligned}$$

where $k = -if_{2,1}\frac{\omega}{h}$. From here onwards, we simply follow the Zassenhaus split and continue to pull out the largest parts of the remainder,

$$W^{[1]} = -i\omega\left(hV + f_{1,1}W\right) = \mathcal{O}\left(\varepsilon^{-1/2} + \varepsilon^{0}\right).$$

Proceeding in the usual fashion leads to

$$W^{[2]} = \tfrac{1}{6}ih^3\omega(\partial_x V)^2 + i\frac{h^3}{\omega}\left\{\partial_x^2,\ (\partial_x^2 V)\right\}_+ - \tfrac{1}{6}f_{2,1}h^2\left[\partial_x^2,\ \int(\partial_x W)(\partial_x^2 V)\right]_- = \mathcal{O}\left(\varepsilon^{1/2}\right).$$

The final step gives

$$\begin{aligned} W^{[3]} = {} & i\omega\left(\left(2f_{3,1} + \tfrac{1}{3}f_{1,1}h^2\right)(\partial_x V) + 2f_{3,2}(\partial_x W)\right)(\partial_x W) \\ & + \tfrac{1}{12}hf_{1,1}f_{2,1}\left[\partial_x^2,\ (\partial_x W)^2\right]_- + i\frac{1}{\omega}\left(4f_{3,1} + \tfrac{1}{12}f_{1,1}h^2\right)\left\{\partial_x^2,\ (\partial_x W)^2\right\}_+ = \mathcal{O}\left(\varepsilon^{1}\right) \end{aligned}$$

We have now reached the precision of the truncated Magnus expansion which gives the method

$$e^{\Theta(0,h)} = e^{\sum_{k=1}^{3}\Theta_k + \mathcal{O}(\varepsilon^{3/2})} = e^{\frac{1}{2}W^{[0]}}e^{\frac{1}{2}W^{[1]}}e^{\frac{1}{2}W^{[2]}}e^{\frac{1}{2}W^{[3]}}e^{\frac{1}{2}W^{[2]}}e^{\frac{1}{2}W^{[1]}}e^{\frac{1}{2}W^{[0]}} + \mathcal{O}\left(\varepsilon^{3/2}\right).$$

Note that all the derivatives and integrals w.r.t. the spatial coordinate of the potentials only have to be computed once and the time-dependency is buried in the functions $f_{j,k}$. This low order method requires very few FFTs, in fact only 2×2 for $W^{[0]}$, 2×3 Lanczos iterations with 4 FFTs for $W^{[2]}$ and two iterations with 4 FFTs for $W^{[3]}$, which totals to 36 FFTs.

Chapter 5

THE GROUND STATE: IMAGINARY TIME PROPAGATION

The exposition is based on the article [6].

We consider the eigenvalue problem for the stationary Schrödinger equation (SE) presented in Section 1.1.4 which is repeated for convenience of the reader

$$H\phi_j(x) = E_j\phi_j(x), \qquad j = 0, 1, 2, \ldots \tag{5.1}$$

where

$$H = T + V(x) = -\frac{1}{2}\Delta + V(x), \tag{5.2}$$

$V(x)$ denotes the interaction potential and Δ is the Laplacian operator. Since the Hamiltonian H is a Hermitian operator, its eigenvalues E_i are real valued, and their corresponding real eigenfunctions $\phi_i(x)$ form a basis of the underlying Hilbert space. This particular problem has attracted great interest among theorists and practitioners [46, 82, 112] due to its relevance for the properties of atomic structures. A widely used approach to solve this problem is based on using the corresponding time-dependent Schrödinger equation in imaginary time ($t = -i\tau$), whose formal solution is given by the evolution operator $\exp(-\tau H)$. In this way, in general, virtually any initial condition, under the action of $\exp(-\tau H)$, converges asymptotically to the ground state solution when $\tau \to \infty$. Notice that the evolution operator $\exp(-\tau H)$ has the same eigenfunctions as the problem (5.1)-(5.2). This technique is usually referred to as the imaginary time propagation method (ITP for short). In this setting, only the action of $\exp(-\tau H)$ on a wave function has to be computed [3, 89].

5.1 Motivation and background

The ITP method can be regarded as an analog of the well-known power method in numerical linear algebra [125]. In this sense, one may also consider the inverse power method: Instead of the iterative application of the exponential operator $\exp(-\tau H)$, the scheme $v_{n+1} = (H - \tilde{E}_j)^{-1} v_n$, $n = 0, 1, 2, \ldots$ is used for some given $\tilde{E}_j$. This iteration is known to converge after normalization to the eigenvector with eigenvalue closest to $\tilde{E}_j$. Although faster convergence than for the ITP method can be observed for an accurate initial guess $\tilde{E}_j \approx E_j$, in general, the algorithm needs more iterations until convergence [1].

However, the benefits of this method are non-negligible if one is interested in a particular high energy eigenstate since, with a suitable initial guess $\tilde{E}_j$, the state can be computed without having to calculate the lower energies E_k, $0 \leq k < j$, previously.

Since the operators $e^{-\tau V}$ and $e^{-\tau T}$ can be exactly computed in the coordinate and momentum space, respectively, the operator splitting technique involving a composition of these exponential operators with appropriate coefficients can be used to approximate $e^{-\tau H}$. The computational cost depends on the number of changes between these coordinates which are cheaply performed by Fast Fourier transforms (FFT).

However, the operator splitting technique has some limitations. In particular, splitting methods of order $p > 2$ require negative time-steps [118, 120] and the instabilities caused thereof are analogous to the ones for the integration of a diffusion equation backwards in time. If it is feasible to compute the gradient of the potential V, generalized splitting methods allow to build methods with positive coefficients up to fourth order [44, 104, 45], but higher order methods also use negative time-steps. In this section, we propose methods to overcome the order barriers for both cases by using complex time-steps. Splitting methods can be tailored to particular equations to achieve better performances and we present criteria based on near-integrability that apply to a wide range of problems and thus yield highly efficient high order schemes. The obtained methods outperform the existing splitting schemes when high accuracy is desired and could be appropriate for elaborating a variable order algorithm. We also report some numerical experiments illustrating the efficiency of the new methods.

For details on the procedure, we refer to the introduction and only elaborate on aspects of the implementation of the process

$$e^{-\tau H} \psi(x, 0) = \sum_i e^{-\tau E_i} \phi_i(x).$$

We will assume that the eigenvalues are distinct and positive, $0 < E_0 < E_1 < \ldots$, the latter can be achieved by appropriately choosing the origin of the potential, which corresponds to adding a physically irrelevant constant global phase to solution. If there is degeneracy, it converges to a linear combination of eigenfunctions, and repeating this process with different initial conditions, one can obtain a complete set of independent vectors of the subspace which can be orthonormalized.

Normalization of the asymptotic value yields the eigenfunction ϕ_0 and the corresponding eigenvalue is computed via $E_0 = \langle \phi_0 | H \phi_0 \rangle$. Excited states can be obtained by propagating different wave functions simultaneously (or successively) in time and using, for example, the

Gram-Schmidt orthonormalization or diagonalization of the overlap matrix [1].

For simplicity in the presentation, the spatial dimension is set to one unless it is explicitly stated, but our results also apply to higher dimensions.

The problem is further simplified by assuming $x \in [a, b]$ with the interval $[a, b]$ sufficiently large such that the wave function and all its derivatives of interest vanish at the boundaries. For numerical computations, the infinite dimensional domain of H has to be truncated, which is done by discretizing the spatial coordinate x: We fix N equally spaced grid points $x_j = x_0 + k\Delta x,\ k = 0, 1, 2, \dots, N-1$, with $a = x_0$ and $b = x_N$. In this way, the interval is divided into N subintervals of size $\Delta x = (b-a)/N$.

The potential V is represented in this grid by a diagonal matrix and the periodicity of the system ($\psi^{(n)}(a) = \psi^{(n)}(b) = 0,\ n = 0, 1, 2, \dots$) allows for the use of spectral methods (in space) for the calculation of T, namely the Fast Fourier Transform after which the matrix representation of T also becomes diagonal. The computational costs for the application of V and T to a vector are thus proportional to N and $N \log N$ operations, respectively. In a d-dimensional space with N mesh points on each dimension, their costs are proportional to N^d and $N^d \log N$, respectively.

5.2 Splitting methods for the Schrödinger equation

To approximate the time evolution (1.17), i.e., the computation of $e^{-\tau H}$ acting on a vector, we propose to use splitting methods, cf. Section 1.3.3, in particular, compositions of the operators $e^{-\tau V}$ and $e^{-\tau T}$ evaluated at different times. For convenience, we express the Strang splitting (1.38) in these terms

$$\Psi_h^{[2]} \equiv e^{-\frac{h}{2}V}\, e^{-hT}\, e^{-\frac{h}{2}V}, \tag{5.3}$$

and verifies $\Psi_h^{[2]} = e^{-hH} + \mathcal{O}(h^3)$ with $h \equiv \Delta\tau$. A general composition is then given by

$$\Psi_h^{[p]} \equiv \prod_{i=1}^{m} e^{-a_i hT}\, e^{-b_i hV}, \tag{5.4}$$

where $\Psi_h^{[p]} = e^{-hH} + \mathcal{O}(h^{p+1})$ if the coefficients a_i, b_i are chosen such that they satisfy a number of order conditions (with m sufficiently large). However, as mentioned earlier, splittings of order greater than two necessarily have negative coefficients. While this is usually not a problem for the coefficients b_i, having negative a_i coefficients makes the algorithm badly conditioned (in the limit $N \to \infty$). Recall that this restriction applies to a more general class of equations: Whenever the operator only creates a semi-group of solutions, the integration has to be computed forward in time.

Composition methods with coefficients b_i positive are also convenient for unbounded potentials, e.g., $V(x) = x^2$, since negative values of b_i can generate large round-off errors in the exponential $e^{-b_i V}$ at the boundaries if the interval-size of the spatial discretization is not appropriately chosen and the potential takes exceedingly large values.

Splitting methods are particularly appropriate for the numerical integration of this problem since the choice of the time step, h, is not affected by the mesh size. Taking a finer mesh (i.e., a

larger value of N) does not necessarily lead to a smaller time step, and the extra computational effort originates only from the FFTs, whose cost is $N\log(N)$ (or $N^d\log(N)$ in a d-dimensional problem with N points on each coordinate). In contrast and as elaborated in the introduction, the Chebyshev polynomial method approximates the exponential as

$$e^{-\tau H} = e^{-\rho(H/\|H\|)} \simeq \sum_{k=0}^{m} a_k(\rho) P_k\left(\tau H/\rho\right), \tag{5.5}$$

where $\rho = \tau\|H\|$, $a_k(\rho) = 2I_k(\rho)$, $k > 0$ and $a_0(\rho) = I_0(\rho)$, with I_n being the modified Bessel functions of the first kind and P_k is the Chebyshev polynomial of degree k. The truncation index m has to be such that $m > \rho$ to reach accuracy. If we take into account that

$$\|H\| \sim V_{max} - V_{min} + \sum_{j=1}^{d}\left(\frac{\pi}{\Delta x_j}\right)^2 \sim N^2,$$

we observe that the number of FFTs is proportional to N^2, and then its computational cost scales as $N^2 \times N^d \log(N)$. Similar considerations apply to other polynomial approximations such as Taylor or Lanczos methods. In fact, in the numerical experiments with $d = 3$ reported in Ref. [89], splitting methods scale as $N^{3.3}$ while Lanczos methods scale as $N^{5.3}$ for a range of values of N, in agreement with the previous estimates.

Nevertheless, from the results in Ref. [89] one might conclude that these polynomial approximations scale better than splitting methods for computing a larger part of the spectrum. Then, splitting schemes are the methods of choice when only relatively few eigenvalues are desired, especially if they are needed with high accuracy (implying a finer mesh, i.e., a larger number of grid points). With this aim in mind, we next explore several families of splitting methods to get approximations to (1.17).

One possible approach to derive the order conditions to be satisfied by the coefficients a_i, b_i consists in applying the Baker-Campbell-Hausdorff formula to the composition (5.4), which we assume consistent ($\sum_i a_i = \sum_i b_i = 1$) [65]. Thus we get $\Psi_h^{[p]} = \exp(-h\mathscr{H})$, with

$$\mathscr{H} = T + V + hf_{2,1}[T,V] + h^2(f_{3,1}[T,[T,V]] + f_{3,2}[V,[T,V]]) + \cdots, \tag{5.6}$$

where $f_{i,j}$ are polynomials of degree i in the coefficients a_k, b_k. Condition $f_{2,1} = 0$ leads to second order methods, and this can always be achieved by taking a left-right symmetric composition in (5.4) because all even terms automatically vanish. Methods of higher orders require in addition $f_{3,1} = f_{3,2} = 0$. Taking into account consistency, these equations can be written as [22]

$$f_{3,1} \quad : \quad \sum_{1\le i<j\le k\le m} a_i b_j a_k = \frac{1}{6}, \tag{5.7}$$

$$f_{3,2} \quad : \quad \sum_{1\le i\le j\le k\le m+1} b_i a_j b_k = \frac{1}{6}. \tag{5.8}$$

These two conditions imply that at least one of the a_i as well as one of the b_i become negative (see [17] and references therein), so that only methods of order two can be used for this problem.

There are several possibilities to circumvent this limitation, and in the following, we enumerate some of them.

Modified potentials If the kinetic energy operator in (5.2) is quadratic in momenta, then the nested commutator

$$[V,[T,V]] = (\nabla V(x))^T (\nabla V(x)) \tag{5.9}$$

is diagonal in coordinate space. For this reason, (5.9) is usually called modifying potential. In consequence, $[V,[V,[T,V]]] = 0$ and we can replace the terms $e^{-b_i h V}$ in (5.4) by the more general operator

$$e^{-b_i h V - c_i h^3 [V,[T,V]]}$$

involving two parameters. As a result, condition (5.8) becomes

$$f_{3,2} \;:\; \sum_{1\le i\le j\le k\le m+1} b_i a_j b_k + \sum_{i=1}^{m} c_i = \frac{1}{6}.$$

This equation can always be satisfied with a proper choice of the coefficients c_i, so that the constraints on the coefficients a_i, b_i reduce to the single condition $f_{3,1} = 0$, allowing for positive coefficients. In addition, solutions with positive c_i coefficients also exist. A first example is the 4th-order composition [86, 44]

$$\Psi_h^{[4]} \equiv e^{-\frac{h}{6}V} e^{-\frac{h}{2}T} e^{-\frac{2h}{3}V - \frac{h^3}{72}[V,[T,V]]} e^{-\frac{h}{2}T} e^{-\frac{h}{6}V}. \tag{5.10}$$

It turns out, however, that 6th-order methods using the operator (5.9) necessarily have some negative coefficients a_i [43].

Near-integrable systems When the Hamiltonian can be considered as a perturbed system, i.e., $H = H_0 + \varepsilon V_\varepsilon(x)$ with an exactly solvable part $H_0 = T + V_0(x)$ and a small perturbation $\varepsilon V_\varepsilon(x)$, we have already pointed out that it is advantageous to split the Hamiltonian into the dominant part H_0 and its perturbation $\varepsilon V_\varepsilon$. For example, if one is interested in the lower excited states, which evolve near the minimum of the potential, it can be useful to separate the quadratic part and to treat the remainder as a perturbation since the harmonic oscillator has a simple and fast solution using FFTs, cf. Section2.1 and Refs. [47, 4].

Notice that in this case, the commutator

$$[\varepsilon V_\varepsilon,[H_0,\varepsilon V_\varepsilon]] = \varepsilon^2 (\nabla V_\varepsilon(x))^T (\nabla V_\varepsilon(x))$$

depends only on the coordinates and modified potentials can also be applied as before. Then, all compositions remain the same except for replacing T by H_0 and V by $\varepsilon V_\varepsilon$. We recall that for potentials $V(x) = |x|^n$, the virial theorem $\langle\phi|T\,\phi\rangle = \langle\phi|\nabla V(x)x\,\phi\rangle$ leads to $\langle T\rangle = n\langle V\rangle$ and for large n, the potential can be considered the dominant part. This is especially relevant for the imaginary-time propagation, since eventual rough initial conditions are smoothed quickly by the diffusion part

Complex coefficients A third possibility consists of considering complex coefficients in the composition (5.4) (with or without modified potentials). In other problems where the presence of negative real coefficients is unacceptable, the use of high-order splitting methods with complex coefficients having positive real part has shown to possess some advantages. In recent years a systematic search for new methods with complex coefficients has been carried out and the resulting schemes have been tested in different settings: Hamiltonian systems in celestial mechanics [41], the time-dependent Schrödinger equation in quantum mechanics [11, 12] and also in the more abstract setting of evolution equations with unbounded operators generating analytic semigroups [40, 66]. It is worth noticing that the propagator $\exp(z\Delta)$ ($z \in \mathbb{C}$) associated with the Laplacian is well-defined (in a reasonable distributional sense) if and only if $\Re(z) \geq 0$ [40], which is the case for the presented methods.

Many of the existing splitting methods with complex coefficients have been constructed by applying the composition technique (1.44) to the symmetric second-order leapfrog scheme (5.3): For example, a fourth-order integrator can be obtained with the symmetric composition

$$\Psi_h^{[4]} = \Psi_{\alpha h}^{[2]}\, \Psi_{\beta h}^{[2]}\, \Psi_{\alpha h}^{[2]}, \tag{5.11}$$

where

$$\alpha = \frac{1}{2 - 2^{1/3} e^{2ik\pi/3}}, \qquad \beta = \frac{2^{1/3} e^{2ik\pi/3}}{2 - 2^{1/3} e^{2ik\pi/3}},$$

and $k = 1, 2$. In both cases, one has $\Re(\alpha), \Re(\beta) > 0$. Higher order composition methods with complex coefficients and positive real part can be found in Refs. [40, 66, 20], where several numerical examples are also reported.

5.2.1 New splitting methods for the ITP problem

In this section, we carry out a systematic search of methods within the classes (a)-(c) above enumerated. The best methods for each subclass are stated online [5] with 25 digits of accuracy whereas the methods used in the numerical examples (Section 5.3) are given in the subsequent tables with 18 digits for simplicity.

We only consider symmetric methods and, since T and V have qualitatively different properties, we analyze both TVT-and VTV-type compositions, defined as

$$\Psi_h^{[p]} = e^{-a_1 hT} e^{-b_1 hV} e^{-a_2 hT} \cdots e^{-a_2 hT} e^{-b_1 hV} e^{-a_1 hT}, \quad \text{and} \tag{5.12}$$

$$\Psi_h^{[p]} = e^{-b_1 hV} e^{-a_1 hT} e^{-b_2 hV} \cdots e^{-b_2 hV} e^{-a_1 hT} e^{-b_1 hV}, \tag{5.13}$$

respectively. In principle, both compositions have the same computational cost for the same number of exponentials. Nevertheless, due to a projection step to the real part after each full time-step, only in the VTV composition we can concatenate the last map in the current step with the first stage in the next one. The TVT compositions thus require two additional FFTs in comparison with the VTV composition, and this is accounted for in the numerical experiments.

The methods we obtain are classified into two families: (I) methods without modified potentials and (II) methods with modified potentials. For each class, we distinguish between methods for general problems (with the unique constraint that $[V, [V, [T, V]]] = 0$) and methods for near-integrable problems (when the main dominant part contains the kinetic energy).

We have explored both TVT and VTV compositions with different number of stages. In some cases we consider extra stages to have free parameters for optimization. When the number and complexity of the order conditions is relatively low, we get all solutions. We then select the solutions having all of their coefficients with positive real part. Finally, we choose the solution which minimizes

$$\sum_i (|a_i| + |b_i|) \tag{5.14}$$

and/or minimizes the absolute value of the real part of the coefficients appearing at the leading error terms. These methods are subsequently tested on several numerical examples. After this process, we collect a number of schemes offering the best performance for most of the problems considered. In practice, however, one has to bear in mind that the relative performance between different methods depends eventually on the particular problem considered, the desired accuracy, the initial conditions, etc.

5.2.2 Methods without modified potentials

TVT and VTV compositions with 3 up to 9 stages have been analyzed. To simplify the notation, we denote compositions (5.12) and (5.13) as

$$\mathrm{T}n_m = a_1\, b_1\, a_2 \cdots a_2\, b_1\, a_1,$$
$$\mathrm{V}n_m = b_1\, a_1\, b_2 \cdots b_2\, a_1\, b_1,$$

respectively. Here n indicates the order (or generalized order) of the method and m corresponds to the number of stages, i.e., the number of b_i coefficients in the TVT composition or the number of a_i coefficients in the VTV composition. The coefficients of the selected TVT methods are collected in Table 5.1, whereas those corresponding to the TVT methods are displayed in Table 5.2.

Methods for general problems

Analogously to (5.6), the symmetric compositions (5.12) and (5.13) can be formally expressed as a single exponential $\Psi_h^{[p]} = \exp(-h\mathscr{H})$ with polynomials $f_{i,j}$ in a_k, b_l multiplying commutators $E_{i,j}$:

$$\begin{aligned}\mathscr{H} &= T + V + h^2(f_{3,1}E_{3,1} + f_{3,2}E_{3,2}) \\ &\quad + h^4(f_{5,1}E_{5,1} + f_{5,2}E_{5,2} + f_{5,3}E_{5,3} + f_{5,4}E_{5,4}) \\ &\quad + h^6(f_{7,1}E_{7,1} + f_{7,2}E_{7,2} + \cdots) + \cdots,\end{aligned}$$

where the $E_{i,j}$ are chosen to form a basis of the algebra of commutators of length i. The chosen basis elements relevant for our exposition are

$$\begin{aligned} E_{3,1} &= [T,[T,V]], & E_{3,2} &= [V,[T,V]], \\ E_{5,1} &= [T,[T,[T,[T,V]]]], & E_{5,2} &= [V,[T,[T,[T,V]]]], \\ E_{5,3} &= [T,[V,[T,[V,T]]]], & E_{5,4} &= [V,[V,[T,[T,V]]]], \\ E_{7,1} &= [T,[T,E_{5,1}]], & E_{7,2} &= [V,[T,E_{5,1}]]. \end{aligned}$$

Here, we summarize some of the methods which have been analyzed:

3-stage compositions A 3-stage composition has sufficient parameters to build 4th-order methods. There is one real solution and two complex solutions (conjugate to each other). For example, the VTV method corresponds to the composition (5.11) when $\Psi_h^{[2]}$ is given by (5.3). The TVT version is obtained by interchanging T and V.

5-stage compositions Fourth-order methods with two free parameters can be obtained using 5-stage symmetric compositions. These two parameters can be used to build methods of effective order 6 (i.e., 4th-order methods that are conjugate to 6th-order methods by a near-identity change of variables). This requires to impose some additional constraints on the leading error terms, $f_{5,j}$, $j = 1, 2, 3, 4$. Specifically, these are $f_{5,1} - f_{5,2} = 0$ and $f_{5,3} + f_{5,4} = 0$ [27]. We have found six solutions for the TVT composition and three solutions for the VTV composition with coefficients having positive real part. The solutions with smallest error terms at order 5 are denoted by $\mathrm{T4}_5$ and $\mathrm{V4}_5$[5].

7-stage compositions In principle, there are sufficient parameters to build 6th-order methods with 7 stages. For the TVT composition, there are 11 solutions with all coefficients having positive real parts. The solution leading to a minimum value of the norm of the error at order 7 can be found online [5].

With respect to the VTV composition, the best method we have found is identical with the most efficient sixth-order method obtained by Chambers [41], where it has been presented as a symmetric composition similar to (5.11) but with 7 stages instead of 3, and with $\Psi_h^{[2]}$ given by (5.3).

Methods for near-integrable problems

Proceeding analogously as before, we arrive at the following methods. We recall that in all compositions one should replace T by H_0 and V by $\varepsilon V_\varepsilon$.

***n*-stage compositions of generalized order** $(2n, 2)$ This class of compositions has real and positive coefficients [94, 87]. A 4-stage VTV composition of generalized order $(8, 2)$ is given by scheme $\mathrm{V84M}_4^{\mathrm{LR}}$ in Table 5.4 with $c_1 = 0$.

5-stage compositions To build a method of generalized order (8,4) the following conditions must be satisfied by a consistent and symmetric method: $f_{3,1} = f_{3,2} = f_{5,1} = f_{7,1} = 0$. It requires at least 5 stages, and in this case only one solution with all coefficients having positive real part is found both for the TVT and VTV compositions. The coefficients of these methods, denoted by $\mathrm{T84}_5$ and $\mathrm{V84}_5$, are collected in Table 5.1 and Table 5.2, respectively.

(8,6,4) methods To build a (8,6,4) method, the coefficients of a consistent and symmetric method must satisfy the following order conditions: $f_{3,1} = f_{3,2} = f_{5,1} = f_{5,2} = f_{5,3} = f_{7,1} = 0$. They therefore require at least 7 stages. In this case, it is possible to get all solutions. Scheme $\mathrm{T864}_7$ corresponds to the solution minimizing (5.14), whereas $\mathrm{V864}_7$ provides the minimum value of $|f_{5,3} + f_{5,4}|$.

(8,6) methods Increasing the number of stages to 9 we have two free parameters, which are used to satisfy in addition the following conditions: $f_{5,4} = f_{7,2} = 0$. In this way, methods of generalized order (8,6) and effective order (10,8,6) are obtained. Two efficient schemes correspond to $\mathrm{T86}_9$ and $\mathrm{V86}_9$ in Table 5.1 and Table 5.2, respectively [102].

5.2.3 Methods with modified potentials

Fourth-order methods incorporating modified potentials do exist with real and positive coefficients. In fact, two- and three-stage schemes have been extensively studied [43, 104, 45]. Methods of generalized order $(n, 4)$ also exist with positive real coefficients [87]. Here we construct new methods of generalized order (6,4) and (8,4) with this property and generalize the treatment to 6th-order schemes with complex coefficients. In all cases, we take compositions TVT and VTV with up to 5 stages and denote them as

$$\begin{aligned} \mathrm{T}n\mathrm{M}_m &= a_1\,(b_1\,c_1)\,a_2 \cdots a_2\,(b_1\,c_1)\,a_1, \\ \mathrm{V}n\mathrm{M}_m &= (b_1\,c_1)\,a_1\,(b_2\,c_2) \cdots (b_2\,c_2)\,a_1\,(b_1\,c_1). \end{aligned}$$

Here, the parenthesis is used to help counting of the number of exponentials, and the letter M indicates that the methods use modified potentials. Notice that the number of free parameters can differ for the TVT and VTV sequences with the same number of exponentials because the exponent of a modified potential contains two parameters. The coefficients of the selected methods are collected in Table 5.3 and Table 5.4 for the TVT and VTV compositions, respectively.

Methods for general problems

4-stage compositions Under the restriction of having real positive coefficients, we have obtained the fourth-order VTV method OMF-4M, already discovered in Ref. [104] (eq. (36) therein).

The VTV composition allows one to build 6th-order methods, whereas the TVT needs an extra stage. There is only one solution (and its complex conjugate) with all coefficients having positive real part. It is denoted by $\mathrm{V6M}_4$ and can be found within the supplementary material [5].

Methods for near-integrable problems

We first consider $(n, 4)$ methods with real and positive coefficients. For schemes of generalized order (8,6) we collect only complex solutions with positive real part.

(6,4) methods They require at least 3 stages to satisfy the following order conditions: $f_{3,1} = f_{3,2} = f_{5,1} = 0$. The coefficients a_i and b_i correspond to the methods (6,2) obtained in Ref. [94] (without modified potentials). We have also considered methods with 4 stages in order to have additional free parameters. As previously mentioned, there is the same number of order conditions as parameters to get a method of order 6 for the VTV sequence, but there are no solutions with coefficients being real and positive. To get a sixth-order method the following conditions must also be satisfied: $f_{5,2} = f_{5,3} = f_{5,4} = 0$. The coefficients c_i only appear in $f_{5,3}$ and $f_{5,4}$ and can only be used to cancel these terms. The VTV sequence has three free parameters which can be used to annihilate $f_{5,3}$ and $f_{5,4}$ and to minimize the absolute value of $f_{5,2}$ under the constraint that all coefficients must be real and positive. The TVT sequence has only two free parameters which can be used to annihilate $f_{5,3}$ and to minimize the absolute value of the dominant term, $f_{5,2}$, under the same constraint on the coefficients. The best methods we have obtained are denoted by $\mathrm{T64M_4}$ and $\mathrm{V64M_4}$ and are published online [5].

(8,4) methods They require at least 4 stages. The coefficients a_i and b_i correspond to the methods (8,2) without using modified potentials and obtained in Ref. [94]. There is one coefficients c_i in the TVT composition which can be used to cancel $f_{5,3}$, and two coefficients c_i in the VTV composition which can be used to annihilate $f_{5,3}$ and $f_{5,4}$. The solution with $c_2 = c_3 = 0$ was already obtained in [87]. We have collected the corresponding coefficients for this method, $\mathrm{V84M_4^{LR}}$, in Table 5.4. We have also considered methods with 5 stages in order to have an additional free parameters. There is the same number of order conditions as parameters to get a method of order (8,6) (which would be of order 6 for a general problem) but obviously, there are no solutions with coefficients real and positive. As in the previous case, the term $f_{5,2}$ can not be zeroed using real positive coefficients. Then in both TVT and VTV compositions, we have chosen the method which, while having real and positive coefficients, minimize its absolute value. The best methods we have obtained are denoted by $\mathrm{T84M_5}$ and $\mathrm{V84M_5}$.

(8,6) methods They require at least 5 stages and do not admit real and positive solutions for the coefficients and we are forced to consider complex solutions. We have found only one solution with positive real part in the coefficients for both TVT and VTV compositions. The coefficients for the methods denoted by $\mathrm{T86M_5}$ and $\mathrm{V86M_5}$ are given in Table 5.3 and Table 5.4, respectively.

Table 5.1: Compositions TVT without modified potentials.

$\mathrm{T84}_5 = a_1\, b_1\, a_2\, b_2\, a_3\, b_3\, a_3\, b_2\, a_2\, b_1\, a_1$
$a_1 = 0.071401131540044698 + 0.010155431019886789i$
$b_1 = 0.178696854264631978 + 0.028197506313218021i$
$a_2 = 0.236383805190074736 + 0.070427007139534522i$
$b_2 = 0.198453474708154649 + 0.082962314733854963i$
$a_3 = 1/2 - (a_1 + a_2) = 0.1922... - 0.0806...i$
$b_3 = 1 - 2(b_1 + b_2) = 0.2457... - 0.2223...i$
$\mathrm{T864}_7 = a_1\, b_1\, a_2\, b_2\, a_3\, b_3\, a_4\, b_4\, a_4\, b_3\, a_3\, b_2\, a_2\, b_1\, a_1$
$a_1 = 0.055705821110864236 + 0.018670384565085049i$
$b_1 = 0.115779449626990422 + 0.046131356173382847i$
$a_2 = 0.118843282163492564 - 0.024151805322796634i$
$b_2 = 0.129128920804026450 - 0.119039413303774209i$
$a_3 = 0.158591515575195578 - 0.076302551893579599i$
$b_3 = 0.184643464154438944 - 0.003053761445376182i$
$a_4 = 1/2 - (a_1 + a_2 + a_3) = 0.1669... + 0.0818...i$
$b_4 = 1 - 2(b_1 + b_2 + b_3) = 0.1409... + 0.1519...i$
$\mathrm{T86}_9 = a_1\, b_1\, a_2\, b_2\, a_3\, b_3\, a_4\, b_4\, a_5\, b_5\, a_5\, b_4\, a_4\, b_3\, a_3\, b_2\, a_2\, b_1\, a_1$
$a_1 = 0.042257897299860339 - 0.014215780224181831i$
$b_1 = 0.094894869367770736 - 0.037963806472588094i$
$a_2 = 0.095260398471830494 + 0.004518725891475591i$
$b_2 = 0.097374660381711248 + 0.088518877931710497i$
$a_3 = 0.099960578944766657 + 0.090271995071312563i$
$b_3 = 0.118584793520055816 + 0.038356250608401259i$
$a_4 = 0.148695530402608487 + 0.011438117187614089i$
$b_4 = 0.136865119760326031 - 0.023587404969570006i$
$a_5 = 1/2 - (a_1 + a_2 + a_3 + a_4) = 0.1138... - 0.0920...i$
$b_5 = 1 - 2(b_1 + b_2 + b_3 + b_4) = 0.1046... - 0.1306...i$

5.3 Numerical results

As test bench for the numerical methods, we consider in the following two qualitatively different cases, the Pöschl-Teller potential and a perturbed harmonic oscillator, the latter being a classic example of a near-integrable system and of practical interest [112]. These two problems can be numerically integrated using modified potentials. However, we compare the relative performance of the methods (with and without modified potentials) separately in order to study the performance of the methods when it is not feasible to compute the gradient of the potential.

The numerical integration proceeds as follows: Starting from random initial data, we iterate with fixed time-step until the sufficiently large final time $T = 100$ and compare the result with the exact solution, $\psi(T)$, which has been obtained by integrating with a much smaller time step. The spatial interval is fixed for all experiments to $[-10, 10]$ and is discretized with $N = 128$ equidistant mesh points. Similar results are obtained for larger $N = 256, 512, 1024$. At each step, we project the obtained vector to its real part and normalize it to one in $\ell_2(\mathbb{R})$,

Table 5.2: Compositions VTV without modified potentials.

$\mathrm{V864}_7 = b_1\,a_1\,b_2\,a_2\,b_3\,a_3\,b_4\,a_4\,b_4\,a_3\,b_3\,a_2\,b_2\,a_1\,b_1$
$b_1 = 0.060017770752528926 - 0.009696150746907738i$
$a_1 = 0.108904710931114447 - 0.075700232434276860i$
$b_2 = 0.067017987316853817 + 0.003927567742822542i$
$a_2 = 0.106594114300156182 + 0.139651903644940761i$
$b_3 = 0.189300872388005476 + 0.091055103879530385i$
$a_3 = 0.204897016414416105 + 0.009719057955143112i$
$b_4 = 1/2 - (b_1 + b_2 + b_3) = 0.1837... - 0.0853...i$
$a_4 = 1 - 2(a_1 + a_2 + a_3) = 0.1592... - 0.1473...i$
$\mathrm{V86}_9 = b_1\,a_1\,b_2\,a_2\,b_3\,a_3\,b_4\,a_4\,b_5\,a_5\,b_5\,a_4\,b_4\,a_3\,b_3\,a_2\,b_2\,a_1\,b_1$
$b_1 = 0.032497706037458608 + 0.010641310380458924i$
$a_1 = 0.087895680441261752 + 0.036052576182866484i$
$b_2 = 0.094180923422602148 + 0.023866875362648754i$
$a_2 = 0.095351855399045611 - 0.065128376035135147i$
$b_3 = 0.101132953097231180 - 0.112201757337044841i$
$a_3 = 0.121865575594908413 - 0.054974002471495827i$
$b_4 = 0.160941382119434892 - 0.016127643896952891i$
$a_4 = 0.141506882718462097 + 0.024607229046524026i$
$b_5 = 1/2 - (b_1 + b_2 + b_3 + b_4) = 0.1112... + 0.0938...i$
$a_5 = 1 - 2(a_1 + a_2 + a_3 + a_4) = 0.1068... + 0.1189...i$

Table 5.3: Compositions TVT with modified potentials.

$\mathrm{T84M}_5 = a_1\,(b_1\,c_1)\,a_2\,(b_2\,c_2)\,a_3\,(b_3\,c_3)\,a_3\,(b_2\,c_2)\,a_2\,(b_1\,c_1)\,a_1$
$a_1 = 0.058520963359694865$
$b_1 = 0.145381537601615725, \qquad c_1 = 0.000245906549261228$
$a_2 = 0.207903047442871771$
$b_2 = 0.244351408696638327, \qquad c_2 = 0.000259178561419125$
$a_3 = 1/2 - (a_1 + a_2) = 0.2336...$
$b_3 = 1 - 2(b_1 + b_2) = 0.2205..., \quad c_3 = 0.000938105701711153$
$\mathrm{T86M}_5 = a_1\,(b_1\,c_1)\,a_2\,(b_2\,c_2)\,a_3\,(b_3\,c_3)\,a_3\,(b_2\,c_2)\,a_2\,(b_1\,c_1)\,a_1$
$a_1 = 0.063556051997493102 + 0.010606890396680920i$
$b_1 = 0.156939525347224563 + 0.027931306200415819i$
$c_1 = 0.000133739181746125 + 0.000085540153220213i$
$a_2 = 0.208998817231756322 + 0.040240203826523395i$
$b_2 = 0.222383136675982213 + 0.026033262090035938i$
$c_2 = 0.000484323504408882 + 0.000241671051573332i$
$a_3 = 1/2 - (a_1 + a_2) = 0.2274... - 0.0508...i$
$b_3 = 1 - 2(b_1 + b_2) = 0.2414... - 0.1079...i$
$c_3 = 0.000179180363327321 - 0.000858304413034511i$

Table 5.4: Compositions VTV with modified potentials.

$\mathrm{V84M}_5 = (b_1\,c_1)\,a_1\,(b_2\,c_2)\,a_2\,(b_3\,c_3)\,a_3(b_3\,c_3)\,a_2\,(b_2\,c_2)\,a_1\,(b_1\,c_1)$		
$b_1 = 0.042308451243127365,$	$c_1 = 0.000232966269565498$	
$a_1 = 0.142939324267716184$		
$b_2 = 0.219303568753387110,$	$c_2 = 5.56677120231130 \cdot 10^{-7}$	
$a_2 = 0.242474508234531493$		
$b_3 = 1/2 - (b_1 + b_2) = 0.2292...,$	$c_3 = 0.000794490777479431$	
$a_3 = 1 - 2(a_1 + a_2) = 0.2384...$		
$\mathrm{V84M}_4^{\mathrm{LR}} = (b_1\,c_1)\,a_1\,(b_2\,c_2)\,a_2\,(b_3\,c_3)\,a_2\,(b_2\,c_2)\,a_1\,(b_1\,c_1)$		
$b_1 = 1/20,$	$c_1 = \frac{3861-791\sqrt{21}}{129600},$	$a_1 = 1/2 - \sqrt{3/28}$
$b_2 = 49/180,$	$c_2 = 0,$	$a_2 = 1/2 - a_1 = \sqrt{3/28}$
$b_3 = 1 - 2(b_1 + b_2) = 16/45,$	$c_3 = 0$	
$\mathrm{V86M}_5 = (b_1\,c_1)\,a_1\,(b_2\,c_2)\,a_2\,(b_3\,c_3)\,a_3(b_3\,c_3)\,a_2\,(b_2\,c_2)\,a_1\,(b_1\,c_1)$		
$b_1 = 0.046213625838152095 - 0.007824529355983108i$		
$c_1 = 0.000035830461339520 + 0.000074370857685421i$		
$a_1 = 0.152650950104799817 - 0.030279967163699065i$		
$b_2 = 0.224258052678856384 - 0.050879282402761772i$		
$c_2 = 0.000338053435041382 - 0.000490508913279372i$		
$a_2 = 0.226364275186039762 - 0.016537249619936515i$		
$b_3 = 1/2 - (b_1 + b_2) = 0.2295... + 0.0587...i$		
$c_3 = 0.000408311644874003 + 0.000484371967433683i$		
$a_3 = 1 - 2(a_1 + a_2) = 0.2420... + 0.0936...i$		

i.e., given the method $\Psi_h^{[p]}$ and initial conditions, $\phi_n \in \mathbb{R}^N$, we compute ϕ_{n+1} as

$$\tilde{\phi}_{n+1} = \Psi_h^{[p]}\,\phi_n;$$

then, since $\tilde{\phi}_{n+1}$ is a complex vector (but $\mathcal{O}(h^p)$ away from a real vector) we project on the real space by removing the imaginary part

$$\bar{\phi}_{n+1} = \Re(\tilde{\phi}_{n+1})$$

and then normalize the solution $\phi_{n+1} = \bar{\phi}_{n+1}/\|\bar{\phi}_{n+1}\|$, where the norm is given by

$$\|w\|^2 \equiv \Delta x \sum_{j=0}^{N-1} w_j^2, \quad w = (w_0, \ldots, w_{N-1}) \in \mathbb{R}^N.$$

The computational cost is estimated by the number of Fourier transforms necessary until the final time. In addition, the methods using complex coefficients are penalized by a factor 2 in the computational cost, which comes from the use of complex Fourier transforms instead of real FFT. We repeat the numerical integrations for different values of the time step, i.e., $h = T/M$ for different values of M and denote the approximate solution by $\phi(T) = \phi_n$ in each case. The error is measured as

$$\text{error} = \|\psi(T) - \phi(T)\|.$$

This procedure will allow us to determine the efficiency of the new splitting methods, which will depend on the desired accuracy, and thereby choose the methods which are most appropriate for implementation with a more efficient algorithm that is based on variable time step and order. We distinguish two types of problems: On the one hand, methods that include modified potentials, the reference methods being Chin-4M (5.10), OMF-4M [104] and V84M$_4^{\mathrm{LR}}$ [87] given in Table 5.4 as well as a differently optimized scheme with three modified potentials SCB-4M[113] and on the other hand, methods without modifying potentials with the reference methods V82 [94], the fourth-order complex triple-jump scheme (5.11), referenced as Yoshida 4 and a 6th-order complex coefficient method by Chambers [41]. As a reference, we also include the results obtained by a 6-stage sixth-order extrapolation method which takes the Strang splitting (5.3) as the basic method with the same decompositions like the other methods ($T + V$ and $H_0 + \varepsilon V_\varepsilon$ for the perturbed problem, respectively), and it is used with time steps h, $h/2$ and $h/3$. We remark that all relevant methods in the cited papers have been tested and the most efficient ones for this problem are included in the plots.

Pöschl-Teller potential

We have chosen the well-known one-dimensional Pöschl-Teller potential for the availability of analytic solutions of the eigenstates

$$H = -\frac{1}{2}\frac{\partial^2}{\partial x^2} - \frac{\lambda(\lambda+1)}{2}\left(\operatorname{sech}(x)^2 - 1\right), \tag{5.15}$$

with $\lambda(\lambda+1) = 10$. The results of our computation are shown in Figure 5.1a. The higher order of the complex coefficient methods outweighs their extra cost starting from moderate accuracy. The optimizations of the error terms can be clearly appreciated in the comparison with the 4th order triple-jump (5.11). When we consider methods with modified potentials, we observe that the new methods show only slight improvements with respect to the method OMF-4M since both parts of the splitting T and V are of comparable size. As the desired precision is increased, the new sixth order methods dominate in efficiency.

Perturbed harmonic oscillator

To illustrate the benefits of methods designed for near integrable systems, we use the Hamiltonian

$$H = -\frac{1}{2}\frac{\partial^2}{\partial x^2} + \frac{1}{2}\omega^2 x^2 + \varepsilon V_\varepsilon(x),$$

and split it in a large part $H_{\mathrm{HO}} = -\frac{1}{2}\frac{\partial^2}{\partial x^2} + \frac{1}{2}\omega^2 x^2$ and a small part $\varepsilon V_\varepsilon(x)$. The trap frequency is set to $\omega = 1$ and the perturbation $\varepsilon V_\varepsilon$ is given by the Pöschl-Teller potential in (5.15), with $\lambda(\lambda+1) = 2/5$. The harmonic part H_{HO} can be solved exactly via an exact splitting using Fourier transforms, cf. Section 2.1, from which we recall

$$e^{-i\delta H_{\mathrm{HO}}} \equiv e^{-i\frac{\omega}{2}\tan(\frac{\delta\omega}{2})x^2}\, e^{-i\frac{1}{2\omega}\sin(\delta\omega)p^2}\, e^{-i\frac{\omega}{2}\tan(\frac{\delta\omega}{2})x^2},$$

for $|\delta\omega| < \pi$ and $p^2 \equiv -\frac{\partial^2}{\partial x^2}$.

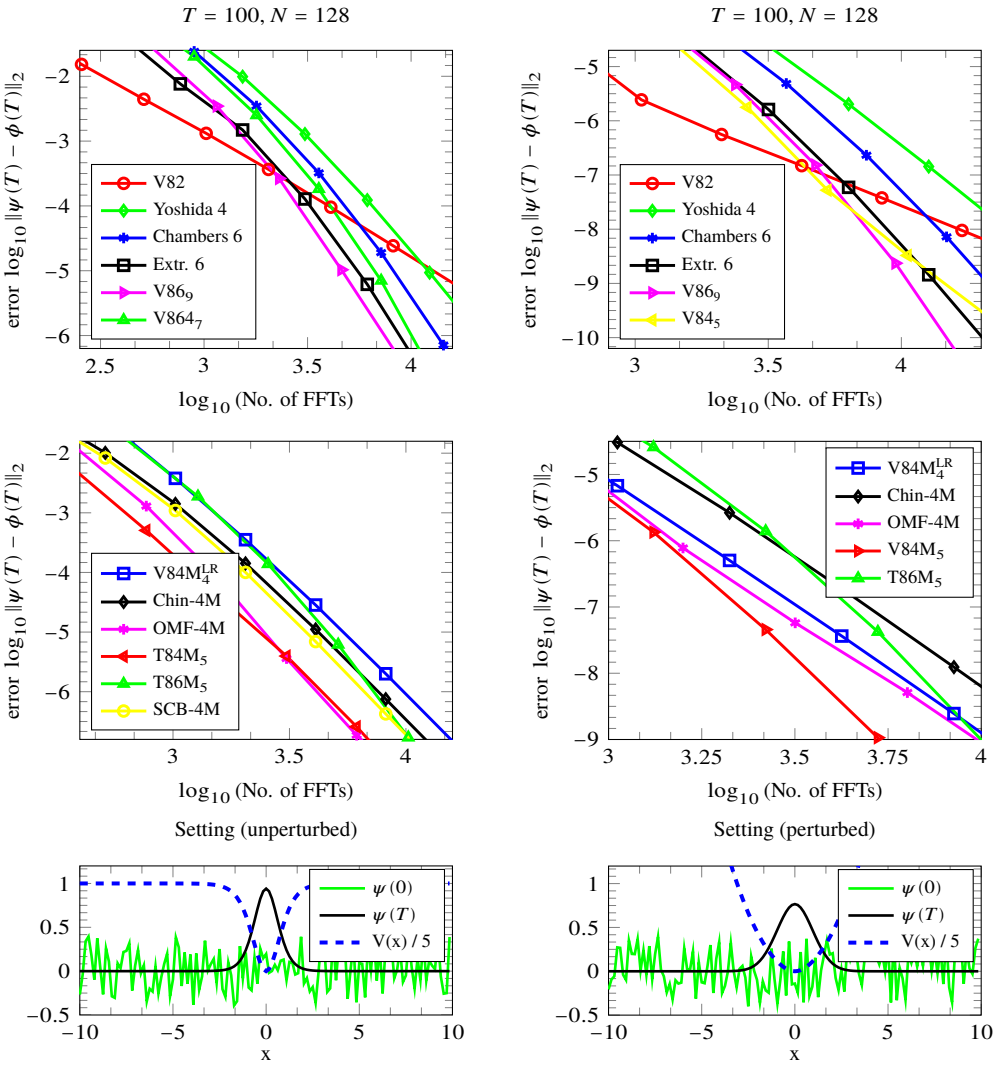

(a) Unperturbed Pöschl-Teller potential

(b) HO perturbed by a Pöschl-Teller potential

Figure 5.1: In the first row, efficiency curves (error vs. number of FFTs) for methods without force evaluations are presented, with the new methods (triangles) performing best for high accuracies. The middle row depicts methods based on modified potentials. In the right column, $T86M_5$ intersects with $V84M_5$ at precision 10^{-13}, whereas it already improves on $T84M_5$ at 10^{-9} for the left column. SCB-4M has the parameters (cf. Ref. [113] for notation) $t_0 = 0.1215$ and $a_1 = 0.33$ and overlaps with Chin-4M in the right plot and has thus been omitted. In the bottom row, the random initial conditions (green), the ground states (black) and the potentials (dashed blue), scaled by $1/5$ to fit the axis, are shown.

From the computational point of view, it is suggested [4] to consider the VTV split instead of the TVT split because it can be concatenated with the perturbation which only depends on the coordinates and no additional FFTs are necessary, i.e.

$$\dots e^{-b_{j+1}\tau\varepsilon V} e^{-a_j\tau H_{\mathrm{HO}}} e^{-b_j\tau\varepsilon V} \dots$$

In Ref. [47], this decomposition is generalized to the two-dimensional problem $H = \frac{1}{2}(p_x^2 + p_y^2) + \frac{1}{2}(w_1^2x^2 + w_2^2y^2) - \Omega(xp_y - yp_x)$ and in Ref. [4] to the non homogeneous and possibly time-dependent one-dimensional problem $H = \frac{1}{2}p^2 + \frac{1}{2}w(t)x^2 + f(t)p + g(t)x$. For a more complete discussion, see Chapter 2.

After the substitution $\delta = -ih$, we have

$$e^{-hH_{\mathrm{HO}}} \equiv e^{-\frac{\omega}{2}\tanh(\frac{h\omega}{2})x^2} e^{-\frac{1}{2\omega}\sinh(h\omega)p^2} e^{-\frac{\omega}{2}\tanh(\frac{h\omega}{2})x^2},$$

for $|\Im(h)\omega| < \pi$ and $\Re(h) > 0$ (for numerical stability) and the perturbation part is easily propagated after discretization by the exponential of a diagonal matrix. In this setting, the higher order in the small parameter is amplified and the efficiency plots in Figure 5.1b indicate that the new methods outperform the existing ones when high precision is sought and overall when modified potentials are allowed. We observe in both examples that, when modified potentials can be computed without exceedingly large computational cost, they should be used.

Further numerical experiments show that the efficiency curves are independent of the mesh size, i.e., the norm of T, and the cost only increases as $N\log(N)$ as expected. The reason for this can be understood by following the evolution of the state vector along the iterations of the algorithm. Whereas in the beginning one has a non-smooth configuration u_0, after a few steps the vector u_i is close to an eigenstate and thus smoothened.

It is important to remark that the methods proposed in this work can be implemented in an algorithm which uses variable step, variable order, variable mesh size and variable simple-double precision. The best implementation can depend on the class of problems to be solved. For illustration, we present an implementation with variable time steps.

5.3.1 Variable step method

The previous examples show that for low accuracies and large time steps, the (8,2) method (with real coefficients) performs best. However, if we allow for variable time steps, as proposed in [1, 89], the computational cost is drastically reduced. We propose an improved time-stepping algorithm that is based on two different estimators for the eigenvalue.

Recall that fixing the time-step and iterating to convergence will yield an eigenvector with the error being of the order of the method $\mathcal{O}(h^p)$ since we are computing exactly the spectrum of a perturbed Hamiltonian. Assume now that we are close to convergence, i.e, one has obtained an eigenvector $u_n = v_0 + \mathcal{O}(h^p)$ and we consider the decomposition in the basis of exact eigenvectors v_i of H,

$$u_n = \sum_{i=0}^{N-1} d_i v_i, \quad \text{where} \quad \sum_{i=0}^{N-1} |d_i|^2 = 1.$$

It is clear that $d_i = \mathcal{O}(h^p),\ i > 1$ and due to the normalization $d_0 = 1 + \mathcal{O}(h^{2p})$. Then, an energy estimation is given by

$$E_{h,1} \equiv u_n^T H u_n = E_0 + \mathcal{O}(h^{2p}).$$

Alternatively, the energy can be estimated by the loss of norm in each time step,

$$\bar{u}_{n+1} = e^{-hH} u_n + \mathcal{O}(h^{p+1}) = e^{-hE_0} v_0 + \mathcal{O}(h^{p+1}),$$

which gives

$$E_{h,2} \equiv \frac{\log\left(\|\bar{u}_{n+1}\|\right)}{h} = E_0 + ch^p + \mathcal{O}\left(h^{p+1}\right).$$

Combining both expressions yields an error estimate for the energy,

$$\Delta E_h \equiv E_{h,2} - E_{h,1} = ch^p + \mathcal{O}(h^{p+1}).$$

The convergence in energy is measured by comparison with the previous time step,

$$\delta E_h^n \equiv E_{h,1}^n - E_{h,1}^{n-1} = dh^{2p} + \mathcal{O}(h^{2p+1}).$$

The time stepper then works as follows: Starting from a large step size, the time step is decreased by a factor $1/2$ whenever the actual reduction in energy of the iteration δE falls below the maximally reachable precision ΔE, i.e., $|\delta E| < (\Delta E)^2$ and the iteration is terminated once the error estimate ΔE has reached a given tolerance.

For the numerical experiments, we use the same configurations as for constant time step but terminate the algorithm when convergence in energy is reached at $\Delta E < 10^{-10}$. The iterations are initialized with random normalized data and a time step of $\tau = 10$. The results are displayed in Figure 5.2a for the Pöschl-Teller potential and in Figure 5.2b for the perturbed harmonic oscillator with the same parameters as in the fixed-step size experiments. The error is measured as the ℓ_2 norm of the difference between the current value of the algorithm $\psi(t)$ and the exact ground state $\phi(T)$ as in the previous experiments, error $= \|\psi(t) - \phi(T)\|$.

As expected, it is apparent that lower order methods show better smoothing behavior for the first steps, when the wave function is still rough (recall that the algorithm is initialized by a worst-case wave function). For higher precisions, the new methods clearly outperform the existing ones, with the sole exception of the unperturbed setting with modified potentials, where the globally optimized OMF-4M method can hardly be improved unless extremely high precision is sought and the 6th-order methods of Table 5.4 and 5.3 become favorable (not shown). Finally, if one is interested in very high accuracies, high order extrapolation methods [46, 24] can be used for the last part of the time integration.

The results indicate that for low precision, i.e., for the first iterations, a lower order method should be used and then, after a certain precision is reached, e.g., when the higher order methods exhibit their superiority the algorithm should change to the optimal method, either $\mathrm{V864}_7$ or $\mathrm{V86M}_5$ until convergence. Further preliminary experiments on this adaptive order strategy have shown that there is plenty of room for optimization, e.g., by changing the initial step-size, adjusting the step-size by a different factor or by modifying the control criterion.

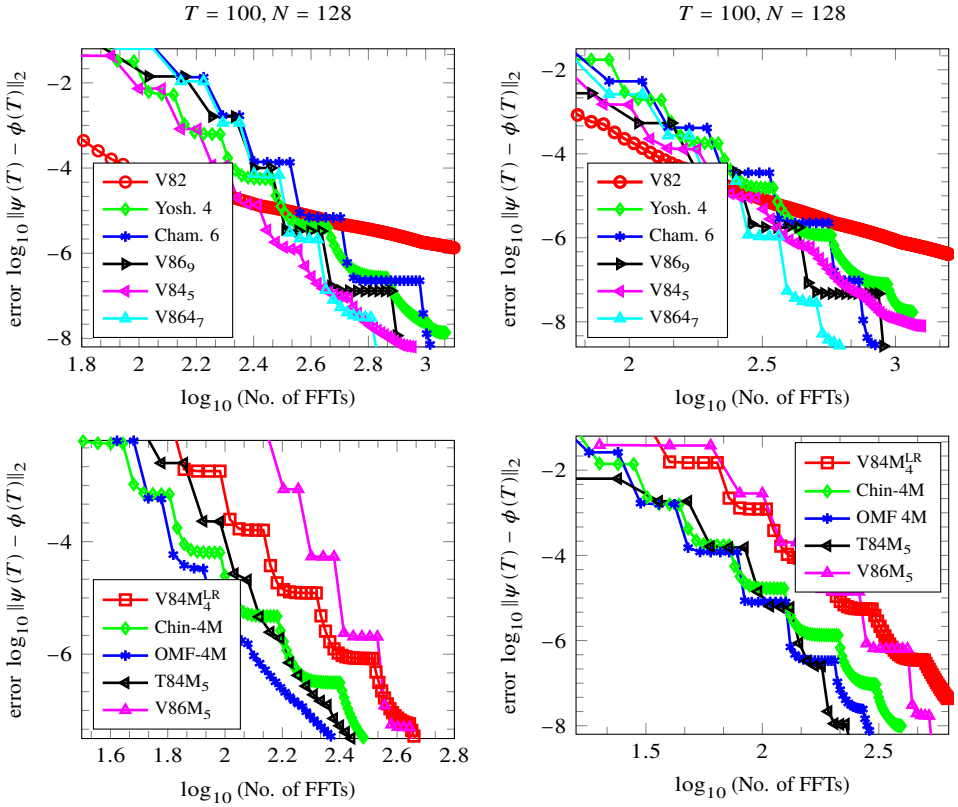

(a) Unperturbed case

(b) Perturbed case

Figure 5.2: Evolution of precision in the discrete L^2 norm of the position vector with the variable time step algorithm described in Section 5.3.1. As in Fig. 5.1, the top row gives the results for standard methods whereas the bottom rows shows methods with modifying potentials.

Each of which has certain advantages and disadvantages, depending on the initial conditions and the range of precision.

For excited states, one expects an even better performance of the new methods since several states have to be computed to high precision in order to avoid error accumulation and the gains of the new methods are thus amplified. We have confirmed this conjecture by numerical experiments. The results thereof are omitted since they do not contribute insight beyond the presented experiments: They are qualitatively identical.

Chapter 6

CONCLUSIONS AND OUTLOOK

We summarize the contributions and conclusions of each chapter and end with a brief introduction to a future line of work that for which this thesis serves as foundation.

6.1 Harmonic oscillators and rotating traps

The first part of this work contains contributions to the solution of a very common problem in quantum mechanics, the harmonic oscillator. Fourier methods have shown a high performance in solving many different problems which can be split into the kinetic part and a remainder that is diagonal in the coordinate space. We have extended the Fourier methods to perturbations of the time-dependent harmonic potential, and refer to them as Hermite-Fourier methods. We introduce a new technique, based on algebraic correspondence between the quantum Lie algebra and its classical mechanical counterpart, to find an expression for the exact solution which is computable using fast Fourier transforms only. The technique extends to arbitrary dimension and is compatible with time-dependencies after some time-averaging like the Magnus expansion has been applied. Due to the finiteness of the harmonic oscillator algebra, the averaged Hamiltonian is shown to be exactly exponentiatable using only FFTs. The decompositions prove to be highly efficient in numerical experiments and should be preferred over the more commonly used expansions in Hermite polynomials. Similar considerations have been applied to Hamiltonians that contain angular momenta. For non-autonomous potentials, the (Magnus-)averaged Hamiltonian is still tractable by our method and we show how to compute efficient approximations for the most general case of quadratic Hamiltonians in two dimensions.

These results have then been combined to introduce Fourier methods for the numerical integration of perturbations of the time dependent harmonic oscillator which are useful for both the Gross-Pitaevskii equation as well as for the linear Schrödinger equation. They solve the linear Schrödinger equation with a time-dependent harmonic potential to the desired order using corresponding Magnus expansions and up to the accuracy given by the spatial discretization.

These methods are fast to compute since FFTs can be applied and show a high accuracy when the problem is a small perturbation of a quadratic Hamiltonian, an important application is the propagation of rotating Bose-Einstein condensates. The principal ingredients were the finiteness of the underlying algebra and the availability of the solution in the corresponding classical mechanical system. Future research could identify other classes of problems where similar algebraic structures allow to find decompositions that are easy to exponentiate by solving the problem in a simpler matrix setting.

6.2 Nonlinear Schrödinger equations

In the third chapter, modified potentials for the nonlinear Schrödinger equation have been developed and successfully applied in numerical examples. Nonlinear modified potentials arise from commutators of Lie derivatives of the separable parts in the Gross-Pitaevskii equation and after suitable reformulation, we show that they can be computed using FFTs only.

Furthermore, complex coefficient splittings have been studied and we have shown how to solve the nonlinear SE in complex time. However, the constraint $\Im(a_i) \leq 0$ and the consistency condition, $\sum_i a_i = 1$, necessarily require $a_i \in \mathbb{R}$, while b_i can be complex. We observed stability problems for unbounded potentials which make current methods impracticable. A large number of new methods have been explored, but the superiority is not yet clear since there exist highly efficient methods with real coefficients for perturbed problems [21, 27] and using modified potentials [25]. These results are pointers to future work, which falls in three classes: – For which kind of nonlinearities is it possible to find cheaply computable perturbations, such as the present modified potential? – Can we find efficient methods with real coefficients a_j and complex b_j that are more efficient than the current (all real) standards? And lastly, how to cure the instabilities that are caused by complex a_j (or equivalently, complex b_j for unbounded potentials)? Numerical results indicate that introducing a cut-off in the exponents, or somewhat similar, an appropriate shrinking of the domain, eases the stability issue. However, it lacks an analysis with respect to the implications on the accuracy.

6.3 Semiclassical Schrödinger equations

The difficulty when treating semiclassical Schrödinger equations arises from the presence of a small parameter ε, which can be interpreted as a long-time integration. Higher-order methods are particularly suitable for this problem since larger time-steps are allowed. The number of exponentials for classical splittings, however, grows exponentially with the order of the method. We show how to apply the symmetric Zassenhaus algorithm to produce arbitrary order methods that grow only linearly in the number of exponentials, but come at the expense of computing commutators. Working in the algebra of linear operators, we show that the commutators can be exponentiated using only a few Lanczos iterations since the Zassenhaus algorithm has already reduced their size drastically. Subsuming the spatial and temporal discretization parameters, Δx and h, respectively, into powers of the semiclassical variable ε, we explicitly derive algorithms of local error $\mathcal{O}\left(\varepsilon^{7/2}\right)$ for $h = \mathcal{O}\left(\sqrt{\varepsilon}\right)$ and $\Delta x = \mathcal{O}(\varepsilon)$.

Thereafter, we briefly address methods that originate from a discretization using Hagedorn-

wavepackets, i.e., shifted and scaled eigenfunctions of the harmonic oscillator. It turns out, that methods recently published [54, 60] can be understood as Magnus integrators and we propose to solve the classical mechanical system for parameters Π using higher-order RKN splitting methods and approximate the evolution of the weights c_k by Magnus integrators.

In the last part, non-autonomous potentials in the semiclassical Hamiltonian are considered. We distinguish between two qualitatively different cases, (ε-independent) slow and fast time-dependencies. It is shown how the Zassenhaus method can be applied in both situations after a previous averaging using the Magnus expansion, for which the truncation error is studied. The initial step of the algorithm consists of an asymmetric splitting in order to guarantee a decrease in size of the exponents along the course of the method. This can be understood as a combination of standard splitting methods with the Zassenhaus-split and can possibly be generalized to standard Magnus integrators in order to reduce the number of commutators. Methods for both situations have been derived explicitly for both cases, using Taylor expansions of the slow potential or integrals of the fast potential. The former can also be carried out using momentum integrals in a straightforward fashion. In the latter case, the fast time-dependency has been assumed to be scalar, and future studies could extend the methodology to more general potentials. Furthermore, it remains to be seen whether the constructions can be turned into efficient algorithms for particular problems, when no closed-form solutions of the spatial and temporal derivatives and integrals of the potential are available.

6.4 Imaginary time

In Chapter 5, we have studied the Schrödinger eigenvalue problem by the imaginary time propagation method and proposed splitting schemes with positive real coefficients using modified potentials as well as with complex coefficients that can overcome the order barrier for parabolic problems since the coefficients have only positive real parts. The obtained sixth order methods are clearly superior to any classical ones for high precisions. On the other hand, when the gradient of the potential can be cheaply evaluated, the high order methods with complex coefficients are efficient only at very high accuracies due to the double cost caused by complex arithmetic.

We have proposed different high order methods to reach highly accurate results. An efficient implementation should take into account, for example, a preliminary time integration on a coarse mesh using simple precision arithmetic in order to get, as fast as possible, a smooth and relatively accurate solution from a random initial guess, and next consider a refined mesh using arithmetic in double precision. For simple precision arithmetic and low accuracies, it suffices to consider only low order methods, and when higher accuracies are desired, we turn to double precision, variable time step and variable order methods. The best algorithm could depend on the class of problems to solve.

It is also important to remark that the form of the exponent allows that the techniques presented in this work can also be transferred to other areas whenever splitting is appropriate and the integration has to be performed forward in time, e.g., statistical mechanics of quantum systems, where one has to compute the Boltzman operator $\exp(-\beta H)$, with $\beta = (kT)^{-1}$ or quantum Monte-Carlo simulations [11].

6.5 Outlook

Many of the presented techniques can be applied to problems arising in the extremely active field of quantum optimal control. In a preliminary study, we have applied geometric integrators to classical mechanical control problems to demonstrate their superiority [7], and we expect that one can improve on the commonly used methods of *Rabitz et al.*, see the review articles [128, 36]. The dynamics of a controlled quantum system are governed by

$$i\partial_t \psi(x,t) = \left(T + V(x) - \varepsilon(t)\mu(x)\right)\psi(x,t), \quad \psi(x,0) = \psi_0(x),$$

with the usual operators for kinetic energy $T = -\frac{\Delta}{2m}$ and the dipole moment μ (usually $\mu = x$).

A suitable objective functional to be maximized is

$$J = \langle\psi(T)|O\psi(T)\rangle - \alpha_0 \int_0^T \varepsilon(t)^2 dt \\ - 2\Re\left[\int_0^T \langle\chi(t)|\frac{\partial}{\partial t} + i\left[T + V - \mu\varepsilon(t)\right]|\psi(t)\rangle dt\right],$$

with the Lagrange multiplier $\chi(t)$. The components lead to maximizing the expectation value of the sought observable O at the final time, minimizing the energy-input in the system, penalized by $\alpha_0 > 0$ and the error in the Schrödinger equation. Setting the variation to zero, $\delta J = 0$, one obtains the set of coupled PDEs

$$\begin{aligned} i\frac{\partial}{\partial t}\psi(t) &= \left[T + V - \mu\varepsilon(t)\right]\psi(t), & \psi(0) &= \psi_0, \\ i\frac{\partial}{\partial t}\chi(t) &= \left[T + V - \mu\varepsilon(t)\right]\chi(t), & \chi(T) &= O\psi(T), \\ \alpha_0\varepsilon(t) &= -\Im\langle\chi(t)|\mu\psi(t)\rangle, \end{aligned}$$

or, equivalently

$$i\frac{\partial}{\partial t}\psi(t) = \left[T + V + \frac{\mu}{\alpha_0}\Im\langle\chi(t)|\mu\psi(t)\rangle\right]\psi(t), \qquad \psi(0) = \psi_0, \tag{6.1}$$

$$i\frac{\partial}{\partial t}\chi(t) = \left[T + V + \frac{\mu}{\alpha_0}\Im\langle\chi(t)|\mu\psi(t)\rangle\right]\chi(t), \qquad \chi(T) = O\psi(T). \tag{6.2}$$

This system is usually solved by iterative methods, e.g., [132, 129, 70]: Initialize with some guess for the laser field $\varepsilon(t)$ (e.g. $\varepsilon = 0$) to compute $\psi^{[0]}(t)$ and then,

1. integrate (6.2) backwards using $\psi^{[0]}$ to obtain $\chi^{[1]}(t)$, with final condition $\chi^{[1]}(T) = O\psi^{[0]}(T)$.
2. integrate (6.1) forwards using $\chi^{[1]}$ to obtain $\psi^{[1]}$.

It can be shown that this method is monotonically convergent, increasing the value of functional in every step. In usual implementations, the Schrödinger equations (6.1),(6.2) are solved with the Strang splitting, however, the procedure requires many iterations until convergence and more accurate, faster converging procedures would be of high impact.

Appendix A

ALGEBRAIC TOOLS

A.1 Algebra

Terms up to order seven of the symmetric BCH formula expressed in a Hall basis.

$$
\begin{aligned}
\mathrm{sBCH}(hX, hY) = {} & h(X+Y) - h^3\left(\tfrac{1}{24}[[Y,X],X] + \tfrac{1}{12}[[Y,X],Y]\right) \\
& + h^5\Big(\tfrac{7}{5760}[[[[Y,X],X],X],X] + \tfrac{7}{1440}[[[[Y,X],X],X],Y] + \tfrac{1}{180}[[[[Y,X],X],Y],Y] \\
& \quad + \tfrac{1}{720}[[[[Y,X],Y],Y],Y] + \tfrac{1}{480}[[[Y,X],X],[Y,X]] - \tfrac{1}{360}[[[Y,X],Y],[Y,X]]\Big) \\
& + h^7\Big(-\tfrac{31}{967680}[[[[[[Y,X],X],X],X],X],X] - \tfrac{31}{161280}[[[[[[Y,X],X],X],X],X],Y] \\
& \quad - \tfrac{13}{30240}[[[[[[Y,X],X],X],X],Y],Y] - \tfrac{53}{120960}[[[[[[Y,X],X],X],Y],Y],Y] \\
& \quad - \tfrac{1}{5040}[[[[[[Y,X],X],Y],Y],Y],Y] - \tfrac{1}{30240}[[[[[[Y,X],Y],Y],Y],Y],Y] \\
& \quad - \tfrac{53}{161280}[[[[[Y,X],X],X],X],[Y,X]] - \tfrac{11}{12096}[[[[[Y,X],X],X],Y],[Y,X]] \\
& \quad - \tfrac{3}{4480}[[[[[Y,X],X],Y],Y],[Y,X]] - \tfrac{1}{10080}[[[[[Y,X],Y],Y],Y],[Y,X]] \\
& \quad - \tfrac{1}{4032}[[[[Y,X],X],[Y,X]],[Y,X]] - \tfrac{1}{6720}[[[[Y,X],Y],[Y,X]],[Y,X]] \\
& \quad - \tfrac{19}{80640}[[[[Y,X],X],X],[[Y,X],X]] - \tfrac{1}{10080}[[[[Y,X],X],Y],[[Y,X],X]] \\
& \quad + \tfrac{17}{40320}[[[[Y,X],Y],Y],[[Y,X],X]] - \tfrac{53}{60480}[[[[Y,X],X],X],[[Y,X],Y]] \\
& \quad - \tfrac{19}{13440}[[[[Y,X],X],Y],[[Y,X],Y]] - \tfrac{1}{5040}[[[[Y,X],Y],Y],[[Y,X],Y]]\Big) \\
& + \mathcal{O}\left(h^9\right). \qquad \text{(A.1)}
\end{aligned}
$$

A.2 Structure coefficients for rotating oscillator

Table A.1: Structure coefficients for the basis elements E_j defined in (2.61). The coefficients have to be read from left to right and multiplied with the imaginary unit i, e.g., $[E_1, E_2] = [x, p_x] = iE_{15} = i$.

	$E_1(x)$	E_2	E_3	E_4	E_5	E_6	E_7	E_8
E_1	0	E_{15}	0	$2E_2$	E_1	0	0	0
E_2	-1	0	$-2E_1$	0	$-E_2$	0	0	0
E_3	0	$2E_1$	0	$4E_5$	$2E_3$	0	0	0
E_4	$-2E_2$	0	$-4E_5$	0	$-2E_4$	0	0	0
E_5	$-E_1$	E_2	$-2E_3$	$2E_4$	0	0	0	0
E_6	0	0	0	0	0	0	E_{15}	0
E_7	0	0	0	0	0	-1	0	$-2E_6$
E_8	0	0	0	0	0	0	$2E_6$	0
E_9	0	0	0	0	0	$-2E_7$	0	$-4E_{10}$
E_{10}	0	0	0	0	0	$-E_6$	E_7	$-2E_8$
E_{11}	0	E_6	0	$2E_{14}$	E_{11}	0	E_1	0
E_{12}	$-E_7$	0	$-2E_{13}$	0	$-E_{12}$	$-E_2$	0	$-2E_{14}$
E_{13}	0	E_7	0	$2E_{12}$	E_{13}	$-E_1$	0	$-2E_{11}$
E_{14}	$-E_6$	0	$-2E_{11}$	0	$-E_{14}$	0	E_2	0

...	E_9	E_{10}	E_{11}	E_{12}	E_{13}	E_{14}
E_1	0	0	0	E_7	0	E_6
E_2	0	0	$-E_6$	0	$-E_7$	0
E_3	0	0	0	$2E_{13}$	0	$2E_{11}$
E_4	0	0	$-2E_{14}$	0	$-2E_{12}$	0
E_5	0	0	$-E_{11}$	E_{12}	$-E_{13}$	E_{14}
E_6	$2E_7$	E_6	0	E_2	E_1	0
E_7	0	$-E_7$	$-E_1$	0	0	$-E_2$
E_8	$4E_{10}$	$2E_8$	0	$2E_{14}$	$2E_{11}$	0
E_9	0	$-2E_9$	$-2E_{13}$	0	0	$-2E_{12}$
E_{10}	$2E_9$	0	$-E_{11}$	E_{12}	E_{13}	$-E_{14}$
E_{11}	$2E_{13}$	E_{11}	0	$(E_5 + E_{10})$	E_3	E_8
E_{12}	0	$-E_{12}$	$-(E_5 + E_{10})$	0	$-E_9$	$-E_4$
E_{13}	0	$-E_{13}$	$-E_3$	E_9	0	$(E_{10} - E_5)$
E_{14}	$2E_{12}$	E_{14}	$-E_8$	E_4	$(E_5 - E_{10})$	0

$$
\begin{aligned}
&E_1 = x, && E_2 = p_x, && E_3 = \tfrac{1}{2}x^2, && E_4 = \tfrac{1}{2}p_x^2, && E_5 = \tfrac{1}{2}\left(xp_x + p_x x\right),\\
&E_6 = y, && E_7 = p_y, && E_8 = \tfrac{1}{2}y^2, && E_9 = \tfrac{1}{2}p_y^2, && E_{10} = \tfrac{1}{2}\left(yp_y + p_y y\right),\\
&E_{11} = xy, && E_{12} = p_x p_y, && E_{13} = xp_y, && E_{14} = yp_x, && E_{15} = 1.
\end{aligned}
$$

A.3 Composition for the rotating oscillator

The composition of flows of classical mechanical systems corresponding to the Hamiltonians given in the exponents can be written as

$$e^{n_1 \frac{x^2}{2}} e^{f_1 \frac{y^2}{2} + g_1 \frac{p_x^2}{2} - e_1 y p_x} e^{f_2 \frac{x^2}{2} + g_2 \frac{p_y^2}{2} + e_2 x p_y} e^{f_3 \frac{y^2}{2} + g_3 \frac{p_x^2}{2} - e_3 y p_x} = A \in \mathbb{R}^{4\times 4}, \tag{A.2}$$

with coefficients of the matrix $A = (a_{i,j})$,

$$\begin{aligned}
a_{1,1} &= 1 - e_1 e_2 - f_2 g_1 \\
a_{2,1} &= e_2 \\
a_{3,1} &= -f_2 + (-1 + e_1 e_2 + f_2 g_1) n_1 \\
a_{4,1} &= -e_2 f_1 - e_1 f_2 \\
a_{1,2} &= e_2 f_3 g_1 + e_3(-1 + f_2 g_1) + e_1(-1 + e_2 e_3 + f_3 g_2) \\
a_{2,2} &= 1 - e_2 e_3 - f_3 g_2 \\
a_{3,2} &= e_3 f_2 + e_2 f_3 - (e_2 f_3 g_1 + e_3(-1 + f_2 g_1) + e_1(-1 + e_2 e_3 + f_3 g_2)) n_1 \\
a_{4,2} &= e_1 e_3 f_2 - f_3 + e_1 e_2 f_3 + f_1(-1 + e_2 e_3 + f_3 g_2) \\
a_{1,3} &= g_3 - e_1(e_3 g_2 + e_2 g_3) - g_1(-1 + e_2 e_3 + f_2 g_3) \\
a_{2,3} &= e_3 g_2 + e_2 g_3 \\
a_{3,3} &= 1 - e_2 e_3 - f_2 g_3 + (e_1 e_3 g_2 - g_3 + e_1 e_2 g_3 + g_1(-1 + e_2 e_3 + f_2 g_3)) n_1 \\
a_{4,3} &= e_1 + e_3 - e_1 e_2 e_3 - e_3 f_1 g_2 - (e_2 f_1 + e_1 f_2) g_3 \\
a_{1,4} &= -e_2 g_1 - e_1 g_2 \\
a_{2,4} &= g_2 \\
a_{3,4} &= e_1 g_2 n_1 + e_2(-1 + g_1 n_1) \\
a_{4,4} &= 1 - e_1 e_2 - f_1 g_2
\end{aligned}$$

The expressions can be derived easily as shown for the the first two exponentials,

$$e^{n_1 \frac{x^2}{2}} \begin{pmatrix} x \\ y \\ p_x \\ p_y \end{pmatrix} = \begin{pmatrix} x \\ y \\ p_x + \{p_x, n_1 \frac{x^2}{2}\}_- \\ p_y \end{pmatrix} = \begin{pmatrix} x \\ y \\ p_x - n_1 x \\ p_y \end{pmatrix} = \begin{pmatrix} 1 & 0 & 0 & 0 \\ 0 & 1 & 0 & 0 \\ -n_1 & 0 & 1 & 0 \\ 0 & 0 & 0 & 1 \end{pmatrix} \begin{pmatrix} x \\ y \\ p_x \\ p_y \end{pmatrix},$$

and

$$\begin{aligned}
e^{f_3 \frac{y^2}{2} + g_3 \frac{p_x^2}{2} - e_3 y p_x} \begin{pmatrix} x \\ y \\ p_x \\ p_y \end{pmatrix} &= \begin{pmatrix} x + \{x, g_3 \frac{p_x^2}{2} - e_3 y p_x\}_- \\ y \\ p_x \\ p_y + \{p_y, f_3 \frac{y^2}{2} - e_3 y p_x\}_- \end{pmatrix} = \begin{pmatrix} x + g_3 p_x - e_3 y \\ y \\ p_x \\ p_y - f_3 y + e_3 p_x \end{pmatrix} \\
&= \begin{pmatrix} 1 & -e_3 & g_3 & 0 \\ 0 & 1 & 0 & 0 \\ 0 & 0 & 1 & 0 \\ 0 & -f_3 & e_3 & 1 \end{pmatrix} \begin{pmatrix} x \\ y \\ p_x \\ p_y \end{pmatrix}.
\end{aligned}$$

REFERENCES

[1] M. Aichinger and E. Krotscheck, A fast configuration space method for solving local Kohn–Sham equations, *Comput. Mater. Sci.* **34** (2005), 188–212.

[2] M. H. Anderson, J. R. Ensher, M. R. Matthews, C. E. Wieman, and E. A. Cornell, Observation of Bose-Einstein condensation in a dilute atomic vapor, *Science* **269** (1995), 198–201.

[3] J. Auer, E. Krotscheck, and S. A. Chin, A fourth-order real-space algorithm for solving local Schrödinger equations, *J. Chem. Phys.* **115** (2001), 6841–6846.

[4] P. Bader and S. Blanes, Fourier methods for the perturbed harmonic oscillator in linear and nonlinear Schrödinger equations, *Phys. Rev. E* **83** (2011), 046711.

[5] P. Bader, S. Blanes, and F. Casas, *See supplementary material for a collection of all obtained methods with 25 digits precision at* `http://dx.doi.org/10.1063/1.4821126`.

[6] P. Bader, S. Blanes, and F. Casas, Solving the Schrödinger eigenvalue problem by the imaginary time propagation technique using splitting methods with complex coefficients, *J. Chem. Phys.* **139** (2013), 124117.

[7] P. Bader, S. Blanes, and E. Ponsoda, Structure preserving integrators for solving (non-)linear quadratic optimal control problems with applications to describe the flight of a quadrotor, *J. Comput. Appl. Math.* **262** (2014), 223–233.

[8] P. Bader and U. R. Fischer, Fragmented many-body ground states for scalar bosons in a single trap, *Phys. Rev. Lett.* **103** (2009), 060402.

[9] P. Bader and U. R. Fischer, Stability of spherically trapped three-dimensional Bose-Einstein condensates against macroscopic fragmentation, *Phys. Rev. A* **87** (2013), 023632.

[10] P. Bader, A. Iserles, K. Kropielnicka, and P. Singh, Effective Approximation for the Semiclassical Schrödinger Equation, *Found. Comput. Math.* (2014), 1–32.

[11] A. D. Bandrauk, E. Dehghanian, and H. Lu, Complex integration steps in decomposition of quantum evolution operators, *Chem. Phys. Lett.* **419** (2006), 346–350.

[12] A. D. Bandrauk and H. Lu, Exponential propagators (integrators) for the time-dependent Schrödinger equation, *J. Theor. Comput. Chem.* **12** (2013), 1340001.

[13] W. Bao, D. Jaksch, and P. Markowich, Numerical solution of the Gross-Pitaevskii equation for Bose-Einstein condensation, *J. Comp. Phys.* **187** (2003), 318–342.

[14] W. Bao, S. Jin, and P. A. Markowich, On Time-Splitting Spectral Approximations for the Schrdinger Equation in the Semiclassical Regime, *J. Comput. Phys.* **175** (2002), 487–524.

[15] W. Bao and J. Shen, A fourth-order time-splitting Laguerre-Hermite pseudo-spectral method for Bose-Einstein condensates, *SIAM J. Sci. Comput.* **26** (2005), 2010–2028.

[16] W. Bao and J. Shen, A fourth-order time-splitting Laguerre-Hermite pseudo-spectral method for Bose-Einstein condensates, *SIAM J. Scient. Comput.* **26** (2005), 2010–2028.

[17] S. Blanes and F. Casas, On the necessity of negative coefficients for operator splitting schemes of order higher than two, *Appl. Num. Math.* **54** (2005), 23–37.

[18] S. Blanes and F. Casas, Optimization of Lie-group methods for differential equations, *Future Gener. Comp. Sys.* **19** (2003), 331–339.

[19] S. Blanes, F. Casas, P. Chartier, and A. Murua, *Optimized high-order splitting methods for some classes of parabolic equations*, arXiv:1102.1622v1 [math.NA], 2011.

[20] S. Blanes, F. Casas, P. Chartier, and A. Murua, Optimized high-order splitting methods for some classes of parabolic equations, *Math. Comput.* **82** (2013), 1559–1576.

[21] S. Blanes, F. Casas, A. Farrés, J. Laskar, J. Makazaga, and A. Murua, New families of symplectic splitting methods for numerical integration in dynamical astronomy, *Appl. Num. Math.* **68** (2013), 58–72.

[22] S. Blanes, F. Casas, and A. Murua, Splitting and composition methods in the numerical integration of differential equations, *Bol. Soc. Esp. Mat. Apl.* **45** (2008), 89–145.

[23] S. Blanes, F. Casas, J. A. Oteo, and J. Ros, The Magnus expansion and some of its applications, *Phys. Rep.* **470** (2009), 151–238.

[24] S. Blanes, F. Casas, and J. Ros, Extrapolation of symplectic integrators, *Celest. Mech. & Dyn. Astron.* **75** (1999), 149–161.

[25] S. Blanes, F. Casas, and J. Ros, High-order Runge-Kutta-Nyström geometric methods with processing, *Appl. Numer. Math.* **39** (2001), 245–259.

[26] S. Blanes, F. Casas, and J. Ros, Improved high order integrators based on the Magnus expansion, *BIT Numer. Math.* **40** (2000), 434–450.

[27] S. Blanes, F. Casas, and J. Ros, Processing symplectic methods for near-integrable Hamiltonian systems, *Celes. Mech. Dyn. Astron.* **77** (2000), 17–35.

[28] S. Blanes, F. Diele, C. Marangi, and S. Ragni, Splitting and composition methods for explicit time dependence in separable dynamical systems, *J. Comput. Appl. Math.* **235** (2010), 646–659.

[29] S. Blanes and P. C. Moan, Practical symplectic partitioned Runge–Kutta and Runge--Kutta-Nyström methods, *J. Comp. Appl. Math.* **142** (2002), 313–330.

[30] S. Blanes and P.C. Moan, Fourth- and sixth-order commutator-free Magnus integrators for linear and non-linear dynamical systems, *Appl. Numer. Math.* **56** (2006), 1519–1537.

[31] S. Blanes and P.C. Moan, Splitting methods for the time-dependent Schrödinger equation, *Phys. Lett. A* **265** (2000), 35–42.

[32] M. Born, Zur Quantenmechanik der Stoßvorgänge, *Zeitschrift für Physik* **38** (1926), 803–827.

[33] M. Born, Zur Quantenmechanik der Stoßvorgänge (Vorläufige Mitteilung), *Zeitschrift für Physik* **37** (1926), 863–867.

[34] M. Born and R. Oppenheimer, Zur Quantentheorie der Molekeln, *Ann. d. Phys.* **84** (1927), 457–484.

[35] C. C. Bradley, C. A. Sackett, J. J. Tollett, and R. G. Hulet, Evidence of Bose-Einstein condensation in an atomic gas with attractive interactions, *Phys. Rev. Lett.* **75** (1995), 1687–1690.

[36] C. Brif, R. Chakrabarti, and H. Rabitz, Control of quantum phenomena: past, present and future, *New Journal of Physics* **12** (2010), 075008.

[37] R. Carles, *Semi-Classical Analysis for Nonlinear Schrödinger Equations*, Singapore: World Scientific, 2008.

[38] F. Casas, Sufficient conditions for the convergence of the Magnus expansion, *J. Phys. A: Math. Theor.* **40** (2007), 15001–15017.

[39] F. Casas and A. Murua, An efficient algorithm for computing the Baker– Campbell–Hausdorff series and some of its applications, *J. Math. Phys.* **50** (2009), 033513-1–033513-23.

[40] F. Castella, P. Chartier, S. Descombes, and G. Vilmart, Splitting methods with complex times for parabolic equations, *BIT Numer. Math.* **49** (2009), 487–508.

[41] J. E. Chambers, Symplectic integrators with complex time steps, *Astron. J.* **126** (2003), 1119–1126.

[42] E. S. Chibrikov, A right normed basis for free Lie algebras and Lyndon–Shirshov words, *J. Algebra* **302** (2006), 593–612.

[43] S. A. Chin, Structure of positive decomposition of exponential operators, *Phys. Rev. E* **71** (2005), 016703.

[44] S. A. Chin, Symplectic integrators from composite operator factorizations, *Phys. Lett. A* **226** (1997), 344–348.

[45] S. A. Chin and C. R. Chen, Gradient symplectic algorithms for solving the Schrödinger equation with time-dependent potentials, *J. Chem. Phys.* **117** (2002), 1409–1415.

[46] S. A. Chin, S. Janecek, and E. Krotscheck, Any order imaginary time propagation method for solving the Schrödinger equation, *Chem. Phys. Lett.* **470** (2009), 342–346.

[47] S. A. Chin and E. Krotscheck, Fourth-order algorithms for solving the imaginary-time Gross-Pitaevskii equation in a rotating anisotropic trap, *Phys. Rev. E* **72** (2005), 036705.

[48] B. E. Davies, *Spectral theory and differential operators*, Cambridge, UK: Cambridge University Press, 1996.

[49] K. B. Davis, M. -O. Mewes, M. R. Andrews, N. J. van Druten, D. S. Durfee, D. M. Kurn, and W. Ketterle, Bose-Einstein condensation in a gas of sodium stoms, *Phys. Rev. Lett.* **75** (1995), 3969–3973.

[50] A. Debussche and E. Faou, Modified Energy for Split-Step Methods Applied to the Linear Schrödinger Equation, *SIAM Journal on Numerical Analysis* **47** (2009), 3705–3719.

[51] C. M. Dion and E. Cancés, Spectral method for the time-dependent Gross-Pitaevskii equation with a harmonic trap, *Phys. Rev. E* **67** (2003), 046706.

[52] E. B. Dynkin, Evaluation of the coefficients of the Campbell-Hausdorff formula, *Dokl. Akad. Nauk SSSR* **57** (1947), 323–326.

[53] E. Faou, *Geometric Numerical Integration and Schrödinger Equations*, Zurich Lectures in Advanced Mathematics, Zürich: Europ. Math. Soc., 2012.

[54] E. Faou, V. Gradinaru, and C. Lubich, Computing semiclassical quantum dynamics with Hagedorn wavepackets, *SIAM J. Sci. Comp.* **31** (2009), 3027–3041.

[55] A. L. Fetter and J. D. Walecka, *Quantum Theory of Many-Particle Physics*, Dover, Mineola, New York: Dover Publications, 2003.

[56] U. R. Fischer and P. Bader, Interacting trapped bosons yield fragmented condensate states in low dimensions, *Phys. Rev. A* **82** (2010), 013607.

[57] T. J. Gil, S. Shi, A. Askar, and H. A. Rabitz, Application of the Born-Oppenheimer principle to classification of time scales in molecules interacting with time-dependent external fields, *Phys. Rev. A* **45** (1992), 6479–6492.

[58] D. Goldman and T. J. Kaper, *n*th-order operator splitting schemes and nonreversible systems, *SIAM J. Numer. Anal.* **33** (1996), 349–367.

[59] G. H. Golub and C. F. Van Loan, *Matrix Computations*, 3rd, Baltimore: Johns Hopkins University Press, 1996.

[60] V. Gradinaru and G. A. Hagedorn, Convergence of a semiclassical wavepacket based time-splitting for the Schrödinger equation, *Numer. Math.* **126** (2014), 53–73.

[61] S. K. Gray and D. E. Manolopoulos, Symplectic integrators tailored to the time-dependent Schrödinger equation, *J. Chem. Phys.* **104** (1996), 7099–7112.

[62] D. J. Griffiths, *Introduction to Quantum Mechanics*, 2nd, Upper Saddle River, NJ: Prentice Hall, 2004.

[63] G. A. Hagedorn, Raising and Lowering Operators for Semiclassical Wave Packets, *Annals of Physics* **269** (1998), 77–104.

[64] G. A. Hagedorn, V. Rousse, and S. W. Jilcott Jr., The AC Stark effect, time-dependent Born-Oppenheimer approximation, and Franck-Condon factors, *Ann. Henri Poincaré* **7** (2006), 1065–1083.

[65] E. Hairer, C. Lubich, and G. Wanner, *Geometric Numerical Integration: Structure-Preserving Algorithms for Ordinary Differential Equations*, 2nd, Berlin: Springer Verlag, 2006.

[66] E. Hansen and A. Ostermann, High order splitting methods for analytic semigroups exist, *BIT Numer. Math.* **49** (2009), 527–542.

[67] E. J. Heller, Time dependent variational approach to semiclassical dynamics, *J. Chem. Phys.* **64** (1976), 63–74.

[68] J. S. Hesthaven, S. Gottlieb, and D. Gottlieb, *Spectral Methods for Time-Dependent Problems*, Cambridge: Cambridge University Press, 2007.

[69] N. J. Higham, *Functions of Matrices: Theory and Computation*, Philadelphia, PA, USA: Society for Industrial and Applied Mathematics, 2008.

[70] T.-S. Ho and H. Rabitz, Accelerated monotonic convergence of optimal control over quantum dynamics, *Phys. Rev. E* **82** (2010), 026703.

[71] M. Hochbruck and C. Lubich, On Krylov subspace approximations to the matrix exponential operator, *SIAM J. Numer. Anal.* **34** (1997), 1911–1925.

[72] M. Hochbruck and C. Lubich, On Magnus Integrators for Time-Dependent Schrödinger Equations, *SIAM J. Numer. Anal.* **41** (2003), 945–963.

[73] H. Hofstätter, O. Koch, and M. Thalhammer, Convergence analysis of high-order time-splitting pseudo-spectral methods for rotational Gross–Pitaevskii equations, *Numerische Mathematik* (2013), 1–50.

[74] R. A. Horn and C. R. Johnson, *Matrix Analysis*, 2nd, Cambridge, UK: Cambridge University Press, 2013.

[75] A. Iserles, *A First Course in the Numerical Analysis of Differential Equations*, 2nd, Cambridge: Cambridge University Press, 2008.

[76] A. Iserles, Think globally, act locally: Solving highly-oscillatory ordinary differential equations, *Appl. Numer. Math.* **43** (2002), 145–160.

[77] A. Iserles and K. Kropielnicka, *Effective approximation for linear time-dependent Schrödinger equation*, Technical Report NA2011/15, DAMTP, University of Cambridge, 2011.

[78] A. Iserles and S. P. Nørsett, On the solution of linear differential equations in Lie Groups, *Phil. Trans. R. Soc. A* **357** (1999), 983–1019.

[79] A. Iserles and S. P. Nørsett, Quadrature methods for multivariate highly oscillatory integrals using derivatives, *Math. Comp.* **75** (2006), 1233–1258.

[80] A. Iserles, S. P. Nørsett, and A.F. Rasmussen, Time symmetry and high-order Magnus methods, *Appl. Numer. Math.* **39** (2001), 379–401.

[81] T. Jahnke and C. Lubich, Error bounds for exponential operator splittings, *BIT* **40** (2000), 735–744.

[82] S. Janecek and E. Krotscheck, A fast and simple program for solving local Schrödinger equations in two and three dimensions, *Comp. Phys. Comm.* **178** (2008), 835–842.

[83] S. Jin, P. Markowich, and C. Sparber, Mathematical and computational methods for semiclassical Schrödinger equations, *Acta Numerica* **20** (2011), 121–209.

[84] M. Khanamiryan, Quadrature methods for highly oscillatory linear and non-linear systems of ordinary differential equations: part II, *BIT Numer. Math.* **52** (2012), 383–405.

[85] K. Kormann, S. Holmgren, and H. O. Karlsson, Accurate time propagation for the Schrödinger equation with an explicitly time-dependent Hamiltonian, *J. Chem. Phys.* **128** (2008).

[86] P.-V. Koseleff, "Calcul Formel pour les méthodes de Lie en mécanique hamiltonienne", PhD thesis, Palaiseau, France: École Polytechnique, 1993.

[87] J. Laskar and P. Robutel, High order symplectic integrators for perturbed Hamiltonian systems, *Cel. Mech. Dyn. Astron.* **80** (2001), 39–62.

[88] A. J. Leggett, Bose-Einstein condensation in the alkali gases: Some fundamental concepts, *Rev. Mod. Phys.* **73** (2001), 307–356.

[89] L. Lehtovaara, J. Toivanen, and J. Eloranta, Solution of time-independent Schrödinger equation by the imaginary time propagation method, *J. Comput. Phys.* **221** (2007), 148–157.

[90] H. R. Lewis and W. B. Riesenfeld, An Exact Quantum Theory of the Time-Dependent Harmonic Oscillator and of a Charged Particle in a Time-Dependent Electromagnetic Field, *J. Math. Phys.* **10** (1969), 1458–1473.

[91] C. Lubich, *From quantum to classical molecular dynamics: reduced models and numerical analysis*, Zurich Lectures in Advanced Mathematics, Zürich: European Mathematical Society, 2008.

[92] Linn M., M. Niemeyer, and A. L. Fetter, Vortex stabilization in a small rotating asymmetric Bose-Einstein condensate, *Phys. Rev. A* **64** (2001), 023602.

[93] W. Magnus, On the exponential solution of differential equations for a linear operator, *Commun. Pure Appl. Math.* **7** (1954), 649–673.

[94] R. I. McLachlan, Composition methods in the presence of small parameters, *BIT Numer. Math.* **35** (1995), 258–268.

[95] R. I. McLachlan and G. R. W. Quispel, Splitting methods, *Acta Numerica* **11** (2002), 341–434.

[96] H.-D. Meyer, U. Manthe, and L. S. Cederbaum, The multi-configurational time-dependent Hartree approach, *Chem. Phys. Lett.* **165** (1990), 73–78.

[97] P. C. Moan, "On Backward Error Analysis and Nekhoroshev Stability in Numerical Analysis of Conservative ODEs", PhD thesis, Cambridge, UK: University of Cambridge, 2002.

[98] P. C. Moan and J. Niesen, Convergence of the Magnus Series, *Found. Comput. Math.* **8** (2008), 291–301.

[99] P. M. Morse, Diatomic Molecules According to the Wave Mechanics. II. Vibrational Levels, *Phys. Rev.* **34** (1929), 57–64.

[100] E. J. Mueller, T.-L. Ho, M. Ueda, and G. Baym, Fragmentation of Bose-Einstein condensates, *Phys. Rev. A* **74** (2006), 033612.

[101] A. Murua, The Hopf Algebra of Rooted Trees, Free Lie Algebras, and Lie Series, English, *Found. Comput. Math.* **6** (2006), 387–426.

[102] A. Murua and J. Makazaga, private communication, 2012.

[103] M. Ö. Oktel, Vortex lattice of a Bose-Einstein condensate in a rotating anisotropic trap, *Phys. Rev. A* **69** (2004), 023618.

[104] I. P. Omelyan, I. M. Mryglod, and R. Folk, On the construction of high-order force gradient algorithms for integration of motion in classical and quantum systems, *Phys. Rev. E* **66** (2002), 026701.

[105] J. A. Oteo, The Baker–Campbell–Hausdorff formula and nested commutator identities, *J. Math. Phys.* **32** (1991), 419–424.

[106] V. M. Pérez-García and X. Liu, Numerical methods for the simulation of trapped nonlinear Schrödinger systems, *Appl. Math. Comp.* **144** (2003), 215–235.

[107] C. J. Pethick and H. Smith, *Bose-Einstein Condensation in Dilute Gases*, 2nd, Cambridge, UK: Cambridge University Press, 2008.

[108] S. E. Pollack, D. Dries, M. Junker, Y. P. Chen, T. A. Corcovilos, and R. G. Hulet, Extreme Tunability of Interactions in a Bose-Einstein Condensate, *Phys. Rev. Lett.* **102** (2009), 090402.

[109] E. Ponsoda, S. Blanes, and P. Bader, New efficient numerical methods to describe the heat transfer in a solid medium, *Mathematical and Computer Modelling* **54** (2011), Mathematical models of addictive behaviour, medicine & engineering, 1858–1862.

[110] G. Pöschl and E. Teller, Bemerkungen zur Quantenmechanik des anharmonischen Oszillators, *Zeitschrift für Physik* **83** (1933), 143–151.

[111] C. Reutenauer, *Free Lie Algebras*, London Maths Soc. Monographs **7**, Oxford: Oxford University Press, 1993.

[112] A. K. Roy, N. Gupta, and B. M. Deb, Time-dependent quantum-mechanical calculation of ground and excited states of anharmonic and double-well oscillators, *Phys. Rev. A* **65** (2001), 012109.

[113] K. Sakkos, J. Casulleras, and J. Boronat, High order Chin actions in path integral Monte Carlo, *J. Chem. Phys.* **130** (2009), 204109.

[114] S. Sánchez, F. Casas, and A. Fernández, New analytic approximations based on the Magnus expansion, *J. Math. Chem.* **49** (2011), 1741–1758.

[115] E. Schrödinger, Der stetige Übergang von der Mikro- zur Makromechanik, *Naturwissenschaften* **14** (1926), 664–666.

[116] E. Schrödinger, Quantisierung als Eigenwertproblem (Erste Mitteilung), *Annalen der Physik* **79** (1926), 361–376.

[117] M. Seydaoğlu and S. Blanes, High-order splitting methods for separable non-autonomous parabolic equations, *Appl. Numer. Math.* **84** (2014), 22–32.

[118] Q. Sheng, Solving linear partial differential equations by exponential splitting, *IMA J. Numer. Anal.* **9** (1989), 199–212.

[119] M. Suzuki, Fractal decomposition of exponential operators with applications to many-body theories and Monte Carlo simulations, *Phys. Lett. A* **146** (1990), 319–323.

[120] M. Suzuki, General theory of fractal path integrals with applications to many-body theories and statistical physics, *J. Math. Phys.* **32** (1991), 400–407.

[121] H. Tal-Ezer and R. Kosloff, An accurate and efficient scheme for propagating the time dependent Schrödinger equation, *J. Chem. Phys.* **81** (1984), 3967–3971.

[122] M. Thalhammer, A Fourth-order Commutator-free Exponential Integrator for Nonautonomous Differential Equations, *SIAM J. Numer. Anal.* **44** (2006), 851–864.

[123] M. Thalhammer, M. Caliari, and C. Neuhauser, High-order time-splitting Hermite and Fourier spectral methods, *J. Comput. Phys.* **228** (2009), 822–832.

[124] L. N. Trefethen, *Spectral Methods in MATLAB*, Philadelphia: SIAM, 2000.

[125] L. N. Trefethen and D. Bau III, *Numerical Linear Algebra*, Philadelphia: SIAM, 1997.

[126] V. S. Varadarajan, *Lie Groups, Lie Algebras, and Their Representations*, 2nd, New York: Springer Verlag, 1984.

[127] J. Wei and E. Norman, Lie Algebraic Solution of Linear Differential Equations, *J. Math. Phys.* **4** (1963), 575–581.

[128] J. Werschnik and E.K.U. Gross, Quantum optimal control theory, *J. Phys. B: At. Mol. Opt. Phys.* **40** (2007), R175.

[129] J. Werschnik and E.K.U. Gross, Tailoring laser pulses with spectral and fluence constraints using optimal control theory, *J. Opt. B: Quantum Semiclass. Opt.* **7** (2005), S300–S312.

[130] R. M. Wilcox, Exponential operators and parameter differentiation in quantum physics, *J. Math. Phys.* **8** (1967), 962–982.

[131] H. Yoshida, Construction of higher order symplectic integrators, *Phys. Lett. A* **150** (1990), 262–268.

[132] W. Zhu and H. Rabitz, A rapid monotonically convergent iteration algorithm for quantum optimal control over the expectation value of a positive definite operator, *J. Chem. Phys.* **109** (1998), 385–391.